Gata2 in Hematopoietic Cell Generation

Mari-Liis Kauts

Gata2 in Hematopoietic Cell Generation

Gata2 in hematopoietische cel generatie

Thesis

to obtain the degree of Doctor from the
Erasmus University Rotterdam
by command of the
rector magnificus

Prof.dr. H.A.P. Pols

and in accordance with the decision of the Doctorate Board.

The public defence shall be held on
Tuesday 11 of April 2017 at 15.30 hours

by

Mari-Liis Kauts

born in Tallinn, Estonia

Erasmus University Rotterdam

Contents

CHAPTER 1

Introduction
Scope of the thesis

Introduction

Hematopoiesis is initiated by a transient wave of primitive blood cell emergence

Blood cells are one of the first differentiated cell/tissue lineages generated in the vertebrate embryo. Surprisingly, they are produced even before the circulation is established (Palis et al., 2001). Transient waves of hematopoietic cell production are first initiated extra-embryonically in the yolk sac (YS) blood islands (Palis et al., 1999) which are derived from mesodermal cells that migrate to the YS at neural plate stage. At embryonic day 7 (E7) the mesodermal aggregates generate the first blood cells (Figure 1) (Haar and Ackerman, 1971; Palis et al., 1999). The emergence of blood cells in the YS is in close relationship to the appearance of endothelial cells that form the first vascular structures. This spatiotemporal association between the emergence of hematopoietic and endothelial cells has led to the hypothesis that they arise from a common bipotential ancestor, which is termed the hemangioblast (Palis et al., 2001).
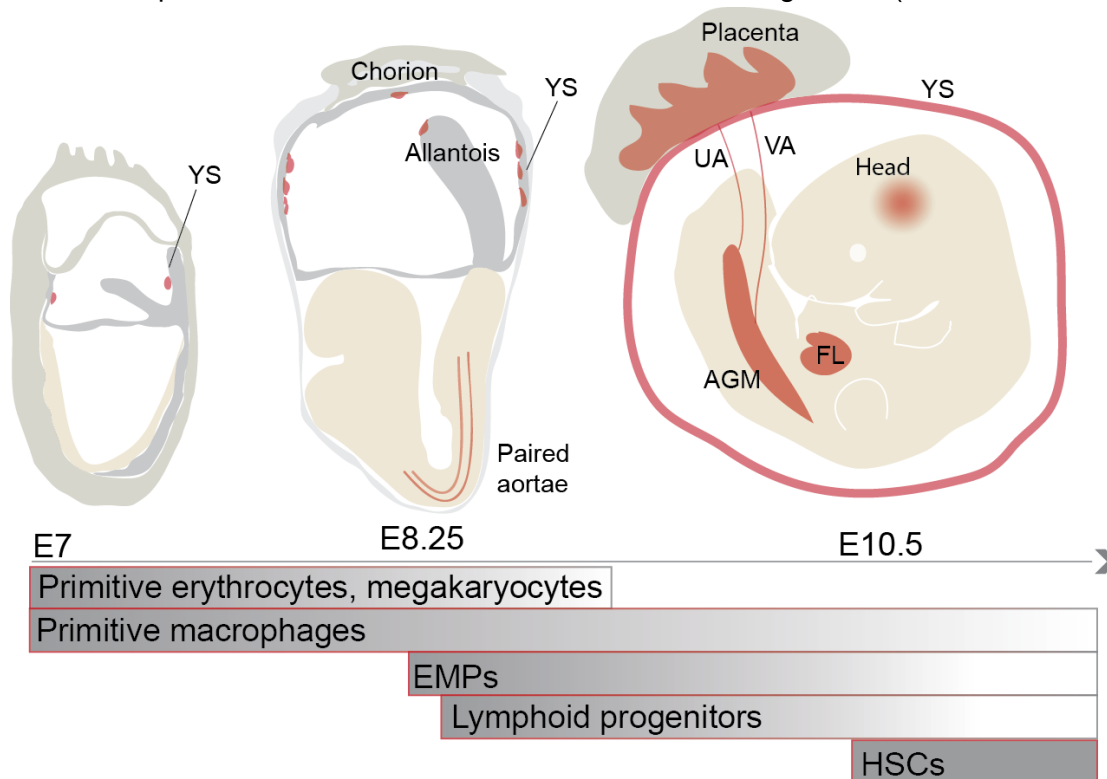

Figure 1. Sites and times of blood cell generation in the mouse embryo.
Blood generation in the mouse embryo starts in the blood islands of extra embryonic yolk sac (YS) at embryonic day 7 (E7) with a transient wave of 'primitive' erythrocyte, megakaryocyte and macrophage production. The erythrocytes and megakaryocytes of that stage are short-lived and disappear by E9. Primitive macrophages are hypothesized to be the source of tissue resident macrophages in the adult brain. The second wave of blood generation gives rise to bipotential erythroid-myeloid progenitors (EMPs) that emerge in the YS from E8.25. Shortly thereafter, lymphoid potential in detected. The paired dorsal aortae contain lymphoid potential as do the allantois/chorion. In the third hematopoietic wave, long-lived transplantable hematopoietic stem cells (HSCs) are generated beginning at E10.5 in the aorta-gonads mesonephros (AGM) region. HSCs are also detected in the vitelline (VA) and umbilical (UA) arteries, YS, placenta and in embryonic head. HSCs and EMPs migrate to the fetal liver (FL) where they expand and reside before migrating to the bone marrow niches.

The first genetic evidence supporting a common precursor for hematopoietic and endothelial lineages came from deletion of the *Flk1* receptor tyrosine kinase gene in the

mouse. *Flk1* expression is detected as early as at E7 in the YS mesoderm (Yamaguchi et al., 1993). Embryos lacking *Flk1* are not viable and interestingly, show a complete absence of mesodermal cell aggregates in the YS. It was concluded that *Flk1* is required for mesodermal cell migration to form YS blood islands and for making hematopoietic and endothelial cells (Shalaby et al., 1995) and suggested that a bipotential hemangioblast generates hematopoietic and endothelial cells. Intriguingly, lineage marking/tracing experiments have shown that there is little/no overlap in the mesodermal precursors that are forming the endothelial and hematopoietic cells in individual blood islands, suggesting a separation in fate early before migration to the YS (Ueno and Weissman, 2006).

Mouse embryonic stem cell (ESC) hematopoietic differentiation studies facilitated the search for putative hemangioblast-like cells. ESCs are self-renewing pluripotent cells derived from the inner cell mass of the blastocyst (Evans and Kaufman, 1981). They are characterised by their ability to contributed to all cells types of the developing embryo, including the germ line when re-introduced into the host blastocyst (Bradley et al., 1984). *In vitro*, they provide a platform for deriving cell types of different lineages (Keller, 1995; Smith, 2001).

ESCs differentiated in in the presence of vascular endothelial growth factor (VEGF) and stem cell factor (SCF) for 2.5 days generated blast-colony forming progenitor cells (BL-CFC) that were able to give rise to both, hematopoietic and endothelial cells (Choi et al., 1998). The BL-CFC (putative hemangioblast) represents a transient population that persists for a very short time in the differentiation culture. It expresses genes common to both hematopoietic and endothelial lineage, including *Flk1* (Kennedy et al., 1997). Later it was shown that the BL-CFC have an additional differentiation potential to cardiomyocyte lineage (Kouskoff et al., 2005) and thus, the physical isolation of the hemangioblast remains difficult. Nonetheless, to better understand embryonic hematopoiesis, *in vitro* ESC hematopoietic differentiation models have been widely used as they recapitulate the early stages of hematopoietic cell development and differentiate to almost all hematopoietic lineages, thus facilitating biochemical analyses of transcription factors and other regulatory molecules involved in development.

The earliest blood cells detected in the embryo are primitive erythrocytes, macrophages and megakaryocytes

Blood cells that emerge in the first wave of hematopoietic cell generation are 'primitive' erythrocytes, macrophages and rare megakaryocyte progenitors (Palis et al., 1999; Tober et al., 2007). This developmental wave is categorized as 'primitive' due to the distinctive characteristics of the erythrocytes and erythrocyte colony forming unit cells (EryP-CFU-Cs). 'Primitive' red blood cells are nucleated and are 3 times larger than fetal and 6 times larger than adult erythrocytes (Kingsley et al., 2006; Kingsley et al., 2004). Moreover, they produce a developmentally distinct embryonic (*βH1*) globin, which is not detected in adult erythrocytes. 'Primitive' erythrocytes peak in numbers at E8.25 and disappear rapidly by E9 (Palis et al., 1999; Tober et al., 2007). The short developmental time of these cells resembles the transient nature of hemangioblast-like cells, thus supporting the hypothesis that they originate from a short-lived precursor.

Concurrently, rare macrophage progenitors are detected in the YS (Bertrand et al., 2005;

Palis et al., 1999). 'Primitive' macrophages from this first YS hematopoietic wave (E7-7.5) are directly derived from the blood islands and do not go through a monocyte intermediate (Naito et al., 1990; Naito et al., 1996; Takahashi et al., 1989) that characterizes the macrophages generated from hematopoietic stem cells (HSC) in the adult bone marrow. Once the bloodstream is established at E8.25-8.5 (McGrath et al., 2003) the YS derived macrophages migrate to the developing tissues where they become 'tissue resident' macrophages expressing high levels of F4/80 macrophage surface marker. These include macrophages in the skin, microglia in the brain, Kupffer cells in the liver and Langerhans cells in the epidermis. Recent lineage tracing studies suggest that 'tissue resident' macrophages in the skin, liver and lung are replaced before birth by 'monocyte derived' macrophages generated in later waves of hematopoietic development (Gomez Perdiguero et al., 2015). In contrast, the labeled brain microglia cells are retained throughout adult life. Unique to these macrophages, as compared to those in the adult, are high F4/80 expression, *c-Myb* transcription factor independence and *PU.1* transcription factor dependence (Gomez Perdiguero et al., 2015; Hoeffel et al., 2015; Kierdorf et al., 2013; Schulz et al., 2012). By E9.5, the quantitative abundance of phenotypic 'primitive' macrophages and megakaryocytes in the embryo further suggests that these cells are directly generated in the first hematopoietic wave and not from the later waves of hematopoietic progenitor and stem cell generation (Bertrand et al., 2005; McGrath et al., 2015).

The need for all the early blood cells in the embryo before the circulation is not yet fully established. However, 'primitive' erythrocytes may be necessary for providing the rapidly growing embryo with oxygen, macrophages for phagocytosis of cells during tissue remodeling and for lymphatic development. The role of megakaryocytes is uncertain, although they are closely associated with red blood cells. Whether some of these primitive cells are directly involved in the emergence of later definitive hematopoietic cell types, remains a to be addressed.

Multipotent progenitors are generated in the YS during a second wave of blood cell generation

After the generation of 'primitive' erythrocytes, macrophages and megakaryocytes, another wave of hematopoietic cell production begins at E8.25 in the YS (Figure 1). It overlaps temporally with the first wave (Palis et al., 1999), but produces functionally more complex bipotential erythroid-myeloid progenitors (EMP). EMP cells express high levels of tyrosine receptor kinase cKit (CD117) and CD41, and by E9.5 are positive for granulocyte-monocyte marker CD16/32 expression (McGrath et al., 2015). EMP-derived erythrocytes are distinguished from their earlier, 'primitive' counterpart by the expression of adult (βmajor) globin (Palis et al., 1999) and by undergoing enucleation. Thus, based in this complexity and the generation of adult-like cells this wave is termed 'definitive' (Frame et al., 2013). However, cKit^{hi}CD41$^+$CD16/32$^+$ EMPs lack lymphoid cell potential, and are able to provide only short-term *in vivo* reconstitution, giving rise to mainly circulating red blood cells (McGrath et al., 2015). Hence, EMPs are distinct from HSCs.

Study of *Ncx1* null mice which lack circulation, show that EMPs are generated in the YS and not in the embryo proper through E9.5 (Lux et al., 2008; McGrath et al., 2015). They appear to emerge from cKit$^+$ cell clusters found in the venous and arterial vessels of the YS (Frame et al., 2016). These cells then colonize the newly forming liver around late E9

(Frame et al., 2013) and give rise to the large numbers of erythrocytes, macrophages, granulocytes and monocytes found before the establishment of a permanent hematopoietic system (Gomez Perdiguero et al., 2015).

Other hematopoietic cells generated in the second wave are rare cells with lymphoid potential, B-1 B cell progenitors. They are detected at E8.5/9.5 in the YS and aorta (Godin et al., 1995; Yokota et al., 2006; Yoshimoto et al., 2012). Mast cells are also found in the YS from E9.5 onwards (Sonoda et al., 1983). Taken together, this 'definitive' wave of hematopoietic cell generation yields more adult-like functionally competent blood cell types. Also, there is growing evidence that these cells may play an interactive role in promoting the third wave of hemogenesis and HSC generation (Espin-Palazon et al., 2014; Li et al., 2014; Travnickova et al., 2015).

The first HSCs emerge intraembryonically in a third wave of blood cell generation

Adult type HSCs are defined by their robust ability to long-term repopulate all blood lineages upon transplantation into irradiated adult recipients. Figure 2 shows hematopoietic hierarchy with HSCs at the top. HSCs are able to reproduce themselves (self-renew) and give rise to all mature blood lineage cells via progenitor intermediates. HSCs are quiescent cells, whereas proliferation capacity is increased in the progenitor cell state.
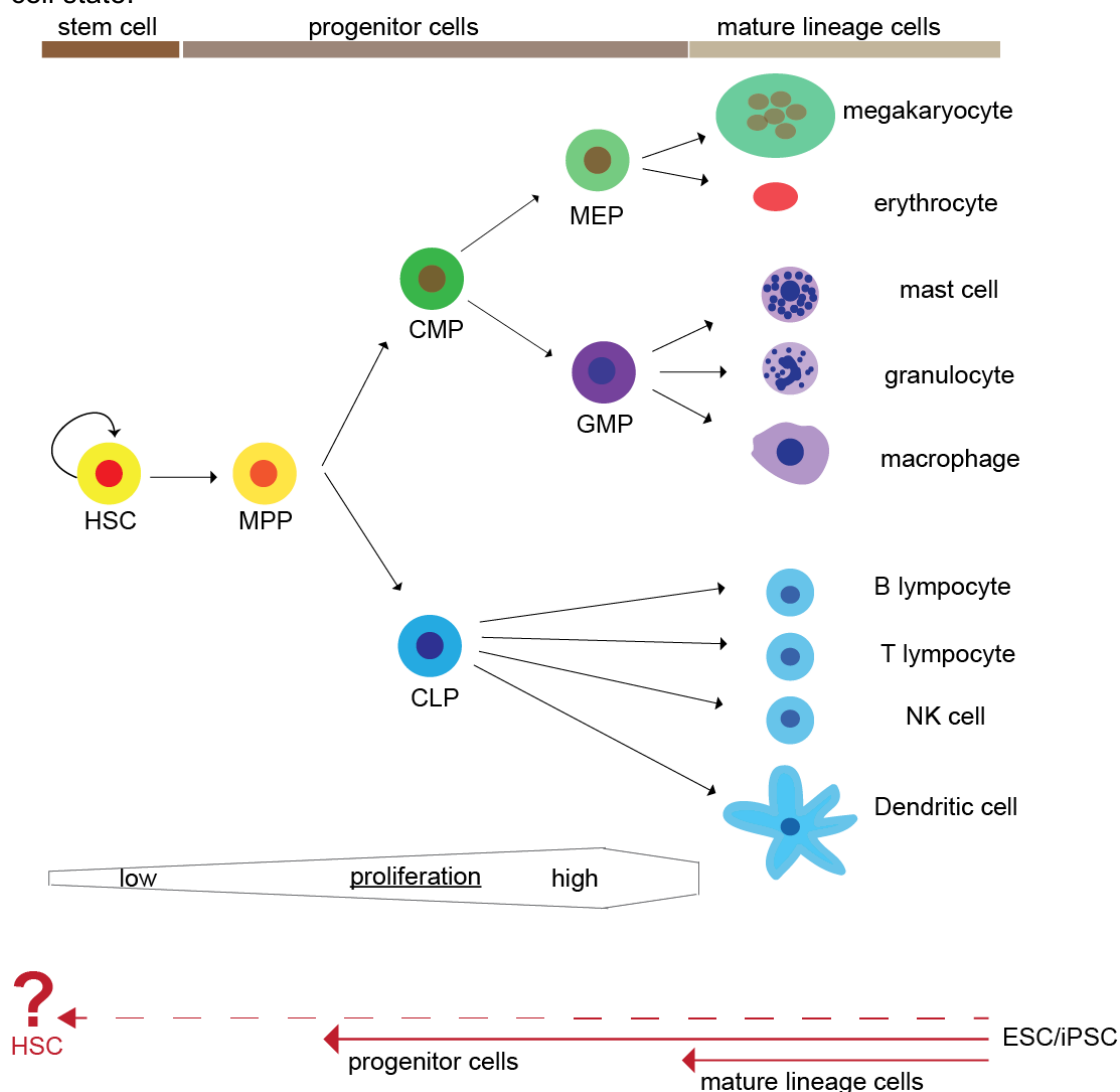
Figure 2. Hematopoietic cell hierarchy. Hematopoietic stem cells (HSC) are at the top of the hematopoietic cell hierarchy. They self-renew and give rise to committed progenitor cells, which differentiate to generate mature cells of all the blood lineages. The progression of rather quiescent HSCs to progenitor cells is associated with the increase in the proliferation rate. Adapted from (Bryder et al., 2006). Generating HSCs *in vitro* from embryonic stem cells (ESC) and induced pluripotent stem cells (iPSC) has been a long term goal of blood research. To date, it has been feasible to derive unipotent cells and (multipotent) progenitors, however, the attempts to robustly convert ESCs/iPSCs into self-renewing multipotent engrafting HSCs, has largely failed. MPP, multipotent progenitor; CMP, common myeloid progenitor; MEP, megakaryocyte/erythroid progenitor; GMP, granulocyte/monocyte progenitor; CLP, common lymphoid progenitor; NK natural killer cell.

In the mouse embryo, the first adult HSCs appear and are autonomously generated in the aorta-gonads-mesonephros (AGM) region at E10.5 (Figure 1) (Medvinsky and Dzierzak, 1996; Muller et al., 1994). They are also found in the vitelline and umbilical arteries (VA, UA) and in the head (de Bruijn et al., 2000; Li et al., 2012). Shortly thereafter, HSCs are detected in the YS, placenta, circulation and fetal liver (FL) (Gekas et al., 2005; Medvinsky and Dzierzak, 1996; Muller et al., 1994; Ottersbach and Dzierzak, 2005). Whereas the YS and placenta may be capable of autonomously generating HSCs, the FL serves only as a niche for the expansion of HSCs (and EMPs) made in the other tissues (Ema and Nakauchi, 2000; Gekas et al., 2005; Kumaravelu et al., 2002). Just before birth HSCs migrate to the bone marrow where they reside throughout mammalian adult life in specialized niches (Mendelson and Frenette, 2014).

HSCs are generated from a subset of embryonic endothelial cells that possess hemogenic potential - the hemogenic endothelial cells (HEC) (Figure 3A) (Dzierzak and Speck, 2008; Jaffredo et al., 2005). They are detected at the time when clusters of hematopoietic cells appear on the ventral wall of the dorsal aorta. These intra-aortic hematopoietic cluster cells (IAHC) are cKit$^+$ and at E10.5, approximately 600 IAHCs (1-19 cKit$^+$ cells per cluster) were found along the length of the embryo by whole mount embryo imaging (Yokomizo and Dzierzak, 2010). Figure 3B shows the *Gata2Venus* mouse model where Gata2 expression is found in almost all IAHCs. The hematopoietic cell clusters are also found in the YS vasculature (Figure 3C). Vital imaging of the mouse embryonic aorta at the time of HSC generation revealed the transition of morphologically flat endothelial cells to cells that bulge out of the vascular wall and form round hematopoietic cells in the lumen of the aorta. This process was visualized in *Ly6a (Sca1) GFP* fluorescent reporter transgenic embryos. GFP is expressed in all embryonic and adult HSCs in the mouse (Chen et al., 2011; de Bruijn et al., 2000; Li et al., 2012; Ma et al., 2002; Ottersbach and Dzierzak, 2005) and hence, is an excellent reporter for observing the emergence of HSCs. To visualize EHT in the aorta by confocal time-lapse imaging, thick sections of *Ly6aGFP* E10.5 embryos were stained with a combination of antibodies against hematopoietic and endothelial cell surface markers (Boisset et al., 2010). HECs that give rise to HSCs could be distinguished from other aortic endothelial cells by the expression of GFP. Rare GFP$^+$cKit$^+$CD41$^+$ cells were observed bulging into the lumen of the aorta directly from GFP$^+$CD31$^+$ ventral aortic endothelial cells, thus facilitating tracking single cells as they transition from an endothelial cell to a HSC/HPC. This process is generally known as the endothelial-to-hematopoietic transition (EHT).
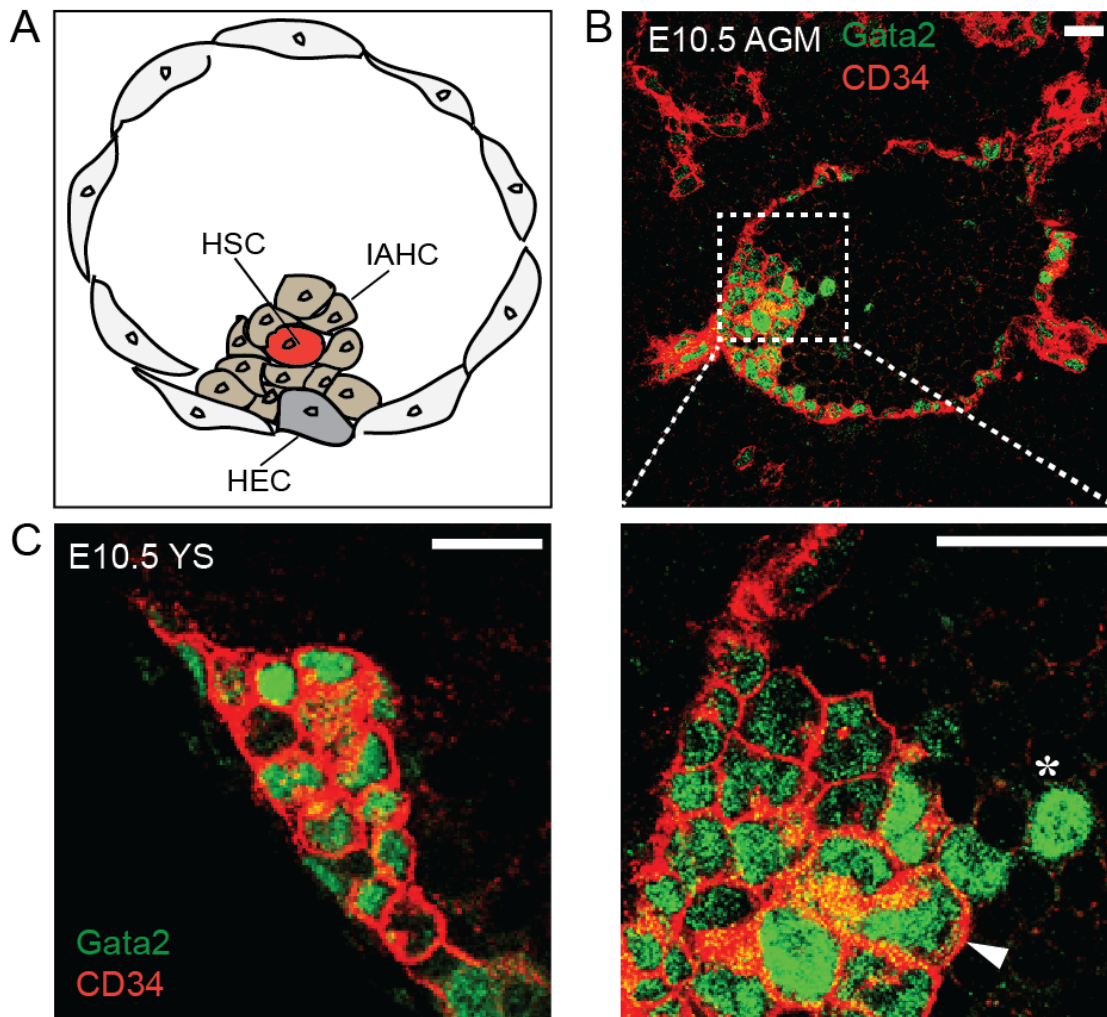
Figure 3. Emergence of HSCs through EHT in the AGM and in the YS.
A) A subset of aortic endothelium – the hemogenic endothelial cells (HEC), transdifferentiate to form intra aortic hematopoietic cluster cells (IAHC) and hematopoietic stem cells (HSC). Drawing of a transverse section through mouse aorta indicating HECs, IAHCs and emerging HSCs. **B)** Gata2 is one of the pivotal transcription factors marking HECs, IAHCs and emerging HSCs. Thus, *Gata2Venus* reporter expression can be exploited to visualize the emergence of HSCs. Upper panel displays an immunostained fluorescent image of a transverse section of embryonic day (E) 10.5 aorta-gonads-mesonephros (AGM) region. Lower panel shows magnified IAHCs in the dotted square region of the upper panel. Gata2 (green) is found in most of the CD34$^+$ (red) IAHCs (arrowhead) and in some endothelial cells. Gata2 is also detected in a few round CD34$^-$ cells (asterisk) that are closely associated with IAHCs suggesting that they arose from clusters. **C)** CD34$^+$Gata2$^+$ clusters are also found in the YS vasculature. Size bars 20 µm.

EHT has also been imaged in zebrafish embryos, however the process is slightly different than that observed in the mouse embryos. The HECs in zebrafish bulge ablumenally, and emerge as hematopoietic cells in the interstitial region between the aorta and axial vein. Moreover, multi-cell clusters do not form. Emerging zebrafish HSCs/HPCs are marked by *c-Myb* expression (Jing and Zon, 2011). Vital time-lapse imaging of compound transgenic *c-Myb-GFP:Kdr1*(*Flk1* endothelial marker)-*mCherry* zebrafish embryos demonstrates that hematopoietic cells acquiring CD41 expression emerge directly from endothelium in the ventral side of the dorsal aorta (Bertrand et al., 2010; Bertrand et al., 2008; Kissa and Herbomel, 2010). They move quickly to extravasate into the lumen of the axial vein where they enter the circulation. They are next found to enter specific

niches in caudal hematopoietic tissue, the equivalent of the mouse fetal liver (Tamplin et al., 2015).

EHT has also been recapitulated *in vitro* and detected by time-lapse imaging of ESC hematopoietic differentiation cultures. ESC-derived cells expressing the endothelial marker Tie2 and cKit, when exposed to hematopoietic culture conditions, give rise to CD41$^+$ hematopoietic cells that down-regulate Tie2 (Eilken et al., 2009; Lancrin et al., 2009). Together these data provide *in vitro* and *in vivo* morphological and phenotypical evidence of HSC/HPC emergence via EHT – a process that is conserved in human ESCs (Rafii et al., 2013) and all vertebrate embryos (Jaffredo et al., 2005) thus far examined.

The Gata2 transcription factor - a pivotal regulator of HSC/HPC development

The Gata2 (GATA binding protein 2) transcription factor is one of the key players in the development of HSCs and HPCs. It belongs to the evolutionarily conserved Gata transcription factor family, together with 5 other members (Gata1-6). They get their name from the DNA motif A/TGATAA/G what they bind to, and they have two conserved zinc finger domains (Bresnick et al., 2010; Ko and Engel, 1993). Three Gata family factors are associated with hematopoiesis - Gata2 with HSCs/HPCs, Gata1 with mainly erythroid development and Gata3 with T lymphopoiesis (Ho et al., 1991; Kitajima et al., 2006). Gata2 and Gata3 expression is also detected in the developing central nervous system (Nardelli et al., 1999) and Gata3 has been associated with the developmental regulation of several tissues such as the ear, kidney and mammary gland (Asselin-Labat et al., 2007, Labastie et al., 1995, Karis et al., 2001). Gata4-6 are involved in cardiac development (Charron and Nemer, 1999; Molkentin et al., 2000). Gata2 is dysregulated in several hematological malignancies, including MonoMac disease, Emberger's syndrome and familial AML and myelodysplastic syndrome reviewed in (Bresnick et al., 2012; Spinner et al., 2014).

The importance of the Gata2 in the process of HSC/HPC generation was first highlighted by the creation of a germline knockout mouse model. Strikingly, *Gata2* homozygous deletions resulted in embryonic lethality at E10.5 (e.g. the time of the first HSC emergence) that was accompanied by severe fetal liver anemia (Okuda et al., 1996; Tsai et al., 1994). Functional studies revealed that *Gata2$^{-/-}$* embryos are defective for 'definitive' hematopoiesis, as demonstrated by greatly reduced progenitor numbers (Ling et al., 2004; Tsai et al., 1994). *In vitro* hematopoietic differentiation experiments with *Gata2$^{-/-}$* ESCs show that they retain the ability to undergo 'primitive' erythroid differentiation, however, at reduced levels. 'Definitive' hematopoietic progenitor generation is profoundly impaired. Analysis of ESC-generated *Gata2$^{-/-}$* chimeric mice revealed a lack of knockout cell contribution to any of the hematopoietic organs (Okuda et al., 1996; Tsai et al., 1994).

The temporal and spatial expression patterns of *Gata2* in the embryo (as determined by *in situ* hybridization and immunostaining) support their important cell-intrinsic role in HSC and HPC generation. *Gata2* is expressed at E8.0 in the YS, which at that time is the main site of hematopoietic cell generation (Minegishi et al., 2003; North et al., 1999; Robert-Moreno et al., 2005). *Gata2* is expressed in IAHCs in the embryonic arteries and all such hematopoietic clusters are absent in the aortae and other major arteries of the *Gata2$^{-/-}$* embryos (Chen et al., 2009; de Pater et al., 2013; Nardelli et al., 1999; North et al., 1999; Pimanda et al., 2007).

The continuum of expression during the transition from endothelial cells to hematopoietic cluster cells in static images of the aorta implicates a role for Gata2 in the process of EHT. Indeed, conditional deletion of *Gata2* in hemogenic endothelium marked by *vascular endothelial-cadherin* (*Vec*) demonstrates that it is essential in the HECs for the formation of hematopoietic clusters and importantly, for the generation of functional HPCs and HSCs (Chen et al., 2011; de Pater et al., 2013; Zovein et al., 2008). *Gata2* continues to be essential in the HSCs after they are made, as demonstrated by Gata2 deletion in *Vav-Cre* (expressed in HSCs) conditional knockout embryos (de Pater et al., 2013). Thus, *Gata2* plays pivotal role in hematopoietic development, affecting mainly the 'definitive' stage in which multipotent HPCs and HSCs are generated, and continues to be required for the maintenance of the emerged HSCs.

Strictly controlled Gata2 expression levels determine the progression of EHT

It is of importance to note that HSC and HPC development is highly dependent on the *Gata2* expression levels. *Gata2*^{+/-} embryos have profoundly reduced numbers of AGM HSCs, HPCs, and IAHCs. The bone marrow of *Gata2*^{+/-} adult mice contains normal quantities of HSCs, but these are qualitatively impaired, as observed in competitive transplantation assays (de Pater et al., 2013; Ling et al., 2004; Rodrigues et al., 2005). Overexpression of *Gata2* also results in abnormal hematopoiesis: it reduces bone marrow colony forming unit-cell (CFU-C) and colony forming unit-spleen (CFU-S) activity and results in a failure of multilineage reconstitution (Gao et al., 2013). Hematopoietic differentiation of ESCs overexpressing *Gata2* suggests that abnormally high *Gata2* expression blocks T and B cell generation, resulting in myeloid-biased cell production (Ikonomi et al., 2000; Nandakumar et al., 2015). Thus, *Gata2* expression levels are likely to be involved in controlling cell fate decisions. Recent transcriptome analysis of placental cells suggests that *Gata2* is continuously expressed in hemogenic and hematopoietic progenitors, but downregulated during commitment to blood lineages (Pereira et al., 2016). Also, *Gata2* expression is downregulated during ESC-derived hemangioblast differentiation into blast cells (Lugus et al., 2007), thus indicating that levels of *Gata2* may play a role in HSC and HPC expansion and potency.

Gata2 functions synergistically with _Runx1_ to regulate its downstream targets

Although deletion of a single allele of *Gata2* or *Runx1* (another pivotal hematopoietic transcription factor) disrupts HSC and HPC development, it does not result in embryonic lethality (Cai et al., 2000; North et al., 1999; Tsai et al., 1994). Strikingly, the analysis of *Gata2*^{+/-}: *Runx1*^{+/-} compound embryos showed a trend towards fewer hematopoietic progenitors and the absence of double haploinsufficient offspring due to embryonic lethality (Wilson et al., 2010). These data suggest that Gata2 functions together with Runx1 in the same cells to control the expression of hematopoietic genes involved in HSC and progenitor cell generation.

Further evidence for combinatorial function of Gata2 and Runx1 comes from an extensive Chromatin Immunoprecipitation Seq (ChIP-seq) and bioinformatics analysis revealing interaction complexes between a heptad of hematopoietic cell specific transcription factors that includes Runx1 and Gata2. The vast majority of heptad bound promoter and

enhancer regions of hematopoietic genes contain a GATA consensus binding sequence. Only approximately 40% of them contain a Runx consensus binding motif, suggesting that the formation of a complex and/or Gata2 binding may be required for the recruitment of Runx1 to the regulatory elements within the complex (Wilson et al., 2010). Similar higher order protein complexes, such as the Ldb1 complexes, are found in erythroid cell development where adaptor molecule Ldb1 mediates the interactions between a variety of binding partners (Meier et al., 2006; Mylona et al., 2013). Combinatorial interactions within the heptad complex result in hematopoietic cell type-specific chromatin binding and downstream gene expression. How exactly the complex functions in cell fate specification is yet unknown. Whether the factors act sequentially or all at the same time, whether they regulate each other, and how individual factor levels affect complex formation is a matter of debate.

Runx1

Similar to Gata2, Runx1 plays a crucial role in HSC/HPC development as was first revealed by the homozygous deletion of *Runx1* that resulted in embryonic lethality (at E12.5) accompanied by severe hematopoietic defects (Okuda et al., 1996; Tsai et al., 1994). Functional studies revealed that although *Runx1*$^{-/-}$ mice make 'primitive' hematopoietic cells, they completely lack 'definitive' hematopoietic progenitors in the YS and fetal liver, and importantly, no HSCs are generated in the AGM (Cai et al., 2000; Okuda et al., 1996). Mutant ESC differentiation studies show that *Runx1*$^{-/-}$ ESCs generate fewer 'primitive' erythroid cells, and the generation of 'definitive' hematopoietic progenitors is profoundly compromised. Like the deletion of *Gata2*, *Runx1*$^{-/-}$ ESCs were unable to contribute to any of the hematopoietic organs (Okuda et al., 1996; Tsai et al., 1994).

Runx1 is expressed at E8.0 in the YS. Slightly thereafter, from E8.5 to E11.5, *Runx1* expression marks the endothelial cells on the ventral side of the aorta, umbilical and vitelline arteries, placenta and IAHCs. As a result of *Runx1* deletion, all hematopoietic clusters are absent in the aortae and other major arteries (Chen et al., 2009; North et al., 1999; Li et al., 2012; Rhodes et al., 2008). Conditional deletion of *Runx1* in *Vec*/*Tie2-Cre* expressing HECs, demonstrates its requirement for the formation of hematopoietic clusters and for the generation of functional HPCs/HSCs (Chen et al., 2011; de Pater et al., 2013; Zovein et al., 2008). It has been shown by tamoxifen-induced deletion of *Runx1* in *Vec*-Cre expressing cells that Runx1 is specifically required for HSC generation between E10.5 and E11.5 (Tober et al., 2013). The vital imaging of *Runx1* morphant zebrafish embryos provided an interesting insight into its role. In the absence of *Runx1*, aortic endothelial cells undergo sudden death as they attempt transition to hematopoietic cells, thus suggesting that *Runx1* is required during EHT for the survival of emerging hematopoietic cells (Kissa and Herbomel, 2010). However, Runx1 is not required for the maintenance of HSCs after they have been generated (Chen et al., 2009, Liakhovitskaia et al., 2014), thus suggesting for a more strict role than Gata2.

Runx1 also functions in a dose dependent manner. *Runx1*$^{+/-}$ embryos generate fewer HPCs and HSCs (Cai et al., 2000; Mukouyama et al., 2000; Robin et al., 2006; Wang et al., 1996). Fascinatingly, *Runx1*$^{+/-}$ embryos experience a temporal shift in the emergence of HSCs. HSCs are detected earlier than normal: at E10 in the AGM and YS, and HSC generation is prematurely terminated in the E11 AGM (Cai et al., 2000). The E10.5/11.5

aorta in *Runx1^{+/-}* embryos have fewer IAHCs, suggesting that Runx1 haploinsufficiency reduces HSC generation, maintenance and/or proliferation.

Taken together, the expression and function of Gata2 greatly overlaps with the one of Runx1, although the requirement for Runx1 is temporally more restricted. The fact that Gata2 and Runx1 double haploinsufficiency is lethal, while single factor haploinsufficiency is not, demonstrates these transcription factors act in concert to regulate HSC/HPC development. Importantly, the dose dependent requirement of both factors illustrates the highly-tuned control over hematopoietic development and suggests that depending on the expression level, they may define different cellular identities.

Gpr56, a downstream target of Gata2, is a novel positive regulator of hematopoiesis

As described in the previous section, downstream hematopoietic gene targets of the heptad transcription factors have been identified through genome-wide analysis in a hematopoietic progenitor cell line, HPC-7 (Wilson et al., 2010). The expression of these heptad factors was recently examined by RNA sequencing of cells undergoing EHT *in vivo* (endothelial cells, hemogenic endothelial cells, HPCs and HSCs) in the AGM at the time of HSC generation (Solaimani Kartalaei et al., 2015). Comparative transcriptome datasets show that heptad transcription factor expression is increasing during EHT, and is accompanied by transcriptional activation of several downstream target genes. One such target gene is the *G-protein coupled receptor 56* (*Gpr56*) that is significantly upregulated (38-fold) in HSCs as compared with hemogenic endothelial cells (Solaimani Kartalaei et al., 2015). Notably, *Gpr56* expression is downregulated as a result of *Gata2* (regulatory element) deletion, which is accompanied with severe disruption of hematopoiesis and embryonic lethality (Gao et al., 2013). Moreover, chromatin immunoprecipitation (ChIP) experiments reveal direct binding of Gata2 to the *Gpr56 +37* enhancer (Solaimani Kartalaei et al., 2015; Chacon et al., 2014) thus indicating that *Gpr56* is a direct target of *Gata2.* The precise function of *Gpr56* in hematopoiesis is as yet unknown. Studies in the 32D cell line show that Gpr56 expression keeps cells in a blast cell stage blocking their terminal differentiation (Solaimani Kartalaei et al., 2015). Hence it is likely that Gpr56 is involved *in vivo* for the acquisition of the self-renewal properties during the embryonic generation of hematopoietic progenitors and/or stem cells. This is supported by the finding of highly upregulated expression of Gpr56 in difficult to treat AMLs where it regulates anti-apoptotic functions (Saito et al., 2013). In zebrafish, it has been shown that *Gpr56* knockdown abrogates HSC/HPC emergence in the dorsal aorta (Solaimani Kartalaei et al., 2015) thereby supporting its functional involvement in EHT, but its function in the process of HSC generation in vertebrate development is as yet unknown.

The concept of preHSCs - do HSCs establish their fate prior to EHT?

Vital imaging of vertebrate embryos demonstrates that HSCs and HPCs are generated by morphological transdifferentiation of specialized endothelial cells (Boisset et al., 2010), and genetic tracing studies show that functional HSCs/HPCs descend from cells expressing endothelial markers (Zovein et al., 2008). But when is hematopoietic fate, and more precisely, when is HSC fate established? Current research interests are addressing the issue of whether HSC fate and function is determined in the endothelium during EHT,

or primed earlier or later in development.

A *Runx1+23 enhancer GFP (+23GFP)* reporter mouse was used to explore this issue (Nottingham et al., 2007; Swiers et al., 2013). Runx1 expression in vast majority of mouse hematopoietic stem and progenitor cells and aortic endothelial cells is controlled by a *Runx1 +23* enhancer, thus the *+23GFP* mouse model allows specific isolation of hemogenic endothelial cells (Nottingham et al., 2007; Swiers et al., 2013). Transcription analysis (Fluidigm) with a panel of endothelial and hematopoietic genes demonstrated that at E8.5 the +23GFP expressing aortic hemogenic endothelium is distinguished from +23GFP negative endothelium by higher expression of hematopoietic regulators such as *Meis1, Gata2, Gata3* and *TAL1*. Single cell transcriptome analysis showed in approximately 50% of +23GFP hemogenic endothelial cells that higher *Meis1* expression is accompanied by downregulation of the endothelial marker *Etv2,* thus arguing for hematopoietic fate establishment earlier than previously recognized (Swiers et al., 2013). At a later developmental time (at E10.5) in the *Ly6a GFP* model, the transcriptome of the aortic hemogenic endothelial fraction (CD31$^+$ckit$^-$GFP$^+$) showed differences to the endothelial fraction (CD31$^+$ckit$^-$GFP$^-$), with heptad transcription factor and Notch gene expression increased (Solaimani Kartalaei et al., 2015). Few indications of hematopoietic gene expression were found in the hemogenic endothelial fraction as compared to the HPC/HSC fraction (CD31$^+$ckit$^+$GFP$^+$). However, these experiments were performed with populations of sorted cells and await single cell transcriptomic analysis. Importantly, the expression of the heptad factors is the first and pivotal step directing a hematopoietic program, and as such *Runx1+23GFP* is an excellent indicator showing that the hemogenic and hematopoietic programs are established already in a subset of endothelial cells at the beginning stage of 'definitive' hematopoietic cell development.

If hematopoietic and HSC commitment occurs earlier than functional HSCs emerge, the aortic endothelium may harbor immature cells that in the proper microenvironment are able to mature into functional HSCs. To test this, an OP9 stromal cell co-aggregation culture was established that facilitates the *ex vivo* maturation of hematopoietic/endothelial cells obtained by multi-surface marker phenotypic sorting (Rybtsov et al., 2011). Using this approach, it was shown that E9.5 dorsal aorta contains a VEC$^+$CD41$^+$CD45$^-$CD43$^-$ cell population (termed pro-HSC) that lacks repopulating activity in direct *in vivo* transplantation assays. However, when co-aggregated with OP9 and *ex vivo* cultured for 7 days in the presence of SCF, IL-3 and Fms-related tyrosine kinase 3 ligand (Flt3L), this population is able to reconstitute the hematopoietic system of the recipient (Rybtsov et al., 2014). These pro-HSCs are almost devoid of endothelial cells and it is thought that they may represent a stage directly downstream of the Runx1+23GFP$^+$ hemogenic endothelium present in the E8.5 AGM (Swiers et al., 2013).

Also, the E10.5 and E11.5 AGM is thought to contain immature HSCs. This VEC$^+$CD41^{low}CD45$^-$CD43$^+$ population (termed pre-HSC) up-regulates CD45 expression when co-aggregated with OP9 and mature into functional, repopulating HSCs (Rybtsov et al., 2011). Interestingly, it has been proposed that the pre-HSCs may be generated independently of *Runx1*, as a developmental block is not observed before the transition of CD41$^+$ cells to CD45$^+$ in *Runx1* deficient mice (Liakhovitskaia et al., 2014). Cells with a pre-HSC phenotype are present also in the E11.5 YS and FL, but they are not able to mature into engrafting HSCs. Thus, functional pre-HSCs are thought to be present mainly in the AGM region and in the extraembryonic arteries (Boisset et al., 2015; Gordon-

Keylock et al., 2013; Rybtsov et al., 2014; Rybtsov et al., 2011).

These data propose that definitive HSCs may be primed for a hematopoietic gene expression program very early in development, making the precise temporal onset of the HSC program debatable. However, it should be taken into account that *ex vivo* manipulations, such as stromal cell and explant (co-)cultures, consequently introduce new variables into the model, that might not be present in *in vivo.* Advances in *in vivo* lineage and vital imaging tracing tools and single cell transcriptomics will assist in further investigations of such cells under more physiologic conditions representative of the *in vivo* embryonic milieu.

The divergence in the HSC emergence path

Recent studies have suggested that mouse embryonic head produces adult HSCs and HPCs independently from other hematopoietic organs and circulation. Lineage tracing experiments show that embryonic head-derived HSC progeny contribute to the adult HSC population (Li et al., 2012). However, to date, it has not been demonstrated that the head HSCs are emerging via an EHT in a similar manner to those in AGM. Moreover, the head vasculature lacks IAHCs (Iizuka et al., 2016; Li et al., 2016). Also, head HSCs do not seem to go through the putative pre-HSC state since no/few pre-HCSs have been reported in the head as demonstrated by OP9 co-aggregation culture of E11.5 head region (Rybtsov et al., 2016). These studies suggest that there may be an alternative way by which functional HSCs are generated, and could include generation in different spatial and temporal frameworks, and different regulatory programs and networks. Defining such mechanisms could contribute to answering questions currently arising in the field of hematopoiesis: for instance, such information may clarify the source of heterogeneity among HSCs – BMP-activated and BMP-non-activated, myeloid or lymphoid biased (Crisan et al., 2015; Yamamoto et al., 2013). Also, it may provide insight into why there are many more HPCs in the IAHCs than HSCs (Boisset et al., 2015), and explain the source of the large cohort of FL HSCs that appears within 24 hours following the generation of the first HSCs in the AGM, and the rapid decrease in the pre-HSC numbers in the AGM (Rybtsov et al., 2016).

Approaches to generate *bone fide* HSCs

The importance of precisely characterizing all the discrete steps and distinct factors required for *in vivo* HSC/HPC development lies in the ability to apply this knowledge to *ex vivo* cell culture strategies with the potential to drive HSC generation. As there is shortage of HSCs for clinical cell replacement therapies to treat blood-related genetic diseases and leukemia, there is a need for their *bone fide* generation, as well as for protocols facilitating their *ex vivo* expansion. Early studies by Doetchman *et al.,* gave initial evidence that mature blood cells can be generated from ESCs (Doetschman et al., 1985). This lead to the thinking that it might be possible to derive HSCs from pluripotent stem cells (Figure 2 lower panel). Indeed, the principle basis of generating long-term engrafting HSCs from pluripotent stem cells has been shown by studies transplanting undifferentiated mouse and human induced pluripotent stem cells (iPSCs) into immunocompromised mice. The teratomas that developed from the injected iPSCs contained donor-cell derived HSCs, and when the putative HSCs were isolated and transplanted, they repopulated the hematopoietic system (Amabile et al., 2013; Suzuki

et al., 2013). Followed the initial study by Doetchman, a few groups reported the successful generation of multilineage repopulating HSCs from mouse ESCs by the use of serum/cytokines (Burt et al., 2004; Palacios et al., 1995). Unfortunately, these results did not lead to the development of a robust HSC generation method. Another approach to obtain engrafting HSCs takes advantage of the genetic manipulation of pluripotent stem cells (PSC) by the overexpression of (transcription) factors (Kitajima et al., 2011; Kyba et al., 2002; Matsumoto et al., 2009; Wang et al., 2005). However, these results have not been translated into a human PSC platform, and the use of genetic manipulation (and possibly oncogenes) hampers the use of these cells in clinical applications. A more recent approach relies on the dogma, introduced by Yamanaka and colleagues (Takahashi and Yamanaka, 2006), that somatic cell fate can be changed by specific transcription factors, known as reprogramming. In these studies, a carefully selected cocktail of hematopoietic transcription factors is expressed in mature cells to convert them phenotypically and functionally into (induced) HSCs (Riddell et al., 2014; Sandler et al., 2014; Vereide et al., 2014). In addition, these studies demonstrate that when knowing the correct factors, a pluripotent state can be bypassed, thus avoiding many of the risks and limitations involved in the PSC differentiation approaches. These studies potentially represent a major advance towards achieving clinically-relevant HSCs, however, so far, no defined cocktail of factors, their essential dosage or temporal expression requirement has been reported that enables robust HSCs derivation. Thus, there is still a long way to go in order to specifically define and describe the path for *in vitro* HSC development. Moreover, most of these studies used integrating vectors, which may lead to insertional mutagenesis, introduces another hurdle that has to be overcome in order to translate this methodology into clinic.

The main goals of this study are to understand the involvement of Gata2 in the stepwise establishment of the adult blood system. We aim to explore how Gata2 functions in the process of the HPC/HSC development *in vivo*, and whether the readout can be applied *in vitro* to better understand the PSC hematopoietic differentiation cultures. We hypothesize that Gata2 has a vital role in the establishment of the *in vivo* HPC/HSC fate and in the generation of blood (progenitor) cells *in vitro*, and thus, Gata2 reporter facilitates the tracing and isolation of hematopoietic (progenitor/stem) cells emerging in the ESC differentiation cultures.

The specific aims of this thesis are:
1.   To explore, compare and contrast Gata2 transcription factor expression during embryonic hematopoietic development in a *Gata2Venus* mouse model and embryonic stem cells.
2.   To investigate the functional potential of Gata2 expressing cells during *in vivo* and *in vitro* hematopoietic development and differentiation.
3.   To examine the role of Gpr56, a Gata2 downstream target signaling molecule in *Gata2Venus* ESCs.

Scope of the thesis

The adult hematopoietic system consists of a hierarchy of cells that progress from a stem cell state to the terminally differentiated cells of over ten functionally distinct blood cell lineages. While hematopoietic stem cells (HSC) are rare, long-lived and self-renewing, there are many intermediate progenitor cell types that lose their multi-lineage and self-renewing potency in a stepwise manner before becoming mature functioning blood cells. The maintenance and homeostasis of the adult hematopoietic system relies on the balanced self-renewal and differentiation of the HSCs. HSC transplantation has been used since the 1950s, and has yielded significant therapeutic success in curing blood cancer and patients with blood-related genetic disease. Nonetheless, several restrictions in using these adult stem cells in transplantation apply, including insufficient availability of compatible donors, shortage of stem cells in samples and inability to expand them *ex vivo*. One way to overcome these limitations is to attempt to generate HSCs *in vitro* by utilizing the recent advance of induced pluripotent stem cell technology and their hematopoietic differentiation. Today, this approach is still challenged by the limited understanding of the signals and factors that drive the stepwise emergence of blood (stem/progenitor) cells *in vivo*, thus subsequently hampering the *in vitro* production of clinically-relevant HSCs for blood cancer therapies.

One of these pivotal components in embryonic generation of HSC is the Gata2 transcription factor, whose role in the differentiation and specification of blood cells is the focus of this thesis.

Chapter 1 is dedicated to introducing the current knowledge about events and factors involved in the stepwise embryonic development of the hematopoietic system and HSCs, and the establishment of the adult hematopoietic cell hierarchy. **Chapter 2** utilizes two embryonic stem cell (ESC) reporter lines (*Gata2Venus* and *Ly6AGFP*) to temporally trace the development and emergence of hematopoietic (progenitor) cells that possess increasingly complex mulitlineage hematopoietic potential. These reporters are well described in the mouse embryogenesis, thus facilitating a comparison between *in vivo* waves of hematopoiesis and *in vitro* ESC differentiation to enrich and isolate functional hematopoietic cells with defined potency. The Gata2 downstream target Gpr56 is potentially a novel positive regulator of HSC/HPC emergence. **Chapter 3** utilizes *Gata2Venus* reporter ESCs to investigate the involvement of Gpr56 hematopoiesis, revealing its redundant requirement for the generation of multipotent hematopoietic progenitors. Besides hematopoietic stem and progenitor cells, Gata2 expression is also specific for mast cells. **Chapter 4** takes advantage of the *Gata2Venus* ESC reporter line to introduce a novel approach in rapidly generating mast cells for inflammation and allergy research. In **Chapter 5,** the *Gata2Venus* mouse model (generated from the *Gata2Venus* ESCs) is described. Venus fluorochrome expression *in vivo* recapitulates the expression of Gata2 and allows for the isolation of live Gata2-expressing cells, revealing that Gata2 marks all functional HSCs, but not all HPCs, thus identifying a Gata2-indepenent progenitor population. Finally, in **Chapter 6,** the main findings of this thesis, their relevance and importance to our understanding of HSC and hematopoietic progenitor generation and differentiation are discussed, together with providing applications and future directions of this work.

References

Amabile, G., Welner, R.S., Nombela-Arrieta, C., D'Alise, A.M., Di Ruscio, A., Ebralidze, A.K., Kraytsberg, Y., Ye, M., Kocher, O., Neuberg, D.S.*, et al.* (2013). In vivo generation of transplantable human hematopoietic cells from induced pluripotent stem cells. Blood *121*, 1255-1264.

Asselin-Labat, M.L., Sutherland, K.D., Barker, H., Thomas, R., Shackleton, M., Forrest, N.C., Hartley, L., Robb, L., Grosveld, F.G., van der Wees, J.*, et al.* (2007). Gata-3 is an essential regulator of mammary-gland morphogenesis and luminal-cell differentiation. Nat Cell Biol *9*, 201-209.

Bertrand, J.Y., Chi, N.C., Santoso, B., Teng, S., Stainier, D.Y., and Traver, D. (2010). Haematopoietic stem cells derive directly from aortic endothelium during development. Nature *464*, 108-111.

Bertrand, J.Y., Jalil, A., Klaine, M., Jung, S., Cumano, A., and Godin, I. (2005). Three pathways to mature macrophages in the early mouse yolk sac. Blood *106*, 3004-3011.

Bertrand, J.Y., Kim, A.D., Teng, S., and Traver, D. (2008). CD41+ cmyb+ precursors colonize the zebrafish pronephros by a novel migration route to initiate adult hematopoiesis. Development *135*, 1853-1862.

Boisset, J.C., Clapes, T., Klaus, A., Papazian, N., Onderwater, J., Mommaas-Kienhuis, M., Cupedo, T., and Robin, C. (2015). Progressive maturation toward hematopoietic stem cells in the mouse embryo aorta. Blood *125*, 465-469.

Boisset, J.C., van Cappellen, W., Andrieu-Soler, C., Galjart, N., Dzierzak, E., and Robin, C. (2010). In vivo imaging of haematopoietic cells emerging from the mouse aortic endothelium. Nature *464*, 116-120.

Bradley, A., Evans, M., Kaufman, M.H., and Robertson, E. (1984). Formation of germ-line chimaeras from embryo-derived teratocarcinoma cell lines. Nature *309*, 255-256.

Bresnick, E.H., Katsumura, K.R., Lee, H.Y., Johnson, K.D., and Perkins, A.S. (2012). Master regulatory GATA transcription factors: mechanistic principles and emerging links to hematologic malignancies. Nucleic Acids Res *40*, 5819-5831.

Bresnick, E.H., Lee, H.Y., Fujiwara, T., Johnson, K.D., and Keles, S. (2010). GATA switches as developmental drivers. J Biol Chem *285*, 31087-31093.

Bryder, D., Rossi, D.J., and Weissman, I.L. (2006). Hematopoietic stem cells: the paradigmatic tissue-specific stem cell. Am J Pathol *169*, 338-346.

Burt, R.K., Verda, L., Kim, D.A., Oyama, Y., Luo, K., and Link, C. (2004). Embryonic stem cells as an alternate marrow donor source: engraftment without graft-versus-host disease. J Exp Med *199*, 895-904.

Cai, Z., de Bruijn, M., Ma, X., Dortland, B., Luteijn, T., Downing, R.J., and Dzierzak, E. (2000). Haploinsufficiency of AML1 affects the temporal and spatial generation of hematopoietic stem cells in the mouse embryo. Immunity *13*, 423-431.

Chacon, D., Beck, D., Perera, D., Wong, J.W., and Pimanda, J.E. (2014). BloodChIP: a database of comparative genome-wide transcription factor binding profiles in human blood cells. Nucleic Acids Res *42*, D172-177.

Charron, F., and Nemer, M. (1999). GATA transcription factors and cardiac development. Semin Cell Dev Biol *10*, 85-91.

Chen, M.J., Li, Y., De Obaldia, M.E., Yang, Q., Yzaguirre, A.D., Yamada-Inagawa, T., Vink, C.S., Bhandoola, A., Dzierzak, E., and Speck, N.A. (2011). Erythroid/myeloid progenitors and hematopoietic stem cells originate from distinct populations of endothelial cells. Cell Stem Cell *9*, 541-552.

Chen, M.J., Yokomizo, T., Zeigler, B.M., Dzierzak, E., and Speck, N.A. (2009). Runx1 is required for the endothelial to haematopoietic cell transition but not thereafter. Nature *457*, 887-891.

Choi, K., Kennedy, M., Kazarov, A., Papadimitriou, J.C., and Keller, G. (1998). A common precursor for hematopoietic and endothelial cells. Development *125*, 725-732.

Crisan, M., Kartalaei, P.S., Vink, C.S., Yamada-Inagawa, T., Bollerot, K., van, I.W., van der Linden, R., de Sousa Lopes, S.M., Monteiro, R., Mummery, C.*, et al.* (2015). BMP signalling differentially regulates distinct haematopoietic stem cell types. Nat Commun *6*, 8040.

de Bruijn, M.F., Speck, N.A., Peeters, M.C., and Dzierzak, E. (2000). Definitive hematopoietic stem cells first develop within the major arterial regions of the mouse embryo. EMBO J *19*, 2465-2474.

de Pater, E., Kaimakis, P., Vink, C.S., Yokomizo, T., Yamada-Inagawa, T., van der Linden, R., Kartalaei, P.S., Camper, S.A., Speck, N., and Dzierzak, E. (2013). Gata2 is required for HSC generation and survival. J Exp Med *210*, 2843-2850.

Doetschman, T.C., Eistetter, H., Katz, M., Schmidt, W., and Kemler, R. (1985). The in vitro development of blastocyst-derived embryonic stem cell lines: formation of visceral yolk sac, blood islands and myocardium. J Embryol Exp Morphol *87*, 27-45.

Dzierzak, E., and Speck, N.A. (2008). Of lineage and legacy: the development of mammalian hematopoietic stem cells. Nat Immunol *9*, 129-136.

Eilken, H.M., Nishikawa, S., and Schroeder, T. (2009). Continuous single-cell imaging of blood generation from haemogenic endothelium. Nature *457*, 896-900.

Ema, H., and Nakauchi, H. (2000). Expansion of hematopoietic stem cells in the developing liver of a mouse embryo. Blood *95*, 2284-2288.

Espin-Palazon, R., Stachura, D.L., Campbell, C.A., Garcia-Moreno, D., Del Cid, N., Kim, A.D., Candel, S., Meseguer, J., Mulero, V., and Traver, D. (2014). Proinflammatory signaling regulates hematopoietic stem cell emergence. Cell *159*, 1070-1085.

Evans, M.J., and Kaufman, M.H. (1981). Establishment in culture of pluripotential cells from mouse embryos. Nature *292*, 154-156.

Frame, J.M., Fegan, K.H., Conway, S.J., McGrath, K.E., and Palis, J. (2016). Definitive Hematopoiesis in the Yolk Sac Emerges from Wnt-Responsive Hemogenic Endothelium Independently of Circulation and Arterial Identity. Stem Cells *34*, 431-444.

Frame, J.M., McGrath, K.E., and Palis, J. (2013). Erythro-myeloid progenitors: "definitive" hematopoiesis in the conceptus prior to the emergence of hematopoietic stem cells. Blood Cells Mol Dis *51*, 220-225.

Gao, X., Johnson, K.D., Chang, Y.I., Boyer, M.E., Dewey, C.N., Zhang, J., and Bresnick, E.H. (2013). Gata2 cis-element is required for hematopoietic stem cell generation in the mammalian embryo. J Exp Med *210*, 2833-2842.

Gekas, C., Dieterlen-Lievre, F., Orkin, S.H., and Mikkola, H.K. (2005). The placenta is a niche for hematopoietic stem cells. Dev Cell *8*, 365-375.

Godin, I., Dieterlen-Lievre, F., and Cumano, A. (1995). Emergence of multipotent hemopoietic cells in the yolk sac and paraaortic splanchnopleura in mouse embryos, beginning at 8.5 days postcoitus. Proc Natl Acad Sci U S A *92*, 773-777.

Gomez Perdiguero, E., Klapproth, K., Schulz, C., Busch, K., Azzoni, E., Crozet, L., Garner, H., Trouillet, C., de Bruijn, M.F., Geissmann, F.*, et al.* (2015). Tissue-resident macrophages originate from yolk-sac-derived erythro-myeloid progenitors. Nature *518*, 547-551.

Gordon-Keylock, S., Sobiesiak, M., Rybtsov, S., Moore, K., and Medvinsky, A. (2013). Mouse extraembryonic arterial vessels harbor precursors capable of maturing into definitive HSCs. Blood *122*, 2338-2345.

Haar, J.L., and Ackerman, G.A. (1971). A phase and electron microscopic study of vasculogenesis and erythropoiesis in the yolk sac of the mouse. Anat Rec *170*, 199-223.

Ho, I.C., Vorhees, P., Marin, N., Oakley, B.K., Tsai, S.F., Orkin, S.H., and Leiden, J.M. (1991). Human GATA-3: a lineage-restricted transcription factor that regulates the expression of the T cell receptor alpha gene. EMBO J *10*, 1187-1192.

Hoeffel, G., Chen, J., Lavin, Y., Low, D., Almeida, F.F., See, P., Beaudin, A.E., Lum, J., Low, I., Forsberg, E.C.*, et al.* (2015). C-Myb(+) erythro-myeloid progenitor-

derived fetal monocytes give rise to adult tissue-resident macrophages. Immunity *42*, 665-678.

Iizuka, K., Yokomizo, T., Watanabe, N., Tanaka, Y., Osato, M., Takaku, T., and Komatsu, N. (2016). Lack of Phenotypical and Morphological Evidences of Endothelial to Hematopoietic Transition in the Murine Embryonic Head during Hematopoietic Stem Cell Emergence. PLoS One *11*, e0156427.

Ikonomi, P., Rivera, C.E., Riordan, M., Washington, G., Schechter, A.N., and Noguchi, C.T. (2000). Overexpression of GATA-2 inhibits erythroid and promotes megakaryocyte differentiation. Exp Hematol *28*, 1423-1431.

Jaffredo, T., Nottingham, W., Liddiard, K., Bollerot, K., Pouget, C., and de Bruijn, M. (2005). From hemangioblast to hematopoietic stem cell: an endothelial connection? Exp Hematol *33*, 1029-1040.

Jing, L., and Zon, L.I. (2011). Zebrafish as a model for normal and malignant hematopoiesis. Dis Model Mech *4*, 433-438.

Kaimakis, P., de Pater, E., Eich, C., Solaimani Kartalaei, P., Kauts, M.L., Vink, C.S., van der Linden, R., Jaegle, M., Yokomizo, T., Meijer, D*., et al.* (2016). Functional and molecular characterization of mouse Gata2-independent hematopoietic progenitors. Blood *127*, 1426-1437.

Karis, A., Pata, I., van Doorninck, J.H., Grosveld, F., de Zeeuw, C.I., de Caprona, D., and Fritzsch, B. (2001). Transcription factor GATA-3 alters pathway selection of olivocochlear neurons and affects morphogenesis of the ear. J Comp Neurol *429*, 615-630.

Keller, G.M. (1995). In vitro differentiation of embryonic stem cells. Curr Opin Cell Biol *7*, 862-869.

Kennedy, M., Firpo, M., Choi, K., Wall, C., Robertson, S., Kabrun, N., and Keller, G. (1997). A common precursor for primitive erythropoiesis and definitive haematopoiesis. Nature *386*, 488-493.

Kierdorf, K., Erny, D., Goldmann, T., Sander, V., Schulz, C., Perdiguero, E.G., Wieghofer, P., Heinrich, A., Riemke, P., Holscher, C*., et al.* (2013). Microglia emerge from erythromyeloid precursors via Pu.1- and Irf8-dependent pathways. Nat Neurosci *16*, 273-280.

Kingsley, P.D., Malik, J., Emerson, R.L., Bushnell, T.P., McGrath, K.E., Bloedorn, L.A., Bulger, M., and Palis, J. (2006). "Maturational" globin switching in primary primitive erythroid cells. Blood *107*, 1665-1672.

Kingsley, P.D., Malik, J., Fantauzzo, K.A., and Palis, J. (2004). Yolk sac-derived primitive erythroblasts enucleate during mammalian embryogenesis. Blood *104*, 19-25.

Kissa, K., and Herbomel, P. (2010). Blood stem cells emerge from aortic endothelium by a novel type of cell transition. Nature *464*, 112-115.

Kitajima, K., Minehata, K., Sakimura, K., Nakano, T., and Hara, T. (2011). In vitro generation of HSC-like cells from murine ESCs/iPSCs by enforced expression of LIM-homeobox transcription factor Lhx2. Blood *117*, 3748-3758.

Kitajima, K., Zheng, J., Yen, H., Sugiyama, D., and Nakano, T. (2006). Multipotential differentiation ability of GATA-1-null erythroid-committed cells. Genes Dev *20*, 654-659.

Ko, L.J., and Engel, J.D. (1993). DNA-binding specificities of the GATA transcription factor family. Mol Cell Biol *13*, 4011-4022.

Kouskoff, V., Lacaud, G., Schwantz, S., Fehling, H.J., and Keller, G. (2005). Sequential development of hematopoietic and cardiac mesoderm during embryonic stem cell differentiation. Proc Natl Acad Sci U S A *102*, 13170-13175.

Kumaravelu, P., Hook, L., Morrison, A.M., Ure, J., Zhao, S., Zuyev, S., Ansell, J., and Medvinsky, A. (2002). Quantitative developmental anatomy of definitive haematopoietic stem cells/long-term repopulating units (HSC/RUs): role of the aorta-gonad-mesonephros (AGM) region and the yolk sac in colonisation of the mouse embryonic liver. Development *129*, 4891-4899.

Kyba, M., Perlingeiro, R.C., and Daley, G.Q. (2002). HoxB4 confers definitive lymphoid-myeloid engraftment potential on embryonic stem cell and yolk sac hematopoietic progenitors. Cell *109*, 29-37.

Lancrin, C., Sroczynska, P., Stephenson, C., Allen, T., Kouskoff, V., and Lacaud, G. (2009). The haemangioblast generates haematopoietic cells through a haemogenic endothelium stage. Nature *457*, 892-895.

Labastie, M.C., Catala, M., Gregoire, J.M., and Peault, B. (1995). The GATA-3 gene is expressed during human kidney embryogenesis. Kidney Int *47*, 1597-1603.

Li, Z., Lan, Y., He, W., Chen, D., Wang, J., Zhou, F., Wang, Y., Sun, H., Chen, X., Xu, C.*, et al.* (2012). Mouse embryonic head as a site for hematopoietic stem cell development. Cell stem cell *11*, 663-675.

Li, Z., Vink, C.S., Mariani, S.A., and Dzierzak, E. (2016). Subregional localization and characterization of Ly6aGFP-expressing hematopoietic cells in the mouse embryonic head. Dev Biol.

Li, Y., Esain, V., Teng, L., Xu, J., Kwan, W., Frost, I.M., Yzaguirre, A.D., Cai, X., Cortes, M., Maijenburg, M.W.*, et al.* (2014). Inflammatory signaling regulates embryonic hematopoietic stem and progenitor cell production. Genes Dev *28*, 2597-2612.

Liakhovitskaia, A., Rybtsov, S., Smith, T., Batsivari, A., Rybtsova, N., Rode, C., de Bruijn, M., Buchholz, F., Gordon-Keylock, S., Zhao, S.*, et al.* (2014). Runx1 is required for progression of CD41+ embryonic precursors into HSCs but not prior to this. Development *141*, 3319-3323.

Ling, K.W., Ottersbach, K., van Hamburg, J.P., Oziemlak, A., Tsai, F.Y., Orkin, S.H., Ploemacher, R., Hendriks, R.W., and Dzierzak, E. (2004). GATA-2 plays two functionally distinct roles during the ontogeny of hematopoietic stem cells. J Exp Med *200*, 871-882.

Lugus, J.J., Chung, Y.S., Mills, J.C., Kim, S.I., Grass, J., Kyba, M., Doherty, J.M., Bresnick, E.H., and Choi, K. (2007). GATA2 functions at multiple steps in hemangioblast development and differentiation. Development *134*, 393-405.

Lux, C.T., Yoshimoto, M., McGrath, K., Conway, S.J., Palis, J., and Yoder, M.C. (2008). All primitive and definitive hematopoietic progenitor cells emerging before E10 in the mouse embryo are products of the yolk sac. Blood *111*, 3435-3438.

Ma, X., de Bruijn, M., Robin, C., Peeters, M., Kong, A.S.J., de Wit, T., Snoijs, C., and Dzierzak, E. (2002). Expression of the Ly-6A (Sca-1) lacZ transgene in mouse haematopoietic stem cells and embryos. Br J Haematol *116*, 401-408.

Matsumoto, K., Isagawa, T., Nishimura, T., Ogaeri, T., Eto, K., Miyazaki, S., Miyazaki, J., Aburatani, H., Nakauchi, H., and Ema, H. (2009). Stepwise development of hematopoietic stem cells from embryonic stem cells. PLoS One *4*, e4820.

McGrath, K.E., Frame, J.M., Fegan, K.H., Bowen, J.R., Conway, S.J., Catherman, S.C., Kingsley, P.D., Koniski, A.D., and Palis, J. (2015). Distinct Sources of Hematopoietic Progenitors Emerge before HSCs and Provide Functional Blood Cells in the Mammalian Embryo. Cell reports *11*, 1892-1904.

McGrath, K.E., Koniski, A.D., Malik, J., and Palis, J. (2003). Circulation is established in a stepwise pattern in the mammalian embryo. Blood *101*, 1669-1676.

Medvinsky, A., and Dzierzak, E. (1996). Definitive hematopoiesis is autonomously initiated by the AGM region. Cell *86*, 897-906.

Meier, N., Krpic, S., Rodriguez, P., Strouboulis, J., Monti, M., Krijgsveld, J., Gering, M., Patient, R., Hostert, A., and Grosveld, F. (2006). Novel binding partners of Ldb1 are required for haematopoietic development. Development *133*, 4913-4923.

Mendelson, A., and Frenette, P.S. (2014). Hematopoietic stem cell niche maintenance during homeostasis and regeneration. Nat Med *20*, 833-846.

Minegishi, N., Suzuki, N., Yokomizo, T., Pan, X., Fujimoto, T., Takahashi, S., Hara, T., Miyajima, A., Nishikawa, S., and Yamamoto, M. (2003). Expression and domain-specific function of GATA-2 during differentiation of the hematopoietic precursor cells in midgestation mouse embryos. Blood *102*, 896-905.

Molkentin, J.D., Antos, C., Mercer, B., Taigen, T., Miano, J.M., and Olson, E.N. (2000). Direct activation of a GATA6 cardiac enhancer by Nkx2.5: evidence for a reinforcing regulatory network of Nkx2.5 and GATA transcription factors in the developing heart. Dev Biol *217*, 301-309.

Mukouyama, Y., Chiba, N., Hara, T., Okada, H., Ito, Y., Kanamaru, R., Miyajima, A., Satake, M., and Watanabe, T. (2000). The AML1 transcription factor functions to

develop and maintain hematogenic precursor cells in the embryonic aorta-gonad-mesonephros region. Dev Biol *220*, 27-36.

Muller, A.M., Medvinsky, A., Strouboulis, J., Grosveld, F., and Dzierzak, E. (1994). Development of hematopoietic stem cell activity in the mouse embryo. Immunity *1*, 291-301.

Mylona, A., Andrieu-Soler, C., Thongjuea, S., Martella, A., Soler, E., Jorna, R., Hou, J., Kockx, C., van Ijcken, W., Lenhard, B.*, et al.* (2013). Genome-wide analysis shows that Ldb1 controls essential hematopoietic genes/pathways in mouse early development and reveals novel players in hematopoiesis. Blood *121*, 2902-2913.

Naito, M., Takahashi, K., and Nishikawa, S. (1990). Development, differentiation, and maturation of macrophages in the fetal mouse liver. J Leukoc Biol *48*, 27-37.

Naito, M., Umeda, S., Yamamoto, T., Moriyama, H., Umezu, H., Hasegawa, G., Usuda, H., Shultz, L.D., and Takahashi, K. (1996). Development, differentiation, and phenotypic heterogeneity of murine tissue macrophages. J Leukoc Biol *59*, 133-138.

Nandakumar, S.K., Johnson, K., Throm, S.L., Pestina, T.I., Neale, G., and Persons, D.A. (2015). Low-level GATA2 overexpression promotes myeloid progenitor self-renewal and blocks lymphoid differentiation in mice. Exp Hematol *43*, 565-577 e561-510.

Nardelli, J., Thiesson, D., Fujiwara, Y., Tsai, F.Y., and Orkin, S.H. (1999). Expression and genetic interaction of transcription factors GATA-2 and GATA-3 during development of the mouse central nervous system. Dev Biol *210*, 305-321.

North, T., Gu, T.L., Stacy, T., Wang, Q., Howard, L., Binder, M., Marin-Padilla, M., and Speck, N.A. (1999). Cbfa2 is required for the formation of intra-aortic hematopoietic clusters. Development *126*, 2563-2575.

Nottingham, W.T., Jarratt, A., Burgess, M., Speck, C.L., Cheng, J.F., Prabhakar, S., Rubin, E.M., Li, P.S., Sloane-Stanley, J., Kong, A.S.J.*, et al.* (2007). Runx1-mediated hematopoietic stem-cell emergence is controlled by a Gata/Ets/TAL1-regulated enhancer. Blood *110*, 4188-4197.

Okuda, T., van Deursen, J., Hiebert, S.W., Grosveld, G., and Downing, J.R. (1996). AML1, the target of multiple chromosomal translocations in human leukemia, is essential for normal fetal liver hematopoiesis. Cell *84*, 321-330.

Ottersbach, K., and Dzierzak, E. (2005). The murine placenta contains hematopoietic stem cells within the vascular labyrinth region. Dev Cell *8*, 377-387.

Palacios, R., Golunski, E., and Samaridis, J. (1995). In vitro generation of hematopoietic stem cells from an embryonic stem cell line. Proc Natl Acad Sci U S A *92*, 7530-7534.

Palis, J., Chan, R.J., Koniski, A., Patel, R., Starr, M., and Yoder, M.C. (2001). Spatial and temporal emergence of high proliferative potential hematopoietic precursors during murine embryogenesis. Proc Natl Acad Sci U S A *98*, 4528-4533.

Palis, J., Robertson, S., Kennedy, M., Wall, C., and Keller, G. (1999). Development of erythroid and myeloid progenitors in the yolk sac and embryo proper of the mouse. Development *126*, 5073-5084.

Pereira, C.F., Chang, B., Gomes, A., Bernitz, J., Papatsenko, D., Niu, X., Swiers, G., Azzoni, E., de Bruijn, M.F., Schaniel, C.*, et al.* (2016). Hematopoietic Reprogramming In Vitro Informs In Vivo Identification of Hemogenic Precursors to Definitive Hematopoietic Stem Cells. Dev Cell *36*, 525-539.

Pimanda, J.E., Ottersbach, K., Knezevic, K., Kinston, S., Chan, W.Y., Wilson, N.K., Landry, J.R., Wood, A.D., Kolb-Kokocinski, A., Green, A.R.*, et al.* (2007). Gata2, Fli1, and Tal1 form a recursively wired gene-regulatory circuit during early hematopoietic development. Proc Natl Acad Sci U S A *104*, 17692-17697.

Rafii, S., Kloss, C.C., Butler, J.M., Ginsberg, M., Gars, E., Lis, R., Zhan, Q., Josipovic, P., Ding, B.S., Xiang, J.*, et al.* (2013). Human ESC-derived hemogenic endothelial cells undergo distinct waves of endothelial to hematopoietic transition. Blood *121*, 770-780.

Rhodes, K.E., Gekas, C., Wang, Y., Lux, C.T., Francis, C.S., Chan, D.N., Conway, S., Orkin, S.H., Yoder, M.C., and Mikkola, H.K. (2008). The emergence of

hematopoietic stem cells is initiated in the placental vasculature in the absence of circulation. Cell Stem Cell *2*, 252-263.

Riddell, J., Gazit, R., Garrison, B.S., Guo, G., Saadatpour, A., Mandal, P.K., Ebina, W., Volchkov, P., Yuan, G.C., Orkin, S.H.*, et al.* (2014). Reprogramming committed murine blood cells to induced hematopoietic stem cells with defined factors. Cell *157*, 549-564.

Robert-Moreno, A., Espinosa, L., de la Pompa, J.L., and Bigas, A. (2005). RBPjkappa-dependent Notch function regulates Gata2 and is essential for the formation of intra-embryonic hematopoietic cells. Development *132*, 1117-1126.

Robin, C., Ottersbach, K., Durand, C., Peeters, M., Vanes, L., Tybulewicz, V., and Dzierzak, E. (2006). An unexpected role for IL-3 in the embryonic development of hematopoietic stem cells. Dev Cell *11*, 171-180.

Rodrigues, N.P., Janzen, V., Forkert, R., Dombkowski, D.M., Boyd, A.S., Orkin, S.H., Enver, T., Vyas, P., and Scadden, D.T. (2005). Haploinsufficiency of GATA-2 perturbs adult hematopoietic stem-cell homeostasis. Blood *106*, 477-484.

Rybtsov, S., Batsivari, A., Bilotkach, K., Paruzina, D., Senserrich, J., Nerushev, O., and Medvinsky, A. (2014). Tracing the origin of the HSC hierarchy reveals an SCF-dependent, IL-3-independent CD43(-) embryonic precursor. Stem Cell Reports *3*, 489-501.

Rybtsov, S., Ivanovs, A., Zhao, S., and Medvinsky, A. (2016). Concealed expansion of immature precursors underpins acute burst of adult HSC activity in foetal liver. Development *143*, 1284-1289.

Rybtsov, S., Sobiesiak, M., Taoudi, S., Souilhol, C., Senserrich, J., Liakhovitskaia, A., Ivanovs, A., Frampton, J., Zhao, S., and Medvinsky, A. (2011). Hierarchical organization and early hematopoietic specification of the developing HSC lineage in the AGM region. J Exp Med *208*, 1305-1315.

Saito, Y., Kaneda, K., Suekane, A., Ichihara, E., Nakahata, S., Yamakawa, N., Nagai, K., Mizuno, N., Kogawa, K., Miura, I.*, et al.* (2013). Maintenance of the hematopoietic stem cell pool in bone marrow niches by EVI1-regulated GPR56. Leukemia *27*, 1637-1649.

Sandler, V.M., Lis, R., Liu, Y., Kedem, A., James, D., Elemento, O., Butler, J.M., Scandura, J.M., and Rafii, S. (2014). Reprogramming human endothelial cells to haematopoietic cells requires vascular induction. Nature *511*, 312-318.

Schulz, C., Gomez Perdiguero, E., Chorro, L., Szabo-Rogers, H., Cagnard, N., Kierdorf, K., Prinz, M., Wu, B., Jacobsen, S.E., Pollard, J.W.*, et al.* (2012). A lineage of myeloid cells independent of Myb and hematopoietic stem cells. Science *336*, 86-90.

Shalaby, F., Rossant, J., Yamaguchi, T.P., Gertsenstein, M., Wu, X.F., Breitman, M.L., and Schuh, A.C. (1995). Failure of blood-island formation and vasculogenesis in Flk-1-deficient mice. Nature *376*, 62-66.

Smith, A.G. (2001). Embryo-derived stem cells: of mice and men. Annu Rev Cell Dev Biol *17*, 435-462.

Solaimani Kartalaei, P., Yamada-Inagawa, T., Vink, C.S., de Pater, E., van der Linden, R., Marks-Bluth, J., van der Sloot, A., van den Hout, M., Yokomizo, T., van Schaick-Solerno, M.L.*, et al.* (2015). Whole-transcriptome analysis of endothelial to hematopoietic stem cell transition reveals a requirement for Gpr56 in HSC generation. J Exp Med *212*, 93-106.

Sonoda, T., Hayashi, C., and Kitamura, Y. (1983). Presence of mast cell precursors in the yolk sac of mice. Dev Biol *97*, 89-94.

Spinner, M.A., Sanchez, L.A., Hsu, A.P., Shaw, P.A., Zerbe, C.S., Calvo, K.R., Arthur, D.C., Gu, W., Gould, C.M., Brewer, C.C.*, et al.* (2014). GATA2 deficiency: a protean disorder of hematopoiesis, lymphatics, and immunity. Blood *123*, 809-821.

Suzuki, N., Yamazaki, S., Yamaguchi, T., Okabe, M., Masaki, H., Takaki, S., Otsu, M., and Nakauchi, H. (2013). Generation of engraftable hematopoietic stem cells from induced pluripotent stem cells by way of teratoma formation. Mol Ther *21*, 1424-1431.

Swiers, G., Baumann, C., O'Rourke, J., Giannoulatou, E., Taylor, S., Joshi, A., Moignard, V., Pina, C., Bee, T., Kokkaliaris, K.D.*, et al.* (2013). Early dynamic fate

changes in haemogenic endothelium characterized at the single-cell level. Nat Commun *4*, 2924.

Zovein, A.C., Hofmann, J.J., Lynch, M., French, W.J., Turlo, K.A., Yang, Y., Becker, M.S., Zanetta, L., Dejana, E., Gasson, J.C.*, et al.* (2008). Fate tracing reveals the endothelial origin of hematopoietic stem cells. Cell Stem Cell *3*, 625-636.

Takahashi, K., Yamamura, F., and Naito, M. (1989). Differentiation, maturation, and proliferation of macrophages in the mouse yolk sac: a light-microscopic, enzyme-cytochemical, immunohistochemical, and ultrastructural study. J Leukoc Biol *45*, 87-96.

Takahashi, K., and Yamanaka, S. (2006). Induction of pluripotent stem cells from mouse embryonic and adult fibroblast cultures by defined factors. Cell *126*, 663-676.

Tamplin, O.J., Durand, E.M., Carr, L.A., Childs, S.J., Hagedorn, E.J., Li, P., Yzaguirre, A.D., Speck, N.A., and Zon, L.I. (2015). Hematopoietic stem cell arrival triggers dynamic remodeling of the perivascular niche. Cell *160*, 241-252.

Tober, J., Koniski, A., McGrath, K.E., Vemishetti, R., Emerson, R., de Mesy-Bentley, K.K., Waugh, R., and Palis, J. (2007). The megakaryocyte lineage originates from hemangioblast precursors and is an integral component both of primitive and of definitive hematopoiesis. Blood *109*, 1433-1441.

Tober, J., Yzaguirre, A.D., Piwarzyk, E., and Speck, N.A. (2013). Distinct temporal requirements for Runx1 in hematopoietic progenitors and stem cells. Development *140*, 3765-3776.

Travnickova, J., Tran Chau, V., Julien, E., Mateos-Langerak, J., Gonzalez, C., Lelievre, E., Lutfalla, G., Tavian, M., and Kissa, K. (2015). Primitive macrophages control HSPC mobilization and definitive haematopoiesis. Nat Commun *6*, 6227.

Tsai, F.Y., Keller, G., Kuo, F.C., Weiss, M., Chen, J., Rosenblatt, M., Alt, F.W., and Orkin, S.H. (1994). An early haematopoietic defect in mice lacking the transcription factor GATA-2. Nature *371*, 221-226.

Ueno, H., and Weissman, I.L. (2006). Clonal analysis of mouse development reveals a polyclonal origin for yolk sac blood islands. Dev Cell *11*, 519-533.

Vereide, D.T., Vickerman, V., Swanson, S.A., Chu, L.F., McIntosh, B.E., and Thomson, J.A. (2014). An expandable, inducible hemangioblast state regulated by fibroblast growth factor. Stem Cell Reports *3*, 1043-1057.

Wang, Q., Stacy, T., Miller, J.D., Lewis, A.F., Gu, T.L., Huang, X., Bushweller, J.H., Bories, J.C., Alt, F.W., Ryan, G.*, et al.* (1996). The CBFbeta subunit is essential for CBFalpha2 (AML1) function in vivo. Cell *87*, 697-708.

Wang, Y., Yates, F., Naveiras, O., Ernst, P., and Daley, G.Q. (2005). Embryonic stem cell-derived hematopoietic stem cells. Proc Natl Acad Sci U S A *102*, 19081-19086.

Wilson, N.K., Foster, S.D., Wang, X., Knezevic, K., Schutte, J., Kaimakis, P., Chilarska, P.M., Kinston, S., Ouwehand, W.H., Dzierzak, E.*, et al.* (2010). Combinatorial transcriptional control in blood stem/progenitor cells: genome-wide analysis of ten major transcriptional regulators. Cell Stem Cell *7*, 532-544.

Yamaguchi, T.P., Dumont, D.J., Conlon, R.A., Breitman, M.L., and Rossant, J. (1993). flk-1, an flt-related receptor tyrosine kinase is an early marker for endothelial cell precursors. Development *118*, 489-498.

Yamamoto, R., Morita, Y., Ooehara, J., Hamanaka, S., Onodera, M., Rudolph, K.L., Ema, H., and Nakauchi, H. (2013). Clonal analysis unveils self-renewing lineage-restricted progenitors generated directly from hematopoietic stem cells. Cell *154*, 1112-1126.

Yokomizo, T., and Dzierzak, E. (2010). Three-dimensional cartography of hematopoietic clusters in the vasculature of whole mouse embryos. Development *137*, 3651-3661.

Yokota, T., Huang, J., Tavian, M., Nagai, Y., Hirose, J., Zuniga-Pflucker, J.C., Peault, B., and Kincade, P.W. (2006). Tracing the first waves of lymphopoiesis in mice. Development *133*, 2041-2051.

Yoshimoto, M., Porayette, P., Glosson, N.L., Conway, S.J., Carlesso, N., Cardoso, A.A., Kaplan, M.H., and Yoder, M.C. (2012). Autonomous murine T-cell progenitor production in the extra-embryonic yolk sac before HSC emergence. Blood *119*, 5706-5714.

CHAPTER 2

Differentiation of *Gata2Venus* and *Ly6aGFP* reporter embryonic stem cells corresponds to *in vivo* waves of hematopoietic cell generation in the mouse embryo

Mari-Liis Kauts[1,2], Polynikis Kaimakis[1], Sandra C. Mendes[1], Carmen Rodríguez Seoane[2], Xabier Cortés-Lavaud[2], Undine Hill[1] and Elaine Dzierzak[1,2] *

*Corresponding author

[1] Erasmus Medical Center Stem Cell Institute, Department of Cell Biology, Erasmus Medical Center, Rotterdam, The Netherlands
[2] Centre for Inflammation Research, Queens Medical Research Institute, University of Edinburgh, Edinburgh, United Kingdom

Abstract

In vivo hematopoietic generation occurs in distinct waves of primitive and definitive progenitor, and hematopoietic stem cell (HSC) emergence. The differentiation of pluripotent stem cells (PSC) potentially offers a source for hematopoietic cell therapies, but, despite many approaches, it is still not possible to robustly generate hematopoietic cells *in vitro.* This is partly due to the inability to trace/enrich hematopoietic emergence by precise temporal programs. We use novel *Gata2Venus* (*G2V*) and *Ly6aGFP (LG)* PSC reporters derived from mice, where they mark emerging hematopoietic progenitor/stem cells. We show that *in vitro* hematopoietic differentiation occurs in distinct waves of primitive and definitive potential traced by the *G2V* reporter. These stages are followed by *LG* expression discriminating a third wave of hematopoietic emergence. These results, facilitated by tracing/enrichment of cells with progressive hematopoietic properties, demonstrate that *in vitro* PSC differentiation is analogous to the waves of hematopoietic cell generation found in the mouse embryo.

Introduction

Since the first report of blood cell production from embryonic stem cells (ESC) more than 30 years ago (Doetschman et al., 1985), it has been a long term goal to use such cultures of pluripotent stem cells (PSC) to produce mature hematopoietic cells, definitive hematopoietic progenitor cells (HPC), and hematopoietic stem cells (HSC). With the advent of patient-specific induced pluripotent stem cells (iPSC), this approach could potentially be used in cell replacement therapies for treating blood disorders without the adverse effects of rejection. Whereas some progress towards differentiation into distinct blood lineages has been made through addition of growth factors to ESC/iPSC differentiation cultures (Doulatov et al., 2013; Kennedy et al., 2012; Pearson et al., 2015; Vodyanik et al., 2005), and some limited *in vivo* repopulation has been achieved by overexpression of transcription factors (Kyba et al., 2002), the *ex vivo* approaches have provided little insight into whether these cultures recapitulate the *in vivo* hematopoietic development.

The natural development of the hematopoietic system begins in the conceptus just after the emergence of mesodermal cells from the primitive streak. It occurs in spatiotemporally distinct waves (reviewed in (Dzierzak and Speck, 2008; Kauts et al., 2016)). The first wave of hematopoietic cell generation occurs in the yolk sac (YS) blood islands at mouse embryonic day 7 (E7), producing a transient cell population consisting mainly of primitive erythrocytes (Palis et al., 1999). Definitive erythrocytes and myeloid cells appear in the YS starting at E8.25 and originate from erythroid-myeloid progenitors (EMP) (Bertrand et al., 2007; Frame et al., 2013). Shortly thereafter, progenitors with erythroid-myeloid-lymphoid potential arise (Godin et al., 1995). The production of HSCs is initiated in the final wave starting at E10.5 in the aorta-gonads-mesonephros region (AGM) (Medvinsky and Dzierzak, 1996; Muller et al., 1994) and is tightly controlled by a combination of extrinsic and intrinsic factors.

The *Gata2* transcription factor plays a pivotal intrinsic role in EMP, HPC and HSC generation in the embryo (de Pater et al., 2013; Gao et al., 2013). *Gata2*$^{-/-}$ mouse and human ESCs show defective hematopoietic differentiation (Huang et al., 2015; Tsai et al., 1994). In our *Gata2Venus* (*G2V*) reporter mice, in which levels of Gata2 expression are normal, it was found that Gata2 expression marks all HSCs and the majority of HPCs (Kaimakis et al., 2016). Gata2 expression is found in endothelial cells of the E8.5 YS and dorsal aorta. It continues to be expressed in the E10.5 YS hematopoietic cells and in the aorta where it is detected in cKit$^+$CD31$^+$ hematopoietic cluster cells (Kaimakis et al., 2016). A recent study reports that the majority of human ESC-derived HPCs are also marked by GATA2 expression (Huang et al., 2016). Thus, fluorescent reporter expression driven from pivotal hematopoietic regulators have facilitated the examination of HPC/HSC as they emerge in the mouse embryo. Another fluorescent reporter that marks hemogenic endothelial cells and some hematopoietic cluster cells in the embryo is *Ly6a(Sca1)GFP* (*LG*). The expression of this transgene marks all HSCs and the HSC/HPC-generating hemogenic endothelium (Chen et al., 2011; de Bruijn et al., 2002; Solaimani Kartalaei et al., 2015) and allowed the observation of endothelial-to-hematopoietic-transition of these cells in the E10.5 mouse aorta (Boisset et al., 2010). However, unlike *G2V*, *LG* expression is initiated in the AGM only beginning of late E9 (Mascarenhas et al., 2009), and thus, it distinguishes the induction of the intraembryonic definitive HPC/HSC program.

Taking into account the highly complicated spatiotemporal organization of *in vivo* blood development, it is likely that the ability to generate definitive HPC/HSC *in vitro* in a robust manner will depend on a better understanding of the precise temporal molecular and cellular programs occurring in the ESC differentiation cultures, and rely on enrichment methodologies with pivotal reporters to identify and isolate the cell populations of interest. Such reporters can provide a powerful tool to study the dynamics of functional HPC/HSC generation in *in vitro* PSC differentiation cultures and their relationship to normal developmental HPC/HSC generation.

Here we examine the temporal expression of the novel *G2V* and *LG* reporters in a stepwise system of induction, enrichment, and differentiation of ESCs to examine the emergence and progress of functional hematopoietic activity. We show that the temporal wave-like expression of the *G2V* reporter during ESC differentiation corresponds to waves of primitive and definitive hematopoietic emergence. *Gata2* is co-expressed in these cells with all hematopoietic heptad transcription factors and marks all functional HPCs emerging in the sequential primitive and EMP-definitive waves. *LG* expression is specific to HPCs that emerge/persist in later differentiation stages, exclusively marking multipotent definitive progenitors. Thus, our models demonstrate that ESC hematopoietic differentiation occurs in a spatiotemporal wave-like manner that is highly analogous to the three *in vivo* waves of hematopoietic cell generation in the mouse embryo.

Experimental procedures

ESC differentiation. ESC differentiation was performed as described in Keller et al., (2002). ESCs were harvested by trypsinization and MEF depleted by incubating in IMDM + 15% FSC (HyClone) + 1 % P/S (Gibco) for 30 minutes. EB formation was induced by culturing 25 000 cells/ml on a shaker at 40 rpm. On day 3, the EB medium containing IMDM +15% FBS (HyClone), +1% P/S, 2mM GlutaMAX (Gibco), 50 µg/ml ascorbic acid (Sigma), 4×10^{-4} M monothgioglycerol (Sigma), 300 µg/ml transferrin (Roche) was supplemented with 5% proteome free hybridoma medium (Gibco). From day 6 onwards, 100 ng/ml SCF, 1 ng/ml IL-3 and 5 ng/ml IL-11 were added. For hemangioblast analysis, 5 ng/ml BMP4 was added on day 0-3 (all PeproTech).

FACS analysis/sorting. EBs were washed 1x with PBS and incubated in TrypLE Express (Gibco) at 37°C for 3-5 minutes. Enzyme was deactivated by adding PBS + 10% FBS + 1% P/S and a homogenous single-cell suspension was obtained by re-suspending with a P1000 pipette. G2V expression could be detected readily in the cells. Antibody staining was performed on ice for 30 minutes at a concentration of 10^6 cells/100 µl. Antibodies are listed in Supplementary Table 1. Dead cells were excluded with Hoechts33342 (Invitrogen). Cells were analyzed on FACS Scan, Fortessa (5LSR, 6LSR) or sorted on FACS Aria III SORP or Fusion (BD). Data analysis was performed with FlowJo software (Tree star).

Hematopoietic progenitor assay. For the generation of blast colonies (BL-CFC assay), day 3 EB derived cells were plated in methylcellulose (Stem Cell Technologies) supplemented with 10% FCS, vascular endothelial growth factor (VEGF, 5 ng/mL) and IL6 (10n g/mL) (both PeproTech). After 4 days in culture, blast cell colonies were

analyzed under the microscope and counted. For the differentiation of hematopoietic precursors, day 6-14 EB derived cells were plated in methylcellulose medium. After 12-14 days in culture, colonies were scored under Zeiss Axiovert25 microscope.

Matrigel assay. On day 4, EBs were sorted into four populations based on Flk1/Venus expression using gating strategy shown in Fig 1B. 2×10^4 cells from each population were pre-cultured in gelatin-coated 96-well plate in DMEM + 20% FBS + 1% P/S for 20 hours. Matrigel-coated wells were prepared using the thin gel method. Briefly: 60 µl matrigel (Qiagen) was plated onto 96-well plate wells and let to polymerize for 30 minutes at 37ºC. Cells were trypsinized, transferred onto matrigel-coated wells, and cultured in EGM-2 medium (Lonza) for 4 hours. Tubule formation was quantified using Angiogenesis Analyzer (Gilles Carpentier ImageJ News 2012) plugin for Fiji.

RNA isolation, cDNA preparation, real-time RT-qPCR. Up to 10^6 cells were lyzed in TRI-Reagent (MRC) and total RNA was isolated according to the manufacturer's protocol. 1 µg of total RNA was subjected to DNase (Invitrogen) treatment. RNA from sorted cell populations was isolated using RNeasy micro kit (Qiagen). cDNA was synthesized using oligo-dT (Invitrogen) and SuperScript III (Life Technologies) according to manufacturer's protocol. qRT-PCR was performed using Fast Sybr Green master mix (Life Technologies) according to manufacturer's instructions. Primers are listed in Supplementary Table 2.

Whole mount staining. Whole mount staining of EBs was performed as described in (Yokomizo et al., 2012). Brief description in Suppl. materials.

Statistical Analysis. Statistical analysis was performed using an unpaired Student's t test, or one-way ANOVA with Bonferroni correction for multiple comparisons. Results were considered to be statistically significant at p value < 0.05 (*p<0.05, **p <0.01, ***p<0.001). All data shown as mean ± SEM. The number of biological replicates is indicated by the n value. Data analysis was done using GraphPad Prism (GraphPad Software).

Results

Hematopoietic and endothelial potential of *Gata2* expressing cells

Hematopoiesis in the mouse embryo and in ESC differentiation cultures is initiated by hemangioblast cells, which are identified by Flk1 expression and their bi-potential capacity to generate endothelial and hematopoietic progenitors (Choi et al., 1998; Huber et al., 2004). In human ESC differentiation cultures, hemangioblasts develop in response to BMP4 stimulation between 72 and 96 hours and represent a transient population that precedes the onset of the primitive hematopoietic program (Kennedy et al., 2007). To directly examine the relationship of *Gata2* expression to hematopoietic differentiation of ESCs, we used a novel *G2V* reporter ESC line (Kaimakis et al., 2016) that facilitates tracing and isolation of live *Gata2* expressing cells by Venus fluorescence expression (Suppl Fig 1), while preserving normal *Gata2* endogenous protein levels. This is important since decreased *Gata2* levels severely affect the production and expansion of HSCs and HPCs in the embryo, and affect HSC robustness in the adult (Ling et al., 2004; Rodrigues et al., 2005). To examine whether Gata2 expressing cells might possess

hemangioblast characteristics, *G2V* ESC differentiation was induced in the presence of BMP4 (Fig 1A) and cells analyzed at days 3-6. Four cell populations, Flk1$^+$V$^-$, Flk1$^-$V$^+$, Flk1$^+$V$^+$ and Flk1$^-$V$^-$, were sorted by flow cytometry (FACS) and evaluated by colony forming unit-cell (CFU-C) and matrigel assays to test the hematopoietic and endothelial potential.

At day 3 and 4, the majority of Venus expressing (V$^+$) cells co-expressed Flk1 (67% and 76%, respectively) (Fig 1B). From day 5 onwards, the V$^+$ single positive population became more prominent and Flk1$^+$ cell frequency decreased (Fig 1B and 1C). Hematopoietic potential was tested at day 3-6 of differentiation (Fig 1D) and CFU-C were found only in cells expressing Venus. CFU-C were detected from day 4 onward and the main colony type observed was EryP (primitive erythroid). Although the majority of colonies were scored in the Flk1$^-$V$^+$ population (24±13; 16±11; 23±10 EryP/10^4 cells at day 4; 5; 6, respectively), EryP were also detected in the Flk1$^+$V$^+$ cells at day 4, indicating that the earliest hematopoietic potential emerges from Gata2 expressing cells.

To test the endothelial potential of the sorted cells at day 4 of ESC differentiation (the time point with the highest EryP potential in the Flk1$^+$V$^+$ population), cells were plated in matrigel and tubule formation was quantified (Fig 1E and 1F). As expected, the highest endothelial potential was found in the Flk1$^+$V$^-$ population (100 tubules/2x10^4 cells). The Flk1$^+$V$^+$ fraction also showed endothelial potential (30 tubules/2x10^4 cells), demonstrating that in addition to the hematopoietic potential, this subset is capable of endothelial differentiation. Together these data suggest a transient Gata2 expressing Flk1$^+$ population emerging at day 4 and rapidly decreasing thereafter, that gives rise to the earliest primitive blood cells and harbors endothelial potential. Thus, it suggests that Gata2$^+$ cells arising during the early stage of differentiation may contain cells with hemangioblast characteristics.
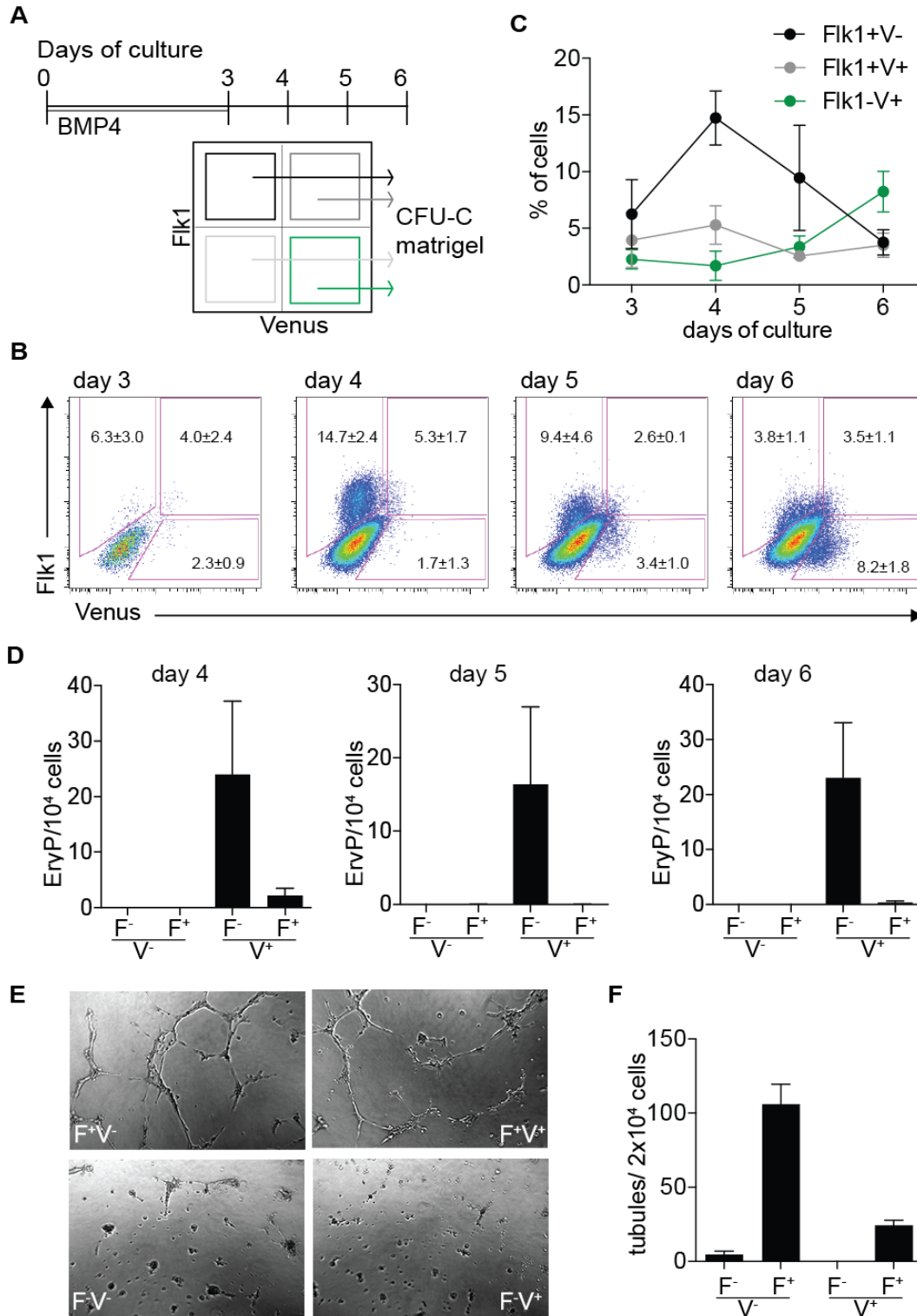
Figure 1. *Gata2Venus* **expressing cells emerging in early differentiation culture possess primitive erythroid and endothelial potential. A)** Scheme of embryonic stem cell (ESC) culture differentiation. ESCs were cultured in the presence of BMP4 from day 0 to 3. Embryoid bodies (EB) were dissociated, cells were FACS analyzed/sorted and tested in CFU-C (colony forming unit-cell) and matrigel assay at indicated time points. **B)** Dot plots with the gating strategy of flow cytometric analysis and sorting of ESCs for Flk1 and Gata2Venus expression at day 3-6 of culture (n=3). **C)** Quantification of FACS analysis in panel (B) showing changes in Flk1$^+$Venus$^-$ (Flk1$^+$V$^-$); Flk1$^+$Venus$^+$ (Flk1$^+$V$^+$) and Flk1$^-$Venus$^+$ (Flk1$^-$V$^+$) cell frequency kinetics from day 3-6 of ESC differentiation (n=3). **D)** Bar graph showing EryP (primitive erythroid) colony output per 10^4 Flk1$^+$Venus$^-$ (F$^+$V$^-$); Flk1$^+$Venus$^+$ (F$^+$V$^+$); Flk1$^-$Venus$^+$ (F$^-$V$^+$) and Flk1$^-$Venus$^-$ (F$^-$V$^-$) cell populations

isolated at day 4-6 culture (n=4). **E)** Representative images of cells showing endothelial tubules generated in matrigel cultures of Flk1$^+$Venus$^-$ (F$^+$V$^-$); Flk1$^+$Venus$^+$ (F$^+$V$^+$); Flk1$^-$Venus$^+$ (F$^-$V$^+$) and Flk1$^-$Venus$^-$ (F$^-$V$^-$) cell populations isolated at day 4 of ESC differentiation. Objective=4x. **F)** Quantification of tubule formation (tubules/2x10^4 cells) shown in panel (E) (n=3).

Two temporally-defined waves of *Gata2* expression are detected during ESC hematopoietic differentiation

To understand the progression of the ESC differentiation towards hematopoietic lineage, the temporal dynamics of Gata2 expression was characterized. The frequency of V$^+$ cells from day 4 to 14 of differentiation was examined by FACS (Fig 2, Suppl Fig 2A). V$^+$ cells were detected throughout the time-course differentiation, and demonstrated wave-like dynamics with 2 peaks of increased V$^+$ cell frequency. As compared to day 4, the percentage of V$^+$ cells was significantly higher (5.5-fold) at day 6 (Fig 2A), and it decreased by day 7-10 as compared to day 6 of culture (3.3-fold). V$^+$ cell frequency was higher again at day 11-12 as compared to day 10 of culture (2.3-fold at day 11). *Venus* and *Gata2* RNA expression correlated with the V$^+$ cell frequency showing 2 temporally-defined expression peaks (Fig 2B). To exclude the possibility that the second *Gata2* expression peak occurs due to remaining undifferentiated cells, we analyzed the expression of pluripotency gene *Nanog. Nanog* RNA was significantly decreased after day 3 of differentiation and was not detectable at day 6 or day 12 at protein level (Suppl Fig 2B and 2C). Also, *Brachyury* expression, indicative of primitive streak/mesodermal commitment, showed the expected dynamics, with increased expression at day 3-6 and downregulated expression thereafter (Suppl Fig 2D), thus supporting the likelihood of two independent waves of induction of *Gata2* expressing cells in ESC differentiation cultures.

Gata2 functions in combinatorial manner with other key hematopoietic transcription factors (heptad factors) to direct HPC/HSC development
(Wilson et al., 2010). The expression of heptad factors *Gata2, Tal1, Lyl1, Lmo2, Fli1, Runx1* and *Erg* was tested (by qRT-PCR) in V$^+$ and V$^-$ sorted cells at day 6 and day 12 (Fig 2C). At both differentiation stages drastically higher expression of all the heptad factors was found in the V$^+$ fraction, with very little/no expression in the V$^-$ fraction. As a control, the expression of a non-heptad ubiquitous transcription factor, *Cbfβ* (Runx1 binding partner) was assessed at day 6 in the same populations (Suppl Fig 2E). In contrast to the heptad factors, *Cbfβ* was expressed similarly in V$^+$ and V$^-$ cells as expected. Thus, these data show that *Gata2* expressing cells exhibit a developmental gen hematopoietic gene expression profile.
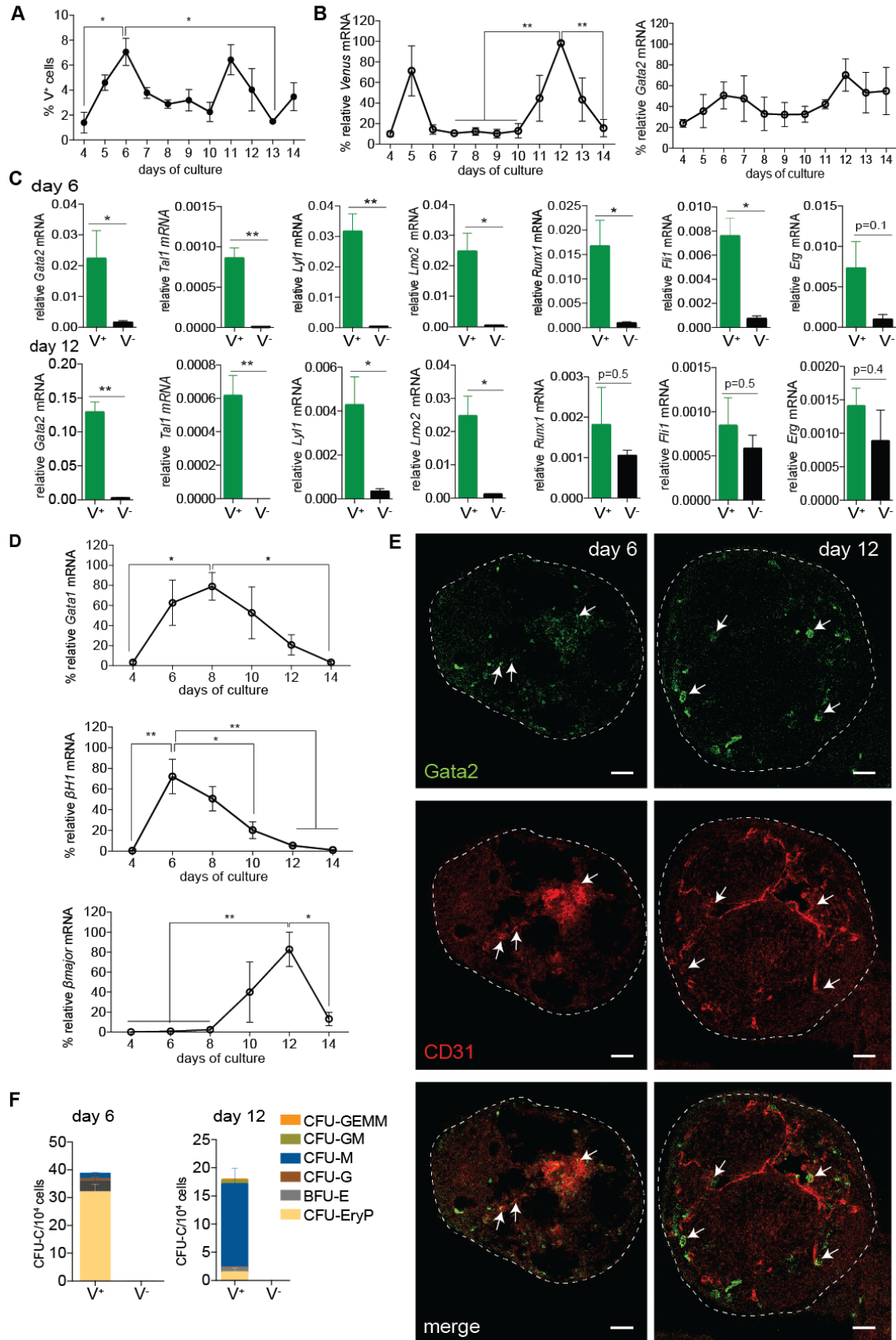
Figure 2. *Gata2Venus* temporal expression defines primitive and definitive hematopoietic stages of ESC differentiation. A) Frequency of Venus expressing (V⁺) cells in day 4-14 differentiated *Gata2Venus* ESC viable cells as measured by FACS (n=3). **B)** Real time qPCR analysis of *Venus* and *Gata2* expression in day 4-14 differentiated *Gata2Venus* ESCs. Expression was normalized to *β-actin*, set as 100% for the sample with the highest expression level.

Expression levels and % of maximum of other samples were calculated accordingly (n=3). **C)** Real time qPCR analysis for *Gata2, Tal1, Lyl1, Lmo2, Runx1, Fli1* and *Erg* expression in FACS sorted Venus$^+$ (V$^+$) and Venus$^-$ (V$^-$) populations isolated at day 6 (upper panel) and at day 12 (lower panel) of *Gata2Venus* ESC culture. Expression levels were normalized to *β-actin* (n=3). **D)** Real time qPCR analysis of *Gata1, βH1* and *βmajor* expression in day 4-14 differentiated *Gata2Venus* ESCs. Expression was normalized to *β-actin*, set as 100% for the sample with the highest expression level. Expression levels and % of maximum of other samples were calculated accordingly (n=3). **E)** Confocal images (representative) of whole mount stained day 6 and day 12 EBs (left and right panels, respectively) showing Venus (green) and CD31 (red) expression. Arrows indicate flat endothelial-like Venus$^+$ cells in day 6 EB and round hematopoietic like Venus$^+$ cells/clusters in day 12 EB. Size-bar=40 µm, 40x objective. **F)** Bar graph showing colony forming unit-cells (CFU-C) per 10^4 cells plated of Venus$^+$ (V$^+$) and Venus$^-$ (V$^-$) cells isolated from day 6 and day 12 *Gata2Venus* differentiated ESCs (n=3). Colony types are indicated by color. CFU-granulocyte, erythrocyte, monocyte, macrophage (GEMM); CFU-granulocyte-macrophage (GM); CFU-macrophage (M); CFU-granulocyte (G); burst-forming-unit erythroid (BFU-E) and CFU-primitive erythroid (EryP).
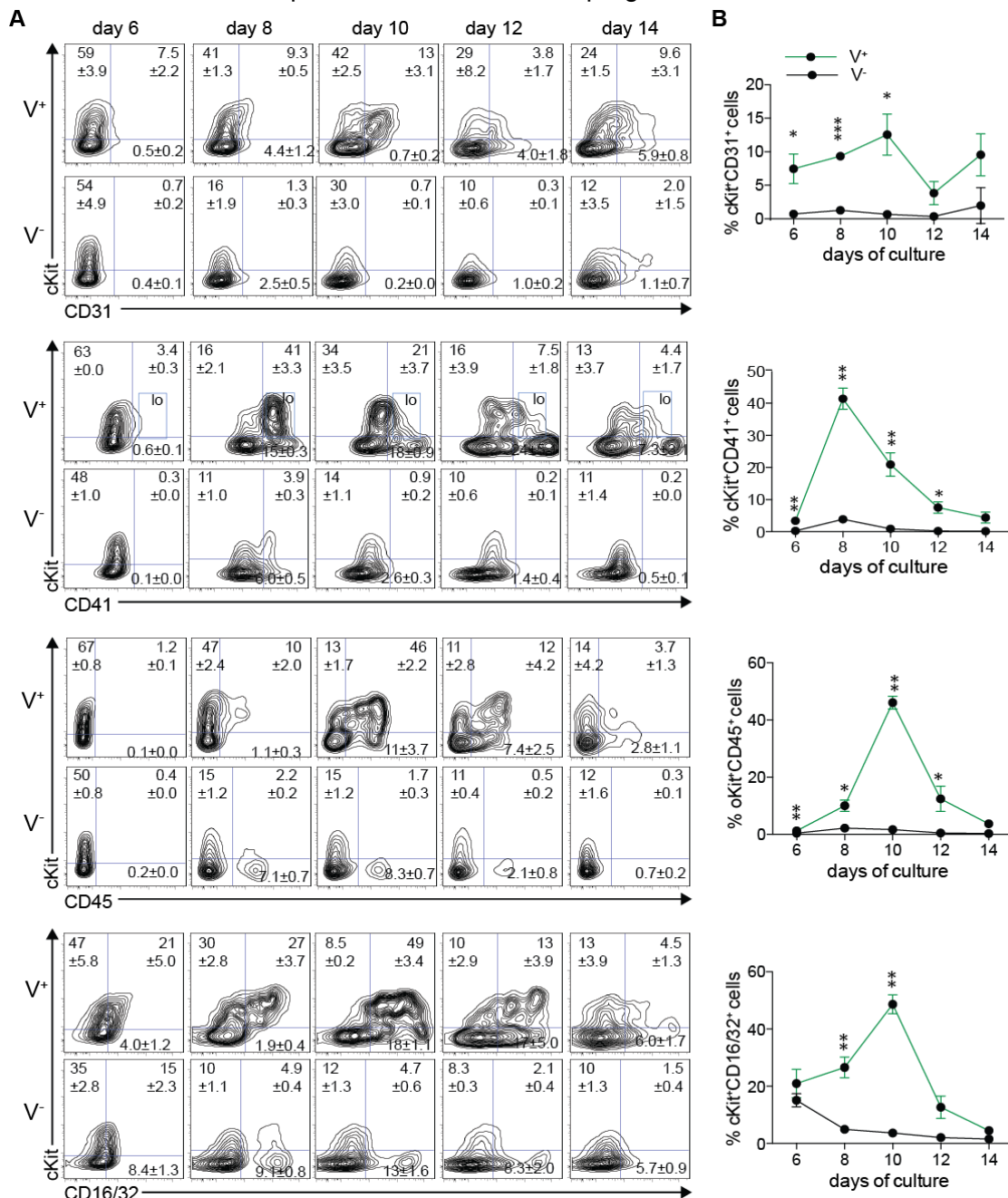
Sequential waves of *Gata2* expressing cell generation correlate with functional primitive and definitive hematopoietic potential

Hematopoiesis in the mouse embryo occurs in stage-specific waves, with a progressive generation of cells with more multipotential hematopoietic properties (reviewed in (Dzierzak and Speck, 2008; Kauts et al., 2016)). To elucidate whether the V$^+$ cells in the two waves express genes indicative of primitive (*βH1*; functions in early erythropoiesis) and/or definitive (*βmajor*; functions in adult erythroid cells) hematopoietic programs (Palis et al., 2010), qRT-PCR was performed (Fig 2D). *Gata1* (a pan-erythropoietic factor) was upregulated after the first peak of *Gata2* expression at day 6-8, and downregulated thereafter (Fig 2D upper panel). As a read-out for Gata1 transcription factor function, its downstream target *βH1* (embryonic globin) showed a peak of expression during the first wave of *Gata2* expression and was significantly downregulated thereafter (Fig 2D middle panel). *βmajor* (adult globin) expression was detectable from day 8 onwards and showed high expression at day 12 of culture (Fig 2D lower panel) correlating with the second *Gata2* expression peak.

The morphology and localization of V$^+$ cells were analyzed at the 2 stages of differentiation (day 6 and day 12) by confocal microscopy of whole EBs. In the mouse embryo, HPCs/HSCs emerge from CD31$^+$ hemogenic endothelial cells (Boisset et al., 2010), thus we immunostained the *G2V* EBs for CD31 to visualize the differentiating vasculature. CD31$^+$, V$^+$ and CD31$^+$V$^+$ cells were detected in the EBs at both time points (Fig 2E). At day 6, CD31$^+$ cells were dispersed throughout the EBs with no distinct structural organization. Flat endothelial-like V$^+$CD31$^+$ cells were scattered in the EBs (Fig 2E left panels). At day 12, CD31$^+$ cells formed a lining around the EB cavities, and round hematopoietic-like V$^+$ CD31$^+$ cells were closely associated with the CD31$^+$ lining (Fig 2E right panels). These imaging data indicate that Gata2 expressing cells in the day 6 and day 12 EBs are morphologically distinct, and thus, may possess different functions.

To test the relationship between *Gata2* expression, stage of ESC differentiation and hematopoietic function, cells from day 6 and day 12 EBs were harvested, FACS sorted into V$^+$ and V$^-$ populations and analyzed by CFU-C assay. Hematopoietic progenitors were found exclusively in the V$^+$ cell fractions (Fig 2F). Day 6 V$^+$ cells gave rise to 39.4±5 CFU-C/10^4 cells (HPC frequency 1:254), whereas day 12 V$^+$ cells generated 17.7±3.6

CFU-C/10^4 cells (HPC frequency 1:564). The majority (82%) of day 6 cells had only EryP (primitive erythroid) potential. A very low frequency of macrophage, granulocyte and definitive erythroid (CFU-M, CFU-G, BFU-E) colonies were also observed. In contrast, day 12 gave rise to a variety of erythroid-myeloid colony types, including mixed multipotent colonies (CFU-GEMM). Moreover, based on the colony size, the colonies derived from day 12 progenitors exhibited significantly increased proliferation capacity compared to the hematopoietic cells isolated from day 6 EBs. No lymphoid cell potential was detected with our culture method in the V$^+$ cells at day 12 of differentiation as assayed by OP9 co-culture (data not shown), and thus, *Gata2* expressin*g* cells possess definitive hematopoietic potential as described for erythroid-myeloid progenitors (EMP). Together these data indicate that *Gata2*-expressing cells proceed through at least 2 different stages of induction in ESC cultures that correlate with distinct primitive and EMP definitive functional cell potentials and molecular programs.

Figure 3. *Gata2Venus* cells progressively gain definitive hematopoietic characteristics. A) Flow cytometric dot plot analyzes of day 6, 8, 10, 12 and 14 differentiated *Gata2Venus* embryoid body (EB) derived cells showing cKit, CD31, CD41, CD45 and CD16/32 expression in Venus$^+$ (V$^+$

42

upper panels) and Venus⁻ (V⁻ lower panels) cell populations (n=3). **B)** Graph showing the temporal kinetics of cKit⁺CD31⁺, cKit⁺CD41⁺, cKit⁺CD45⁺ and cKit⁺CD16/32⁺ cell frequencies in Venus⁺ (V⁺, green line) and Venus⁻ (V⁻, black line) cell fractions of day 6, 8, 10, 12 and 14 *Gata2Venus* ESC differentiation cultures. Significant differences between indicated cell frequencies in V⁺ and V⁻ populations are designated with asterisks (n=3).

Gata2 expressing cells show progressive gain of definitive phenotypic characteristics during the waves of ESC differentiation

To characterize the phenotype of V⁺ and V⁻ cells during the waves of ESC differentiation, the expression of cell-surface markers cKit (expressed on all intra-aortic hematopoietic cluster cells), CD31 (expressed on all endothelial cells and intra-aortic hematopoietic cluster cells), CD41 (marks the earliest HPCs and megakaryocytes), CD45 (pan-hematopoietic marker) and CD16/32 (marks EMP when co-expressed with cKit) was measured by FACS (Fig 3A and 3B). CD31⁺cKit⁺ cells were detected predominantly in V⁺ fraction (0.7%-13%), whereas very few V⁻ cells (0.3%-2%) showed this phenotype. The percentages of CD31⁺cKit⁺ cells in the V⁺ fraction increased steadily from day 6 to day 10, decreased to a low point at day 12, and then rose again, suggesting a late wave of hematopoietic cell production. CD41 expression was detected in 4% of day 6 V⁺ cells and increased concomitantly with cKit co-expression to peak at day 8 (41±3.3% CD41⁺cKit⁺), followed by decreased percentages of these cells at day 10-14. Interestingly, cKit expression was mainly detected in V⁺CD41ˡᵒ and not in V⁺CD41ʰⁱ cells and is in line with published data showing that AGM HPCs/HSCs express CD41 at low/intermediate levels (Robin et al., 2011). Very few V⁻ cells were CD41⁺ throughout all time points analyzed, thus suggesting that co-expression of Gata2, CD41ˡᵒ and cKit define a HPC/HSC population during ESC differentiation. CD45 expression was barely detectable in V⁺ cells at day 6 of differentiation (1.3%). There was a profound increase and peak at day 10 with 46±2.2% of V⁺ cells CD45⁺cKit⁺ (as compared to the peak of CD41⁺cKit⁺ cells at day 8) and this was followed by decreased CD45⁺cKit⁺ cell percentages at day 12 and day 14. Very few V⁻ cells were CD45⁺cKit⁺ (0.4-2.2%) throughout differentiation. Thus, CD45 is confirmed as a later marker of hematopoietic cells. In contrast to the other markers, CD16/32 was expressed in both, V⁻ and in V⁺ cells at day 6 (15±2.3% and 21±5.0% respectively). This is expected and is in line with the *in vivo* results showing *Gata2* independent HPCs (Kaimakis et al., 2016). However, as with the other hematopoietic markers, CD16/32 was co-expressed with cKit more abundantly in the V⁺ fraction, and cell frequencies peaked at day 10 (49±3.4%) followed by a rapid decline. Together these data demonstrate that Gata2 expression defines almost all phenotypic hematopoietic cells generated throughout ESC differentiation (both early and later) and that these phenotypic markers show wave-like kinetics.
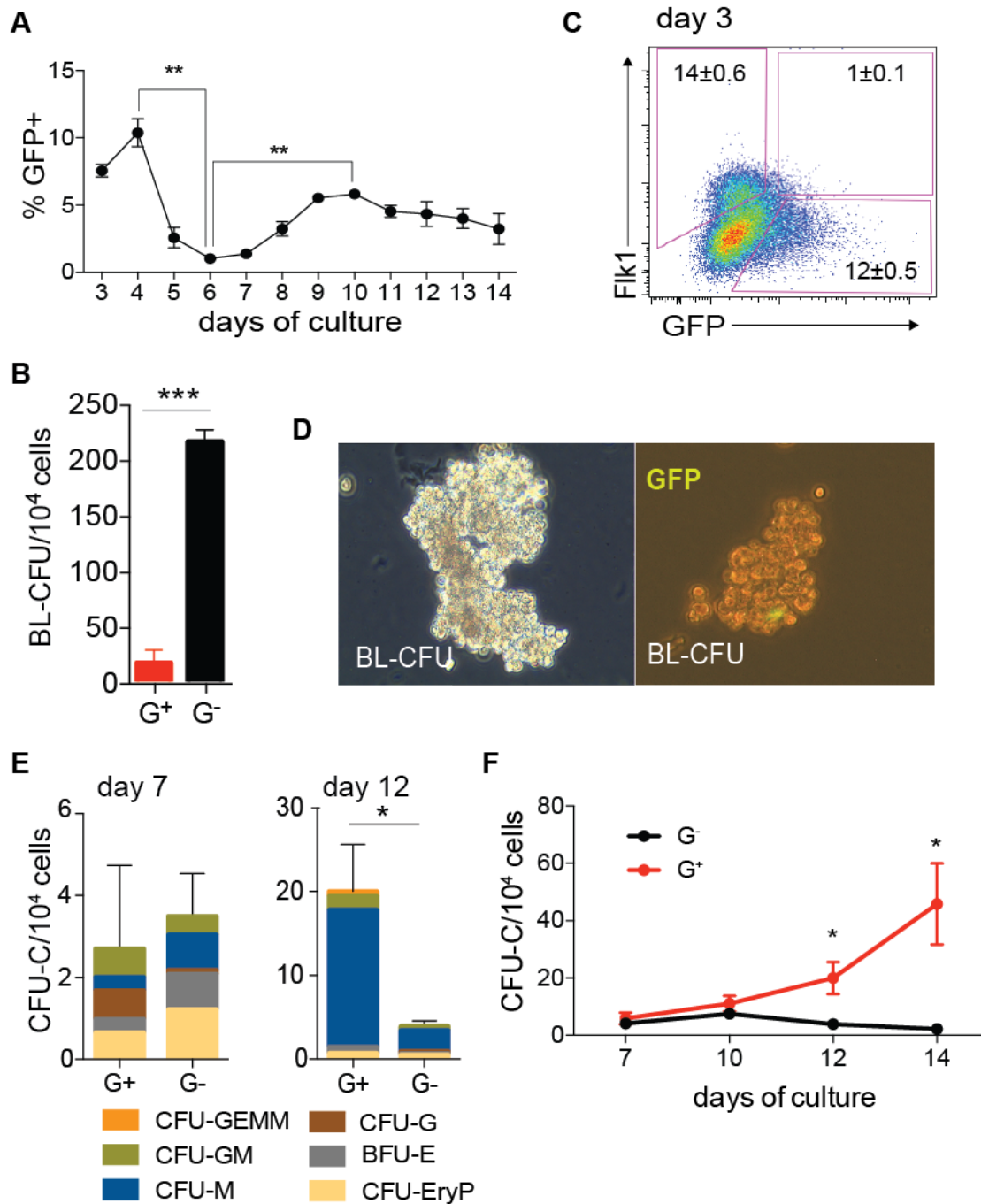
Figure 4. *Ly6a(Sca1)GFP* expression distinguishes functional hematopoietic cells in the definitive stage of ESC differentiation. A) Frequency of *Ly6a(Sca1)GFP* expressing (G$^+$) cells in day 4-14 differentiated *Ly6a(Sca1)GFP* embryoid bodies (EB) as measured by FACS (n=3). **B)** Blast colony (BL-CFU) potential in *Ly6a(Sca1)GFP$^+$* (G$^+$) and *Ly6a(Sca1)GFP$^-$* (G$^-$) cells sorted from day 3 *Ly6a(Sca1)GFP* EBs (n=3). **C)** Representative FACS plot for expression of Flk1 and Ly6a(Sca1)GFP expression in day 3 *Ly6a(Sca1)GFP* EBs. **D)** Representative BL-CFU colony originating from a G$^-$ cell sorted from day 3 *Ly6a(Sca1)GFP* EBs (left). Representative fluorescent image of day 4 BL-CFC originating from a G$^-$ cell sorted from day 3 *Ly6a(Sca1)GFP* EBs (right). The emergence of G$^+$ cells within the colony can be observed. **E)** CFU-C potential of day 7 (left panel) and 12 (right panel) G$^+$ and G$^-$ cells sorted from *Ly6a(Sca1)GFP* EBs. Colony forming unit-cell (CFU-C) number per 10^4 cells is shown (n=4). Colony types are indicated by color. CFU-granulocyte, erythrocyte, monocyte, macrophage (GEMM); CFU-granulocyte-macrophage (GM); CFU-macrophage (M); CFU-granulocyte (G); burst-forming-unit erythroid (BFU-E) and CFU-primitive erythroid (EryP). **F)** Graph showing time course of CFU-C frequency in day 3 to day 14 *Ly6a(Sca1)GFP* EB-derived sorted G$^+$ and G$^-$ cells. Significant differences between CFU-C/10^4 G$^+$ and G$^-$ cells are indicated (n=4).

The *Ly6a(Sca1)GFP* reporter distinguishes definitive hematopoietic cell potential after the *Gata2Venus* defined EMP stage

Unlike the *G2V* reporter in the embryos which marks almost all hematopoietic cells from the earliest time of generation, the *LG* reporter *in vivo* marks fewer hematopoietic cells, and cells generated at later developmental time points. To examine whether the *LG* reporter shows different kinetics and marks the later wave of hematopoietic generation in ESC differentiation cultures, LG ESC line was established from the *LG* mouse model. FACS analysis of the temporal appearance of GFP-positive (G^+) cells in the time course of ESC differentiation (Fig 4A) showed the presence of G^+ cells already at day 3 (7%) and day 4 (10%), followed by a rapid 5-fold decrease. Percentages of G^+ cells began to increase at day 7 showing a peak at day 9-10 of differentiation (3-fold increase; 6% at day 10). These two peaks of G^+ cell frequency occurred approximately 2 days earlier than V^+ cells (Fig 2A).

To investigate whether GFP expression correlates with hematopoietic activity in the ESC differentiation culture, we performed hematopoietic colony forming assays. At early differentiation stages (day 3-4), bipotent endothelial/hematopoietic precursors, the putative hemangioblast, can be detected as blast colony forming cells (BL-CFC). BL-CFC culture, established with FACS sorted G^+ and G^- cells derived from day 3 EBs, revealed that significantly more blast colonies were formed in the G^- fraction (215±11 in G^-; 17±12 in G^+) (Fig 4B). Accordingly, only very few G^+ cells (1±0.1% of the total live population) expressed Flk1 (Fig 4C). However, examination of BL colonies during growth phase showed a few G^+ cells starting to emerge (Fig 4D), suggesting that *LG* expression in the hematopoietic lineage begins just after the hemangioblast stage. CFU-C assay with G^+ and G^- cells derived from later stage (day 7) EBs revealed that HPCs were found equally in both fractions (Fig 4E). However, at day 12 significantly more of these (including all the CFU-GEMMs) were found in the G^+ population. Time course CFU-C assays (Fig 4F) demonstrated that from day 7 to 10 of differentiation, HPCs were contained in both fractions, at day 12 there were significantly more HPCs generated by G^+ cells, and by day 14 virtually all HPC activity was found in G^+ cells. The frequency of hematopoietic cells in the G^+ and G^- fractions at day 6-14 of ESCs was determined by FACS for cKit and co-expression of CD31, CD41, CD45 and CD16/32 (Fig 5). $CD31^+cKit^+$ cells were detected at day 6 at similar levels (6.9±0.4% and 6.9±1.3%) in G^+ and G^- fractions respectively. From day 10 onwards, the frequency of $CD31^+cKit^+$ cells increased in the G^+ fraction (rising to 26.0±6.2%) as compared to the G^- fraction. $CD41^+cKit^+$ cells were detected beginning at day 8 in G^+ cells (0.9±0.2%) and frequencies gradually increased to day 14, when they were profoundly higher (14±3.0%). At all time points, CD41 expression was low in the G^- fraction, thus $CD41^+cKit^+$ cell frequency in the G^- fraction was negligible. CD45cKit expression showed a similar trend as $CD41^+cKit^+$ cells being detected in the G^+ fraction from day 8 (0.2±0.1%) onwards, with a significantly higher frequency after day 12 of culture and raising to 18±5.1% at day 14, as compared to the G^- fraction, in which no/very few $CD45^+cKit^+$ cells were found. Phenotypic EMPs ($cKit^+CD16/32^+$ cells) were detected from day 6 onwards in both G^+ and G^- fractions (1.8±0.6% and 0.1±0.0% respectively). With progression of differentiation (day 10-12), the frequency of $cKit^+CD16/32^+$ cells increased considerably in the G^+ fraction, while the frequency decreased in the G^- fraction. These data indicate that *LG* specifically marks phenotypic hematopoietic cells in later stages of the ESC differentiation, e.g. from day 10-12 onwards, and that a subset of hematopoietic progenitors is generated and/or acquire this marker later in the culture than the *G2V* defined EMP wave, thus potentially distinguishing

a third multipotent EMP definitive wave of hematopoietic emergence in the ESC differentiation cultures (Model, Fig 6).
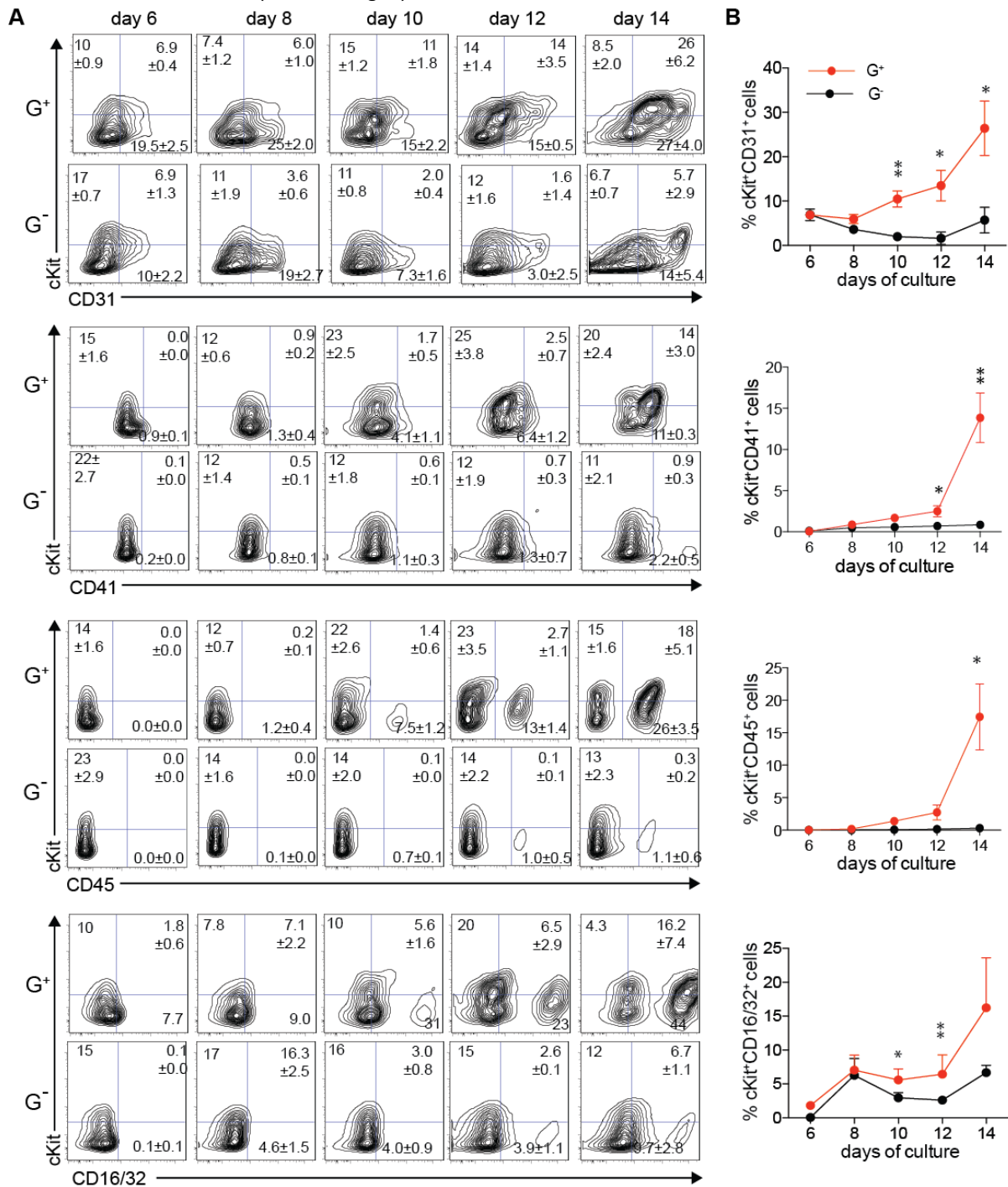

Figure 5. *Ly6a(Sca1)GFP* expression marks phenotypic hematopoietic cells after the *Gata2Venus*-defined EMP stage. A) Flow cytometric dot plot analyzes of day 6, 8, 10, 12 and 14 *Ly6a(Sca1)GFP* embryoid body (EB) derived cells showing cKit, CD31, CD41, CD45 and CD16/32 expression in Ly6a(Sca1)GFP-expressing (G$^+$) and non-expressing (G$^-$) cell fractions (n=4). **B)** Graph showing the temporal kinetics of cKit$^+$CD31$^+$, cKit$^+$CD41$^+$, cKit$^+$CD45$^+$ and cKit$^+$CD16/32$^+$ cell frequencies in Ly6a(Sca1)GFP-expressing (G$^+$, red line) and non-expressing (G$^-$, black line) fractions of day 6, 8, 10, 12 and 14 differentiated *Ly6a(Sca1)GFP* EBs. Significant differences between indicated cell frequencies in G$^+$ and G$^-$ populations are designated with asterisks (n=4).
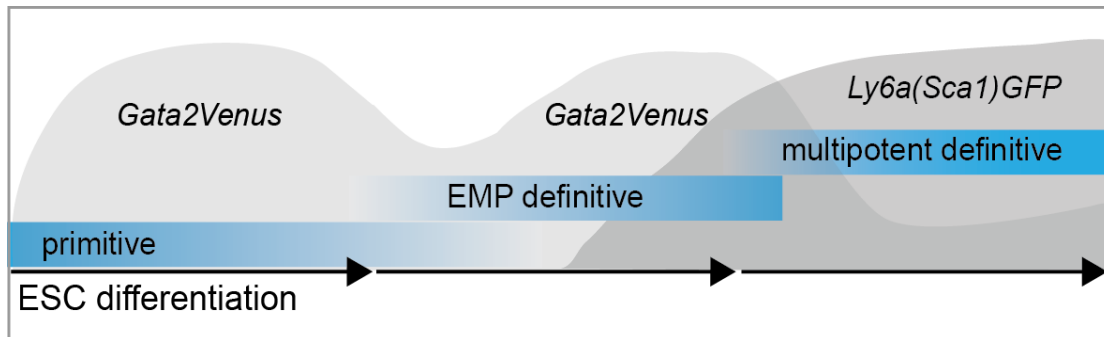
Figure 6. *Gata2Venus* and *Ly6a(Sca1)GFP* expression mark primitive and definitive hematopoietic progenitor generation stages in ESC differentiation cultures. Within the first few days of ESC differentiation, *Gata2Venus* expression defines cells with primitive hematopoietic potential. A subsequent decrease in *Gata2Venus* expressing cells is followed by the emergence of EMP-definitive potential in the second wave of *Gata2Venus*-expressing cells. In a later stage of ESC differentiation culture, *Ly6a(Sca1)GFP* and *Gata2Venus* expression distinguishes a third wave of hematopoietic emergence that defines multipotent definitive hematopoietic cells.

Discussion

In this study, we show that ESC differentiation progresses through three stages of functional hematopoietic cell production that can be discriminated by the temporal expression of the *G2V* or *LG* reporters. These reporters are excellent *in vivo* indicators of normal temporal and spatial generation of hematopoietic cells in the mouse embryo, ensuring high fidelity in their use to examine the stages of hematopoietic emergence *in vitro*. These novel reporter ESC lines, when enriched during the differentiation culture, demonstrate functional hematopoietic properties that are analogous to the cells generated in the three *in vivo* waves of hematopoietic emergence found in the mouse embryo.

Hematopoiesis in the mouse embryo starts in the YS with a transient wave of primitive hematopoiesis. This program is characterized by a short lived bi-potential Flk1$^+$ hemangioblast that gives rise to the earliest blood cells and entotheliium (Choi et al., 1998; Kennedy et al., 1997; Palis et al., 1999; Shalaby et al., 1997). Our analysis of early *G2V* EB differentiation reveals a transient V$^+$Flk1$^+$ population that differentiates into endothelial and primitive erythroid cells. In contrast, no Flk1 expression or hemangioblast function is found in the G$^+$cells of *LG* EB. Thus the earliest functional hematopoietic cells in the ESC cultures are defined by *Gata2* expression. *Gata2*, and also *Gata1,* are first detected in the YS mesoderm at E7 resulting in high expression of the developmentally distinct embryonic globin from E7.5, that is not detected later in the adult erythroid cells (Silver and Palis, 1997). In the embryo, *Gata2* is involved in the initial activation of *Gata1*, and when *Gata1* is expressed, it subsequently suppresses *Gata2*. This is referred as the Gata factor switch (Ferreira et al., 2005). Our kinetic analysis of *Gata* factor expression is consistent with this switch. As a readout for *Gata* function, high level of embryonic globin is detected at day 6, e.g. during the first *Gata2* expression peak, but not thereafter (day 12-14). This agrees with the single cell transcriptomic data in which a pseudotemporal ordering of cells (posterior Flk1$^+$ mesodermal cells arising from the posterior primitive streak) in the E7.5-7.75 embryo show upregulation of *Gata1,* embryonic globin and *Itga2b* after *Brachyury* detection indicative of primitive streak specification (Scialdone et al., 2016). Therefore, the early stage of our EB differentiation culture as defined by the first *Gata2* expression peak related with *Gata1*, embryonic

globin and CD41 expression, closely follows the formation of early mesoderm in gastrulating embryos.

Interestingly, EryP colonies and the expression of embryonic globin declined in the culture in parallel with the onset of the second *Gata2* expression wave that is accompanied by expression of adult globin and the appearance of multipotent EMPs. Thus, the *Gata2* expression peaks discriminate functional primitive and EMP-definitive stages in the ESC differentiation. It is likely that the first and second wave cells are derived from independent cohorts of cells as supported by the data of (Scialdone et al., 2016) and from the human ESC differentiation cultures of (Ditadi et al., 2015; Sturgeon et al., 2014), but this is in contrast to the day 3 differentiation cultures of (Pearson et al., 2015) suggesting that all waves of hematopoietic activity and *in vivo* repopulating cells (albeit low-level repopulating) arise in these early cultures. Additionally, the temporal dynamics of *Gata2* defined primitive/definitive stages are consistent with studies from other groups reporting waves of distinct hemogenic endothelium and hematopoietic cell generation in mouse and human ESC differentiation cultures (Nakano et al., 1996; Rafii et al., 2013; Zambidis et al., 2005). Our results show for the first time that these stage-specific hematopoietic cells can be traced and isolated using a single relevant reporter.

Morphological observation of the *Gata2*$^+$ cells in the differentiating EBs corroborates both developmental and functional stage changes. Whole mount imaging of day 12 (but not day 6) EBs show the presence of CD31$^+$ cells lining vascular tubules and the close association of clusters of V$^+$CD31$^+$ cells, mainly near the cavities of the EBs. This observation is supported by our FACS data showing an increased frequency of cKit$^+$CD31$^+$V$^+$ cells after day 6 of differentiation. This could represent the endothelial-to-hematopoietic-transition occurring in E8.25-E11 circulation deficient YS where EMPs emergence from cKit$^+$ clustering was observed (Frame et al., 2016). However, we previously showed by immunostained E10.5 *G2V* AGM tissue that endothelial and hematopoietic cluster cells of the aorta are CD31$^+$V$^+$ (Kaimakis et al., 2016), indicating a structural resemblance between the day 12 EBs and the dorsal aorta. Also, a recent study with day 23-33 differentiated human ESCs showed similar aortic and cluster-like structures (Ng et al., 2016). All together these data show that the second wave defines EMP development, which is morphologically close to *in vivo* definitive hematogenesis.

In the mouse embryo, although all HSCs are *Gata2*$^+$, a few *Gata2* independent progenitors are generated (Kaimakis et al., 2016). HPC activity is enriched in the *GATA2* expressing fraction of human ESC differentiation cultures (Huang et al., 2016). Here we have shown that the functional hematopoietic activity in the *G2V* EBs is exclusively found in the V$^+$ population. However, some phenotypic HPCs are found in the V$^-$ fraction as assayed by FACS. High enrichment of hematopoietic activity of V$^+$ cells is further highlighted by dramatically higher expression of all heptad hematopoietic transcription factors as compared to V$^-$ cells suggesting that V$^+$ cells are more potent/robust.

Surface marker analysis of *G2V* ESC-derived cells revealed that the highest frequency of phenotypic V$^+$ hematopoietic cells is detected at day 8 (cKit$^+$CD41$^+$ cells) and at day 10 (cKit$^+$CD45$^+$; cKit$^+$CD16/32$^+$; cKit$^+$CD31$^+$ cells), and thereafter the frequency is greatly reduced. This wave-like activity is in line with several human ESC differentiation studies that use gene expression profiling and surface markers suggesting waves of hematopoietic generation (Irion et al., 2010; Nakano et al., 1996; Rafii et al., 2013;

Zambidis et al., 2005). HPC potential in our cultures continues at day 12 and thereafter, and the definitive HPC potential specifically expresses *LG*. *LG* expression did not report hemangioblast stage primitive progenitors. However, in BL-CFC rare G$^+$ cells were found. During the first stage of EB differentiation (e.g. day 6-10) HPCs are found in both, G$^+$ and G$^-$ fractions. After day 12, HPC activity is significantly enriched in the G$^+$ cells. These data are in contrast to HPC activity in the differentiated *G2V* ESCs where all HPCs are V$^+$ throughout the differentiation. Distribution in progenitor activity in the *LG* EBs is consistent with the distribution of HPC activity in the *LG* mouse embryos. In the *LG* YS, most HPCs are G$^-$. This is in contrast to the E10.5/E11.5 AGM lymphoid progenitors and multipotent HPCs/HSCs, that are found in the G$^+$ population at much higher frequency than in the G$^-$ fraction (Li et al., 2014; Solaimani Kartalaei et al., 2015). *LG* expression reports hemogenic endothelial cells and all emerging HSCs in the E10.5 aorta *in vivo* (Boisset et al., 2010; de Bruijn et al., 2002). Thus, *LG* expression specifically reports aortic HSCs and cells with lymphoid potential, but not the YS stage progenitors. Taken together, these data propose that in the ESC differentiation culture the *LG* reporter distinguishes definitive aorta-like hematopoietic progenitors that appear/persist in the culture after the EMP stage defined by the *G2V* expression.

In conclusion, we demonstrate that three waves of hematopoietic generation can be prospectively traced and isolated by the *G2V* and *LG* reporter expression in ESC differentiation cultures. Further experiments will elucidate whether the late waves of hematopoietic cells generated in the *G2V* and *LG* ESC cultures possess lymphoid, and even more robust hematopoietic potentials. Such findings will facilitate better understanding of the hematopoietic development in PSC differentiation cultures, and may ultimately enable the recapitulation of physiologic HSC emergence for the *de novo* generation of transplantable HSCs for therapeutic strategies.

Acknowledgements

References

Bertrand, J.Y., Kim, A.D., Violette, E.P., Stachura, D.L., Cisson, J.L., and Traver, D. (2007). Definitive hematopoiesis initiates through a committed erythromyeloid progenitor in the zebrafish embryo. Development *134*, 4147-4156.

Boisset, J.C., van Cappellen, W., Andrieu-Soler, C., Galjart, N., Dzierzak, E., and Robin, C. (2010). In vivo imaging of haematopoietic cells emerging from the mouse aortic endothelium. Nature *464*, 116-120.

Bryja, V., Bonilla, S., and Arenas, E. (2006). Derivation of mouse embryonic stem cells. Nat Protoc *1*, 2082-2087.

Chen, M.J., Li, Y., De Obaldia, M.E., Yang, Q., Yzaguirre, A.D., Yamada-Inagawa, T., Vink, C.S., Bhandoola, A., Dzierzak, E., and Speck, N.A. (2011). Erythroid/myeloid progenitors and hematopoietic stem cells originate from distinct populations of endothelial cells. Cell Stem Cell *9*, 541-552.

Choi, K., Kennedy, M., Kazarov, A., Papadimitriou, J.C., and Keller, G. (1998). A common precursor for hematopoietic and endothelial cells. Development *125*, 725-732.

de Bruijn, M.F., Ma, X., Robin, C., Ottersbach, K., Sanchez, M.J., and Dzierzak, E. (2002). Hematopoietic stem cells localize to the endothelial cell layer in the midgestation mouse aorta. Immunity *16*, 673-683.

de Pater, E., Kaimakis, P., Vink, C.S., Yokomizo, T., Yamada-Inagawa, T., van der Linden, R., Kartalaei, P.S., Camper, S.A., Speck, N., and Dzierzak, E. (2013). Gata2 is required for HSC generation and survival. J Exp Med *210*, 2843-2850.

Ditadi, A., Sturgeon, C.M., Tober, J., Awong, G., Kennedy, M., Yzaguirre, A.D., Azzola, L., Ng, E.S., Stanley, E.G., French, D.L.*, et al.* (2015). Human definitive haemogenic endothelium and arterial vascular endothelium represent distinct lineages. Nat Cell Biol *17*, 580-591.

Doetschman, T.C., Eistetter, H., Katz, M., Schmidt, W., and Kemler, R. (1985). The in vitro development of blastocyst-derived embryonic stem cell lines: formation of visceral yolk sac, blood islands and myocardium. J Embryol Exp Morphol *87*, 27-45.

Doulatov, S., Vo, L.T., Chou, S.S., Kim, P.G., Arora, N., Li, H., Hadland, B.K., Bernstein, I.D., Collins, J.J., Zon, L.I.*, et al.* (2013). Induction of multipotential hematopoietic progenitors from human pluripotent stem cells via respecification of lineage-restricted precursors. Cell Stem Cell *13*, 459-470.

Dzierzak, E., and Speck, N.A. (2008). Of lineage and legacy: the development of mammalian hematopoietic stem cells. Nat Immunol *9*, 129-136.

Ferreira, R., Ohneda, K., Yamamoto, M., and Philipsen, S. (2005). GATA1 function, a paradigm for transcription factors in hematopoiesis. Mol Cell Biol *25*, 1215-1227.

Frame, J.M., Fegan, K.H., Conway, S.J., McGrath, K.E., and Palis, J. (2016). Definitive Hematopoiesis in the Yolk Sac Emerges from Wnt-Responsive Hemogenic Endothelium Independently of Circulation and Arterial Identity. Stem Cells *34*, 431-444.

Frame, J.M., McGrath, K.E., and Palis, J. (2013). Erythro-myeloid progenitors: "definitive" hematopoiesis in the conceptus prior to the emergence of hematopoietic stem cells. Blood Cells Mol Dis *51*, 220-225.

Gao, X., Johnson, K.D., Chang, Y.I., Boyer, M.E., Dewey, C.N., Zhang, J., and Bresnick, E.H. (2013). Gata2 cis-element is required for hematopoietic stem cell generation in the mammalian embryo. J Exp Med *210*, 2833-2842.

Godin, I., Dieterlen-Lievre, F., and Cumano, A. (1995). Emergence of multipotent hemopoietic cells in the yolk sac and paraaortic splanchnopleura in mouse embryos, beginning at 8.5 days postcoitus. Proc Natl Acad Sci U S A *92*, 773-777.

Huang, K., Du, J., Ma, N., Liu, J., Wu, P., Dong, X., Meng, M., Wang, W., Chen, X., Shi, X.*, et al.* (2015). GATA2(-/-) human ESCs undergo attenuated endothelial to hematopoietic transition and thereafter granulocyte commitment. Cell Regen (Lond) *4*, 4.

Huang, K., Gao, J., Du, J., Ma, N., Zhu, Y., Wu, P., Zhang, T., Wang, W., Li, Y., Chen, Q.*, et al.* (2016). Generation and Analysis of GATA2w/eGFP Human ESCs Reveal ITGB3/CD61 as a Reliable Marker for Defining Hemogenic Endothelial Cells during Hematopoiesis. Stem Cell Reports *7*, 854-868.

Huber, T.L., Kouskoff, V., Fehling, H.J., Palis, J., and Keller, G. (2004). Haemangioblast commitment is initiated in the primitive streak of the mouse embryo. Nature *432*, 625-630.

Irion, S., Clarke, R.L., Luche, H., Kim, I., Morrison, S.J., Fehling, H.J., and Keller, G.M. (2010). Temporal specification of blood progenitors from mouse embryonic stem cells and induced pluripotent stem cells. Development *137*, 2829-2839.

Kaimakis, P., de Pater, E., Eich, C., Solaimani Kartalaei, P., Kauts, M.L., Vink, C.S., van der Linden, R., Jaegle, M., Yokomizo, T., Meijer, D.*, et al.* (2016). Functional and molecular characterization of mouse Gata2-independent hematopoietic progenitors. Blood *127*, 1426-1437.

Kauts, M.L., Vink, C.S., and Dzierzak, E. (2016). Hematopoietic (stem) cell development-how divergent are the roads taken? FEBS Lett.

Keller, G.M., Webb, S., and Kennedy, M. (2002). Hematopoietic Development of ES Cells in Culture. Methods Mol Med *63*, 209-230.

Kennedy, M., Awong, G., Sturgeon, C.M., Ditadi, A., LaMotte-Mohs, R., Zuniga-Pflucker, J.C., and Keller, G. (2012). T lymphocyte potential marks the emergence of definitive hematopoietic progenitors in human pluripotent stem cell differentiation cultures. Cell Rep *2*, 1722-1735.

Kennedy, M., D'Souza, S.L., Lynch-Kattman, M., Schwantz, S., and Keller, G. (2007). Development of the hemangioblast defines the onset of hematopoiesis in human ES cell differentiation cultures. Blood *109*, 2679-2687.

Kennedy, M., Firpo, M., Choi, K., Wall, C., Robertson, S., Kabrun, N., and Keller, G. (1997). A common precursor for primitive erythropoiesis and definitive haematopoiesis. Nature *386*, 488-493.

Kyba, M., Perlingeiro, R.C., and Daley, G.Q. (2002). HoxB4 confers definitive lymphoid-myeloid engraftment potential on embryonic stem cell and yolk sac hematopoietic progenitors. Cell *109*, 29-37.

Li, Y., Esain, V., Teng, L., Xu, J., Kwan, W., Frost, I.M., Yzaguirre, A.D., Cai, X., Cortes, M., Maijenburg, M.W.*, et al.* (2014). Inflammatory signaling regulates embryonic hematopoietic stem and progenitor cell production. Genes Dev *28*, 2597-2612.

Ling, K.W., Ottersbach, K., van Hamburg, J.P., Oziemlak, A., Tsai, F.Y., Orkin, S.H., Ploemacher, R., Hendriks, R.W., and Dzierzak, E. (2004). GATA-2 plays two functionally distinct roles during the ontogeny of hematopoietic stem cells. J Exp Med *200*, 871-882.

Mascarenhas, M.I., Parker, A., Dzierzak, E., and Ottersbach, K. (2009). Identification of novel regulators of hematopoietic stem cell development through refinement of stem cell localization and expression profiling. Blood *114*, 4645-4653.

Medvinsky, A., and Dzierzak, E. (1996). Definitive hematopoiesis is autonomously initiated by the AGM region. Cell *86*, 897-906.

Muller, A.M., Medvinsky, A., Strouboulis, J., Grosveld, F., and Dzierzak, E. (1994). Development of hematopoietic stem cell activity in the mouse embryo. Immunity *1*, 291-301.

Nakano, T., Kodama, H., and Honjo, T. (1996). In vitro development of primitive and definitive erythrocytes from different precursors. Science *272*, 722-724.

Ng, E.S., Azzola, L., Bruveris, F.F., Calvanese, V., Phipson, B., Vlahos, K., Hirst, C., Jokubaitis, V.J., Yu, Q.C., Maksimovic, J.*, et al.* (2016). Differentiation of human embryonic stem cells to HOXA+ hemogenic vasculature that resembles the aorta-gonad-mesonephros. Nat Biotechnol *34*, 1168-1179.

Palis, J., Malik, J., McGrath, K.E., and Kingsley, P.D. (2010). Primitive erythropoiesis in the mammalian embryo. Int J Dev Biol *54*, 1011-1018.

Palis, J., Robertson, S., Kennedy, M., Wall, C., and Keller, G. (1999). Development of erythroid and myeloid progenitors in the yolk sac and embryo proper of the mouse. Development *126*, 5073-5084.

Pearson, S., Cuvertino, S., Fleury, M., Lacaud, G., and Kouskoff, V. (2015). In vivo repopulating activity emerges at the onset of hematopoietic specification during embryonic stem cell differentiation. Stem Cell Reports *4*, 431-444.

Rafii, S., Kloss, C.C., Butler, J.M., Ginsberg, M., Gars, E., Lis, R., Zhan, Q., Josipovic, P., Ding, B.S., Xiang, J.*, et al.* (2013). Human ESC-derived hemogenic endothelial cells undergo distinct waves of endothelial to hematopoietic transition. Blood *121*, 770-780.

Robin, C., Ottersbach, K., Boisset, J.C., Oziemlak, A., and Dzierzak, E. (2011). CD41 is developmentally regulated and differentially expressed on mouse hematopoietic stem cells. Blood *117*, 5088-5091.

Rodrigues, N.P., Janzen, V., Forkert, R., Dombkowski, D.M., Boyd, A.S., Orkin, S.H., Enver, T., Vyas, P., and Scadden, D.T. (2005). Haploinsufficiency of GATA-2 perturbs adult hematopoietic stem-cell homeostasis. Blood *106*, 477-484.

Scialdone, A., Tanaka, Y., Jawaid, W., Moignard, V., Wilson, N.K., Macaulay, I.C., Marioni, J.C., and Gottgens, B. (2016). Resolving early mesoderm diversification through single-cell expression profiling. Nature *535*, 289-293.

Shalaby, F., Ho, J., Stanford, W.L., Fischer, K.D., Schuh, A.C., Schwartz, L., Bernstein, A., and Rossant, J. (1997). A requirement for Flk1 in primitive and definitive hematopoiesis and vasculogenesis. Cell *89*, 981-990.

Silver, L., and Palis, J. (1997). Initiation of murine embryonic erythropoiesis: a spatial analysis. Blood *89*, 1154-1164.

Solaimani Kartalaei, P., Yamada-Inagawa, T., Vink, C.S., de Pater, E., van der Linden, R., Marks-Bluth, J., van der Sloot, A., van den Hout, M., Yokomizo, T., van Schaick-Solerno, M.L.*, et al.* (2015). Whole-transcriptome analysis of endothelial to hematopoietic stem cell transition reveals a requirement for Gpr56 in HSC generation. J Exp Med *212*, 93-106.

Sturgeon, C.M., Ditadi, A., Awong, G., Kennedy, M., and Keller, G. (2014). Wnt signaling controls the specification of definitive and primitive hematopoiesis from human pluripotent stem cells. Nat Biotechnol *32*, 554-561.

Zambidis, E.T., Peault, B., Park, T.S., Bunz, F., and Civin, C.I. (2005). Hematopoietic differentiation of human embryonic stem cells progresses through sequential hematoendothelial, primitive, and definitive stages resembling human yolk sac development. Blood *106*, 860-870.

Tsai, F.Y., Keller, G., Kuo, F.C., Weiss, M., Chen, J., Rosenblatt, M., Alt, F.W., and Orkin, S.H. (1994). An early haematopoietic defect in mice lacking the transcription factor GATA-2. Nature *371*, 221-226.

Vodyanik, M.A., Bork, J.A., Thomson, J.A., and Slukvin, II (2005). Human embryonic stem cell-derived CD34+ cells: efficient production in the coculture with OP9 stromal cells and analysis of lymphohematopoietic potential. Blood *105*, 617-626.

Wilson, N.K., Foster, S.D., Wang, X., Knezevic, K., Schutte, J., Kaimakis, P., Chilarska, P.M., Kinston, S., Ouwehand, W.H., Dzierzak, E.*, et al.* (2010). Combinatorial transcriptional control in blood stem/progenitor cells: genome-wide analysis of ten major transcriptional regulators. Cell Stem Cell *7*, 532-544.

Yokomizo, T., Yamada-Inagawa, T., Yzaguirre, A.D., Chen, M.J., Speck, N.A., and Dzierzak, E. (2012). Whole-mount three-dimensional imaging of internally localized immunostained cells within mouse embryos. Nat Protoc 7, 421-431.
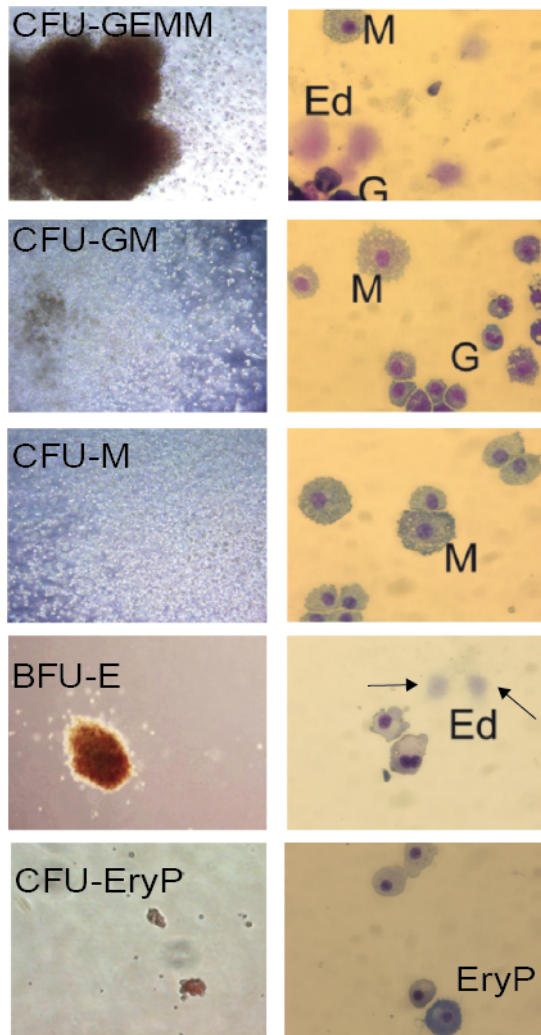
Supplementary data

A

B

C
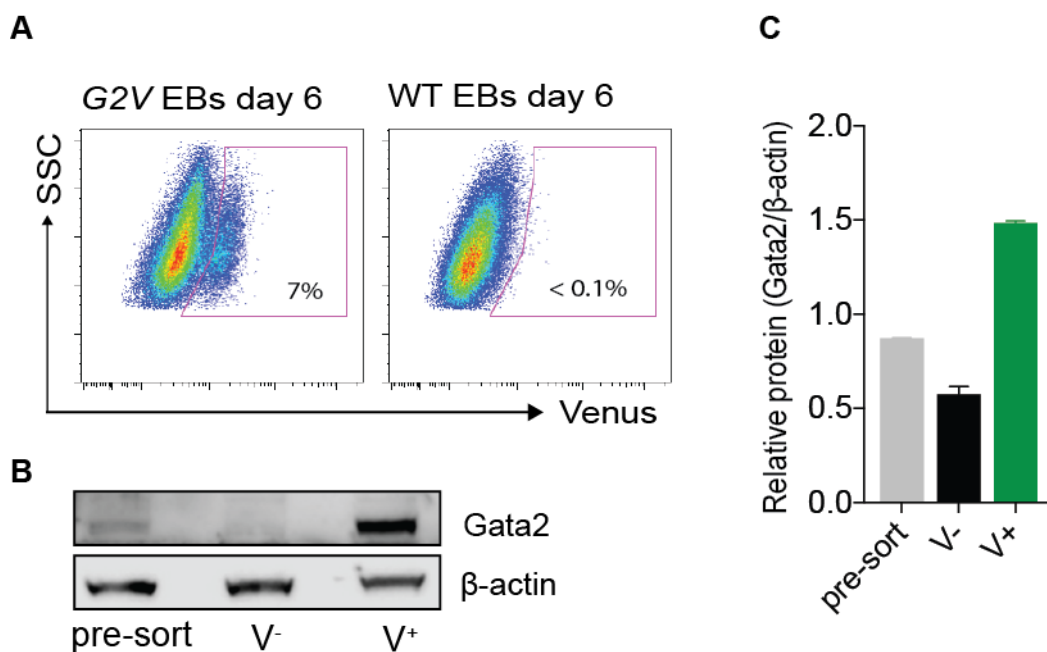
Supplementary figure 1. Validation of *Gata2Venus* ESC reporter. A) FACS dot plots showing percentage of Venus expressing cells in day 6 *Gata2Venus (G2V*, left) ESC differentiation cultures. Differentiated wild type (WT, right) ESCs were used as a negative control. **B)** Western blot analysis of whole cell extracts of pre-sorted or Venus⁻ (V⁻) and Venus⁺ (V⁺) populations from day 6 differentiated *Gata2Venus* ESC cultures. A Gata2 protein band (40 kDa) is observed in unsorted and V⁺ cells. -actin is the protein normalization control. Representative plot (n=2). **C)** Quantification of Gata2 protein in Western blot shown in panel B. Values represent Gata2 protein quantity relative to β-actin expression. Mean ± SEM (n=2).
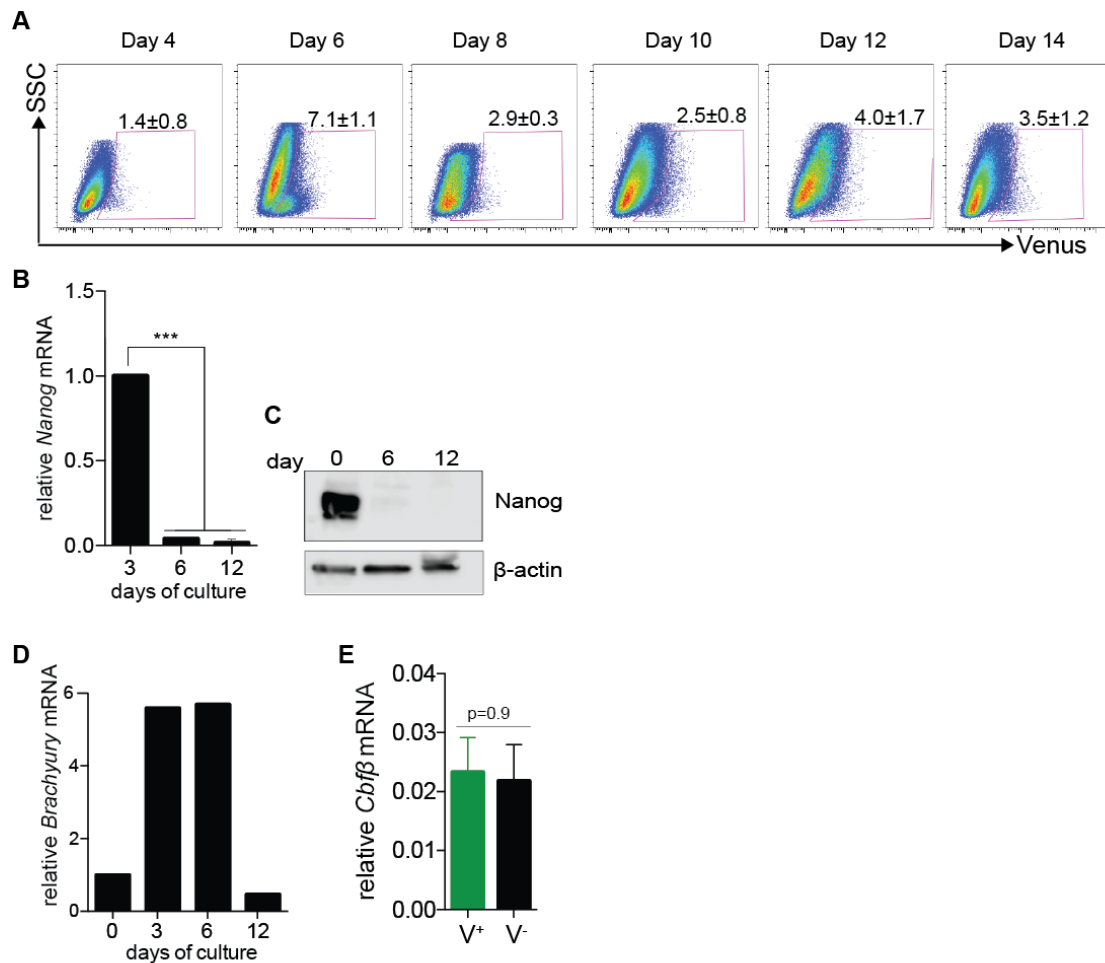
Supplementary Figure 2. *Gata2Venus* expression kinetics during ESC hematopoietic differentiation. A) FACS dot plots showing Venus[+] cell frequency in day 4-14 *Gata2Venus* ESC differentiation cultures (n=3). **B)** Real time qPCR analysis of *Nanog* expression in day 3-12 *Gata2Venus* ESC differentiation cultures. Expression was normalized to β-*actin* and set as 1 in the day 3 sample, and the other samples were calculated accordingly (n=3). **C)** Western blot analysis of Nanog protein expression in day 0, 6 and 12 differentiated *Gata2Venus* ESCs. β-actin was used as the protein normalization control. Representative plot (n=2). **D)** Real time qPCR analysis of *Brachyury* expression in day 0, 3, 6 and 12 differentiated *Gata2Venus* ESCs. Expression was normalized to β-*actin* and set as 1 in day 0 sample, and the other samples were calculated accordingly. Representative data. **E)** Real time qPCR analysis of *Cbfβ* expression in FACS sorted Venus[+] (V[+]) and Venus[-] (V^{-}) cells derived from day 6 ESC differentiation cultures. Gene expression was normalized to β-*actin* expression (n=3).
Data shown as mean ± SEM, if not stated otherwise. ****p*<0.001.

Supplementary Figure 3. Myeloid potential of *Gata2Venus* ESC derived Venus^{+} cells. Representative photos of CFU-C colonies (left) and May-Grünwald/Giemsa staining of cytospinned colony cells (right) from Venus^{+} cells derived from day 6 or day 12 *Gata2Venus* differentiated ESCs. Objective=4x (left panels), =40x (right panels). CFU-granulocyte, erythrocyte, monocyte, macrophage (GEMM); CFU-granulocyte-macrophage (GM); CFU-macrophage (M); CFU-granulocyte (G); burst-forming-unit erythroid (BFU-E) and CFU-primitive erythroid (EryP). Ed=definitive erythrocyte.

Supplementary experimental procedures

Establishment and maintenance of ESC lines. ESC lines (WT from WT 129/Ola mice, *G2V* from *Gata2Venus* mice (Kaimakis et al. 2016) and *LG* from *Ly6a(Sca1)GFP* mice (de Bruijn et al. 2002)) were established as described by Bryja et al., (2006). Blastocysts were isolated at E3.5 and placed onto irradiated mouse embryonic fibroblasts (MEFs) and cultured in SR-ES medium (Knockout DMEM supplemented with 20% Knockout Serum Replacement (Gibco), 1% penicillin/streptomycin (P/S) (Gicbo), 2 mM L-glutamine (Gicbo), 1x NEAA (Gibco), 100 mM β-mercaptoethanol (Sigma) and recombinant mouse LIF (1000 U/ml) (Chemicon International)). After an attachment phase of 2 days, the medium was changed every two days to allow for expansion of the inner cell mass (ICM). After sufficient outgrowth, the ICM was trypsinized and transferred to a 12-well format coated with inactivated MEFs. Afterwards, the ESCs were maintained in DMEM (Lonza) + 15% FBS (HyClone), 2mM GlutaMAX, 1mM Na-pyruvate, 1% P/S, 50µM β-mercaptoethanol (all Gibco), 0.1mM NEAA (Lonza) and 1000U/ml LIF (Sigma) at 37°C in the presence of 5% CO_2.

Protein extraction and Western Blotting. Cells were washed 2x with PBS and re-suspended in ice cold RIPA buffer + protease and phosphatase inhibitors (Thermo Fisher) and incubated for 30 minutes on ice. Samples were homogenized by sonication and centrifuged at 13 000 rpm for 15 minutes, total protein in the supernatant was quantified using BSA kit (BioRad) following the manufacturer's instructions. Total protein concentration was calculated based on a BSA standard curve. Equal amounts of protein for each sample were boiled (95°C for 5 minutes) in SDS sample buffer (BioRad). Proteins were separated in SDS-polyacrylamide gel (NuStep) and blotted for 30 minutes at 20 volts on a nitrocellulose membrane (Amersham). The membrane was blocked with 5% semi-skimmed milk in TBS-Tween 20 (TBS-T) immunostained overnight at 4°C in 2.5% semi-skimmed milk in TBS-T. After 3 x 5 minute washes with TBS-T the membrane was immunostained with secondary antibody at RT for 1 hour. Membranes were analyzed with Odyssey FC (Li-Cor) using Image Studio Lite™ (Li-Cor) software. Used antibodies are listed in Supplementary Table 1.

Whole mount staining and confocal imaging. Fixing: EB were washed with PBS, fixed in PBS + 2% PFA (Sigma) for 10 minutes on ice following triple washing in PBS for 10 minutes on ice. Dehydration: dehydration was performed 1x in 50% methanol + PBS and 2x in 100% methanol on ice for 10 minutes. Rehydration: EBs were incubated 1x in 1:1 methanol + PBS and 1x in 100% methanol on ice for 10 minutes and washed 1x with cold PBS on ice for 10 minutes. Blocking: EBs were incubated in PBS + 1% semi skimmed milk + 0.005% Tween X100 (Sigma) (PBS-MT) + 10% bovine serum albumin (BSA) (Sigma) and 0.1% goat serum on ice for 4-6 hours. Primary and secondary antibody incubations were performed overnight at 4°C in PBS-MT solution following 3x washing with PBS-MT on ice each for at least 2 hours. Dehydration: EBs were rinsed in PBS-T and incubated for 10 minutes on ice first in 1:1 methanol/PBS and then in 100% methanol. Clearing and mounting: EBs were transferred onto a fast well and washed 4 x for 30 seconds in 100% methanol following clearing first 4x for 30 seconds in 1:1 benzyl alcohol + benzyl benzoate (BABB) + methanol following in 100% BABB. Fast well was covered with coverslip and EBs were imaged in 100% BABB with Leica SP5 confocal microscope. Antibodies are listed in Supplementary Table 1.

Cytospin and May-Grünwald/Giemsa staining. Single colonies from methylcellulose culture were picked, washed 1x with PBS + 10% FBS. Cells were re-suspended in 50 μl PBS and transferred into sample chamber containing a glass slide. Samples were centrifuged for 5 minutes at 200 rpm. Cells were stained with Rapid Romanowsky Stain Pack kit (TCS Biosciences) according to the manufacturer's protocol. Slides were washed 2x in tap water and examined under Zeiss Axioskop2 microscope.

Supplementary Table 1. Antibody list

FACS antibodies	Provider, cat#	Dilution
CD41-ef450	eBioscience, 48-0411	1:100
CD45-AF700	BioLegend, 103127	1:400
CD31-PE	BD Biosciences, 553373	1:1000
CD16/32-PE	eBioscience, 12-0161	1:200
cKit-APCef780	eBioscience, 47-1171-80	1:800
Flk1-PE	BD Biosciences, 3221709	1:600
Western Blot antibodies		
Gata2	Santa Cruz, sc9008	1:200
Nanog	Chambers lab (Edinburgh) inhouse	1:2000
β-actin	Santa Cruz	1:1000
Whole mount antibodies		
GFP (used for Venus)	MBL, MBL 598	1:2000
CD31-biotin	BD Biosciences, 553371	1:500

Supplementary Table 2. Real time qPCR primer list

qRT-PCR	forward 5'-3'	reverse 5'-3'
β-actin	CACCACACCTTCTTACAATGAG	GTCTCAAACATGATCTGGGTC
Gpr56	TCTGCTCTGGCTTGTGTCTTC	AGGTTCATGTGGACTTTGATGG
Gpr97	CTGGGATATGGCTAAAGGAGAC	AAGGCGAAGAAGGTCAAGTG
Gpr114	TCACTGCTCAATAACTATGTCC	ACTGTATACCCTTCCAGACTC
βH1	AGTCCCCATGGAGTCAAAGA	CTCAAGGAGACCTTTGCTCA
βmajor	CTGACAGATGCTCTCTTGGG	CACAACCCCAGAAACAGACA
Gata1	TGCCTGTGGCTTGTATCA	TGTTGTAGTGGTCGTTTGAC
Runx1	TTTGATGGCTCTATGGTAGGTG	CAGGTAGCGAGATTCAAAGA
Brachyury	TGTCCTCCCTTGTTGCCTTAGAGT	AGTAGGCATGTTCCAAGGGCAGAA
Cbfβ	CAGGAAGATGCATTAGCACAA	AGATCATCACCGCCACCTAA
Fli1	ATGGACGGGACTATTAAGGAGG	GAAGCAGTCATATCTGCCTTGG
Nanog	CACAGTTTGCCTAGTTCTGAGG	GCAAGAATAGTTCTCGGGATGAA
Tal1	TCCCCATATGAGATGGAGATT	ATTGATGTACTTCATGGCAAG
Lyl1	CAGGACCCTTCAGCATCTTC	ACGGCTGTTGGTGAACACTC
Erg	GGCAGCTACATGGAGGAGAA	TATTCTTTCACCGCCCACTC
Lmo2	ATGTCCTCGGCCATCGAAAG	CGGTCCCCTATGTTCTGCTG
Venus	ATCTTCTTCAAGGACGACGG	GGCTGTTGTAGTTGTACTCC

CHAPTER 3

**The Gata2 target gene *Gpr56* is a positive regulator
of hematopoietic differentiation**

Mari-Liis Kauts[1,2], Samanta A. Mariani[2], Carmen Rodriguez Seoane[2] and
Elaine Dzierzak[1,2]

[1] Erasmus Stem Cell Institute, Department of Cell Biology, Erasmus
Medical Center, Rotterdam, The Netherlands
[2] Centre for Inflammation Research, Queen's Medical Research Institute,
University of Edinburgh, Edinburgh, United Kingdom

Work in progress

Introduction

Hematopoietic stem cells (HSC), the cells that provide life-long maintenance of the adult hematopoietic system, are generated via a transdifferentiation process, known as the endothelial to hematopoietic cell transition (EHT) reviewed in Kaimakis et al., (2013). In that stepwise process, specialized vascular endothelial cells, known as the hemogenic endothelial cells (HEC) suppress their endothelial program to turn on the hematopoietic identity. In mice, the first HSCs are generated in the aorta-gonad-mesonephros (AGM) region at embryonic day (E) 10.5 (Medvinsky and Dzierzak, 1996; Muller et al., 1994). Their development is temporally associated with the appearance of hematopoietic clusters in the endothelium of the dorsal aorta (de Bruijn et al., 2000; Garcia-Porrero et al., 1995; North et al., 1999). Vital imaging of the mouse embryonic aorta at the time of the first HSC emergence has revealed the transition of morphologically flat endothelial cells into round hematopoietic cells that are bulging out from the wall of the aorta into the lumen (Boisset et al., 2011). The use of elegant tracing methods supported by transplantation of stringently enriched populations, have provided further evidence of the endothelial origin of the HSCs (Chen et al., 2009; de Bruijn et al., 2002; North et al., 2002; Zovein et al., 2008). The emergence of round hematopoietic cells from flat endothelial cells has also been observed in the zebrafish model, thus suggesting that the development of HSCs through EHT is a process that is conserved between vertebrate species (Bertrand et al., 2010; Kissa and Herbomel, 2010).

Several markers/the combination of different markers has facilitated studies examining the emergence of HSCs. The appearance of newly generated HSCs via EHT has been visualized in the *Ly6a (Sca1) GFP* fluorescent reporter transgenic embryos. GFP reporter marks all embryonic and adult HSCs (Chen et al., 2011; de Bruijn et al., 2000; Li et al., 2016; Ma et al., 2002; Ottersbach and Dzierzak, 2005), therefore, serves as an excellent reporter for observing the emergence of HSCs. Vital time-lapse imaging of thick *Lya6A-GFP* E10.5 embryo sections, that were immunostained with endothelial (CD31) and hematopoietic (cKit, CD41) markers, revealed the bulging of some GFP$^+$cKit$^+$CD41$^+$ cells into the lumen of the aorta. They were directly transdifferentiating from the CD31$^+$GFP$^+$ cells, where GFP specifically distinguished the HECs from other endothelial cells, thus revealing the EHT process in real time (Boisset et al., 2011).

Although marker expression of cells going through EHT has given some insight into this process, and allows for the enrichment of emerging HSCs, the precise molecular program of each step in this process has not been characterized extensively. Thus, it is as yet unclear what drives the emergence of HSCs from HECs. A recent transcriptome sequencing of the *Ly6A-GFP* E10.5 AGM sorted EHT cell subsets (endothelial cells, CD31$^+$GFP$^-$; HECs, CD31$^+$GFP$^+$; differentiated hematopoietic cells, CD31$^+$cKit$^+$GFP$^-$ and HPCs/HSCs, CD31$^+$cKit$^+$GFP$^+$) has identified 530 differentially expressed genes. *Gpr56* was identified as the top differentially expressed novel gene in the HEC to HSC transition (Solaimani Kartalaei et al., 2015). As a surface receptor, is it of interest to study as a candidate signaling molecule involved in EHT.

Gpr56 is a member of the largest family of cell surface receptors that mediate various external stimuli as well as signals from other cells. The G protein coupled receptors (GPCR) share a conserved seven transmembrane (7TM) polypeptide chain and use a trimeric GTP-binding protein (G protein) to relay the signal to intracellular target proteins (Rosenbaum et al., 2009) (Figure 1). About 150 genes encode for orphan GPCRs,

meaning that their ligands are unknown. The largest group of orphan GPCRs is the adhesion receptor group. Adhesion GPCRs have an extremely long N-terminal tail that almost always contains a GPCR proteolytic site (GPC) motif (Paavola and Hall, 2012). The GPC site harbors similarities with known self-cleaving domains proteins (Paulus, 2000). The physiological significance of the large N-terminus remains largely unknown, however, mutations in it often result in disease (Piao et al., 2004). Interestingly, it has been shown that removal of the N-terminus causes the constitutive activation of adhesion GPCRs (Paavola et al., 2011; Ward et al., 2011).
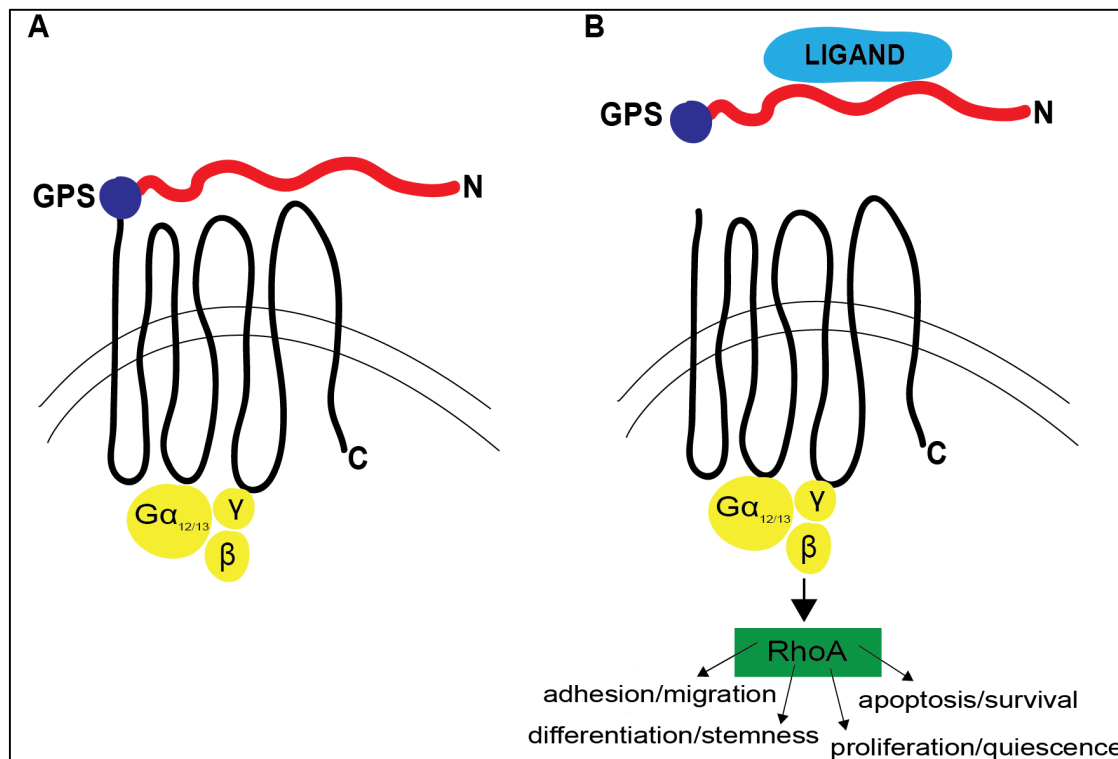
Figure 1. Schematic illustration of the Gpr56 structure and proposed activation mechanism. A) Gpr56 has a conserved seven transmembrane (7TM) polypeptide region (black) and a long N-terminal tail (red). Gpr56 uses trimeric GTP-binding protein (G-protein, yellow) to relay the signal. The long N-terminal tail is cleaved from the 7TM region at the GPCR proteolytic site (GPS, blue), but the two halves of the receptor remain non-covalently associated, and the receptor is inactive. **B)** The binding of the N-terminal tail by an adhesive ligand (such as Collagen III) (Luo et al., 2011a) (turquoise) can lead to receptor's conformational changes causing the removal of the N-terminal tail from the 7TM region leading to the induction of receptor signaling via activation of RhoA. Gpr56 expression and signaling has been associated with several functions, such as cell migration/adhesion, apoptosis/survival, proliferation/quiescence and differentiation/stemness (Saito et al., 2013; Shashidhar et al., 2005; Xu et al., 2006; Xu and Hynes, 2007; Yang et al., 2011; Solaimani Kartalaei et al., 2015).

Gpr56 is one of the approximately 30 orphan adhesion GPCRs (Langenhan et al., 2013). Gpr56 function is mainly studied in the context of brain development, as its high expression has been observed in the developing mouse neocortex and neural stem cells, where the RhoA dependent activation leads to actin fiber reorganization and suppression of their migration (Bae et al., 2014; Iguchi et al., 2008; Piao et al., 2004). Mutations in Gpr56 cause a severe brain malformation known as the bilateral frontoparietal polymicrogyria (BFPP). Gpr56 is required for normal oligodendrocyte development as loss of Gpr56 impairs axon myelination through impaired oligodendrocyte maturation (Ackerman et al., 2015; Giera et al., 2015). The expression levels of *Gpr56* have been correlated with several cancer types and their progression. It has been proposed that

Gpr56 acts as a tumor growth suppressor, as its downregulation leads to melanoma metastasis (Xu et al., 2006). On the other hand, high *Gpr56* levels have also been shown to induce melanoma progression (Ke et al., 2007). Furthermore, high *Gpr56* expression levels have been found in epithelial ovarian cancer patients (Liu et al., 2017), in glioma cells where they induce growth and metastasis (Shashidhar et al., 2005) and in leukemic stem cells contributing to acute myeloid leukemia (AML) progression (Daria et al., 2016). Gpr56 has been identified as a candidate target molecule of the ectopic viral integration site-1 (EVI1) transcription factor positive AML cells, where it regulates cell adhesion and anti-apoptotic function (Saito et al., 2013). EVI1 positive cancers are known for their poor prognosis and clinical outcome (Barjesteh van Waalwijk van Doorn-Khosrovani et al., 2003). Thus Gpr56 serves as a potential drug target. The role of Gpr56 in different diseases is mainly associated with adhesion and cell migration, however, the precise function seems to be cell type specific.

Gpr56 has been suggested to interact with several extracellular molecules, such as tetraspanins (CD9, CD81) and a major ECM crosslinking protein transglutaminase 2 (TG2) (Xu et al., 2006). The biological meaning of the interactions with tetraspanins is still unknown. The Gpr56-TG2 interaction has been proposed to be anti-metastatic and suppress the growth of tumor cells (Xu and Hynes, 2007; Yang et al., 2011). Another proposed binding partner is Collagen III, which in the development of cerebral cortex, binds to the N-terminus of Gpr56, resulting in the coupling to $G\alpha_{12/13}$ and the activation of RhoA pathway (Luo et al., 2011b). Collagen III is the major collagen in connective tissues. The homozygous deletion of the *Collagen III* encoding gene in mice (*Col3a1*) results in perinatal lethality in 90% of the mice caused by the rupture of the major blood vessels (Liu et al., 1997) as seen in patients with type IV Ehlers Danlos syndrome (Pope et al., 1975), and cobblestone-like malformation of the cerebral cortex (Bahi-Buisson et al., 2010) a highly similar phenotype to the *Gpr56* knockout mice (Li et al., 2008). Besides the central nervous system, Collagen III binds Gpr56 in pancreatic β-cells, where it is required for normal β-cell function (Duner et al., 2016). Whether any of these ligands act as Gpr56 activators in hematopoietic cells, remains to be addressed.

The expression of *Gpr5*6 in HSC has been reported long ago (Terskikh et al., 2001), however its function in hematopoietic development is largely unexplored. Studies with *Gpr56* knockdown mice have given insight into Gpr56 requirement for HSC biology. Saito *et al* has detected decreased bone marrow HSC numbers and impaired HSC reconstitution ability in the *Gpr56*^{-/-} mice suggesting that Gpr56 is involved in the maintenance of the adult HSC quiescence and in the interactions with the bone marrow niche (Saito et al., 2013). On the other hand, although Rao et al detected *Gpr56* mRNA expression in the E11 AGM and E14 fetal liver HSCs by quantitative RT-PCR, their functional studies with *Gpr56*^{-/-} derived embryonic HSCs revealed no hematopoietic defects or significant differences in the potential of HSCs (Rao et al., 2015). It is important to note that the strategy to generate *Gpr56*^{-/-} mouse model aimed to delete exons 2 and 3, which harbor translational start sites. However, murine *Gpr56* has an alternative splice variant (S4) translated from exon 4. Thus, it is possible that the *Gpr56*^{-/-} mice have residual Gpr56 protein expression that is sufficient to overcome profound hematopoietic defects (Rao et al., 2015). Corroborating with the *Gpr56* expression pattern in HSCs detected by Rao *et al*, in situ hybridization by us shows *Gpr56* expression in the Ly6A-GFP[+] E10.5 AGM hematopoietic cells (Solaimani Kartalaei et al., 2015). Knockdown experiments in zebrafish show that phenotypic HPCs/HSCs are abolished upon *Gpr56*

morpholino injection and this phenotype is rescued by mouse and human *Gpr56* cDNA injection (Solaimani Kartalaei et al., 2015). Thus these data strongly suggest that Gpr56 signaling axis functions in the development of definitive hematopoiesis, however, its precise role and temporal requirement remains to be explored.

In this study, we take advantage of a novel *Gata2Venus* (*G2V)* reporter mouse embryonic stem cell (ESC) model, that allows the isolation of live Gata2$^+$ cells by Venus fluorochrome expression, to investigate the requirement of Gpr56 in early hematopoiesis. ESCs serve as a valuable tool to recapitulate aspects of early embryonic development, including EHT (Lancrin et al., 2009; Tamplin et al., 2015). The *Gata2* transcription factor belongs to the heptad transcription complex of hematopoietic transcription factors (Wilson et al., 2010) that function as transcriptional hubs for the progression of EHT. In the mouse genome, there is a heptad factor consensus region located 37 kb upstream of the *Gpr56* translational start site (Gpr56-37 enhancer) and enrichment of Gata2 and the heptad factors has been indicated at the Gpr57-37 enhancer (Solaimani Kartalaei et al., 2015). Also, Gpr56 expression is negatively affected upon the deletion of *Gata2* regulatory element (+9.5 cis element) that is required for the generation of HSCs (Gao et al., 2013). Previous studies by us and others demonstrate that the *Gata2* transcription factor has a pivotal role in hematopoiesis (de Pater et al., 2013; Kaimakis et al., 2016; Ling et al., 2004; Rodrigues et al., 2005; Tsai et al., 1994; Tsai and Orkin, 1997). Our lab generated a *G2V* reporter knock-in mouse model and found that all AGM HSCs and most hematopoietic progenitor cells (HPC) are Venus$^+$ (Kaimakis et al., 2016). By differentiating *G2V* ESCs, we have shown that G2V expression facilitates the isolation of all functional HPCs generated in the ESC differentiation culture (Kauts *et al.,* submitted). As *Gpr56* is a downstream target of *Gata2,* the novel *G2V* hematopoietic reporter ESC line serves as an advantageous tool to study the role of Gpr56 in hematopoietic development. Here we show that Gpr56 is increasingly expressed during hematopoietic commitment of ESCs and suggest that Collagen III, the putative ligand of Gpr56, serves as a positive regulator of hematopoiesis, possibly via Gpr56 signaling. Our studies with Gpr56 knockout ESCs reveal a functional redundancy between Gpr56 and Gpr97, and demonstrate that Gpr56 is required for the generation of multipotent hematopoietic progenitors.

Materials and methods

Maintenance of ESC lines. WT and *G2V* (derived as described in (Kaimakis et al., 2016)) ESC lines (129/Ola background) were maintained on gelatinized tissue culture plates in a 12-well format on mouse embryonic feeders (MEF) in DMEM (Lonza) + 15% FBS (HyClone), 2mM GlutaMAX, 1mM Na-pyruvate, 1% P/S, 50µM β-mercaptoethanol (all Gibco), 0.1mM NEAA (Lonza) and 1000U/ml LIF (Sigma) at 37°C in the presence of 5% CO_2. Cell medium was refreshed daily and cells were passaged by trypsinization every other day.

Establishment of G2V hematopoietic reporter GPCR knockout cell ESC lines:

CRISPR/Cas9 technology. CRISPR/Cas9 technology was performed as described in (Ran et al., 2013). Guide RNAs (gRNA) (sequences listed in Supplementary Table 1) were designed to target the exon 2 of the *Gpr56* and *Gpr97* genes, and exons 1+2 in *Gpr114* (Supplementary Fig1). BbsI cohesive ends were added on the 5' of each strand. The insert gRNA duplex was prepared by annealing, followed by ligation into the pSpCas9(BB)-2AGFP (PX458, Addgene) vector. Bacterial transformation was performed followed bacterial plasmid DNA isolation (miniprep). Correct gRNA integration was tested by BbsI restriction (BbsI site is lost after successful integration) and positive clones were sequenced. Clones with correct integration were subjected to high yield bacterial DNA isolation (maxiprep).

ESC transfection. Gata2Venus ESC transfection was performed using DreamFectStem (Oz Biosciences) according to manufacturer's instructions. The cells were seeded on MEFs on a 24-well plate one the day before the transfection. On the day of transfection, medium was changed to growth medium with no P/S and +5% FBS. 0.5 µg of total Psp-Cas9-2A-GFP plasmid containing preferred gRNA, combination of different gRNAs or no gRNA for Gpr56-97-115 wild type control, was added to 50 µl DMEM and mixed with another 50 µl of DMEM containing 2 µl of DreamFectStem and incubated at RT for 20 minutes. The mixture was then added dropwise to the cells. Medium was changed to full growth medium after 4-6 hours. Following 48-72 hours, cells were harvested by trypsinization and single GFP expressing cells were FACS sorted onto 96-well plate containing MEFs. After approximately 5 days of culture, single colonies were trypsinized and transferred to a 12-well plate. After extra 5 days of culture, the cells were split into a 6-well plate. When the well reached 80% confluency, ½ of the cells were harvested for protein analysis, ¼ for RNA analysis and the rest was frozen down and stored in liquid nitrogen. Following protein and RNA analysis, clones with desired gene/protein expression profile were subjected to karyotyping.

ESC differentiation. ESC differentiation was performed as described in (Keller et al., 2002). ESCs were harvested by trypsinization and MEF depleted by incubating in IMDM + 15% FSC (HyClone) + 1 % P/S (Gibco) for 30 minutes. EB formation was induced by culturing 25 000 cells/ml on a shaker at 40 rpm. On day 3, the EB medium containing IMDM +15% FBS (HyClone), +1% P/S, 2mM GlutaMAX (Gibco), 50 µg/ml ascorbic acid (Sigma), 4×10^{-4} M monothgioglycerol (Sigma), 300 µg/ml transferrin (Roche) was supplemented with 5% proteome free hybridoma medium (Gibco). From day 6 onwards, 100 ng/ml SCF, 1 ng/ml IL-3 and 5 ng/ml IL-11 were added and cell medium including fresh cytokines was changed every other day. Y-27632 inhibitor (at concentration of

10µM) and Collagen III (at concentration of 0.84nM or 8.4nM, as indicated) treatments were started at day 4 of culture, fresh reagents were added every other day.

FACS analysis/sorting. EBs were washed 1x with PBS and incubated in TrypLE Express (Gibco) at 37°C for 3-5 minutes. Enzyme was deactivated by adding PBS + 10% FBS + 1% P/S and homogenous single-cell suspension was obtained by re-suspending with a P1000 pipette or mechanically crushing the EBs on a nylon mesh. G2V expression could be readily detected in the cells. cKit-PE antibody (BD Biosciences, dilution 1:600) staining was performed on ice for 30 minutes at a concentration of 10^6 cells/100 µl. Dead cells were excluded with Hoechts33342 (Invitrogen). Cells were sorted on FACS Aria III SORP or Fusion. Data analysis was performed with FlowJo software (Tree star).

RNA isolation, cDNA preparation, real-time qRT-PCR. RNA was isolated using RNeasy micro kit (Qiagen). cDNA was synthesized using oligo-dT (Invitrogen) and SuperScript III (Life Technologies) according to manufacturer's protocol. qRT-PCR was performed using Fast Sybr Green master mix (Life Technologies) according to manufacturer's instructions. Primers are listed in Supplementary Table 2.

Protein extraction and Western Blotting. Cells were washed 2x with PBS and re-suspended in ice cold RIPA buffer + protease and phosphatase inhibitors (Thermo Fisher) and incubated for 30 minutes on ice. Samples were homogenized by sonication and centrifuged at 13 000 rpm for 15 minutes, total protein in the supernatant was quantified using BSA kit (BioRad) following the manufacturer's instructions. Total protein concentration was calculated based on a BSA standard curve. Equal amounts of protein for each sample were boiled (95°C for 5 minutes) in SDS sample buffer (BioRad). Proteins were separated in SDS-polyacrylamide gel (NuStep) and blotted for 30 minutes at 20 volts on a nitrocellulose membrane (Amersham). The membrane was blocked with 5% semi-skimmed milk in TBS-Tween 20 (TBS-T) immunostained overnight at 4°C in 1%/1.5%/2.5% (for Gpr97/Gpr56/β-actin detection, respectively) semi-skimmed milk in TBS-T. Incubation for β-actin detection for performed at RT for 2 hours. After 3 x 5 minute washes with TBS-T the membrane was immunostained with secondary antibody at RT for 1 hour. Membranes were analyzed with Odyssey FC (Li-Cor) using Image Studio Lite™ (Li-Cor) software. The following primary antibodies were used: Gpr56 mouse monoclonal (Millipore, dilution 1:250), Gpr97 goat anti mouse (Santa Cruz, dilution 1:1000), β-actin anti-mouse-HRP conjugated (Santa Cruz, dilution 1:1000).

Hematopoietic progenitor assay. For the differentiation of hematopoietic precursors, the Venus[+] population was sorted from day 12 EB derived cells. Sorted cells were plated in methylcellulose medium (Stem Cell Technologies). After 12-14 days in culture, colonies were scored under Zeiss Axiovert25 microscope and results calculated as colonies per 10^4 Venus^{+} cells.

Statistical Analysis. Statistical analysis was performed using an unpaired Student's t test. Results were considered to be statistically significant at p value < 0.05 (*p<0.05, **p <0.01). All data are shown as a mean ± SEM. The number of biological replicates is indicated by the n value. Data analysis was done using GraphPad Prism (GraphPad Software).

Results

Gpr56 expression is specific for ESC-derived hematopoietic cells

We first assessed the expression dynamics of Gpr56 during mouse *G2V* ESC hematopoietic differentiation. Gene and protein expression analysis showed a trend of *Gpr56* transcript (Fig 2A) and Gpr56 protein (Fig 2B) upregulation at day 12 of differentiation culture, suggesting that Gpr56 may function in hematopoietic commitment. To assess whether Gpr56 expression is detected in hematopoietic cells, day 6 (represents primitive hematopoietic cells) and day 12 (definitive) (Kauts et al., submitted) differentiated Venus expressing (Venus$^+$) and non-expressing (Venus$^-$) G2V ESCs were sorted. A significantly higher *Gpr56* transcript expression was found in the Venus$^+$ fraction at day 6, the same trend was observed at day 12 (Fig 2C). Western blot analysis confirmed the profoundly higher Gpr56 protein expression in day 6 Venus$^+$ fraction (Fig 2D). Thus, suggesting that *Gpr56* is specifically expressed in Gata2 expressing cells that possess hematopoietic characteristics.

GPCR signaling affects HPC generation

Gpr56 signals via RhoA by coupling to Gα$_{12/13}$ (Luo et al., 2011a). We used Y-27632, a selective inhibitor of Rho associated protein kinases (ROCK1 and ROCK2) as an antagonist to GPCR to assess Gpr56 requirement in the generation of HPCs. The Y-27632 (10µM) treatment of day 12 differentiated *G2V* ESCs resulted in diminished hematopoietic progenitor potential as described by colony forming unit cell (CFU-C) activity of the Venus$^+$ cells (Fig 2E) (9 fold as compared with untreated sample). Importantly, no bi-or multipotent progenitors were generated upon GPCR inhibition. When the expression of hematopoietic genes *βH1* and *βmajor* (encoding for embryonic and adult globin, respectively) and *Gata1* in the total EB-derived cell population showed a trend of downregulation upon Y-27632 treatment (Fig 2F), the levels of Runx1 were mainly unchanged. Thus, suggesting an involvement of ROCK signaling in HPC and erythroid differentiation.

Collagen III, a putative ligand of Gpr56, is a positive stimulator of ESC hematopoietic differentiation

The ligand of Gpr56 in the hematopoietic system remains to be characterized. It has been proposed that Collagen III (Col III) binds and activates Gpr56 in the neural system (Luo et al., 2011a) and *Col3a1* was found to be most highly expressed in AGM ECs in the RNA Sequencing datasets (Solaimani Kartalaei et al., 2015). Hence, we supplemented the *G2V* ESC differentiation cultures with Col III to assess the hematopoietic cell output at day 12 of culture. A CFU-C assay revealed that an increased number of CFU-Cs were generated when Col III was present (1.4-fold increase as compared to untreated control) (Fig 2E and Supplementary Fig 1), and there was an increase in the bi-and multipotent progenitors (CFU-GM and CFU-GEMM). *Gata1,* and as a result of its function*, βmajor* expression were significantly upregulated upon Col III treatment, whereas *βH1 and Runx1* showed only a slight trend of upregulation. The increased expression of *βmajor, βH1* and *Gata1* was concentration dependent. A role for Col III in the hematopoietic development/differentiation, was also supported by its expression in hematopoietic supportive stromal cell lines (Fig 2G). *Col31a* gene showed high expression in OP9

stromal cells, which have been used efficiently to induce hematopoietic differentiation of pluripotent stem cells and promote EHT (Lynch et al., 2011). AM201B4 and UG261B6 cell lines, derived from the AGM region of mouse embryos, that have been reported to support HSCs but not their generation (Oostendorp et al., 2002a; Oostendorp et al., 2002b), were also found to express *Col31a*, but at lower level. Together, these data suggest that Col III may be a novel dose dependent positive regulator of hematopoiesis, and that hematopoietic induction may occur via the Col III-Gpr56 axis.
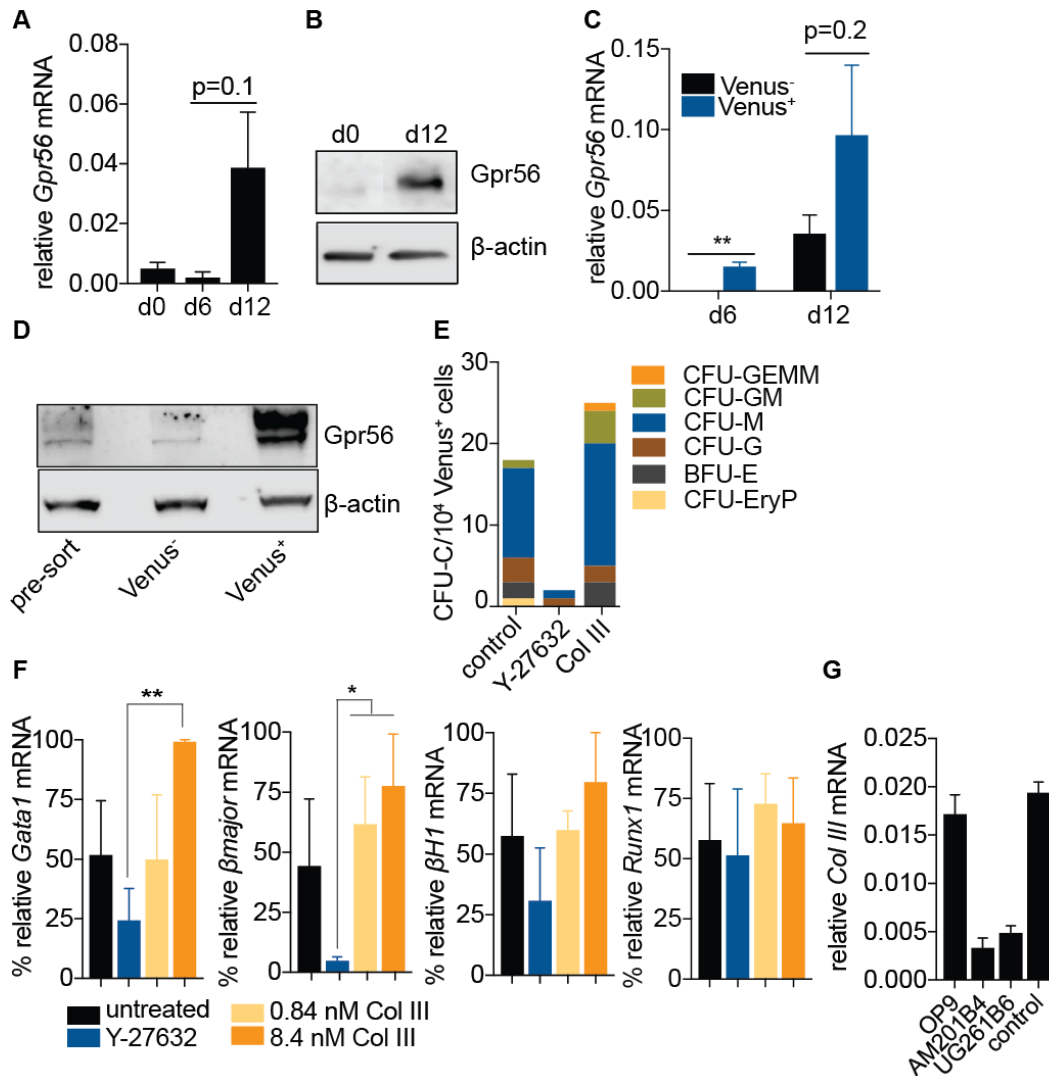
Figure 2. Gpr56 expression in the differentiating ESCs is hematopoietic specific. A) qRT-PCR gene expression analysis of *Gpr56* in undifferentiated day 0 (d0), day 6 and day 12 *Gata2Venus* (*G2V*) ESCs. *Gpr56* expression levels were normalized to *β-actin* (n=3). **B)** A representative Western Blotting analysis of Gpr56 (52kDa) protein expression in undifferentiated (day 0) and day 12 differentiated *G2V* ESCs. β-actin (42 kDa) was used as a loading control. 15 μg of total protein was loaded per lane. **C)** qRT-PCR gene expression analysis of *Gpr56* in Gata2 expressing (Venus⁺) and non-expressing (Venus⁻) fractions flow cytometrically (FACS) sorted from day 6 and day 12 differentiated *G2V* ESCs. *Gpr56* expression levels were normalized to *β-actin* (n=3). **D)** Western Blotting analysis of Gpr56 protein expression in total population (pre-sort), Venus⁺ and Venus⁻ cells FACS sorted from day 6 differentiated *G2V* ESCs. β-actin was used as a loading control. Total protein from 0.7×10^6 cells was loaded per lane (n=2). **E)** Representative hematopoietic colony forming unit-cell (CFU-C) analysis of Venus⁺ cells sorted from day 12 differentiated untreated (control), 10 μM Y-27632 or 0.84 nM Collagen III (Col III) stimulated *G2V* ESCs. CFU-C potential per 10^4 Venus⁺ cells is shown. Colony types are indicated by color. CFU-granulocyte, erythrocyte, monocyte, macrophage (GEMM); CFU-granulocyte-macrophage (GM); CFU-macrophage (M); CFU-granulocyte (G); burst-forming-unit erythroid (BFU-E) and CFU-primitive erythroid (EryP) (n=4). **F)** qRT-PCR gene expression analysis of *Gata1, βmajor* (*adult*

globin), $\beta H1$ (*embryonic globin*) and *Runx1* hematopoietic genes in day 12 differentiated untreated (control), 10 μM Y-27632, 0.84nM Col III or 8.4nM Col III treated *G2V* ESCs. Expression was normalized to β-*actin*, set as 100% for the sample with the highest expression level. Expression levels and % of maximum of other samples were calculated accordingly (n=3). **G)** qRT-PCR gene expression analysis of *Col3a1* in AM201B4 and UG201B6 embryonic cell lines derived from aorta-gonads-mesonephros region (Oostendorp, 2002; Oostendorp, 2002) and in OP9 stromal cell line. Expression in NIH3T3 fibroblastic cell line was used as a positive control. *Col3a1* expression levels were normalized to β-*actin* (n=3).

Gpr56 and *Gpr97* expression is redundant

Our data indicate that ESC hematopoietic differentiation is negatively affected upon GPCR signaling inhibition by Y-27632. To specifically study the role of Gpr56 in hematopoiesis, we took advantage of the *CRISPR/Cas9* technology to delete *Gpr56* in *G2V* reporter ESCs. We generated two clones of Gpr56 KO *G2V* ESCs (56 KO1 and 56 KO2) and 2 clones of mock controls (56 WT1 and 56 WT2). Reduced mRNA expression levels as compared with 56 WT2 cells, and lack of Gpr56 protein in 56 KO1 and 56 KO2 lines was confirmed by qRT-PCR and Western Blotting (Fig 3A-B). Surprisingly, the hematopoietic output, as measured by the frequency of Venus^{+} cells at day 12 of differentiation culture, showed a slight (1.6-fold), but significant increase in the 56 null *G2V* ESCs (56 KO2 vs 56 WT2) (Fig 3C). This was accompanied by significantly higher CFU-C frequency of the Venus^{+} cells (total CFU-C count 3.8 fold higher in 56 KO2 vs 56 WT2) (Fig 3D). These data suggest that Gpr56 could be a negative regulator of hematopoietic differentiation.

Based on previous contradictory data of (Rao et al., 2015), who reported no hematopoietic defects in a Gpr56 KO mouse model; and zebrafish data showing that Gpr56 is a novel positive HSC/HPC regulator (Solaimani Kartalaei et al., 2015), we proposed that the function of Gpr56 may be redundant. In the mouse genome, *Gpr56* is located on chromosome 8, with 2 other adhesion GPCRs: The *Gpr114* located 77 kb upstream and *Gpr97* 48 kb downstream from *Gpr56*. And, importantly, our RNA Sequencing datasets revealed that *Gpr97* (and to a lesser extent *Gpr114*) was upregulated in EHT (Solaimani Kartalaei et al., 2015). To assess, whether the higher CFU-C and Venus[+] hematopoietic cell frequency in the *56* KO cells was observed due to a compensatory mechanism by redundant GPCRs, the *G2V* ESCs were differentiated for 6 days, and Venus[+] and Venus^{-} cells were sorted. qRT-PCR analysis revealed that *Gpr97* showed a profoundly higher expression in the Venus[+] fraction (Fig 3E). Same trend, however, at much lower level, was observed for *Gpr114*. Thus, *Gpr97* (and to lesser extent *Gpr114*) are expressed in the same cells as *Gpr56*. We next analysed whether the levels of these receptors were affected by the deletion of Gpr56 in the total population of undifferentiated 56 KO *G2V* ESCs. qRT-PCR showed a 25-fold *Gpr97* mRNA expression level increase in 56 KO1 and 56 KO2 lines (Fig 3F). No upregulation of *Gpr114* was observed (data not shown) likely due to overall very low expression of *Gpr114* in ESCs, and also in the hematopoietic sites of the mouse embryo (Solaimani Kartalaei et al., 2015). These data suggest that there is a redundancy between *Gpr56* and *Gpr97,* and, that strong compensatory mechanisms leading to higher hematopoietic progenitor output, are seen due to the upregulation of *Gpr97* when *Gpr56* is not present (Fig 2G).
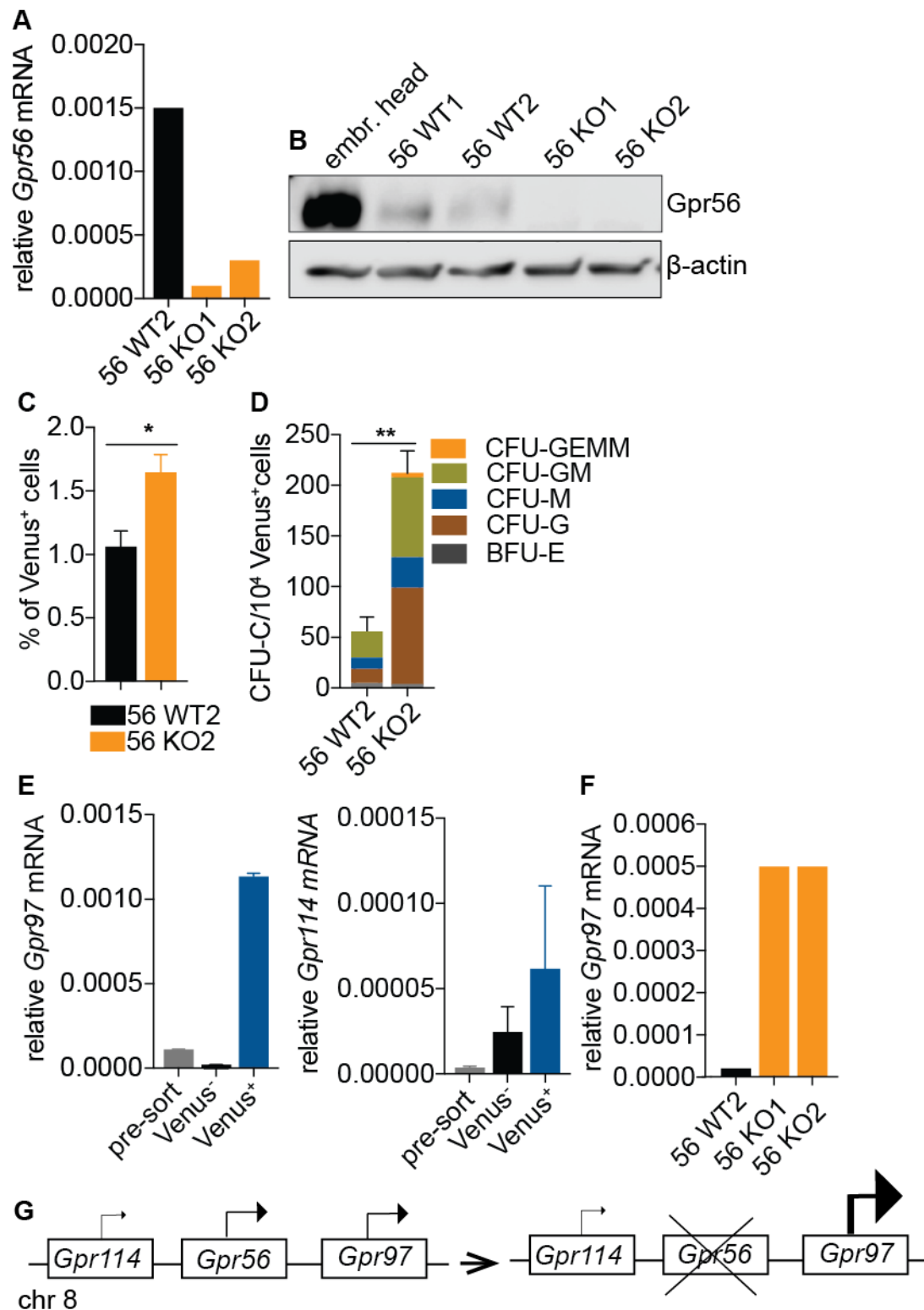
Figure 3. Gpr56 and Gpr97 redundancy. A) A representative qRT-PCR gene expression analysis of undifferentiated *Gata2Venus* (*G2V)* ESCs encoding wild type *Gpr56* gene (56 WT2) that were transfected with Cas9-GFP vector without gRNA, and in 2 clones of *G2V* ESCs that were targeted with Cas9-GFP vector together with *Gpr56* specific gRNA (56 KO1, 56 KO2). *Gpr56* expression levels were normalized to *β-actin.* **B)** A representative Western Blotting analysis of Gpr56 (52kDa) protein expression in embryonic head that was used as a positive control (embr. head) and in two clones of Gpr56 WT and Gpr56 KO *G2V* ESCs. 10 μg of total protein was loaded per lane. β-actin (42 kDa) was used as a loading control. **C)** Frequency of Gata2 expressing (Venus^{+}) cells in day 12 differentiated Gpr56 WT2 and Gpr56 KO2 *G2V* ESCs (n=3). **D)** Hematopoietic colony forming unit-cell (CFU-C) analysis of Venus^{+} cells sorted from day 12 differentiated Gpr56 WT2 and Gpr56 KO2 *G2V* ESCs. CFU-C potential per 10[4] Venus^{+} cells is

shown. Colony types are indicated by color. CFU-granulocyte, erythrocyte, monocyte, macrophage (GEMM); CFU-granulocyte-macrophage (GM); CFU-macrophage (M); CFU-granulocyte (G) and burst-forming-unit erythroid (BFU-E) (n=3). **E)** qRT-PCR gene expression analysis of *Gpr97* and *Gpr114* in total cells (pre-sort), Gata2 expressing (Venus$^+$) and non-expressing (Venus$^-$) cell fractions FACS sorted from day 6 differentiated *G2V* ESCs. *Gene* expression levels were normalized to *β-actin* (n=2). **F)** A representative qRT-PCR gene expression analysis of *Gpr97* in undifferentiated Gpr56 WT2, Gpr56 KO1 and Gpr56 KO2 *G2V* ESCs. *Gpr97* expression levels were normalized to *β-actin*. **G)** A schematic representation of mouse chromosome 8 locus harboring *Gpr56; Gpr97 and Gpr114 genes.* Due to redundancy *by Gpr97*, the deletion of *Gpr56* results in induction of *Gpr97* expression and function.

Gpr56 function is required for normal hematopoietic differentiation

In order to generate *Gpr56* KO cells that lacks the redundant function of other GPCRs at this locus, *Gpr97* and *Gpr114* were deleted. Therefore, we targeted the *G2V* ESCs with guide RNAs specific for *Gpr56*, *Gpr97* and *Gpr114,* to block their protein expression (Supplementary Fig 2). No Gpr56 protein, and reduced levels of Gpr97 protein were found in the KO *G2V* ESCs (56-97-114 KO) as compared with the mock control cells (56-97-114 WT) (Fig 4A). Quantification of Gpr97 protein expression showed 2-fold decreased levels, thus suggesting that the Gpr56-97-114 KO ESCs only have one deleted *Gpr97* allele (Fig 4B). We could not detect Gpr114 protein in Gpr56-97-114 WT cells, and the RNA levels were very low, thus we were not able to confirm whether it was knocked out. Due to very low initial level we neglected its expression/function in further experiments.

We differentiated the Gpr56-97-114 WT and Gpr56-97-114 KO *G2V* ESCs and analysed the hematopoietic cell output. FACS analysis revealed that there were significantly (2-fold) less hematopoietic cells generated at day 12 of differentiation from the Gpr56-97-114 KO *G2V* ESCs as demonstrated by decreased frequency of Venus$^+$ cells (Fig 4C). This is in contrast to the Venus$^+$ cell frequency increase observed in Gpr56 KO cells. Interestingly, we noticed significantly increased frequency of cKit (CD117) expressing cells in the day 12 differentiated Gpr56-97-114 KO *G2V* ESCs as compared to the Gpr56-97-114 WT ESCs (Fig 4D-E) and overall increased viable cell numbers (Fig 4F). When we visually assed the day 12 differentiated EBs generated from Gpr56-97-114 WT, Gpr56 KO2 and Gpr56-97-114 KO cells, the latter failed to show globin expression, which is indicated by red colour of the EBs (Fig 4G), thus, suggesting that erythropoietic differentiation is affected. These data are in line with the decreased globin mRNA levels upon Y-27632 treatment (Fig 2F). Red color was also observed in the 56 KO2 EBs, as expected based on the presence of BFU-E colonies in the day 12 EB derived Venus$^+$ cells (Fig 2D). When we assessed the hematopoietic potential of the generated Venus$^+$ cells, we detected significantly (4.1 fold) lower CFU-C yield. Importantly, there were no bi- or multipotent colonies (CFU-GM; CFU-GEMM) generated from the Gpr56-97-114 KO cells (Fig 4H) demonstrating that hematopoietic progenitor cell generation is abrogated, and most severely affected is the definitive multipotent compartment which represents the cells that are most similar to the HSCs.
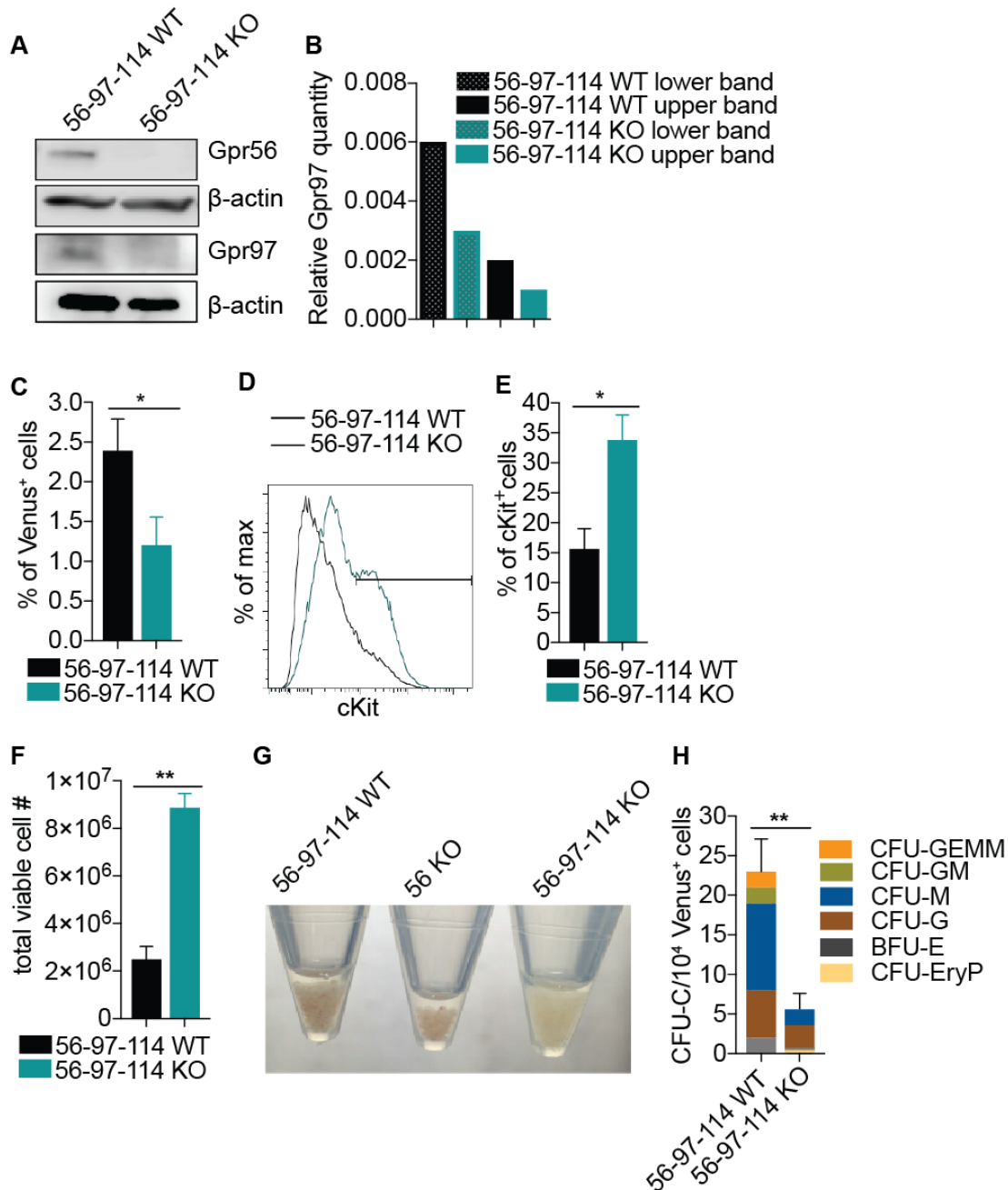
Figure 4. Gpr56 function is required for the generation of multipotent definitive hematopoietic progenitors. A) To generate a triple knockout cell line, we used CRISPR/Cas9 to target *Gpr56, Gpr97* and *Gpr114* genes in the *Gata2Venus (G2V)* reporter ESCs. A representative Western Blotting protein expression analysis of Gpr56 and Gpr97 in undifferentiated *G2V* ESCs encoding wild type *Gpr56*, *Gpr97* and *Gpr114* genes (Gpr56-97-114 WT) that were transfected with Cas9-GFP vector without gRNA, and in *G2V* ESCs with that were targeted with Cas9-GFP vector together with *Gpr56*, *Gpr97* and *Gpr114* specific gRNAs (Gpr56-97-114 KO). β-actin was used as a loading control. 15 μg of total protein was loaded per lane. **B)** Quantification of Gpr97 protein expression in panel A. Values represent Gpr97 protein quantity relative to β-actin expression. **C)** Quantification of Venus expressing cell frequency in day 12 differentiated Gpr56-97-114 WT and Gpr56-97-114 KO *G2V* ESCs (n=6). **D)** Representative FACS histogram of cKit expression in day 12 differentiated Gpr56-97-114 WT (black line) and Gpr56-97-114 KO (green line) *G2V* ESCs. **E)** Quantification of FACS data in panel D, n=4. **F)** Quantification of total live cell number in day 12 differentiated Gpr56-97-114 WT and Gpr56-97-114 KO *G2V* ESCs (n=4). **G)** Representative picture of day 12 differentiated Gpr56-97-114 WT, Gpr56 KO2 and Gpr56-97-114 KO *G2V* ESCs. Red color indicates globin expression. **H)** Hematopoietic colony forming unit-cell (CFU-C) analysis of Venus$^+$ cells sorted from day 12 differentiated Gpr56-97-114 WT and Gpr56-97-114 KO *G2V* ESCs. CFU-C potential per 10^4

Venus^{+} cells is shown. Colony types are indicated by color. CFU-granulocyte, erythrocyte, monocyte, macrophage (GEMM); CFU-granulocyte-macrophage (GM); CFU-macrophage (M); CFU-granulocyte (G); burst-forming-unit erythroid (BFU-E) and CFU-primitive erythroid (EryP) (n=4).

Discussion

Whole transcriptome analysis of EHT provides valuable information to identify the key players in the gene regulatory networks that orchestrate the development of HSCs. A recent RNA Seq dataset revealed *Gpr56* as a possible new positive regulator of HSC/HPC emergence in EHT (Solaimani Kartalaei et al., 2015). Gpr56 signaling in hematopoiesis has been poorly studied and many aspects of its function and regulation remain to be addressed. Here we have taken advantage of a *G2V* reporter mouse ESC line, where the expression of *Gata2* (direct regulator of Gpr56) can be traced by Venus fluorochrome expression. We have previously shown that all functional HPCs are found in the Gata2 expressing fraction, and thus, can be isolated by Venus reporter (Kauts et al., submitted). *In vivo* studies of the midgestation AGM are limited due to the extremely low cell numbers, thus hampering (biochemical) studies, therefore *G2V* reporter ESC line is an advantageous tool to study the involvement and role of Gpr56 in the establishment of HSCs/HPCs.

Consistent with *Gpr56* expression in the HSCs/HPCs (Rao et al., 2015; Saito et al., 2013; Solaimani Kartalaei et al., 2015), we found *Gpr56* to be co-expressed with Gata2^{+} hematopoietic progenitors and its expression upregulated during the commitment of definitive hematopoietic progenitors, therefore supporting the hypothesis that Gpr56 functions as a positive regulator of the HPC/HSC development. The signals which stimulate Gpr56 in the blood cells, are not known. Several interacting partners, including Collagen III, have been suggested, but their signaling has not been studied in hematopoietic cells. Rao *et al.,* reported Collagen III encoding gene *Col3a1* expression by qRT-PCR in the E11 AGM mesenchymal cells (Rao et al., 2015), thus demonstrating the spatiotemporal vicinity of Collagen III to the developing HSCs/HPCs. We detected *Col3a1* expression in other stromal cells that are used as a hematopoiesis inductive environment in embryonic and induced pluripotent stem cell hematopoietic differentiation approaches, further indicating for its possible role as a stimulator of hematopoiesis. Moreover, Collagen III seems to have a positive effect on the hematopoietic differentiation as it induced hematopoietic gene expression in ESC differentiation and increased the definitive hematopoietic potential of Venus^{+} cells. Thus, these data suggest that Collagen III is a positive regulator of hematopoietic differentiation, possibly via the Collagen III-Gpr56 axis. Our further experiments with Gpr56 KO cells aim to confirm the specificity of Collagen III-Gpr56 signaling. Also, biochemical analysis of Gpr56 expressing Venus[+] hematopoietic progenitors will allow us to identify possible new ligands of the Gpr56 receptor that could be used as external stimulators of pluripotent stem cell hematopoietic differentiation in order to establish protocols for the *in vivo* HSC generation.

To investigate the requirement of Gpr56 for the hematopoietic development, we established Gpr56 KO *G2V* reporter ESCs, and to our surprise, found that there were significantly more Gata2 expressing cells generated in their hematopoietic differentiation, and those cells gave rise to 4-fold more definitive hematopoietic colonies. Consistent with our data, Rao et al investigated hematopoiesis in Gpr56^{-/-} mice and did not report negative

effect on embryonic HSC/HPC development, maintenance, or reconstitution ability (Rao et al., 2015). Strikingly, we observed that the expression of another GPCR, *Gpr97* was upregulated in both of our Gpr56 KO ESC clones, demonstrating for the first time a direct redundancy between Gpr56 and Gpr97. Functional redundancy between other adhesion GPRC has been proposed previously. Gpr65, a pH sensing GPCR, has a critical role in glucocortical-induced thymocyte apoptosis (Malone et al., 2004; Tosa et al., 2003), however, Gpr65 KO mice show no immune defects, thus suggesting for a redundancy by other GPCR with similar expression pattern, such as G2A (Radu et al., 2006). Increased *Gpr97* expression was detected during EHT specifically in the HSC compartment (Solaimani Kartalaei et al., 2015). Upon deletion of Gata2 cis-regulatory element at 9.5 kb downstream of its promoter (+9.5 element), *Gpr97* transcript levels were decreased more than 100 fold (Gao et al., 2016). In line with this study, we detected *Gpr97* specifically in the Venus expressing cells, thus suggesting that *Gpr97* and *Gpr56* are expressed in the same hematopoietic cells and upon the deletion of Gpr56, compensatory mechanisms are activated that result in higher progenitor output. Further studies are needed to specify the direct mechanisms activated upon Gpr56 ablation, and whether this phenomenon could be rescued by Gpr56 expression. Also, it is attractive to propose that the compensatory mechanisms caused by functionally redundant Gpr56 and Gpr97 may be the causing the loss of abnormalities in the *Gpr56* KO embryos (Rao et al., 2015). When *Gpr97* was knocked down in *Gpr56* KO ESC, the hematopoietic program was severely abrogated. These data corroborate the proposed redundancy between *Gpr56* and *Gpr97* and demonstrate that *Gpr97* knockdown is sufficient to suppress normal HPC development in the absence of *Gpr56* activity.

Double knockdown of *Gpr56* and *Gpr97* mainly affected the generation of bi- and multipotent progenitor compartment, some unipotent cells were detected, thus suggesting that Gpr56 function may be specifically required for the generation/maintenance of definitive multipotent progenitors. Previously published data suggest that Gpr56 may function in the maintenance of stem cell properties. Overexpression of constitutively signaling *Gpr56* mutant form in neutrophil cell line resulted in a blockage of differentiation, thus demonstrating that Gpr56 is keeping progenitor cells in undifferentiated state (Solaimani Kartalaei et al., 2015). This is in line with Gpr56 activity in adult bone marrow, where it sustains the HSC pool (Saito et al., 2013). Gpr56 seems to have a similar role of sustaining stemness properties also in cancer stem cells, where high *Gpr56* expression in the AML cells has been noted to correlate with higher repopulating activity of the cells (Daria et al., 2016; Pabst et al., 2016). Taken together, these data suggest that lower multipotent CFU-C activity in Gpr56-97-114 KO cell differentiation may be seen due to the abrogated maintenance mechanism of the progenitor/stemness properties in the generated progenitor cells.

Interestingly, we detected increased frequency of cells with high cKit expression in the double knockout cell line. cKit is a receptor tyrosine kinase that is essential for hematopoiesis. It is expressed in HSCs and in lineage progenitor cells and is downregulated in most of the mature lineage cells, except for mast cells that retain high cKit expression. Our hematopoietic progenitor assay data agree with this expression pattern as a complete loss of bi- and multipotent hematopoietic progenitors upon Gpr97 knockdown in the Gpr56 KO cells was observed, however, the CFU-G fraction, which contain mast cells, was only marginally affected. cKit receptor has been reported to directly interact with other growth factor receptors, such as the receptors for GM-CSF,

Epo, IL-7 and IL-33 (Drube et al., 2010; Jahn et al., 2007; Lennartsson et al., 2004; Wu et al., 1995). Thus, one possible way how to explain the higher frequency of cells expressing high cKit levels is that Gpr56 is involved in the maintenance of normal cKit expression levels by directly interacting with cKit receptor. Our ongoing experiments will investigate the Gpr56-cKit interactions and aim to reveal whether one means by which Gpr56 controls hematopoiesis is via cKit regulation.

We detected profoundly increased viable cell counts upon Gpr56-97-114 deletion in the differentiating cells. This may be a secondary effect caused by higher frequency of cKit expressing cells, as SCF-cKit axis regulates cell growth and proliferation. However, stem cells are slowly cycling cells (Fig 2 Chapter 1) and the expression of Gpr56 in stem cells has been associated with the maintenance for their quiescence. Also, Gp56 has been proposed to suppress cancer cell growth *in vivo*. Thus, the higher viable cell number seen in the Gpr56-97-114 KO cells may be seen due to decreased numbers of quiescent stem/progenitor cells and subsequently, higher proportion of proliferating non progenitor/stem cells.

Our study proposes that Gpr56 is involved in the regulation of HPC generation, possibly via Collagen III signaling axis, and reveals a functional redundancy between Gpr56 and Gpr97. Our data suggest that Gpr56 may be involved in the maintenance of stem/progenitor cell properties, however, the precise role of how Gpr56 signaling functions in hematopoietic cells needs further investigation. Gpr56 signaling is activated via the cleavage and additional binding of its long N-terminal tail by an adhesive ligand to relieve the inhibitory influence of the N-terminal tail (Figure 1). The removal of the N-terminus results in the generation of a constitutively active form of Gpr56 (Paavola et al., 2011). Our ongoing experiments aim to generate an ESC line expressing inducible constitutively signaling Gpr56 form to analyze the temporal requirement of Gpr56 signaling for HPC/HSC generation. This approach facilitates studying the downstream pathways that are activated by Gpr56 signaling and potentially, will reveal the mechanism of how Gpr56 functions in EHT to induce HSC/HPC emergence. Moreover, we aim to investigate whether overexpression of Gpr56 has a positive effect on hematopoietic differentiation of pluripotent stem cells, possibly allowing the generation of repopulating HSCs *in vitro,* which has been a long term goal in blood research.

References

Ackerman, S.D., Garcia, C., Piao, X., Gutmann, D.H., and Monk, K.R. (2015). The adhesion GPCR Gpr56 regulates oligodendrocyte development via interactions with Galpha12/13 and RhoA. Nat Commun *6*, 6122.

Bae, B.I., Tietjen, I., Atabay, K.D., Evrony, G.D., Johnson, M.B., Asare, E., Wang, P.P., Murayama, A.Y., Im, K., Lisgo, S.N.*, et al.* (2014). Evolutionarily dynamic alternative splicing of GPR56 regulates regional cerebral cortical patterning. Science *343*, 764-768.

Bahi-Buisson, N., Poirier, K., Boddaert, N., Fallet-Bianco, C., Specchio, N., Bertini, E., Caglayan, O., Lascelles, K., Elie, C., Rambaud, J.*, et al.* (2010). GPR56-related bilateral frontoparietal polymicrogyria: further evidence for an overlap with the cobblestone complex. Brain *133*, 3194-3209.

Barjesteh van Waalwijk van Doorn-Khosrovani, S., Erpelinck, C., van Putten, W.L., Valk, P.J., van der Poel-van de Luytgaarde, S., Hack, R., Slater, R., Smit, E.M., Beverloo, H.B., Verhoef, G.*, et al.* (2003). High EVI1 expression predicts poor survival in acute myeloid leukemia: a study of 319 de novo AML patients. Blood *101*, 837-845.

Bertrand, J.Y., Chi, N.C., Santoso, B., Teng, S., Stainier, D.Y., and Traver, D. (2010). Haematopoietic stem cells derive directly from aortic endothelium during development. Nature *464*, 108-111.

Boisset, J.C., Andrieu-Soler, C., van Cappellen, W.A., Clapes, T., and Robin, C. (2011). Ex vivo time-lapse confocal imaging of the mouse embryo aorta. Nat Protoc *6*, 1792-1805.

Chen, M.J., Li, Y., De Obaldia, M.E., Yang, Q., Yzaguirre, A.D., Yamada-Inagawa, T., Vink, C.S., Bhandoola, A., Dzierzak, E., and Speck, N.A. (2011). Erythroid/myeloid progenitors and hematopoietic stem cells originate from distinct populations of endothelial cells. Cell Stem Cell *9*, 541-552.

Chen, M.J., Yokomizo, T., Zeigler, B.M., Dzierzak, E., and Speck, N.A. (2009). Runx1 is required for the endothelial to haematopoietic cell transition but not thereafter. Nature *457*, 887-891.

Daria, D., Kirsten, N., Muranyi, A., Mulaw, M., Ihme, S., Kechter, A., Hollnagel, M., Bullinger, L., Dohner, K., Dohner, H.*, et al.* (2016). GPR56 contributes to the development of acute myeloid leukemia in mice. Leukemia *30*, 1734-1741.

de Bruijn, M.F., Ma, X., Robin, C., Ottersbach, K., Sanchez, M.J., and Dzierzak, E. (2002). Hematopoietic stem cells localize to the endothelial cell layer in the midgestation mouse aorta. Immunity *16*, 673-683.

de Bruijn, M.F., Speck, N.A., Peeters, M.C., and Dzierzak, E. (2000). Definitive hematopoietic stem cells first develop within the major arterial regions of the mouse embryo. EMBO J *19*, 2465-2474.

de Pater, E., Kaimakis, P., Vink, C.S., Yokomizo, T., Yamada-Inagawa, T., van der Linden, R., Kartalaei, P.S., Camper, S.A., Speck, N., and Dzierzak, E. (2013). Gata2 is required for HSC generation and survival. J Exp Med *210*, 2843-2850.

Drube, S., Heink, S., Walter, S., Lohn, T., Grusser, M., Gerbaulet, A., Berod, L., Schons, J., Dudeck, A., Freitag, J.*, et al.* (2010). The receptor tyrosine kinase c-Kit controls IL-33 receptor signaling in mast cells. Blood *115*, 3899-3906.

Duner, P., Al-Amily, I.M., Soni, A., Asplund, O., Safi, F., Storm, P., Groop, L., Amisten, S., and Salehi, A. (2016). Adhesion G Protein-Coupled Receptor G1 (ADGRG1/GPR56) and Pancreatic beta-Cell Function. J Clin Endocrinol Metab *101*, 4637-4645.

Gao, X., Johnson, K.D., Chang, Y.I., Boyer, M.E., Dewey, C.N., Zhang, J., and Bresnick, E.H. (2013). Gata2 cis-element is required for hematopoietic stem cell generation in the mammalian embryo. J Exp Med *210*, 2833-2842.

Gao, X., Wu, T., Johnson, K.D., Lahvic, J.L., Ranheim, E.A., Zon, L.I., and Bresnick, E.H. (2016). GATA Factor-G-Protein-Coupled Receptor Circuit Suppresses Hematopoiesis. Stem Cell Reports *6*, 368-382.

Garcia-Porrero, J.A., Godin, I.E., and Dieterlen-Lievre, F. (1995). Potential intraembryonic hemogenic sites at pre-liver stages in the mouse. Anat Embryol (Berl) *192*, 425-435.

Giera, S., Deng, Y., Luo, R., Ackerman, S.D., Mogha, A., Monk, K.R., Ying, Y., Jeong, S.J., Makinodan, M., Bialas, A.R.*, et al.* (2015). The adhesion G protein-coupled receptor GPR56 is a cell-autonomous regulator of oligodendrocyte development. Nat Commun *6*, 6121.

Iguchi, T., Sakata, K., Yoshizaki, K., Tago, K., Mizuno, N., and Itoh, H. (2008). Orphan G protein-coupled receptor GPR56 regulates neural progenitor cell migration via a G alpha 12/13 and Rho pathway. J Biol Chem *283*, 14469-14478.

Jahn, T., Sindhu, S., Gooch, S., Seipel, P., Lavori, P., Leifheit, E., and Weinberg, K. (2007). Direct interaction between Kit and the interleukin-7 receptor. Blood *110*, 1840-1847.

Kaimakis, P., Crisan, M., and Dzierzak, E. (2013). The biochemistry of hematopoietic stem cell development. Biochim Biophys Acta *1830*, 2395-2403.

Kaimakis, P., de Pater, E., Eich, C., Solaimani Kartalaei, P., Kauts, M.L., Vink, C.S., van der Linden, R., Jaegle, M., Yokomizo, T., Meijer, D.*, et al.* (2016). Functional and molecular characterization of mouse Gata2-independent hematopoietic progenitors. Blood *127*, 1426-1437.

Kauts, M.L., Kaimakis, P., Hill, U., Cortes, X., Mendez, S., Dzierzak, E. Differentiation of *Gata2Venus* and *Ly6aGFP* reporter embryonic stem cells corresponds to *in vivo* waves of hematopoietic cell generation in the mouse embryo. (submitted)

Ke, N., Sundaram, R., Liu, G., Chionis, J., Fan, W., Rogers, C., Awad, T., Grifman, M., Yu, D., Wong-Staal, F*., et al.* (2007). Orphan G protein-coupled receptor GPR56 plays a role in cell transformation and tumorigenesis involving the cell adhesion pathway. Mol Cancer Ther *6*, 1840-1850.

Keller, G.M., Webb, S., and Kennedy, M. (2002). Hematopoietic Development of ES Cells in Culture. Methods Mol Med *63*, 209-230.

Kissa, K., and Herbomel, P. (2010). Blood stem cells emerge from aortic endothelium by a novel type of cell transition. Nature *464*, 112-115.

Lancrin, C., Sroczynska, P., Stephenson, C., Allen, T., Kouskoff, V., and Lacaud, G. (2009). The haemangioblast generates haematopoietic cells through a haemogenic endothelium stage. Nature *457*, 892-895.

Langenhan, T., Aust, G., and Hamann, J. (2013). Sticky signaling--adhesion class G protein-coupled receptors take the stage. Sci Signal *6*, re3.

Lennartsson, J., Shivakrupa, R., and Linnekin, D. (2004). Synergistic growth of stem cell factor and granulocyte macrophage colony-stimulating factor involves kinase-dependent and -independent contributions from c-Kit. J Biol Chem *279*, 44544-44553.

Li, S., Jin, Z., Koirala, S., Bu, L., Xu, L., Hynes, R.O., Walsh, C.A., Corfas, G., and Piao, X. (2008). GPR56 regulates pial basement membrane integrity and cortical lamination. J Neurosci *28*, 5817-5826.

Li, Z., Vink, C.S., Mariani, S.A., and Dzierzak, E. (2016). Subregional localization and characterization of Ly6aGFP-expressing hematopoietic cells in the mouse embryonic head. Dev Biol *416*, 34-41.

Ling, K.W., Ottersbach, K., van Hamburg, J.P., Oziemlak, A., Tsai, F.Y., Orkin, S.H., Ploemacher, R., Hendriks, R.W., and Dzierzak, E. (2004). GATA-2 plays two functionally distinct roles during the ontogeny of hematopoietic stem cells. J Exp Med *200*, 871-882.

Liu, Z., Huang, Z., Yang, W., Li, Z., Xing, S., Li, H., Hu, B., and Li, P. (2017). Expression of orphan GPR56 correlates with tumor progression in human epithelial ovarian cancer. Neoplasma *64*, 32-39.

Liu, X., Wu, H., Byrne, M., Krane, S., and Jaenisch, R. (1997). Type III collagen is crucial for collagen I fibrillogenesis and for normal cardiovascular development. Proc Natl Acad Sci U S A *94*, 1852-1856.

Luo, R., Jeong, S.J., Jin, Z., Strokes, N., Li, S., and Piao, X. (2011a). G protein-coupled receptor 56 and collagen III, a receptor-ligand pair, regulates cortical development and lamination. Proc Natl Acad Sci U S A *108*, 12925-12930.

Luo, R., Yang, H.M., Jin, Z., Halley, D.J., Chang, B.S., MacPherson, L., Brueton, L., and Piao, X. (2011b). A novel GPR56 mutation causes bilateral frontoparietal polymicrogyria. Pediatr Neurol *45*, 49-53.

Lynch, M.R., Gasson, J.C., and Paz, H. (2011). Modified ES / OP9 co-culture protocol provides enhanced characterization of hematopoietic progeny. J Vis Exp.

Ma, X., de Bruijn, M., Robin, C., Peeters, M., Kong, A.S.J., de Wit, T., Snoijs, C., and Dzierzak, E. (2002). Expression of the Ly-6A (Sca-1) lacZ transgene in mouse haematopoietic stem cells and embryos. Br J Haematol *116*, 401-408.

Malone, M.H., Wang, Z., and Distelhorst, C.W. (2004). The glucocorticoid-induced gene tdag8 encodes a pro-apoptotic G protein-coupled receptor whose activation promotes glucocorticoid-induced apoptosis. J Biol Chem *279*, 52850-52859.

Medvinsky, A., and Dzierzak, E. (1996). Definitive hematopoiesis is autonomously initiated by the AGM region. Cell *86*, 897-906.

Muller, A.M., Medvinsky, A., Strouboulis, J., Grosveld, F., and Dzierzak, E. (1994). Development of hematopoietic stem cell activity in the mouse embryo. Immunity *1*, 291-301.

North, T., Gu, T.L., Stacy, T., Wang, Q., Howard, L., Binder, M., Marin-Padilla, M., and Speck, N.A. (1999). Cbfa2 is required for the formation of intra-aortic hematopoietic clusters. Development *126*, 2563-2575.

North, T.E., de Bruijn, M.F., Stacy, T., Talebian, L., Lind, E., Robin, C., Binder, M., Dzierzak, E., and Speck, N.A. (2002). Runx1 expression marks long-term repopulating hematopoietic stem cells in the midgestation mouse embryo. Immunity *16*, 661-672.

Oostendorp, R.A., Harvey, K.N., Kusadasi, N., de Bruijn, M.F., Saris, C., Ploemacher, R.E., Medvinsky, A.L., and Dzierzak, E.A. (2002a). Stromal cell lines from mouse aorta-gonads-mesonephros subregions are potent supporters of hematopoietic stem cell activity. Blood *99*, 1183-1189.

Oostendorp, R.A., Medvinsky, A.J., Kusadasi, N., Nakayama, N., Harvey, K., Orelio, C., Ottersbach, K., Covey, T., Ploemacher, R.E., Saris, C*., et al.* (2002b). Embryonal subregion-derived stromal cell lines from novel temperature-sensitive SV40 T antigen transgenic mice support hematopoiesis. J Cell Sci *115*, 2099-2108.

Ottersbach, K., and Dzierzak, E. (2005). The murine placenta contains hematopoietic stem cells within the vascular labyrinth region. Dev Cell *8*, 377-387.

Paavola, K.J., and Hall, R.A. (2012). Adhesion G protein-coupled receptors: signaling, pharmacology, and mechanisms of activation. Mol Pharmacol *82*, 777-783.

Paavola, K.J., Stephenson, J.R., Ritter, S.L., Alter, S.P., and Hall, R.A. (2011). The N terminus of the adhesion G protein-coupled receptor GPR56 controls receptor signaling activity. J Biol Chem *286*, 28914-28921.

Pabst, C., Bergeron, A., Lavallee, V.P., Yeh, J., Gendron, P., Norddahl, G.L., Krosl, J., Boivin, I., Deneault, E., Simard, J*., et al.* (2016). GPR56 identifies primary human acute myeloid leukemia cells with high repopulating potential in vivo. Blood *127*, 2018-2027.

Paulus, H. (2000). Protein splicing and related forms of protein autoprocessing. Annu Rev Biochem *69*, 447-496.

Piao, X., Hill, R.S., Bodell, A., Chang, B.S., Basel-Vanagaite, L., Straussberg, R., Dobyns, W.B., Qasrawi, B., Winter, R.M., Innes, A.M*., et al.* (2004). G protein-coupled receptor-dependent development of human frontal cortex. Science *303*, 2033-2036.

Pope, F.M., Martin, G.R., Lichtenstein, J.R., Penttinen, R., Gerson, B., Rowe, D.W., and McKusick, V.A. (1975). Patients with Ehlers-Danlos syndrome type IV lack type III collagen. Proc Natl Acad Sci U S A *72*, 1314-1316.

Radu, C.G., Cheng, D., Nijagal, A., Riedinger, M., McLaughlin, J., Yang, L.V., Johnson, J., and Witte, O.N. (2006). Normal immune development and glucocorticoid-induced thymocyte apoptosis in mice deficient for the T-cell death-associated gene 8 receptor. Mol Cell Biol *26*, 668-677.

Ran, F.A., Hsu, P.D., Wright, J., Agarwala, V., Scott, D.A., and Zhang, F. (2013). Genome engineering using the CRISPR-Cas9 system. Nat Protoc *8*, 2281-2308.

Rao, T.N., Marks-Bluth, J., Sullivan, J., Gupta, M.K., Chandrakanthan, V., Fitch, S.R., Ottersbach, K., Jang, Y.C., Piao, X., Kulkarni, R.N*., et al.* (2015). High-level Gpr56 expression is dispensable for the maintenance and function of hematopoietic stem and progenitor cells in mice. Stem Cell Res *14*, 307-322.

Rodrigues, N.P., Janzen, V., Forkert, R., Dombkowski, D.M., Boyd, A.S., Orkin, S.H., Enver, T., Vyas, P., and Scadden, D.T. (2005). Haploinsufficiency of GATA-2 perturbs adult hematopoietic stem-cell homeostasis. Blood *106*, 477-484.

Rosenbaum, D.M., Rasmussen, S.G., and Kobilka, B.K. (2009). The structure and function of G-protein-coupled receptors. Nature *459*, 356-363.

Saito, Y., Kaneda, K., Suekane, A., Ichihara, E., Nakahata, S., Yamakawa, N., Nagai, K., Mizuno, N., Kogawa, K., Miura, I*., et al.* (2013). Maintenance of the hematopoietic stem cell pool in bone marrow niches by EVI1-regulated GPR56. Leukemia *27*, 1637-1649.

Shashidhar, S., Lorente, G., Nagavarapu, U., Nelson, A., Kuo, J., Cummins, J., Nikolich, K., Urfer, R., and Foehr, E.D. (2005). GPR56 is a GPCR that is overexpressed in gliomas and functions in tumor cell adhesion. Oncogene *24*, 1673-1682.

Solaimani Kartalaei, P., Yamada-Inagawa, T., Vink, C.S., de Pater, E., van der Linden, R., Marks-Bluth, J., van der Sloot, A., van den Hout, M., Yokomizo, T., van Schaick-Solerno, M.L*., et al.* (2015). Whole-transcriptome analysis of endothelial to

hematopoietic stem cell transition reveals a requirement for Gpr56 in HSC generation. J Exp Med *212*, 93-106.

Zovein, A.C., Hofmann, J.J., Lynch, M., French, W.J., Turlo, K.A., Yang, Y., Becker, M.S., Zanetta, L., Dejana, E., Gasson, J.C.*, et al.* (2008). Fate tracing reveals the endothelial origin of hematopoietic stem cells. Cell Stem Cell *3*, 625-636.

Tamplin, O.J., Durand, E.M., Carr, L.A., Childs, S.J., Hagedorn, E.J., Li, P., Yzaguirre, A.D., Speck, N.A., and Zon, L.I. (2015). Hematopoietic stem cell arrival triggers dynamic remodeling of the perivascular niche. Cell *160*, 241-252.

Terskikh, A.V., Easterday, M.C., Li, L., Hood, L., Kornblum, H.I., Geschwind, D.H., and Weissman, I.L. (2001). From hematopoiesis to neuropoiesis: evidence of overlapping genetic programs. Proc Natl Acad Sci U S A *98*, 7934-7939.

Tosa, N., Murakami, M., Jia, W.Y., Yokoyama, M., Masunaga, T., Iwabuchi, C., Inobe, M., Iwabuchi, K., Miyazaki, T., Onoe, K.*, et al.* (2003). Critical function of T cell death-associated gene 8 in glucocorticoid-induced thymocyte apoptosis. Int Immunol *15*, 741-749.

Tsai, F.Y., Keller, G., Kuo, F.C., Weiss, M., Chen, J., Rosenblatt, M., Alt, F.W., and Orkin, S.H. (1994). An early haematopoietic defect in mice lacking the transcription factor GATA-2. Nature *371*, 221-226.

Tsai, F.Y., and Orkin, S.H. (1997). Transcription factor GATA-2 is required for proliferation/survival of early hematopoietic cells and mast cell formation, but not for erythroid and myeloid terminal differentiation. Blood *89*, 3636-3643.

Ward, Y., Lake, R., Yin, J.J., Heger, C.D., Raffeld, M., Goldsmith, P.K., Merino, M., and Kelly, K. (2011). LPA receptor heterodimerizes with CD97 to amplify LPA-initiated RHO-dependent signaling and invasion in prostate cancer cells. Cancer Res *71*, 7301-7311.

Wilson, N.K., Foster, S.D., Wang, X., Knezevic, K., Schutte, J., Kaimakis, P., Chilarska, P.M., Kinston, S., Ouwehand, W.H., Dzierzak, E.*, et al.* (2010). Combinatorial transcriptional control in blood stem/progenitor cells: genome-wide analysis of ten major transcriptional regulators. Cell Stem Cell *7*, 532-544.

Wu, H., Klingmuller, U., Besmer, P., and Lodish, H.F. (1995). Interaction of the erythropoietin and stem-cell-factor receptors. Nature *377*, 242-246.

Xu, L., Begum, S., Hearn, J.D., and Hynes, R.O. (2006). GPR56, an atypical G protein-coupled receptor, binds tissue transglutaminase, TG2, and inhibits melanoma tumor growth and metastasis. Proc Natl Acad Sci U S A *103*, 9023-9028.

Xu, L., and Hynes, R.O. (2007). GPR56 and TG2: possible roles in suppression of tumor growth by the microenvironment. Cell Cycle *6*, 160-165.

Yang, L., Chen, G., Mohanty, S., Scott, G., Fazal, F., Rahman, A., Begum, S., Hynes, R.O., and Xu, L. (2011). GPR56 Regulates VEGF production and angiogenesis during melanoma progression. Cancer Res *71*, 5558-5568.

Supplementary data
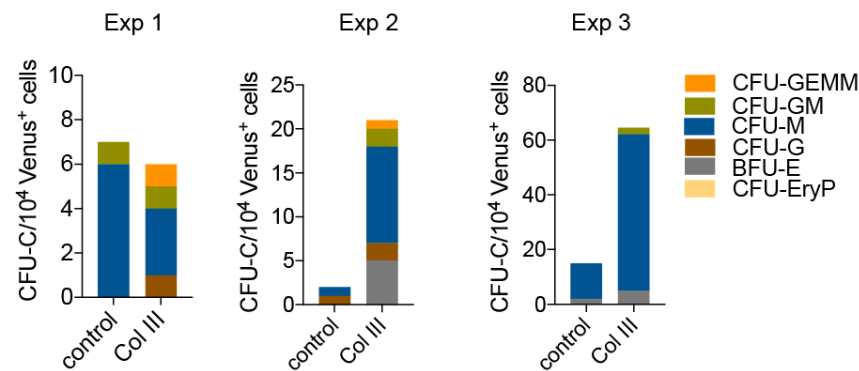
Supplementary Figure 1. Hematopoietic progenitor potential of Collagen III treated G2V ESCs. Hematopoietic colony forming unit-cell (CFU-C) analysis of Venus^{+} cells sorted from day 12 differentiated *G2V* ESCs. Data from 3 biological replicates are presented. Colony types are indicated by color. CFU-granulocyte, erythrocyte, monocyte, macrophage (GEMM); CFU-granulocyte-macrophage (GM); CFU-macrophage (M); CFU-granulocyte (G); burst-forming-unit erythroid (BFU-E) and CFU-primitive erythroid (EryP).
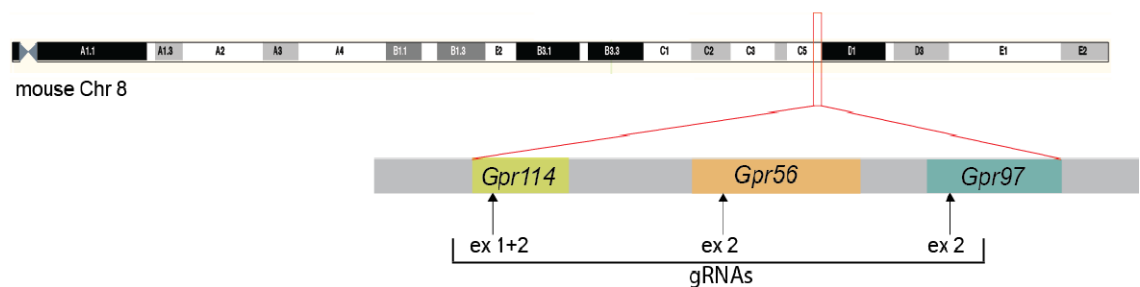
Supplementary Figure 2. Generation of Gp56-97-114 knockout *G2V* ESCs by CRISPR/Cas9 strategy A schematic representation of the *Gpr114*, *Gpr56* and *Gpr97* locus on mouse chromosome 8. Guide RNAs (gRNA) targeting exon 1+2 on *Gpr114* and exon 2 on *Gp56* and *Gpr97* were used to disrupt the locus by Non-Homologous End Joining DNA repair pathway, which may lead to the deletion of the complete locus, or specific fragments, or a frameshift, ultimately causing a loss of Gpr56, Gpr97 and Gpr114 protein expression.

Supplementary Table 1. CRISPR/Cas9 gRNA sequences

Gpr56 exon 2	Top	CACCGTCTGTTGGGTCTGGTTCCGC
	Bottom	AAACGCGGAACCAGACCCAACAGAC
Gpr97 exon 2	Top	CACCGGAATGTCTGCCGTCGGCTTC
	Bottom	AAACGAAGCCGACGGCAGACATTCC
Gpr114 exon 1+2	Top	CACCGCTTGAGCAGCCCGTAGGCCG
	Bottom	AAACCGGCCTACGGGCTGCTCAAGC

Guide RNAs (gRNA) designed to target the exons that harbour ATG start sites in *Gpr56*, *Gpr97* and *Gpr114* genes (top) and their deduced reverse complement sequences (bottom). The gRNA sequences (black) contain overhangs (red) for ligation into the pair of BbsI sites in the pSP-Cas9-A2-GFP plasmid. A G-C base pair (blue) is added at the 5′ end of the guide sequence to facilitate transcription from the U6 promoter that is contained in the pSP-Cas9-A2-GFP plasmid directly upstream from the ligated gRNA sequence.

Supplementary Table 2. qRT-PCR primer sequences

qRT-PCR	forward 5'-3'	reverse 5'-3'
β-actin	CACCACACCTTCTTACAATGAG	GTCTCAAACATGATCTGGGTC
Gpr56	TCTGCTCTGGCTTGTGTCTTC	AGGTTCATGTGGACTTTGATGG
Gpr97	CTGGGATATGGCTAAAGGAGAC	AAGGCGAAGAAGGTCAAGTG
Gpr114	TCACTGCTCAATAACTATGTCC	ACTGTATACCCTTCCAGACTC
βH1	AGTCCCCATGGAGTCAAAGA	CTCAAGGAGACCTTTGCTCA
βmajor	CTGACAGATGCTCTCTTGGG	CACAACCCCAGAAACAGACA
Gata1	TGCCTGTGGCTTGTATCA	TGTTGTAGTGGTCGTTTGAC
Runx1	TTTGATGGCTCTATGGTAGGTG	CAGGTAGCGAGATTCAAAGA
Col3a1	GAATCTGTGAATCATGTCCAACTG	CCACCCATTCCTCCCACTC

CHAPTER 4

An innovative approach to rapidly generate functionally mature mast cells from Gata2 reporter pluripotent stem cells

Mari-Liis Kauts[1,2], Bianca De Leo[2], Polynikis Kaimakis[1], Carmen Rodriguez Seoane[2], Fokion Glykofrydis[2], Helen Taylor[3], Lesley Forrester[3], Adam C. Wilkinson[4], Berthold Göttgens[4], Philippa Saunders[2], and Elaine Dzierzak[1,2*]

*Corresponding author

[1] Erasmus Stem Cell Institute, Department of Cell Biology, Erasmus Medical Center, Rotterdam, The Netherlands
[2] Centre for Inflammation Research, Queen's Medical Research Institute, University of Edinburgh, Edinburgh, United Kingdom
[3] Centre for Regenerative Medicine, University of Edinburgh, Edinburgh, United Kingdom
[4] Wellcome Trust and MRC Cambridge Stem Cell Institute, University of Cambridge, Cambridge, United Kingdom

Abstract

Mast cells are tissue resident immune cells. Aberrant or uncontrolled activation of mast cells can result in a wide range of common, distressing and sometimes life-threatening disorders, including asthma, psoriasis, anaphylaxsis and mastocytosis (Figure 1) (Theoharides et al., 2016; Theoharides et al., 2015). Drug discovery efforts have been hampered by the cell culture systems which have used immature (cancer-derived) cell lines or primary cells that provide low efficiency yield and reproducibility, and require a 12-week culture period before mature mast cells are obtained (Holm et al., 2006; Saito et al., 2006; Shimizu et al., 2002; Wang et al., 2006). To address this problem, we developed a novel method for the rapid and robust production of mature mast cells from pluripotent stem cells (PSC) - which represent an unlimited source. Our protocol utilizes an advantageous *Gata2Venus* reporter (Kaimakis et al., 2016) that marks and enables the isolation of all mast cells and precursors as they are produced from PSCs. Highly proliferating mast cells emerge after less than 2 weeks of culture. These mast cells are fully functional and degranulate after activation. Unlike primary tissue-derived mast cells, this approach will enable the production of sufficient numbers of physiologically relevant human mast cells for high-throughput drug discovery and, in combination with patient-specific iPSCs, the study of mast cell-associated hematological disorders, thus opening the field for personalized medicine.
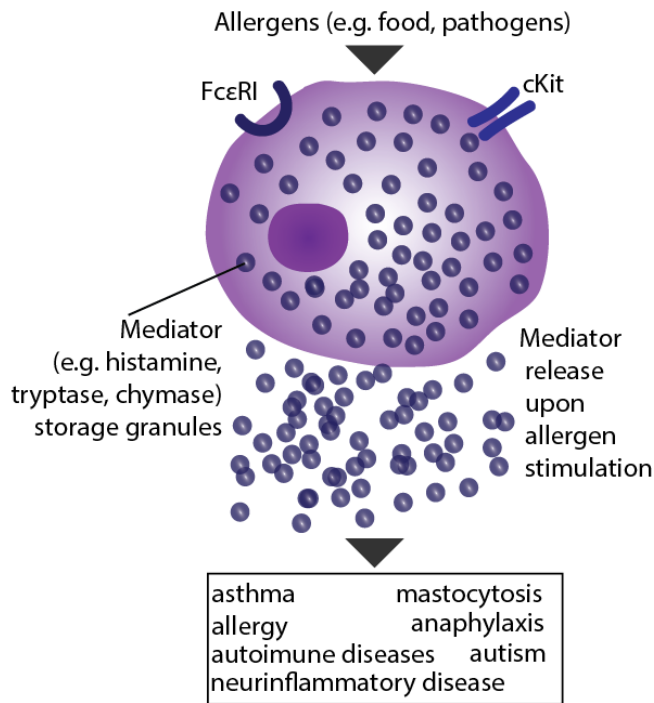
Figure 1. Mast cell activation. Mast cells are white blood cells that play a key role in inflammatory processes (Theoharides et al., 2016; Theoharides et al., 2015). They express ckit (CD117) and FcεRIα (IgE high affinity receptor) and contain cytoplasmic granules rich in proteases. When they are activated by an allergen, degranulation is triggered resulting in chemical mediator release and inflammation.

Results

Mast cells are the key effectors in common immunological disorders affecting worldwide populations. These include allergies, autism, asthma, eosinophilic esophagitis, celiac disease, mastocytosis, atopic dermatitis and psoriasis. To date, treatment options focusing on the modulation of mast cells are limited and development of new therapies are hampered by challenges in generating sufficient phenotypically mature mast cells for biomedical discovery and drug screening (Holm et al., 2006; Saito et al., 2006; Shimizu et al., 2002; Wang et al., 2006). Currently, direct isolation of mast cells is inefficient and results in an altered phenotype. The *ex vivo* generation of mast cells from blood precursors involves extended culture periods, expensive reagents and low/variable yields (Table 1).

Pluripotent stem cells (PSC) offer an alternative source for obtaining mature mast cells for research. However, the published protocols are again laborious and time-consuming, as mast cells emerge after extensive 4-8 weeks of mouse ESC culture (Moller et al., 2007; Tsai et al., 2002; Westerberg et al., 2012) and only after 10 weeks of human ESC culture (Kovarova et al., 2010) (Table 1). Further prolonged culture is needed to increase mast cell yield, as the cells are cumulatively harvested, and do not enable prompt production of large numbers of mast cells. Thus, the lack of an efficient protocol to rapidly obtain large numbers of mature mast cells for research has severely hampered drug development and progress in understanding and treating mast cell-related disorders. Here we report a novel method for the rapid (12-14 days) and abundant production of functionally mature mast cells from PSCs (mouse and human) that relies on a *Gata2Venus* (*G2V*) reporter.

Table 1. Duration of cultures used for mast cell generation from different cell/tissue sources.

Source	Culture time	Ref
hPB	12 weeks	(Saito et al., 2006; Wang et al., 2006)
hCB	12 weeks	(Holm et al., 2006)
hBM	12 weeks	(Shimizu et al., 2002)
WT mESC	4-8 weeks	(Moller et al., 2007; Tsai et al., 2002; Westerberg et al., 2012)
WT hESC	10 weeks	(Kovarova et al., 2010)
G2V mESC	14 days	This study
G2V hESC/iPSC	12 days	This study

Duration of cultures for human mast cell generation from progenitors isolated from primary tissue sources such as peripheral blood (hPB), cord blood (hCB) and bone marrow (hBM) and from wild type (WT) and *Gata2Venus* (*G2V*) reporter mouse embryonic stem cells (mESC) and human ESC (hESC) or induced pluripotent stem cells (iPSC).

The rationale for this reporter is that the Gata2 transcription factor is highly expressed in mast cells (Jippo et al., 1996) and its expression is essential for mast cell precursor development (Tsai and Orkin, 1997), expansion (Tsai and Orkin, 1997), and the function of mature mast cells (Masuda et al., 2007). We have previously shown that Venus reporter expression in the mouse G2V ESCs (Kauts et al., submitted) and embryos (Kaimakis et al., 2016) mirrors that of Gata2 without affecting its expression levels, and that Gata2 is expressed in all hematopoietic stem cells (HSC) and progenitors (HPC) (Kaimakis et al., 2016). Gata2 is downregulated when immature HPCs differentiate into mature lineage cells, with the exception of mast cells, thus making it a specific reporter for this lineage.

Our recent data show that all the functional erythroid-myeloid progenitors (EMPs) generated in the G2V ESC differentiation cultures are Gata2-expressing and the highest frequency of EMPs is found at day 10 of culture (Kauts et al., submitted). To induce EMP development, mouse G2V ESCs were differentiated to embryoid bodies (EB) for 10 days (Fig 2A). Venus+ cells were sorted (1.6 % of total live EB-derived cells) and cultured on a monolayer of OP9 stromal cells (Fig 2B). The average number of Venus+ cells obtained from day 10 EBs (starting ESC number=3×10^4) was 1.5 ± 0.3 $\times10^4$ (Suppl Table 1). After 2-3 days, round non-adherent hematopoietic cells appeared in the co-culture (Fig 3A) and after 4 days, 37 ± 6.8 % of the cells expressed high levels of Venus (Fig 2C). Only Venus+ cells specifically co-expressed the pan-leukocyte receptor CD45. 99 ± 0.6 % of the Venus+CD45+ cells were positive for the cKit (CD117) HSC, HPC and mast cell marker (Fig2C-D) and 84 ± 3.8 % of the Venus+CD45 +cKit+ cells were expressing the high affinity IgE immunoglobulin receptor 1α (FceRIα), a mast cell and basophil marker (Fig 2C-D). Whereas 5.7 ± 3.5 % of the Venus- cells were expressing low levels of cKit, none of the cells had acquired FcεRIα expression (Fig 2C, lower left panel). These data demonstrate that the great majority of Venus+ cells have acquired a mast cell phenotype after 4 days of OP9 co-culture and this phenotype is specific only for Venus-expressing cells.
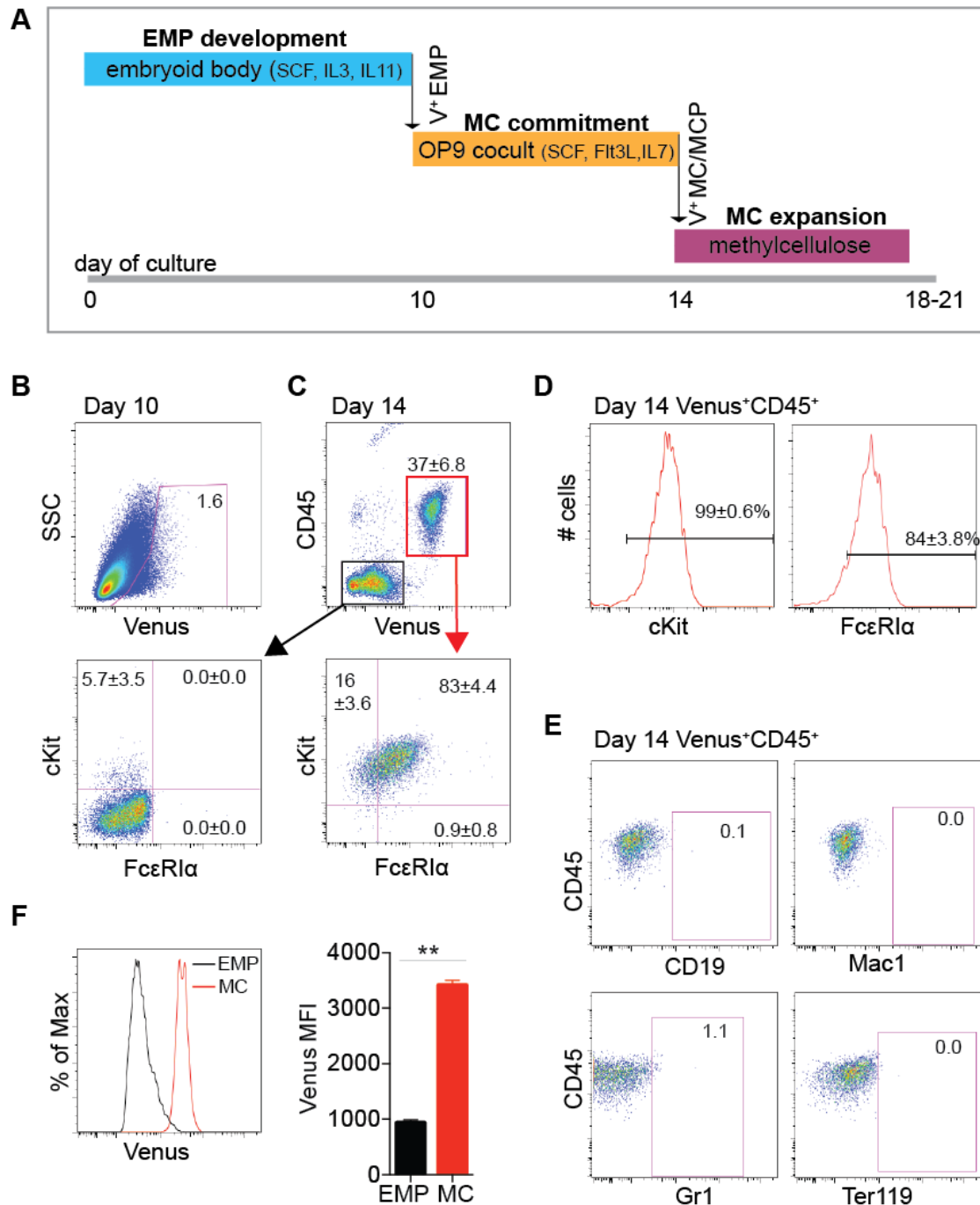
Figure 2. *Gata2Venus* **ESC differentiation and Venus enrichment facilitates rapid and robust mast cell generation. (A)** Hematopoietic commitment is induced during a 10 day embryoid body culture (blue line, day 0-10). At day 10, Venus$^+$ (V$^+$) erythroid-myeloid progenitors (EMP) are flow cytometrically sorted and plated onto OP9 stromal cells where mast cell (MC) commitment is induced (orange line, day 10-14). Highly proliferating phenotypic mast cells appear after 3-4 days of co-culture in the presence of Flt3L, IL-7 and SCF. By day 14, phenotypic mast cells/mast cell progenitors (MCP) can be isolated by Venus expression for analysis, or for further clonal expansion in methylcellulose (crimson line, day 14-18/21). **(B)** Representative FACS dot plot of day 10 mouse *Gata2Venus* ESC differentiation demonstrating gating strategy used for sorting Venus$^+$ erythroid-myeloid progenitors (1.6%) that were seeded on OP9 cells. **(C)** FACS analysis of cells after 4 days of OP9 co-culture. 37±6.8 % of the cells expressed Venus and CD45 (upper left panel) of which 16±3.6 % were cKit$^+$ mast cell progenitors, and 83±4.4 % mast cells (upper right panel). No phenotypic mast cells were generated from Venus$^-$ cells (lower left panel). **(D)** FACS histogram plots of cKit and FcεRIα expression in Venus$^+$CD45$^+$ cells derived after 4 days of OP9 co-culture. Values indicate mean±SEM, n=6 (upper panels). **(E)** FACS analysis showing lack of B-cell (CD19), macrophage (Mac1), granulocyte/basophil (Gr1) and erythrocyte (Ter119) lineage cells in Venus$^+$CD45$^+$ population after 4 days of OP9 co-culture. **(F)** FACS

histogram of Venus expression in EMPs at day 10 of culture (black line) and mast cells at day 14 of culture (MC, red line) (upper panel). Quantification of Venus mean fluorescence intensity (MFI) in EMP (black bar) and MC (red bar) showing significantly higher Venus protein levels in mast cells. Mean±SEM, ** p<0.01, n=3 (lower panel).

To assess the purity of the Venus$^+$CD45$^+$ cell population, the expression of other blood lineage markers, such as Mac1 (macrophage), Gr1 (granulocyte/monocyte), CD19 (lymphocyte) and Ter119 (erythroid) was analysed (Fig 2E). None of these markers were found to be expressed on the Venus$^+$CD45$^+$ cells. As HSCs express Gata2 (Kaimakis et al., 2016), cKit (Sanchez et al., 1996) and CD45 (McKinney-Freeman et al., 2009), to examine the possibility that some HSC-like cells were generated in the differentiation culture, we transplanted Venus$^+$CD45$^+$Lin$^-$ cells into lethally-irradiated adult mice. Spleen analysis at day 8 post-transplantation showed no donor-derived colony forming unit-spleen activity (data not shown). Thus, the majority, if not all of Venus$^+$CD45$^+$ cells are mast cells and/or mast cell progenitors. Interestingly, a significant shift in the intensity of Venus expression was seen between EMPs and mast cells/progenitors (Fig 2F). The geometrical mean of Venus fluorescence intensity in mast cells/progenitors was 3.5 fold higher than in EMPs, thus supporting the view that the direct induction of high Gata2 expression is a prerequisite for the rapid commitment to the functional mast cell lineage (Sasaki et al., 2016).

Mature mast cells produce high levels of inflammatory mediators that are stored in the cytoplasmic secretory granules (Schwartz and Austen, 1980). The expression of genes encoding the inflammatory mediators of connective tissue mast cells (*mMCP-5* chymase and *mMCP-6* tryptase, and *CPA-3* carboxypeptidase A) and of mucosal mast cells (*mMCP-1* chymase) was examined in undifferentiated ESCs, day 10 EMPs and methylcellulose expanded mast cells before and after clonal re-plating (Fig 3E). High expression of *mMCP-1*; *mMCP-5* and *mMCP-6* was found in all mast cells samples before and after serial re-plating, with only low/negligible expression in some ESC or EMP samples. Mast cell receptors *cKit* and *FcεR1α* were similarly expressed before and after re-plating in all mast cell samples with some low *cKit* expression in ESCs. As expected, high levels of *Gata2* were detected in EMPs and in mast cells before and after re-plating. The fact that the clonal expansion capacity, cellular morphology and gene expression profile of the mast cells were retained after serial plating (Fig 3D and 3E) suggests that these cultures maintain the self-renewal properties of mast cell progenitors. Gene expression of the chemical mediators and mast cell receptors in ESC-derived mast cells was compared to expression in murine ear tissue which is known to contain mast cells. *cKit*, *FcεR1α* and *FcεR1γ* were expressed 560±39, 2802±1690 and 644±66 times more respectively than ear tissue and mediator proteases *mMCP-5*, *mMCP-6* and *CPA-3* were expressed at 1727±402, 570±58 and 3818±621 times higher than in the ear (Fig 3F). These data confirm the highly enriched production of mast cells from G2V ESCs and strongly suggest that these mast cells are functional.
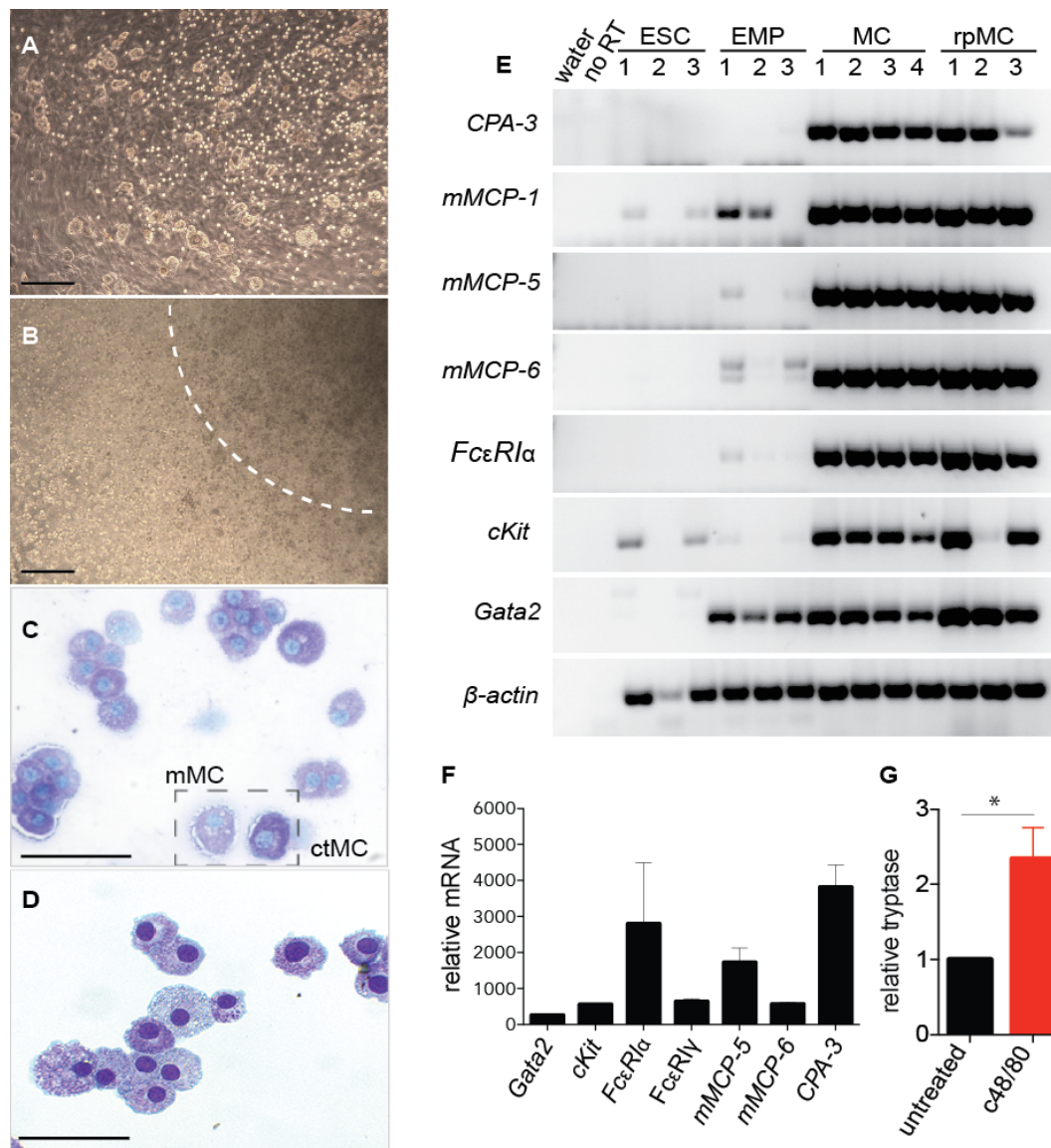
Figure 3. Gata2Venus enrichment results in the generation of functional mucosal and connective tissue type mast cells that express high levels of chemical mediators. (A) Representative image demonstrating the expansion capacity of single Venus$^+$ mast cells derived from d14 of culture. Arrows indicate the centers of two macroscopic colonies that were each derived from single cells. Objective=4x. **(B)** Representative image of Toluidine blue staining of mast cells generated after methylcellulose expansion. Light staining indicates mucosal mast cells (mMC), dark staining connective tissue like mast cells (ctMC), objective=40x. **(C)** Representative image of toluidine blue stained mast cells generated after 2x clonal re-plating of methylcellulose colony, objective 4x. **(D)** Mast cell specific gene expression analysis of undifferentiated embryonic stem cells (ESC, n=3), erythroid-myeloid progenitors (EMP, n=3), methylcellulose expanded mast cells (MC, n=4) and mast cells after clonal re-plating (rpMC, n=3). No RT, no reverse transcription; CPA-3, carboxypeptidase; mMCP, mouse mast cell proteases. **(E)** Quantitative gene expression analysis of mast cell specific genes in methylcellulose expanded mast cells. Expression level of all genes was normalized to *18S* expression and compared to the normalized levels in the mouse ear tissue that is known to contain mast cells. Mean ± SEM, n=3. **(F)** ELISA assay of relative released tryptase concentration in the medium of untreated and 5 μM c48/80 treated mast cells. Tryptase levels were calculated based on a tryptase standard curve. Level was set as 1 in untreated sample and level in c48/80 samples was calculated accordingly, *p<0.05, n=5.

To analyze the proliferative capacity of the Venus⁺ mast cells/progenitors, single Venus⁺ cells harvested after 4 days of co-culture on OP9 cells (Fig 3A) were plated in methylcellulose. After 3-4 days, macroscopic homogenous single cell-derived colonies appeared, indicating a large degree of rapid expansion (Fig 3B). The proliferative capacity of a single day 14 derived mast cell/mast cell progenitor was up to 10^4 fold (average $2.2\pm1.4 \times10^3$ fold). In total, a starting culture of 3×10^4 ESC can yield up to 3.8×10^6 mature mast cells (average $1.6\pm0.5 \times10^6$) (Suppl Table 1). This is up to 8-fold more cells generated in 21 days than previously published protocols in 5 or more weeks (0.5×10^6 cells) (Westerberg et al., 2012). Mast cell identity was confirmed by Toluidine blue staining (specific for intracellular granules). 100% of these cells were toluidine blue positive and both types of mast cells - connective tissue (dark staining due to heparin and high histamine levels; found mainly in skin) and mucosal mast cells (light-staining due to no heparin and low levels of histamine; found in digestive tract and lung mucosa (Bischoff and Kramer, 2007; Welle, 1997) were present in the cultures (Fig 3C).

Allergic responses *in vivo* result from the activation and degranulation of mast cells. To test whether *G2V* ESC-derived mast cells can be activated and degranulate, they were treated with the synthetic polyamine compound 48/80 (c48/80) (Lagunoff et al., 1983) which is one of the secretagogues of mast cells that include neuropeptides and opiates. After 60 minutes of c48/80 stimulus (5 µg/ml) a significantly 1.6-fold higher tryptase level was found in the cell medium as compared to the control unstimulated sample (Fig 3G), thus demonstrating that the *G2V* ESC-derived mast cells are functionally active and respond to common mast cell activating extracellular stimuli by releasing chemical mediators.

The known high conservation between mouse and human hematopoietic development, Gata2 expression and function, suggests that *GATA2* could enrich human mast cells. To test this, we generated and characterized *GATA2Venus* reporter human ESCs (*G2V*-hESC) and 2 clones of iPSCs (*G2V*-hiPCS-1; *G2V*-hiPCS-2) (Suppl Fig 1). Phenotypic (Fig 4A) and functional (Fig 4B) hematopoietic cells were enriched in the Venus⁺ fraction upon serum-free hESC/hiPSC hematopoietic differentiation, and are in line with previous analyses of mouse ESCs (Kauts et al., submitted) and human ESC/iPSC (Huang et al., 2016). Venus⁺ cells sorted on days 7, 8 and 11 following differentiation were co-cultured with OP9 cells. After 4-5 days of co-culture, 5.5%-19% of the Venus⁺ cells, which constituted 3.0%-5.5% of the co-culture cells, were of the cKit⁺FCεRIα⁺ mast cell phenotype, whereas no/few phenotypic mast cells were generated from Venus⁻ fraction (Fig 4C). Toluidine blue staining of methylcellulose expanded colonies confirmed the mast cell morphology (Fig 4D). These results were consistent between *G2V*-hESCs and *G2V*-hiPSC clones demonstrating the robustness of our approach, which, with further optimization, will deliver a platform for the robust generation of human mast cells. Our novel and innovative Gata2 reporter-based pluripotent stem cell differentiation approach for the rapid and efficient production of functional mast cells, represents a major advance that can now provide sufficient numbers of mast cells (including patient-specific mast cells) for high throughput drug discovery and mechanistic studies on mast-cell related disorders.
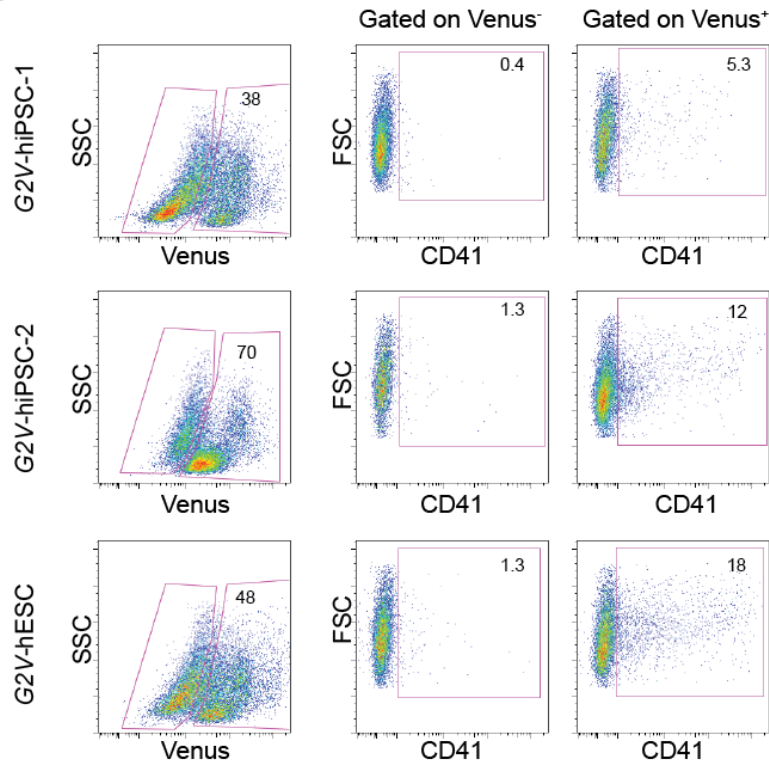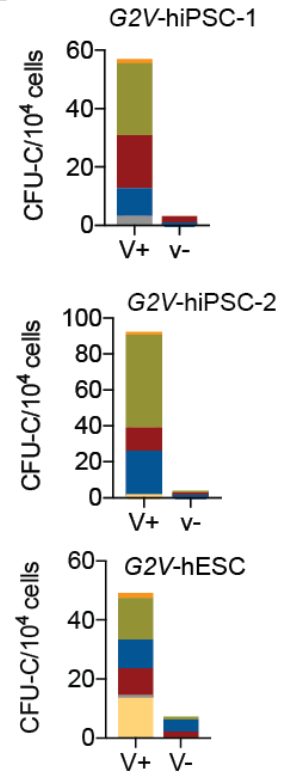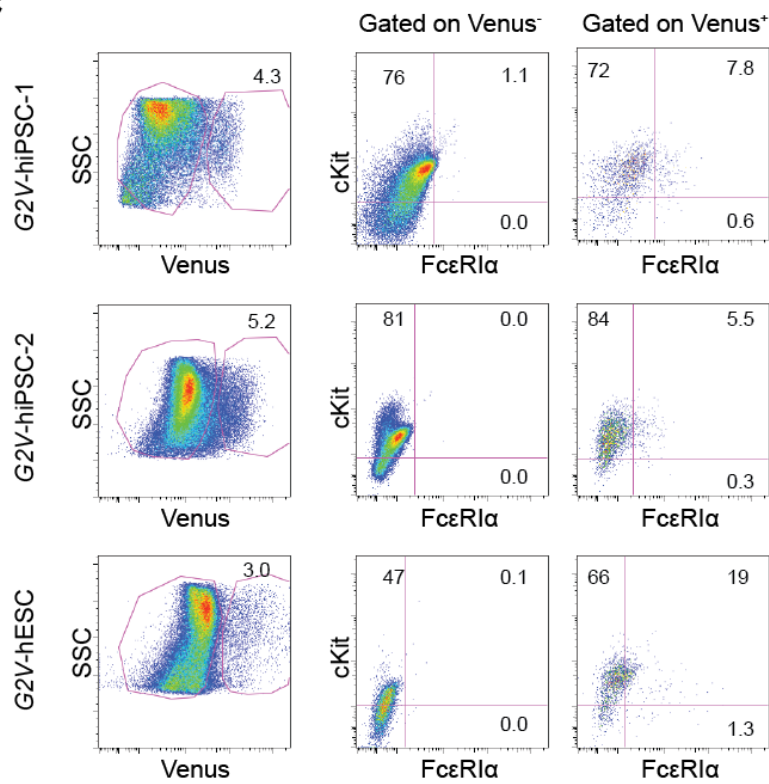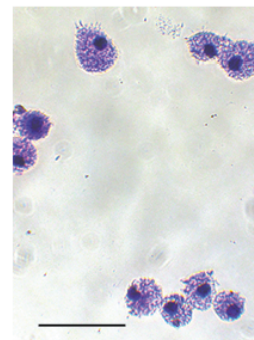
Figure 4. *Gata2Venus* hiPSC/ESC differentiation and generation of mast cells. (A) FACS analysis of hematopoietic cell surface marker CD41 expression on Venus$^-$ and Venus$^+$ populations of day 12 differentiated *G2V*-hESCs and G2V-hiPSCs. **(B)** Hematopoietic progenitor potential of Venus$^+$ (V$^+$) and Venus$^-$ (V$^-$) cells isolated from day 12 differentiated *G2V*-hES and *G2V*-hiPSC. Number of colony forming unit-cells (CFU-C) per 10^4 FACS sorted cells is shown. Colony types are indicated by color. CFU-granulocyte, erythrocyte, monocyte, macrophage (GEMM); CFU-granulocyte-macrophage (GM); CFU-macrophage (M); CFU-granulocyte (G); burst-forming-unit erythroid (BFU-E) and CFU-primitive erythroid (EryP). Representative data. **(C)** Mast cell differentiation approach as described for murine culture in Figure 1A was applied to *G2V*-hESCs and *G2V*-iPSCs to generate human mast cells. Venus$^+$ cells were sorted from day 11 (*G2V*-hES), day 7 (G2V-hiPSC-1) or day 8 (G2V-hiPSC-2) differentiated embryoid bodies and subjected to OP9 co-culture. After 5 (G2V-hESC; G2V-hiPSC-2) or 4 days (G2V-hiPSC-1) of co-culture, Venus+ and Venus- cells were analyzed for mast cell surface markers cKit and FCeRIa by FACS. **(D)** Representative image of Toluidine blue staining of mast cell generated after 5 days of methylcellulose expansion, objective=40x.

Methods

Mouse and human G2V reporter pluripotent stem cells. G2V and wild type (IB10) mouse ESCs were derived and cultured as undifferentiated cells as described by Kaimakis et al., (2016) and in Kauts et al., (submitted). hESC (line WA01 from WiCell) and iPSC lines (line SFCi55 from Lesley Forrester and CENSO Biotechnologies Ltd) (Yang et al., 2016) were maintained on MEFs seeded on 0.1% gelatin-coated plates, in DMEM/F12 supplemented with Knock-out Serum Replacement (ThermoFisher), GlutaMAX (Gibco), Minimum Essential Medium Non-essential Amino Acids (Lonza), 50 μM β-mercaptoethanol (Gibco) and 10 μg/ml bFGF (PeproTech). Medium was replaced daily. The human GATA2Venus reporter PSCs were generated by CRISPR/Cas9 engineering. The *GATA2*-stop codon-targeting gRNA was designed and its reverse complement deduced. BbsI cohesive ends were added on the 5' of each strand as appropriate. The insert DNA duplex was prepared by annealing, and ligated into the pSpCas9(BB)-2AGFP (PX458) (Addgene) vector as described by (Ran et al., 2013).

The *GATA2-T2A-H2B-Venus-pA-EF1α-Puro-pA* donor vector was generated from a BAC (CTD-3248G10; Life Technologies). Bacterial lines were transformed with pSIM18Hygro (kind gift from P. Liu, Wellcome Trust Sanger Institute) to generate bacterial strains with heat-inducible recombinase expression. Four mini-homology arms (5'-out, 3'-out, 5'-in and 3'-in) were initially generated by PCR amplification of BAC DNA using the following PCR primers:
GATA2 Out-5-F ttgcggccgc GCAAAATTCCCAGGACCTGCTC
GATA2 Out-5-R ccaagctt TGCAAAACAAACAGGAGAAAGGACC
GATA2 Out-3-F ccaagcttggatcc TCCTACCTGATGCATAGTGGC
GATA2 Out-3-R ccctcgag GAGTTCTGGGGCCTAGAGCTATGG
GATA2 In-5-F cggaattc CTGGCTTCCTGGGACCCTCAG
GATA2 In-5-R gggctagcgtcgac GCCCATGGCGGTCACCATG
GATA2 In-3-F ccctcgagggcgcgcc GGAACAGATGGACGTCGAGGACC
GATA2 In-3-R aggcggccgc AGGACTTGGGACAGCTCAGACCAC

5'-out arm were digested with NotI/HindIII and 3'-out arm with XhoI/HindIII. Digested 5' and 3' out-arms were ligated into XhoI/NotI digested and gel purified pBlueScript to generate outarm-pBlueScript. 5'-in arm were digested with EcoRI/NheI and 3'-in arm with XhoI/NotI. Digested 5'- and 3'-in arms were ligated with a NheI/AscI digested ZeoR cassette (kind gift from P.Liu) and EcoRI/NotI digested pBlueScript to generate 5'in-arm-ZeoR-3'in-arm-pBlueScript. The entire out-arm-pBlueScript backbone was PCR amplified for recombineering. Competent BAC/pSIM18Hygro bacteria were transformed with PCR amplified out-arm-pBlueScript to generate the full homology region within pBlueScript. This full homology region-pBluescrip and a EcoRV/NotI linearised 5'in-arm-ZeoR 3'in-arm fragment were then transformed into competent SIM18 E.coli (a strain with stable phage incorporated SIM18 recombinase; Chan et al., 2007) to replace the GATA2 stop codon with the ZeoR cassette. The ZeoR cassette was digested from the homology arms using SalI/AscI and homology arms ligated with a SpeI/AscI digested T2A-Venus-pA-EF1a-PuroR-pA DNA fragment (plasmid kindly provided by W. Wang, Wellcome Trust Sanger Institute). Sequencing was used to verify homology arm sequences.

8x10^5 hPSCs were electroporated using the Human Stem Cell Nucleofector Kit 2 (A-023 programme) of the AMAXA Nucleofector (Lonza) according to the supplier's protocol. 3 µg of GATA2-T2A-H2B-Venus-pA-EF1α-Puro-pA-pBlueScript together with 2 µg of gRNA-pSpCas9(BB)-2A-GFP were used for transfection. Transfected cells were seeded on puromycin resistant MEF feeders (DR4, ATCC). 48hours post-transfection, 1 µg/ml puromycin selection was initiated for 1 week. In total, 33 iPSC and 16 ESC prospective *GATA2Venus* clones were established and subjected to PCR based genotyping with primers spanning over the 3' (4795 bp) and 5' (5025 bp) junctions of the construct and the *GATA2* genomic sequence (Supplementary Figure 1). Primers detecting *GATA2* WT allele (240 bp) were used to assess the homo-/heterozygousity of the insertion. Clones with correct integration were subjected to karyotyping. 1 clone of *G2V*-hESC and 2 clones of *G2V*-hiPSC with normal karyotype were used for experiments.

Multistep culture for PSC differentiation and mast cell generation.
The three step culture procedure is summarized in Fig 2A.

1. EMP differentiation (day 0-10). Mouse *G2V* ESCs were harvested by trypsinization and feeder depleted by incubation in the Iscove modified Dulbecco medium (IMDM) containing 20% fetal bovoine serum (FBC) (HyClone) and 1% penicillin/streptomycin (P/S) for 30 minutes at 37°C. *G2V* ESC differentiation was induced by forming EBs. Cells were allowed to aggregate by culturing them at a density of 25,000 cells/ml in EB differentiation medium (IMDM containing 15% FBS, 2mM GlutaMAX (Gibco), 50 µg/ml ascorbic acid (Sigma), 4x10^{-4} monothioglycerol (Sigma), 300 µg/ml transferrin (Roche)) in bacterial petri dishes. 72 h later the medium was refreshed and supplemented with 5%proteome free hybridoma medium (Gibco). At day 6 of differentiation, the medium was supplemented with murine stem cell factor (SCF, 100 ng/ml), IL-3 (1 ng/ml) and IL-11 (5 ng/ml) (PeproTech). Medium was refreshed every other day.

The differentiation of hPSC to EMPs was performed as previously described (Kennedy et al., 2012). Briefly, hPSCs were non-enzymatically cut using StemPro EZPassage Disposable Stem Cell Passaging Tool (Thermo Fisher) and aggregates were re-suspended in Stem-Pro-34 (Invitrogen), supplemented with 10 ng/ml P/S, 2 mM L-glutamine (Gibco), 1 mM ascorbic acid (Sigma-Aldrich), 4x10^{-4} M monothioglycerol (Sigma-Aldrich), and 150 mg/ml transferrin (Roche). Human BMP-4 (10 ng/ml), bFGF (5 ng/ml), Activin A, 6 mM SB, VEGF (15 ng/ml), Dkk (150 ng/ml), IL-6 (10 ng/ml), IGF-1 (25 ng/ml), IL-11 (5 ng/ml), SCF (50 ng/ml), EPO (2 U/ml), TPO (30 ng/ml), IL-3 (30 ng/ml), and Flt-3L (10 ng/ml) (all from PeproTech) were added as indicated (Kennedy et al., 2012).

2. Isolation of EMPs, mast cell commitment (day 10-14). At day 10 of differentiation, EBs were washed with PBS and incubated with TrypLE Express enzyme (Gibco) at 37°C for 3-5 minutes. Enzyme was deactivated by adding PBS + 10% FCS + 1% P/S and homogenous single-cell suspension was obtained by re-suspending with a P1000 pipette.

10,000 Venus$^+$ cells were sorted and plated on 30,000 OP9 cells pre-seeded one day earlier in 24 well plate. Cells were cultured in α-MEM + 10% heat inactivated FBS + 1% P/S co-culture medium supplemented with murine Flt3L, IL-7 (20 ng/ml) and SCF (50 ng/ml) (all from PeproTech). For human PSC culture, same concentration of human cytokines was used (PeproTech). Venus$^+$ mast cells appeared in the culture after 2-4 days, they could be readily isolated for experiments or further expansion by Venus$^+$ expression.

3. Expansion. After 4 days of OP9 co-culture, Venus$^+$ cells were isolated by FACS and plated in methylcellulose medium (Stem Cell Technologies) at concentration of 500 cells/ml. After 3-4 days of expansion, big bright dense colonies appeared. Colonies were counted after 3-7 days of methylcellulose culture and cells were harvested by dissolving methylcellulose in PBS. Cells were counted by trypan blue exclusion. For colony re-plating, colonies were picked and single cells were plated into fresh methylcellulose.

Human mast cell generation was performed essentially as described for murine culture, but with the use of human cytokines.

FACS analysis, cell sorting. Venus fluorochrome expression was readily detected in the reporter cell lines by FACS. Surface receptor expression was analyzed using the following antibodies purchased from eBioscience, BioLegend or BD Pharmingen: CD45-AF700 (1:400), CD19-PE (1:200), Gr1-APC-Cy7 (1:400), CD11b-PerCP-Cy5.5 (1:500), Ter119-BV421 (1:400), cKit-APCeFluor780 (1:800) and FcεR1α -PE (1:200, clone MAR-1) (for murine cells) and CD41-ef450 (1:50), FcεRIα-PE (1:50), cKit-PECy7 (1:50) (for human cells). Dead cells were excluded with Hoechts33342 (Life Technologies). Cells were sorted and analyzed on FACS Aria II SORP (BD Biosciences). Results analysis was performed by FlowJo software (Tree star).

Cytospin, toluidine blue staining. 15,000 mast cells isolated after expansion in methylcellulose were re-suspended in 50 µl PBS and transferred into sample chamber containing a glass slide. Samples were centrifuged for 5 min at 200 rpm. Cells were fixed in methanol for 30 seconds and stained in Toluidine blue in 0.5N HCl for 1 h (mouse). Slides with human sample were stained with Rapid Romanowsky Stain Pack kit (TCS Biosciences) according to the manufacturer's protocol. Slides were washed 2x in tap water and examined under Axioskop2 (Zeiss) microscope using 40x objective.

Mast cell activation and ELISA. 1 x 10^6 mast cells after methylcellulose expansion were re-suspended in 1 ml of PBS and stimulated with 5 μg/ml of compound 48/80 (Sigma) for 60 min at 37°C in the presence of 5% CO_2. Cell suspension was centrifuged and supernatant was collected. Tryptase concentration in the medium was quantified using Mouse Mast Cell Tryptase (Rosenbaum et al.) ELISA Kit (Cusabio) according to manufacturer's instructions. Tryptase standard curve was generated using a four parameter logistic (4-PL) curve-fit and tryptase concentrations in the sample medium were calculated accordingly.

RNA extraction, cDNA synthesis, PCR and qRT-PCR. Murine and human cell total RNA was extracted using RNA mini or micro kit (Qiagen) according to manufacturer's protocol. For murine samples, all RNA samples were standardized to 100 ng/ml, optimal RNA concentration needed for reverse transcription. Synthesis of cDNA was performed using

the Superscript VILO synthesis kit (Invitrogen) according to manufacturer's protocol. Sample mixes were run at 25°C for 10 minutes, 42°C for 60 minutes (primer extension phase) and 85°C for 5 minutes (inactivation of reverse transcription phase) in a thermal cycler (MJ Research PTC 200 Thermo Cycler, BC-MJPC200). A cDNA standard curve for qPCR primer efficiency validation was made using a 10-fold serial dilutions of a RNA mix from pooled concentrated RNAs. Together with R^2 value for the standard curve, efficiency (E, %) of all the primer sets was calculated by the formula $E=(10^{(-1/slope)}-1) \times 100$ 10 and 2-fold dilutions. $\Delta\Delta Ct$ analysis was performed for primer sets with an efficiency range of 95-105% (all primers in this study). Taqman PCR technique was used for real time RNA quantification following manufacturer's guidelines. Primer sets were specifically designed using "Universal ProbeLibrary Assay Design Center" (Supplementary Table 3). Semi-quantitative RT-PCR was performed using BioMix Red (Bioline) according to manufacturer's manual using the following primers (Supplementary Table 3). For human VENUS sorted samples total RNA was isolated and reverse transcribed using oligo-dT (Life Technologies) and SuperScript III (Life Technologies) according to manufacturer's protocol. qRT-PCR was performed using Fast Sybr Green master mix (Life Technologies) according to manufacturer's instructions. Primers are listed in Supplementary Table 3.

Statistical Analysis. Statistical analysis was performed using an unpaired Student's t test. Results were considered to be statistically significant at p value < 0.05 (*p<0.05, **p <0.01). Data are shown as a mean ± SEM. The number of biological replicates is indicated by the n value. Data analysis was done using GraphPad Prism (GraphPad Software).

Acknowledgements

References

Bertrand, J., Boucherle, B., Billet, A., Melin-Heschel, P., Dannhoffer, L., Vandebrouck, C., Jayle, C., Routaboul, C., Molina, M.C., Decout, J.L*., et al.* (2010). Identification of a novel water-soluble activator of wild-type and F508del CFTR: GPact-11a. Eur Respir J *36*, 311-322.

Bischoff, S.C., and Kramer, S. (2007). Human mast cells, bacteria, and intestinal immunity. Immunological reviews *217*, 329-337.

Holm, M., Kvistgaard, H., Dahl, C., Andersen, H.B., Hansen, T.K., Schiotz, P.O., and Junker, S. (2006). Modulation of chemokine gene expression in CD133+ cord blood-derived human mast cells by cyclosporin A and dexamethasone. Scand J Immunol *64*, 571-579.

Huang, K., Gao, J., Du, J., Ma, N., Zhu, Y., Wu, P., Zhang, T., Wang, W., Li, Y., Chen, Q*., et al.* (2016). Generation and Analysis of GATA2w/eGFP Human ESCs Reveal

ITGB3/CD61 as a Reliable Marker for Defining Hemogenic Endothelial Cells during Hematopoiesis. Stem Cell Reports *7*, 854-868.

Jippo, T., Mizuno, H., Xu, Z., Nomura, S., Yamamoto, M., and Kitamura, Y. (1996). Abundant expression of transcription factor GATA-2 in proliferating but not in differentiated mast cells in tissues of mice: demonstration by in situ hybridization. Blood *87*, 993-998.

Kaimakis, P., de Pater, E., Eich, C., Solaimani Kartalaei, P., Kauts, M.L., Vink, C.S., van der Linden, R., Jaegle, M., Yokomizo, T., Meijer, D.*, et al.* (2016). Functional and molecular characterization of mouse Gata2-independent hematopoietic progenitors. Blood.

Kauts, M.L., Kaimakis, P., Hill, U., Cortes, X., Mendez, S., Dzierzak, E. Differentiation of *Gata2Venus* and *Ly6aGFP* reporter embryonic stem cells corresponds to *in vivo* waves of hematopoietic cell generation in the mouse embryo. (submitted)

Kennedy, M., Awong, G., Sturgeon, C.M., Ditadi, A., LaMotte-Mohs, R., Zuniga-Pflucker, J.C., and Keller, G. (2012). T lymphocyte potential marks the emergence of definitive hematopoietic progenitors in human pluripotent stem cell differentiation cultures. Cell Rep *2*, 1722-1735.

Kovarova, M., Latour, A.M., Chason, K.D., Tilley, S.L., and Koller, B.H. (2010). Human embryonic stem cells: a source of mast cells for the study of allergic and inflammatory diseases. Blood *115*, 3695-3703.

Lagunoff, D., Martin, T.W., and Read, G. (1983). Agents that release histamine from mast cells. Annual review of pharmacology and toxicology *23*, 331-351.

Masuda, A., Hashimoto, K., Yokoi, T., Doi, T., Kodama, T., Kume, H., Ohno, K., and Matsuguchi, T. (2007). Essential role of GATA transcriptional factors in the activation of mast cells. J Immunol *178*, 360-368.

McKinney-Freeman, S.L., Naveiras, O., Yates, F., Loewer, S., Philitas, M., Curran, M., Park, P.J., and Daley, G.Q. (2009). Surface antigen phenotypes of hematopoietic stem cells from embryos and murine embryonic stem cells. Blood *114*, 268-278.

Moller, C., Karlberg, M., Abrink, M., Nakayama, K.I., Motoyama, N., and Nilsson, G. (2007). Bcl-2 and Bcl-XL are indispensable for the late phase of mast cell development from mouse embryonic stem cells. Exp Hematol *35*, 385-393.

Ran, F.A., Hsu, P.D., Wright, J., Agarwala, V., Scott, D.A., and Zhang, F. (2013). Genome engineering using the CRISPR-Cas9 system. Nat Protoc *8*, 2281-2308.

Rosenbaum, B.P., Gorrindo, T.L., Patel, S.G., McTigue, M.P., Rodgers, S.M., and Miller, B.M. (2009). Medical student involvement in website development. Med Teach *31*, 627-633.

Saito, H., Kato, A., Matsumoto, K., and Okayama, Y. (2006). Culture of human mast cells from peripheral blood progenitors. Nat Protoc *1*, 2178-2183.

Sanchez, M.J., Holmes, A., Miles, C., and Dzierzak, E. (1996). Characterization of the first definitive hematopoietic stem cells in the AGM and liver of the mouse embryo. Immunity *5*, 513-525.

Sasaki, H., Kurotaki, D., and Tamura, T. (2016). Regulation of basophil and mast cell development by transcription factors. Allergol Int *65*, 127-134.

Schwartz, L.B., and Austen, K.F. (1980). Enzymes of the mast cell granule. The Journal of investigative dermatology *74*, 349-353.

Shimizu, Y., Sakai, K., Miura, T., Narita, T., Tsukagoshi, H., Satoh, Y., Ishikawa, S., Morishita, Y., Takai, S., Miyazaki, M.*, et al.* (2002). Characterization of 'adult-type' mast cells derived from human bone marrow CD34(+) cells cultured in the presence of

stem cell factor and interleukin-6. Interleukin-4 is not required for constitutive expression of CD54, Fc epsilon RI alpha and chymase, and CD13 expression is reduced during differentiation. Clin Exp Allergy *32*, 872-880.

Theoharides, T.C., Stewart, J.M., Panagiotidou, S., and Melamed, I. (2016). Mast cells, brain inflammation and autism. Eur J Pharmacol *778*, 96-102.

Theoharides, T.C., Valent, P., and Akin, C. (2015). Mast Cells, Mastocytosis, and Related Disorders. N Engl J Med *373*, 1885-1886.

Tsai, F.Y., and Orkin, S.H. (1997). Transcription factor GATA-2 is required for proliferation/survival of early hematopoietic cells and mast cell formation, but not for erythroid and myeloid terminal differentiation. Blood *89*, 3636-3643.

Tsai, M., Tam, S.Y., Wedemeyer, J., and Galli, S.J. (2002). Mast cells derived from embryonic stem cells: a model system for studying the effects of genetic manipulations on mast cell development, phenotype, and function in vitro and in vivo. Int J Hematol *75*, 345-349.

Wang, X.S., Sam, S.W., Yip, K.H., and Lau, H.Y. (2006). Functional characterization of human mast cells cultured from adult peripheral blood. Int Immunopharmacol *6*, 839-847.

Welle, M. (1997). Development, significance, and heterogeneity of mast cells with particular regard to the mast cell-specific proteases chymase and tryptase. Journal of leukocyte biology *61*, 233-245.

Westerberg, C.M., Ulleras, E., and Nilsson, G. (2012). Differentiation of mast cell subpopulations from mouse embryonic stem cells. J Immunol Methods *382*, 160-166.

Yang, C.T., Ma, R., Axton, R.A., Jackson, M., Taylor, A.H., Fidanza, A., Marenah, L., Frayne, J., Mountford, J.C., and Forrester, L.M. (2016). Activation of KLF1 Enhances the Differentiation and Maturation of Red Blood Cells from Human Pluripotent Stem Cells. Stem Cells.

Supplementary data
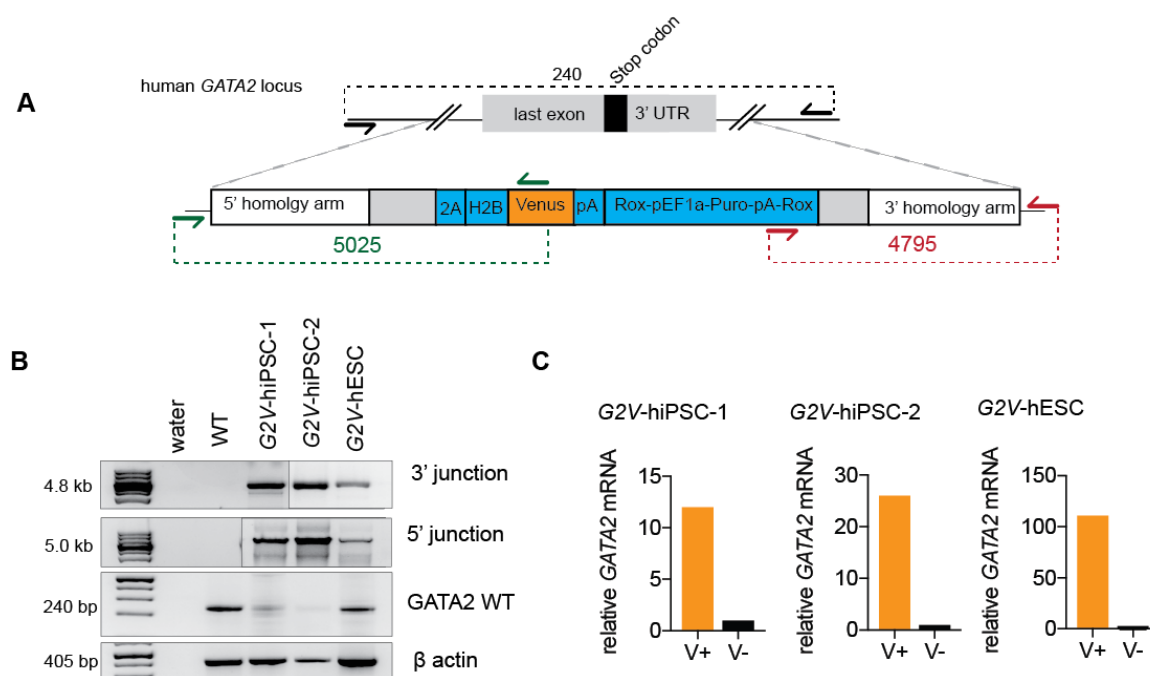
Supplementary Figure 1. Generation of human *GATA2Venus* reporter pluripotent stem cells. (A) Schematic diagram of the 2A-H2B-*Venus* reporter and Rox site flanked puromycin selection cassette insertion into the 3' untranslated region (UTR) of the human *GATA2* locus. Primers used for detection of the WT and recombined alleles are indicated by colors (Black, WT; green, 5'-junction; red, 3'-junction). **(B)** PCR analysis of the genomic locus of GATA2 in untargeted (WT) and targeted ES (*G2V*-hESC) and iPSC clones (*G2V*-hiPSC). **(C)** Representative data of *GATA2* gene expression in Venus[+] (V[+]) and Venus[-] (V[-]) FACS sorted cells from day 6 differentiated *G2V*-hESCs and *G2V*-iPSCs. Gene expression was normalized to *HPRT1*, set as 1 in Venus[-] fraction, fold of expression in Venus[+] was calculated accordingly.

Supplementary Table 1. Mast cell generation and frequency in the *G2V* ESC multistep cultures

exp	d10 EMP from 3x10^4 ESC	d14 MC/MCP from 3x10^4 ESC	d18-21 MC yield from 3x10^4 ESC
1	11,504	14,923	1,242,200
2	30,000	2,781	937,000
3	7,541	2,623	3,834,375
4	9,653	1,990	570,313
5	20,087	6,421	1,156,250
6	13,764	6,875	1,906,250
mean	**15,425**	**5,936**	**1,607,731**
±SEM	3,405	1,986	479,952

Number of Venus[+] erythroid-myeloid progenitors (EMP) at day 10 (d10), Venus^{+} mast cells/mast cell progenitors (MC/MPC) after OP9 co-culture at day 14, and total mast cell yield after methylcellulose expansion at day 18-21 from 3×10^4 input *Gata2Venus* mouse ES cells, n=6, mean±SEM.

Supplementary Table 2. Primer sequences

Murine RT-PCR	forward 5'-3'	reverse 5'-3'
cKit	CCATCCATCCATCCAGCACA	CTGTTGCTGCACGTGTATGT
FcεR1α	ACCGTTCAAGACAGTGGAAA	AGACGGGGCTCTCATAACTG
mMCP-6	TAATGACGAGCCTCTCCCAC	CAGCCAGGTACCCTTCACTT
mMCP-5	TCATCTGCTGCTCCTTCTCC	ATAGACCTTCCCGCACAGTG
Gata2	ATGGCAGCAGTCTCTTCCAT	CACAGGCATTGCACAGGTAG
MMCP-1	CCACACTCCCGTCCTTACAT	ACATCATGAGCTCCAAGGGT
CPA-3	ACACCAACAAACCATGCCTC	TGGTGGTTAGGAGGCAGTTT
β-actin	CACCACACCTTCTTACAATGAG	GTCTCAAACA TGATCTGGGTC
Murine qRT-PCR		
cKit	GATCTGCTCTGCGTCCTGTT	CTTGCAGATGGCTGAGACG
FcεR1α	CCATGGATCCTTTGACATCAG	GATCACCTTGCGGACATTC
FcεR1γ	CTTACCCTACTCTACTGTCGACTCAA	AGGCCCGTGTAGACAGCAT
Gata2	TGGCACCACAGTTGACACA	TGGCACCACAGTTGACACA
mMCP-5	ATCTGCTGCTCCTTCTCCTG	ACTCCGTGCCTCCAATGA
mMCP-6	TGCTGTGTGCTGGAAATACC	CCCTTCACTTTGCAGACCA
CPA-3	GCTATTAATTCCTTATGGCTACACATT	GTGGCAATCCTTGCAACTTT
human RT-PCR		
GATA2	CAGCAAGGCTCGTTCCTGTT	GGCTTGATGAGTGGTCGGT
HPRT-1	CCTGGCGTCGTGATTAGTGAT	AGACGTTCAGTCCTGTCCATAA
human PCS genotyping		
β-ACTIN	AGCTGTCACATCCAGGGTCC-	CCTCGGCCACATTGTGAACT
5'-junction	AGTGCTTCCAGTGTACCCCCA	TGGTCGAGCTGGACGGCGA
3'-junction	GAAGGACCGCGCACCTGGT	GATTCTGAGGTCTGGGCTCTGG
GATA2 WT	ACCTCCCGCCCTTCAGCC	GAGGGGGTGCTGGGCCGAG

CHAPTER 5

Functional and molecular characterization of mouse Gata2-independent hematopoietic progenitors

Polynikis Kaimakis,[1,*] Emma de Pater,[1,2,*] Christina Eich,[1,*] Parham Solaimani Kartalaei,[1] Mari-Liis Kauts,[1,3] Chris S. Vink,[1,3] Reinier van der Linden,[1] Martine Jaegle,[1] Tomomasa Yokomizo,[1] Dies Meijer,[1,4] and Elaine Dzierzak[1,3‡]

*Co-first author
‡Corresponding author

[1]Erasmus Medical Center Stem Cell Institute, Departments of Cell Biology and Genetics,
[2]Department of Hematology, Erasmus Medical Center, Rotterdam, The Netherlands;
[3]Centre for Inflammation Research, Queens Medical Research Institute,
[4]Centre for Neuro Regeneration, University of Edinburgh, Edinburgh, United Kingdom

Functional and molecular characterization of mouse Gata2-independent hematopoietic progenitors

Polynikis Kaimakis, Emma de Pater, Christina Eich, Parham Solaimani Kartalaei, Mari-Liis Kauts, Chris S. Vink, Reinier van der Linden, Martine Jaegle, Tomomasa Yokomizo, Dies Meijer and Elaine Dzierzak

---

Regular Article

HEMATOPOIESIS AND STEM CELLS

Functional and molecular characterization of mouse Gata2-independent hematopoietic progenitors

Polynikis Kaimakis,[1,*] Emma de Pater,[1,2,*] Christina Eich,[1,*] Parham Solaimani Kartalaei,[1] Mari-Liis Kauts,[1,3] Chris S. Vink,[1,3] Reinier van der Linden,[1] Martine Jaegle,[1] Tomomasa Yokomizo,[1] Dies Meijer,[1,4] and Elaine Dzierzak[1,3]

[1]Erasmus Medical Center Stem Cell Institute, Departments of Cell Biology and Genetics, and [2]Department of Hematology, Erasmus Medical Center, Rotterdam, The Netherlands; and [3]Centre for Inflammation Research, Queens Medical Research Institute, and [4]Centre for NeuroRegeneration, University of Edinburgh, Edinburgh, United Kingdom

---

Key Points

- A new Gata2 reporter indicates that all HSCs express Gata2 and corroborates findings that Gata2 is not required for generation of all HPCs.
- Isolatable non–Gata2-expressing HPCs show less potency and a distinct genetic program, thus having implications for reprogramming strategies.

The Gata2 transcription factor is a pivotal regulator of hematopoietic cell development and maintenance, highlighted by the fact that *Gata2* haploinsufficiency has been identified as the cause of some familial cases of acute myelogenous leukemia/myelodysplastic syndrome and in MonoMac syndrome. Genetic deletion in mice has shown that Gata2 is pivotal to the embryonic generation of hematopoietic stem cells (HSCs) and hematopoietic progenitor cells (HPCs). It functions in the embryo during endothelial cell to hematopoietic cell transition to affect hematopoietic cluster, HPC, and HSC formation. *Gata2* conditional deletion and overexpression studies show the importance of Gata2 levels in hematopoiesis, during all developmental stages. Although previous studies of cell populations phenotypically enriched in HPCs and HSCs show expression of *Gata2*, there has been no direct study of Gata2 expressing cells during normal hematopoiesis. In this study, we generate a *Gata2Venus* reporter mouse model with unperturbed Gata2 expression to examine the hematopoietic function and transcriptome of Gata2 expressing and nonexpressing cells. We show that all the HSCs are Gata2 expressing. However, not all HPCs in the aorta, vitelline and umbilical arteries, and fetal liver require or express Gata2. These Gata2-independent HPCs exhibit a different functional output and genetic program, including Ras and cyclic AMP response element-binding protein pathways and other Gata factors, compared with Gata2-dependent HPCs. Our results, indicating that Gata2 is of major importance in programming toward HSC fate but not in all cells with HPC fate, have implications for current reprogramming strategies. (*Blood*. 2016;127(11):1426-1437)

Introduction

Gata2 is one of the "heptad" transcription factors that acts on regulatory regions of hematopoietic genes.[1] It is upregulated in vivo in Ly6aGFP^{+} cells undergoing endothelial-to-hematopoietic cell transition (EHT), a process by which definitive hematopoietic progenitors (HPCs) and hematopoietic stem cells (HSCs) are generated in the embryo.[2,3] As one of the major regulators of HPC and HSC generation, germline deficiency of *Gata2* results in embryonic lethality between embryonic day (E)10 and E10.5 and an anemic phenotype, with a decreased number of primitive and definitive HPCs in the yolk sac (YS) and in *Gata2*^{−/−} embryonic stem (ES) cell hematopoietic differentiation cultures.[4-6] Chimeric embryo generation with *Gata2*^{−/−} ES cells revealed defective production of all hematopoietic lineages.[5] The E10.5 lethality of *Gata2*^{−/−} embryos precludes the study of HSC generation in the aorta-gonad-mesonephros (AGM) region, the first site of de novo HSC production. *Gata2*^{+/−} embryos contain greatly reduced number of HSCs in the AGM region.[7,8] Gata2 haploinsufficiency

perturbs adult HSC homeostasis in mice[9] and, in humans, leads to MonoMac syndrome,[10] which is associated with sporadic myelodysplasia and myeloid leukemia. Also, rearrangement of the remote *Gata2* enhancer drives acute myeloid leukemogenesis by activating *Evi1* expression.[11,12] Overexpression studies also reveal that levels of Gata2 expression are important for its hematopoietic function.[13-15] In situ hybridization studies localize *Gata2* expression to aortic endothelial cells, intra-aortic hematopoietic cluster cells, placenta (PL), and fetal liver (FL) in the midgestation mouse.[16-18] Conditional knockout of *Gata2* or *Gata2* regulatory elements in vascular endothelial cells indicates that Gata2 is essential for hematopoietic cluster formation and HSC generation.[7,19,20] Gata2 plays a role in the emergence of cKit-expressing hematopoietic cells from the endothelium.[7] Later, as shown in *VavCre* conditional knockout mice, *Gata2* is essential for HSC maintenance,[7] thus demonstrating a role for Gata2 as previously recognized in bone marrow LSK HSCs.[21]

To date, the correlation between Gata2 and hematopoietic cell generation in the embryo has been made in the absence of prospective isolation of viable Gata2-expressing cells.[16] Although some hematopoietic cells remain in the embryo in the absence of Gata2,[5-8] the identity of these cells is unknown. In this study, to further understand the requirement for Gata2 in normal hematopoietic development, we create and use a mouse model in which a fluorescent reporter for Gata2 (IRES-Venus knock-in gene) does not affect the normal level or function of Gata2. We demonstrate that all long-term repopulating HSCs and a large percentage of HPCs in the midgestation mouse embryo are Venus[+]. We isolate and characterize a Venus[−] HPC population that corresponds to the HPCs found in Gata2-null embryos. Gata2-independent hematopoietic progenitors are functionally less complex and do not follow the same genetic program as Gata2-dependent HPCs.

Materials and methods

Gata2Venus ES cells and mice

Generation of the Gata2-Venus mouse model is described in the supplemental Methods, available on the Blood Web site. In short, an IRES-Venus fragment and a loxP-PGK-Puro-loxP fragment were inserted in the Gata2 3′ untranslated region (UTR). IB10 ES cells were transfected and puromycin selected, and 360 clones were polymerase chain reaction (PCR) screened for Gata2Venus (right arm junction, 2292 bp). Correct integration was verified by Southern blot (left arm) for 2 clones with normal karyotype. Founders were identified by Venus PCR. First-generation G2V offspring were crossed with CAG-Cre mice[22] and backcrossed (>10 generations) with C57BL/6.

Mice and embryo production

Gata2^{+/−} mice,[5] Ly5.1 (6-8 weeks) and C57BL/6 mice were obtained/maintained (Harlan or locally) and genotyped by PCR (supplemental Methods). Day of plug discovery is E0. Embryos were staged by somite pair (sp): E9.5 = 16 to 28 sp, E10 = 28 to 40 sp, early E10 = 28 to 34 sp, E10.5 = 35 to 40 sp, and E11 = 40 to 50 sp. All mouse experimentation was performed under the UK Animals Scientific Procedures Act 1986 Project License 70/8076 and NL Ethics Committee approval and performed in compliance with Standards for Care and Use of Laboratory Animals.

Immunostaining

Whole-mount conceptuses were stained and imaged[23]; cryosections and cells for flow cytometry were stained[8] using anti-CD34-biotin (1:50; BD), anti-Gata3 (1:10 KT122, 111207H09; Absea), anti-Gata4 (1:50 H-112, sc-9053; SantaCruz), and anti-green fluorescent protein antibodies. For flow cytometry,[8] cells were stained with anti-CD31 (390; BD), anti-CD34 (RAM34; BD), anti-cKit (2B8; BD), anti-CD41 (MWReg3; SantaCruz), anti-Sca1 (D7; Ebiosciences), and anti-CD16/32 (2.4G2; BD) antibodies and Hoechst 33258 (BD) and analyzed (FACSARIAIII; SORP).

Hematopoietic assays

Venus-sorted E9 to E11 AGM, vitelline+umbilical arteries (VA+UA), PL, and YS and E10 FL or Gata2-deficient E9 to E10 AGM, VA+UA, and PL were seeded in 3.6 mL methylcellulose (1 mL per dish; M3434; Stem Cell Tech) for 10 to 12 days.[24] Colonies were counted, isolated, and washed, and Venus expression was examined (FACSARIAIII; Fortessa). Sorted G2V E11 AGM (Ly5.1/Ly5.2) cells were transplanted[24] into 9.5-Gy irradiated (C57BL/6X129) F1 recipients (Ly5.2/Ly5.2) together with 2×10^5 spleen cells from the recipient strain. Peripheral blood (PB) donor chimerism was determined by Venus PCR and/or fluorescence-activated cell sorter (FACS) at 4 months after transplantation and scored positive if PB donor chimerism was >10%.

RNA analyses

Detailed RNA procedures are provided in supplemental Methods. The Gene Expression Omnibus data accession number is GSE76254. Briefly, RNA was isolated from E10.5 AGM CD31 and cKit sorted cells with the mirVana miRNA Kit (Ambion), and quality/quantity was assessed using the 2100 Bioanalyzer (Agilent; RNA Nano/Pico chip). For RNA sequencing, samples were prepared with the SMARTER protocol and analyzed on an Illumina HiSeq200 system.[25-27] For quantitative reverse transcription-PCR (qRT-PCR), SuperScriptII/III ReverseTranscriptase (LifeTechnologies) was used for first-strand cDNA synthesis. Primers are specified in supplemental Table 1.

Results

Generation and validation of a novel Gata2 reporter mouse model

Previously, analysis of Gata2-expressing cells has been limited to a reporter mouse model that results in Gata2 haploinsufficiency.[16] Our approach allows for the expression of the reporter within the Gata2 genomic locus without affecting the levels of Gata2 expression or protein function. This is particularly important because Gata2 haploinsufficiency greatly reduces the number of HS/PCs generated during development.[7,8,19,20,28] Briefly, an internal ribosome entry site sequence (IRES) followed by the Venus fluorochrome gene was recombined into the Gata2 3′UTR (Figure 1A) in ES cells. The resulting Gata2Venus (G2V) mice bred normally and showed no overt growth or hematopoietic defects.

To determine whether Venus reporter expression parallels that of Gata2, G2V bone marrow (BM) cells were sorted into Venus-expressing (Venus[+]) and nonexpressing (Venus[−]) fractions (Figure 1B). qRT-PCR for Gata2 and Venus transcripts (Gata2[V/+] BM) demonstrated that only Venus^{+} cells express Venus and Gata2 mRNA (Figure 1C). Western blot analysis revealed that equivalent amounts of Gata2 protein were present in Gata2^{+/+} and Gata2[V/V] adult BM cells (data not shown). FACS analysis showed that Gata2[v/v] BM LSK frequency (388/10[5] cells) are comparable to wild-type (WT) BM LSK frequency (378/10[5] cells). Importantly, the results of competitive limiting dilution transplantation analyses of Gata2[V/V] and WT BM cells demonstrate that HSCs are qualitatively and quantitatively normal in this mouse model (Figure 1D). Thus, Venus expression correctly reports Gata2 expression without interfering with its normal expression levels or function.

Gata2 is expressed in emerging aortic hematopoietic cluster cells and other embryonic hematopoietic tissues

Venus expression was examined in midgestation G2V hematopoietic tissues. Flow cytometry revealed that E9 to E11 AGM, YS, PL, and FL contained Venus^{+} cells (Figure 1E). At E9, 6.28 ± 0.47% of viable YS cells and 1.82 ± 0.31% of AGM cells are Venus[+]. At E10.5 (when the first HSCs are generated), 3.27 ± 0.52% of AGM cells are Venus[+], and this increases to 7.86 ± 1.1% at E11. Table 1 shows the frequencies of Gata2-expressing cells.[29,30]

Whole-mount images of E10 and E11 G2V embryos immunostained with anti-CD31 antibody (marks all endothelial cells and hematopoietic cluster cells) shows Venus^{+} cells along the aorta (DA). Venus^{+} cells are also observed in cells of the neural tube (NT), olfactory bulb (OB), and FL (Figure 2A-C). In the E10.5 AGM region (4,6 diamidino-2-phenylindole [DAPI] and CD31 stained [blue and red, respectively]), Venus expression is found in endothelial and hematopoietic cluster cells mainly on the ventral side of the DA and in
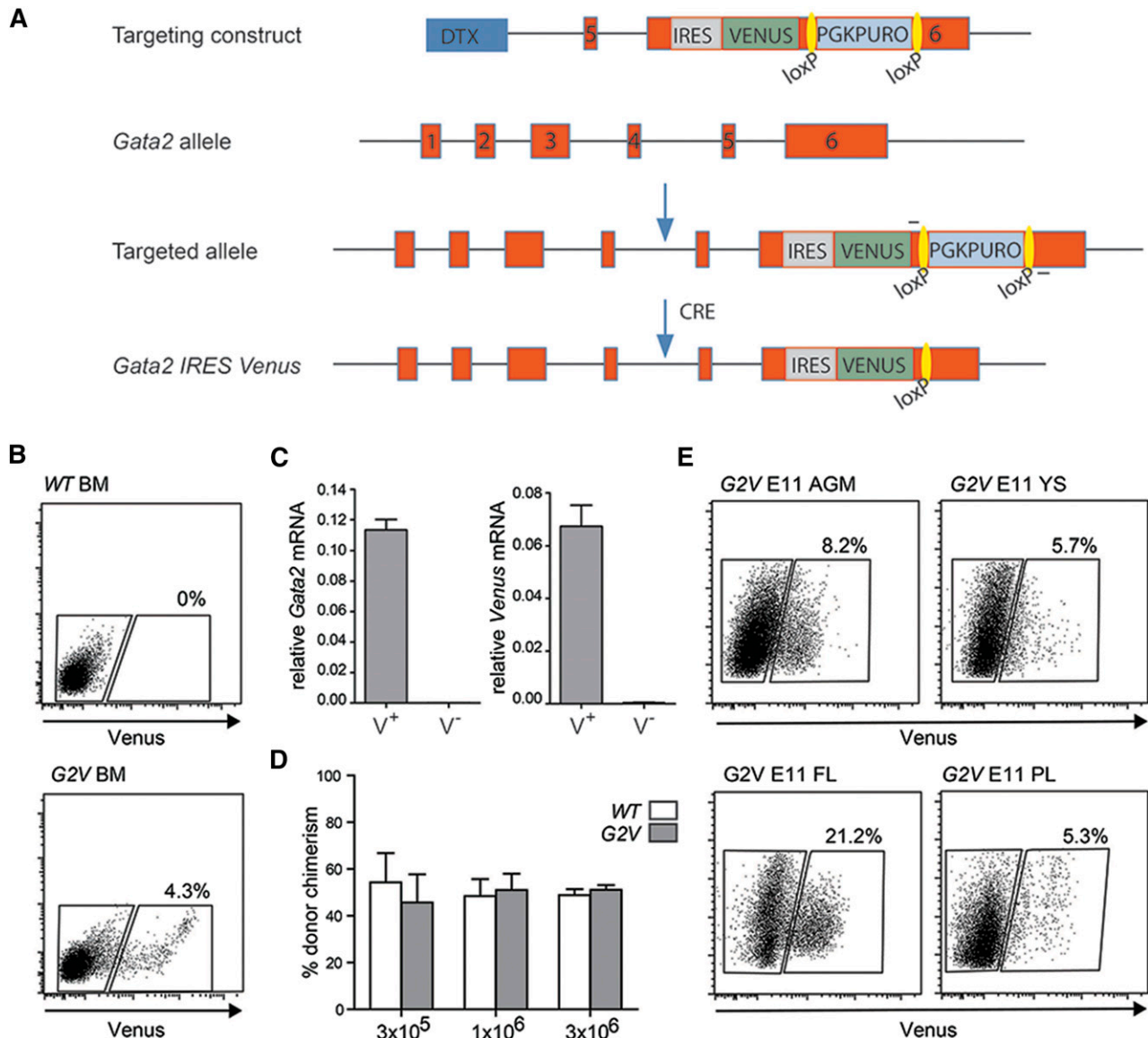
Figure 1. Gata2 Venus reporter construction and validation. (A) Schematic diagram of the *IRES Venus* reporter selection cassette insertion in the 3′UTR of the mouse *Gata2* locus and Cre-mediated removal of *lox PGK-Puro lox*. Primers used for detection of the targeted and recombined alleles are indicated flanking the loxP sites (yellow). (B) Representative flow cytometric analysis and sorting plot of Venus-expressing cells in the BM of adult *Gata2 Venus* (*G2V*) mice. Gated regions show percentage positive and negative viable cells. (C) Relative levels of *Gata2* and *Venus* mRNA in sorted Venus$^+$ and Venus$^-$ *Gata2*$^{V/+}$ BM cells as determined by qRT-PCR. *Gata2* transcripts in Venus$^+$ cells = 0.11337 ± 0.00681 and Venus$^-$ cells = 0.00012 ± 0.00003 (*P* = .000076). *Venus* transcripts in Venus$^+$ cells = 0.06722 ± 0.00799 and Venus$^-$ cells = 0.00036 ± 0.00010 (*P* = .00112). Mean ± standard error of the mean (SEM), n = 3. (D) Competitive limiting dilution transplantation strategy used to test the quantity and robustness of *Gata2*$^{V/V}$ BM HSCs compared with wild type. Percentage of donor cell chimerism in adult irradiated recipients cotransplanted with the same number of wild-type (WT) Ly5.1/5.2 and *Gata2 Venus* (*G2*$^{V/V}$) Ly5.2 BM cells. Varying numbers (1 × 10^5, 3 × 10^5, 3 × 10^6) of BM cells of each genotype were injected, and peripheral blood of recipients was analyzed for donor cell engraftment by FACS at 1 and 4 months after transplantation. n = 2 (5 mice per group). (E) Representative FACS plots demonstrating frequency of Venus expressing cells in E11 AGM, YS, PL, and FL. Gates indicate Venus$^-$ and Venus$^+$ cell fractions. Percentages represent the frequency of Venus$^+$ cells within the viable cell fraction (Table 1).

the urogenital (UG) region (Figure 2D-E). In the FL, Venus-expressing cells are found in a punctate distribution pattern (Figure 2D,F). At E9, Venus is expressed in some of the CD34$^+$ (red) endothelial cells of the paired aorta (Figure 2G, arrowhead) and also in some of the endothelial and hematopoietic cluster cells of the UA (Figure 2H). Venus continues to be expressed at E11 in some aortic endothelial cells and emerging/ other hematopoietic cluster cells (Figure 2I, arrowhead). The E10.5 YS shows Venus expression in some of the CD31$^+$ (red) endothelial cells. Overall, Venus expression is similar to what has been previously documented for *Gata2* in situ hybridization analysis.[31,32] Thus, our model allows for the prospective identification, isolation, and characterization of Gata2-expressing cells during normal development.

All HSCs, but not all HPCs, express Gata2

To test for HSC activity, E11 AGM Venus$^+$ and Venus$^-$ cells were transplanted into irradiated adult recipients. All long-term repopulating HSCs were found in the Gata2Venus-expressing fraction (Figure 3A). Nine of 19 recipients receiving Venus$^+$ cells were engrafted (15-71%), whereas none of the 14 Venus$^-$ recipients showed donor-derived hematopoietic cells. These HSCs were multilineage repopulating (supplemental Figure 1) and self-renewing (8 repopulated of 12 transplanted with 3 × 10^6 BM cells from primary repopulated mice; n = 4).

The relationship between Gata2 expression and HPC function was also examined. E9 and E10 AGM Venus$^+$ and Venus$^-$ cells were

Table 1. Frequency of Venus$^+$ cells in embryonic tissues of *G2V* embryos

Tissue	Stage	Number of experiments, embryos analyzed	% Venus$^+$ cells/tissue
AGM	E9, 16-25 sp	n = 4, 22	1.82 ± 0.31
	E10, 28-36 sp	n = 4, 29	3.27 ± 0.52
	E11, 43-49 sp	n = 4, 25	7.86 ± 1.1
FL	E9	nd	nd
	E10, 28-36 sp	n = 4, 10	13.89 ± 0.7
	E11, 43-49 sp	n = 4, 19	19.27 ± 2.14
YS	E9, 16-25 sp	n = 5, 8	6.28 ± 0.47
	E10, 28-36 sp	n = 6, 9	6.17 ± 0.86
	E11, 42-46 sp	n = 1, 3	5.25 ± 0.59
PL	E9, 17-23 sp	n = 3, 4	10.91 ± 0.49
	E10, 28-35 sp	n = 3, 6	10.8 ± 1.92
	E11, 42-46 sp	n = 1, 3	10.01 ± 4.64

The frequency of Venus$^+$ cells within the viable cell fraction of embryonic tissues per embryo is presented. FACS analysis of single cell suspensions of dissected embryonic tissues was performed to define the percentage of cells expressing Venus. AGM contains part of the vitelline and umbilical arteries. Our data for the total number of cells in each tissue (data not shown) correlated with published data for YS and E9.5 AGM[29] and for FL.[30] The data represent mean ± SEM of 3 to 6 independent experiments, with the exception of E11 YS and PL data (data represent the mean ± standard deviation of 1 experiment. E, embryonic day; n, number of independent experiments, number of individual embryos analyzed; nd, not done; sp, somite pairs.

plated in the colony forming unit–culture (CFU-C) assay. High enrichment of HPCs was found in the Venus$^+$ fractions (Table 2). Surprisingly, HPCs were found also in the Venus$^-$ fraction, although there were very few. At E9, the Venus$^+$ and Venus$^-$ fractions, respectively, yielded 8.0 ± 2.1 and 0.4 ± 0.4 CFU-C per AGM. CFU-C numbers increased in the Venus$^+$ cell fraction at E10 (69.0 ± 7.1) and the Venus$^-$ fraction increased to 8.0 ± 2.3 CFU per AGM. However, bi- and multipotent progenitors were found only in the Venus$^+$ fraction (Figure 3B).

HPC activity was also examined in the Venus$^+$ and Venus$^-$ fractions of other hematopoietic tissues (Table 2). E9 and E10 VA+UA (Figure 3C), YS (Figure 3D), and PL (Figure 3E), and E10 FL (Figure 3F) contained progenitors in both fractions. Most HPCs were Venus$^+$. The greatest number of CFU-C arising from Venus$^-$ cells was found in the E9 YS (270.0 ± 69.8 CFU-C/YS). These data indicate that some HPCs are not expressing Gata2. BFU-E, CFU-G, and CFU-M were the predominant colony types in both fractions, and in contrast to the Venus$^+$ fractions, the Venus$^-$ fractions of VA+UA, YS, FL, and PL yielded few or no CFU-GEMM. Thus, all AGM HSCs express Gata2, Gata2 expression is associated with immature HPCs, but not all HPCs are Gata2 expressing.

Some HPCs and vascular cluster cells are formed in the absence of *Gata2*

Because the Venus$^-$ fractions of midgestation *G2V* hematopoietic tissues contain CFU-C, we tested whether such hematopoietic progenitors are present in *Gata2*-deleted embryos. CFU-Cs were detected in the *Gata2*$^{-/-}$ E9 AGM, E10 AGM (Figure 4A), and E10 VA+UA (Figure 4B), although significantly fewer compared with WT (Table 3). *Gata2*$^{+/-}$ tissues also contained fewer CFU-Cs compared with WT. The E9 *Gata2*$^{-/-}$ YS contained the most CFU-C (64.4 ± 12.2; Figure 4C). In *VEC-Cre:Gata*$^{f/f}$ embryos, E10 PL showed significantly decreased CFU-C numbers (Figure 4D), as did E10 AGM and YS[7] compared with WT. The CFU-C remaining in *Gata2*$^{-/-}$ embryos are predominantly CFU-G and CFU-M. Very few *Gata2*$^{-/-}$ CFU-GM and no CFU-GEMM were observed. These data support and validate our findings in *G2V* embryos that not all HPCs are Gata2-expressing, Gata2-independent progenitors exist in each of the early hematopoietic tissues, and the Gata2-expressing cell fraction is more enriched in multipotent progenitors.

Because hematopoietic clusters appear in the VA and UA prior to appearance in the aorta, and are larger than in the AGM,[33] we further examined these vessels. Whole-mount microscopic analysis demonstrates that clusters form in the absence of Gata2. The number and size of cKit$^+$ hematopoietic clusters in early E10 *Gata2*$^{+/-}$ and *Gata2*$^{-/-}$ VA+UA are decreased compared with WT (Figure 4E). The number of cKit$^+$ cells decreases 20-fold in the E10 *Gata2*$^{-/-}$ VA+UA (Figure 4F) in correspondence to the decrease in VA+UA CFU-C (Figure 4B), suggesting that these emerging cKit$^+$ hematopoietic cluster cells are part of the cohort of Gata2-independent HPCs.

Alternative genetic program is expressed in Venus$^-$ hematopoietic cells

The molecular basis for the functional differences observed in Gata2-dependent and -independent HPCs was examined by RNA sequencing. As most CD31$^+$Venus$^-$ HPCs showed cKit intermediate expression, we compared this population to CD31$^+$Venus$^+$cKit^{int} HPCs (Figure 5A). Gene set enrichment analysis on genes sorted by log ratio of Venus$^+$ vs Venus$^-$ FPKMs revealed that genes in the Ras signaling pathway were significantly enriched in the Venus$^+$ compared with the Venus$^-$ fraction (Figure 5B). Genes upregulated by Ras were enriched in the Venus$^+$ fraction, and highly upregulated genes included *Kras, Grb2* (Ras adaptor), and *Sos1* and *Sos2* (RasGEF activators) (Figure 5C). Genes downregulated by Ras were enriched in the Venus$^-$ fraction. RasGAP gene (renders Ras inactive) *Rasa2* was highly upregulated in the Venus$^-$ fraction, whereas *Rasa1* and *Rasa3* were highly upregulated in the Venus$^+$ fraction. *Rasa4* and *NF1* were expressed to similar levels. Also, Venus$^+$ HPCs showed increased levels of *CREB* and *CBP* expression compared with Venus$^-$ HPCs and express protein kinase A catalytic subunit genes, suggesting that Venus$^+$ HPCs have the potential to activate CREB target genes. *Gata2* has *CREB response element* consensus sites (-3 kb, -300 bp upstream transcription start site), suggesting that it is a downstream target.[34,35] As *Gata2* is a Notch target,[18] a two- to fourfold higher expression of *Notch1* and *Notch4* was found in the Venus$^+$ fraction (Figure 5D). Moreover, *Snw1* and *Maml1* (transcriptional coactivators in the Notch pathway that interact with Notch) were upregulated (2- and 30-fold, respectively) in Gata2-expressing HPCs.

Because Venus$^-$ HPCs are mainly restricted in their differentiation potential to the macrophage and granulocytic lineages, we evaluated their similarity to YS-derived erythromyeloid progenitors (EMPs) that give rise to tissue-resident macrophages. Flow cytometric analysis for EMP markers[36] showed that 3.89% of E10 YS and 0.72% of E10 AGM cells were EMPs (Sca1$^-$cKit$^+$CD41$^+$CD16/32$^+$). The majority of EMPs were Venus$^-$ (74% in YS, 85% in AGM; Figure 5F). At E11, the frequency of EMPs in the E11 YS and AGM decreased to 2.11% and 0.11%, respectively (Figure 5F), with 60% of YS and 77% of AGM EMPs now being Venus$^+$. Published transcriptome data on mouse YS EMPs show the low expression of several chemokine receptors/ligands (*Cx3cr1, Cx3cl1, Ccl2, Ccr1, Ccl9,* and *Ccr7*).[37] The expression of these genes was low or absent in Venus$^-$ AGM cells compared with Venus$^+$ cells (Figure 5F). Also, *Cxcr4* (highly expressed in EMPs) was highly expressed in Venus$^-$ AGM cells compared with Venus$^+$ cells. These results suggest that the Venus$^-$ population shares similarities to EMPs at the transcription level.

Analysis of FPKMs for heptad transcription factors previously described as expressed in AGM HSCs and HPCs[1-3] showed expression in both the Venus$^+$ and Venus$^-$ AGM fractions (data not shown). Also, other Gata factors were expressed in both fractions. In the mouse, *Gata1, 2,* and *3* are hematopoietic transcription factors, whereas the *Gata4, 5,* and *6* factors are not directly related to hematopoiesis.
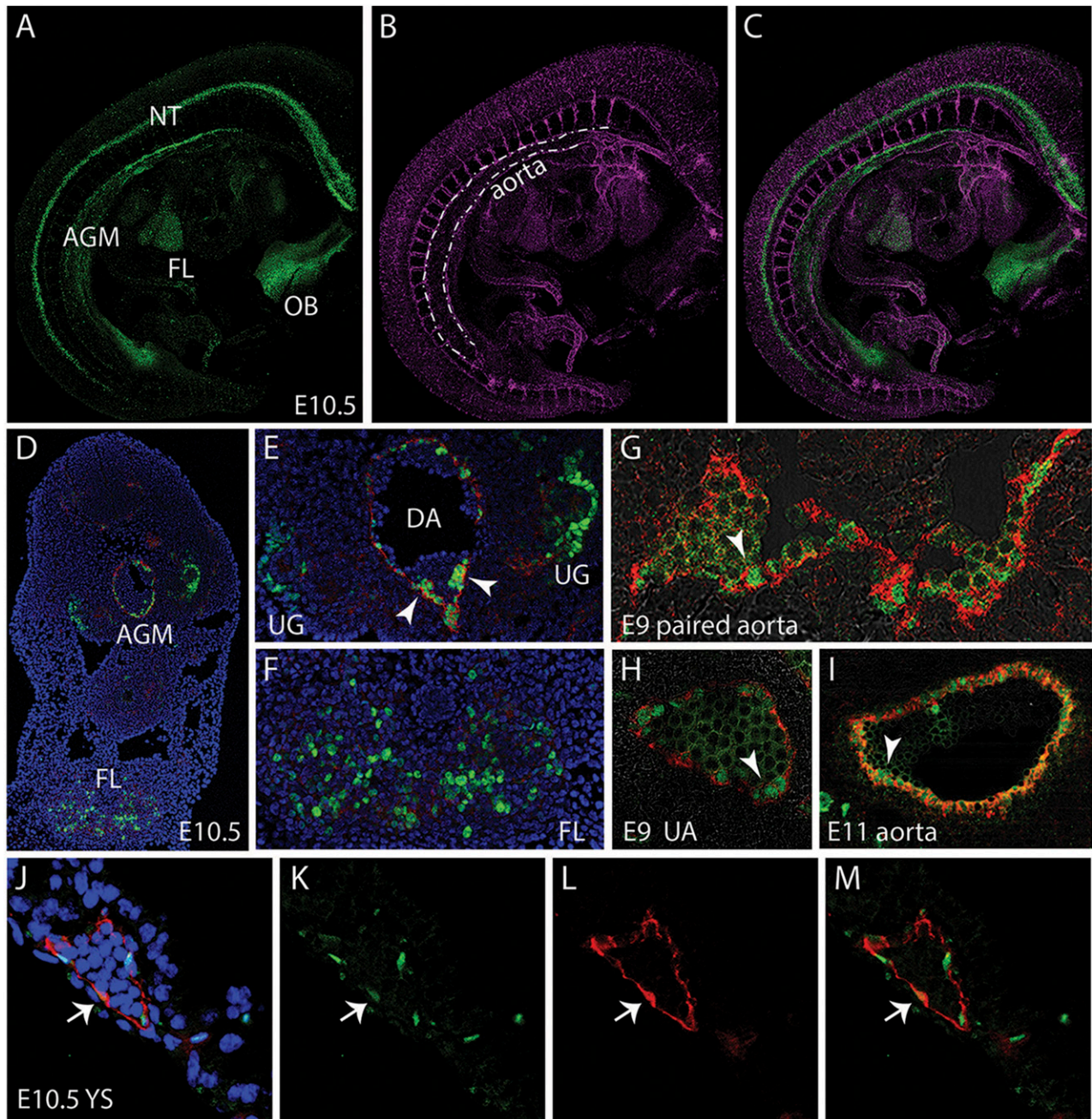
Figure 2. Localization of Gata2Venus-expressing cells in embryonic hematopoietic sites. Confocal images of a whole mount immunostained E10.5 Gata2Venus embryo showing (A) Venus (green), (B) CD31 (magenta), and (C) merged expression. Venus-expressing cells are detected in the AGM along the wall of the dorsal aorta (dotted lines), the FL, NT, and OB. (D) Confocal image of a transverse section through the E10.5 AGM. DAPI staining (blue), CD31 (red), and Venus fluorescence (green) revealed Gata2-expressing aortic endothelial and hematopoietic cluster cells and UG and FL cells. Enlarged images of D showing Gata2-expressing cells in (E) AGM (DA, dorsal aorta; UG, urogenital ridges; arrowheads indicate hematopoietic cluster) and (F) FL. Venus (green) and CD34 (red) fluorescence showing endothelial and hematopoietic cluster cells in (G) E9 paired aorta, (H) umbilical artery (UA) at E9, and (I) E11 aorta. Arrowheads indicate hematopoietic cluster. (J-M) Images of E10.5 YS section showing DAPI merged, Venus, CD31, and merged fluorescence. Arrow denotes an endothelial cell expressing Venus and CD31.

qRT-PCR performed on E10.5 AGM CD31$^+$cKit$^+$ cells (Figure 6A) confirmed *Gata3* expression by both the Venus$^+$ and Venus$^-$ fractions, and *Gata4* was significantly higher in the Venus$^-$ fraction. *Gata1, 5,* and *6* transcripts were low/not detected. Immunostaining of E10.5 AGM (WT) showed Gata3-expressing cells in the mesenchyme underlying the ventral aspect of the aorta, aortic endothelial cells, and some cells emerging from the aortic wall (Figure 6B) in agreement with Fitch.[38] *G2V* E10.5 AGM confirmed that some aortic endothelial cells coexpress Gata3 and Gata2 (Figure 6C). Gata4 expression was also found in aortic endothelial (CD34$^+$) cells, but it did not overlap with Gata2 expression

(Figure 6D). Together, these results suggest that Gata3 and/or Gata4 may provide some function in Gata2-independent hematopoietic cells.

Discussion

In this study, we prospectively enriched and characterized Gata2-dependent and -independent HPC subsets from our novel *Gata2Venus* reporter mouse. Molecular analyses, together with the fact that some

Figure 3. Quantitation of functional HSCs and HPCs in *G2V* embryonic hematopoietic tissues. HSCs in sorted Venus[+] and Venus[−] cell fractions of E11 AGM were analyzed by transplantation into irradiated adult recipients. (A) Percentage donor cell chimerism was determined by Venus PCR of peripheral blood DNA at 4 months after transplantation. Each dot represents 1 recipient receiving 1.7 to 6.5 embryo equivalent (ee) of AGM cells. n = 7. **P = .0089. (B-F) Hematopoietic progenitor number per tissue in sorted Venus[+] and Venus[−] cell fractions of (B) E9 and E10 AGM, (C) E9 and E10 VA+UA, (D) E9 and E10 YS, (E) E9 and E10 PL, and (F) E10 FL. CFU-C per 1 ee of tissue is shown. Colony types designated by colored bars are CFU-granulocyte, erythroid, monocyte, megakaryocyte (GEMM); CFU-granulocyte, macrophage (GM); CFU-macrophage (M); CFU-granulocyte (G), and burst forming unit-erythroid (BFU-E). SEM of total CFU-C is shown; 2 ee of somite pair–matched tissues were pooled for sorting and yielded 1 ee for colony analysis.
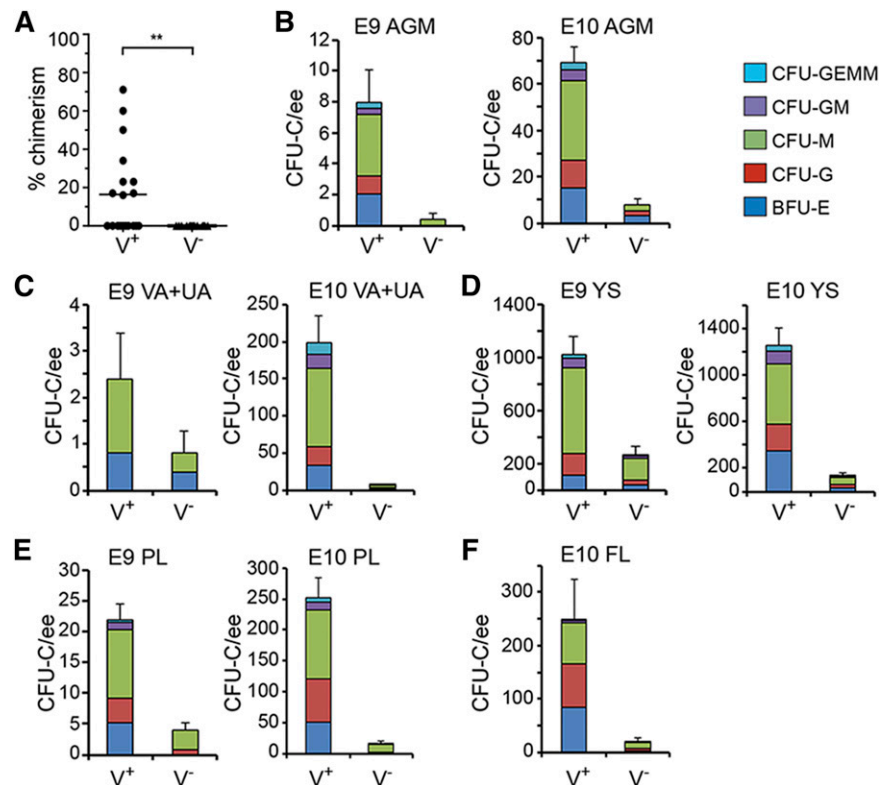
vascular hematopoietic cluster cells and HPCs persist in the absence of Gata2 expression, suggest that an alternative genetic program exists for the production of HPCs. The transcriptome differences observed between Venus[+] and Venus[−] HPCs may offer possibilities for pathway modifications to achieve the programming complexities necessary for the generation/function of normal definitive HPCs and provide insights into the factors involved in myeloid leukemogenesis.

Gata2 expression in the developing hematopoietic system

We showed the temporal and quantitatively coordinate transcription of *Venus* and *Gata2* in our *G2V* mouse model. The strategy used[39] eliminates expression level and protein alterations that affect HP/SC development. In *G2V* embryos, we showed that the cells with the most robust and complex hematopoietic potential (all HSCs and most HPCs) are Gata2 expressing. Imaging and FACS analyses of *G2V* embryos confirm that Gata2 is expressed in all hematopoietic sites during midgestation and that the numbers of Gata2-expressing cells reflect the developmental and temporal hematopoietic changes occurring in each

site. At E9, Gata2-expressing cells are found predominantly in the YS, which at this time produces the highest numbers of the hematopoietic progenitors (EMP) in the conceptus. Slightly later as hematopoiesis begins in the AGM and FL, the numbers of Gata2-expressing cells also increase. The highest numbers of CD31^{+}cKit^{+} cluster cells are found in the aorta, VA, and UA at E10.5, as quantitated by whole-mount embryo imaging.[33] Most, but not all, hematopoietic cluster cells express Gata2, and *Gata2* expression may be downregulated as HPCs differentiate. However, we found some hematopoietic cluster cells and HPCs in the E10 *Gata2*^{−/−} vasculature, confirming the existence of Gata2-independent HPCs.[5]

Importantly, Gata2 is expressed in the endothelial cells of the DA. Already at E8.5, endothelial cells lining the paired dorsal aortae express Gata2, and it continues to be expressed in the E10.5 aorta when HSCs are generated, thus highlighting an involvement of Gata2 in the hemogenic program of endothelial cells. Data in *VE-cadherin* conditional *Gata2*-deficient mice and other models[7,19,28,40] strongly support the notion that Gata2 is required in hemogenic endothelium

Table 2. CFU-C number in Venus[+] and Venus[−] cell fractions of *G2V* embryonic tissues

			CFU-C/tissue/sorted cell fraction	
Tissue	Stage	Number of experiments, embryos analyzed	Venus[−]	Venus[+]
AGM	E9, 20-23sp	n = 2, 5	0.4 ± 0.4	8.0 ± 2.1
	E10, 32-35sp	n = 2, 6	8.0 ± 2.3	69.0 ± 7.1
VA+UA	E9, 20-23sp	n = 2, 5	0.8 ± 0.5	2.4 ± 1.0
	E10, 32-35sp	n = 2, 6	7.0 ± 1.5	197.7 ± 36.9
YS	E9, 20-23sp	n = 2, 5	270.0 ± 69.8	1020 ± 137.3
	E10, 32-35sp	n = 2, 5	130.0 ± 25.5	1252.0 ± 156.0
PL	E9, 20-23sp	n = 2, 5	4.0 ± 1.3	22.0 ± 2.5
	E10, 32-35sp	n = 2, 6	14.5 ± 5.3	251.7 ± 32.4
FL	E10, 32-35sp	n = 2, 6	20.5 ± 7.6	248.7 ± 75.2

Number of total CFU-C (mean ± SEM) per tissue per *G2V* embryo for the sorted Venus[−] and Venus[+] cell fractions at E9 and E10.
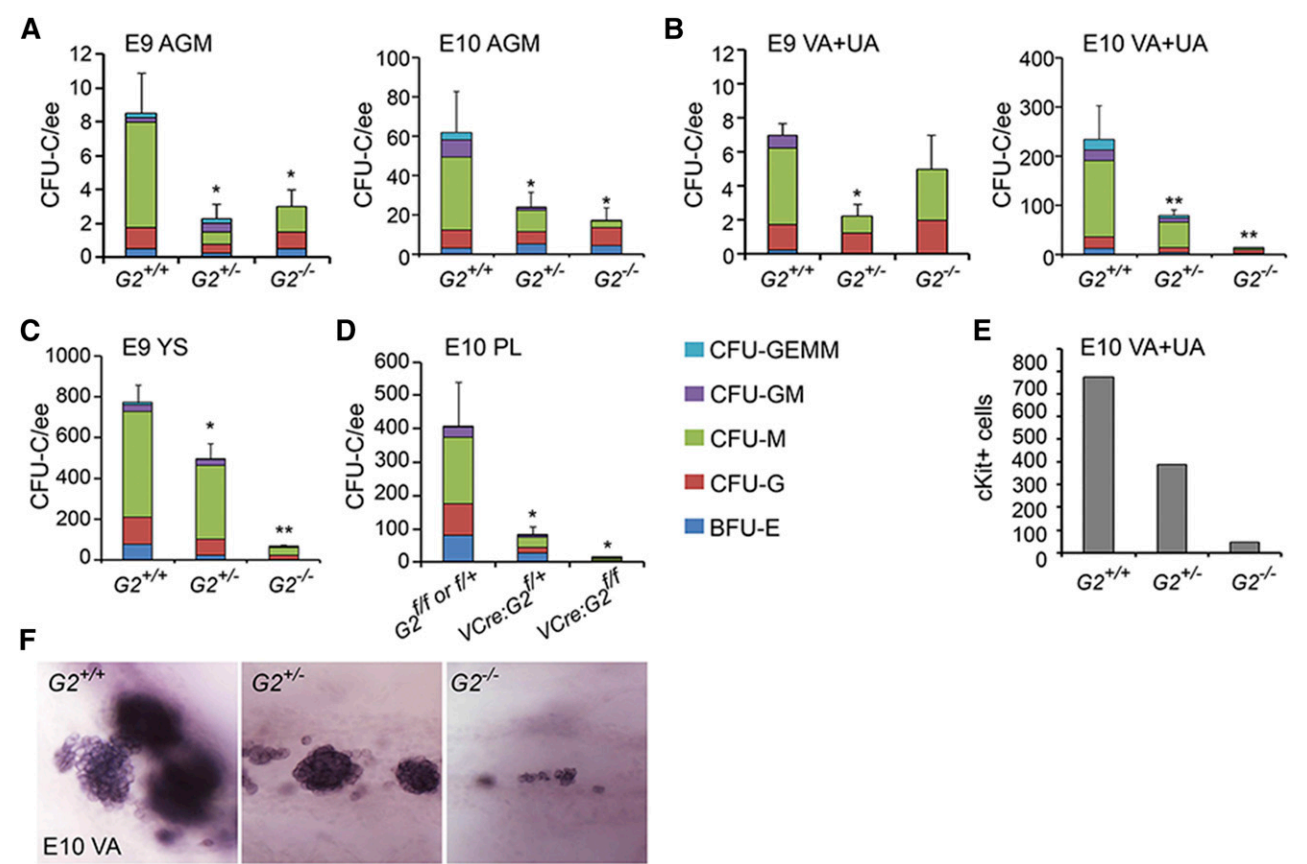
Figure 4. CFU-C numbers and vascular hematopoietic clusters in Gata2$^{-/-}$ embryos. CFU-C numbers per ee found in (A) E9 and E10 AGM, (B) E9 and E10 VA+UA, (C) E9 and E10 YS, and (D) E10 placenta. *P < .05; **P < .01. (E) Quantitation of cKit$^+$ hematopoietic cluster cells in VA+UA of E10 Gata2$^{+/+}$, Gata2$^{+/-}$, and Gata2$^{-/-}$ embryos. (F) Representative whole mount images of hematopoietic cluster cells in the VA of E10 Gata2$^{+/+}$ (30 sp), Gata2$^{+/-}$ (31 sp), and Gata2$^{-/-}$ (30 sp) embryos stained for cKit expression.

for the emergence of HSCs, as does the morpholino knockdown of Gata2b in zebrafish.[41]

Gata2 and the relationship with hematopoietic function

Prospective isolation and in vivo transplantation showed that all HSCs are Gata2 expressing. In contrast, some HPCs are present in the Venus$^-$ cell fractions of G2V hematopoietic tissues and Gata2$^{-/-}$ hematopoietic tissues. In both cases, the HPCs are restricted in their differentiation potential to predominantly the macrophage and granulocytic lineages. Currently, the EMP population is of high interest as a novel hematopoietic cell subset providing tissue resident macrophages.[37,42-44] Our FACS data revealed that EMPs are mainly in the Venus$^-$ cell population of E10 YS and AGM and increased in the Venus$^+$ population at E11. Chemokine receptor/ligand gene sets obtained from a study on EMP/microglia transcriptome comparisons allowed us to find similarities in chemokine receptor/ligand expression between EMPs and the Venus$^-$ HPC fraction.

Despite prevalence of EMPs in the Venus$^-$ cell population in E10 YS and AGM, definitive progenitors are largely Venus$^+$. The co-existence of these HPC subsets highlights the fact that there is more diversity in the types of progenitors generated in the embryo than was

Table 3. CFU-C number per E9-E10 Gata2-deleted hematopoietic tissues

Tissue	Stage	Genotype					
		WT		Gata2$^{+/-}$		Gata2$^{-/-}$	
AGM	E9, 20-23sp	8.5 ± 2.3	n = 1, 4	2.25 ± 0.9*	n = 1, 4	3.0 ± 1.0	n = 1, 2
	E10, 28-34sp	62.4 ± 20.8	n = 3, 7	24.0 ± 7.4*	n = 3, 13	16.7 ± 6.8*	n = 3, 9
VA+UA	E9, 20-23sp	7.0 ± 0.6	n = 1, 4	2.25 ± 0.6*	n = 1, 4	5.0 ± 2.0	n = 1, 2
	E10, 28-34sp	241.1 ± 67.8	n = 3, 7	78.7 ± 12.3**	n = 3, 13	12.0 ± 2.5**	n = 3, 9
YS	E9, 20-23sp	772.5 ± 85.3	n = 1, 4	500.0 ± 71.5*	n = 1, 4	64.4 ± 12.2**	n = 1, 2
	E10, 28-34sp	918.6 ± 147.9	n = 3, 7	584.6 ± 89.0**	n = 3, 9	25.7 ± 8.0**	n = 2, 3
		Gata2$^{f/+}$ or Gata2$^{f/f}$		VEC-Cre:Gata2$^{f/+}$		VEC-Cre:Gata2$^{-/-}$	
FL	E10, 30-34sp	115.8 ± 35.0	n = 2, 5	83.0 ± 20.8	n = 2, 6	22.2 ± 6.7*	n = 2, 6
PL	E10, 30-34sp	406.0 ± 134.0	n = 2, 5	81.0 ± 25.0*	n = 2, 6	12.0 ± 4.0*	n = 2, 6

Number of total CFU-C (mean ± SEM) per tissue shown for WT, Gata2 germline, and conditional knockout embryos at E9 and E10.
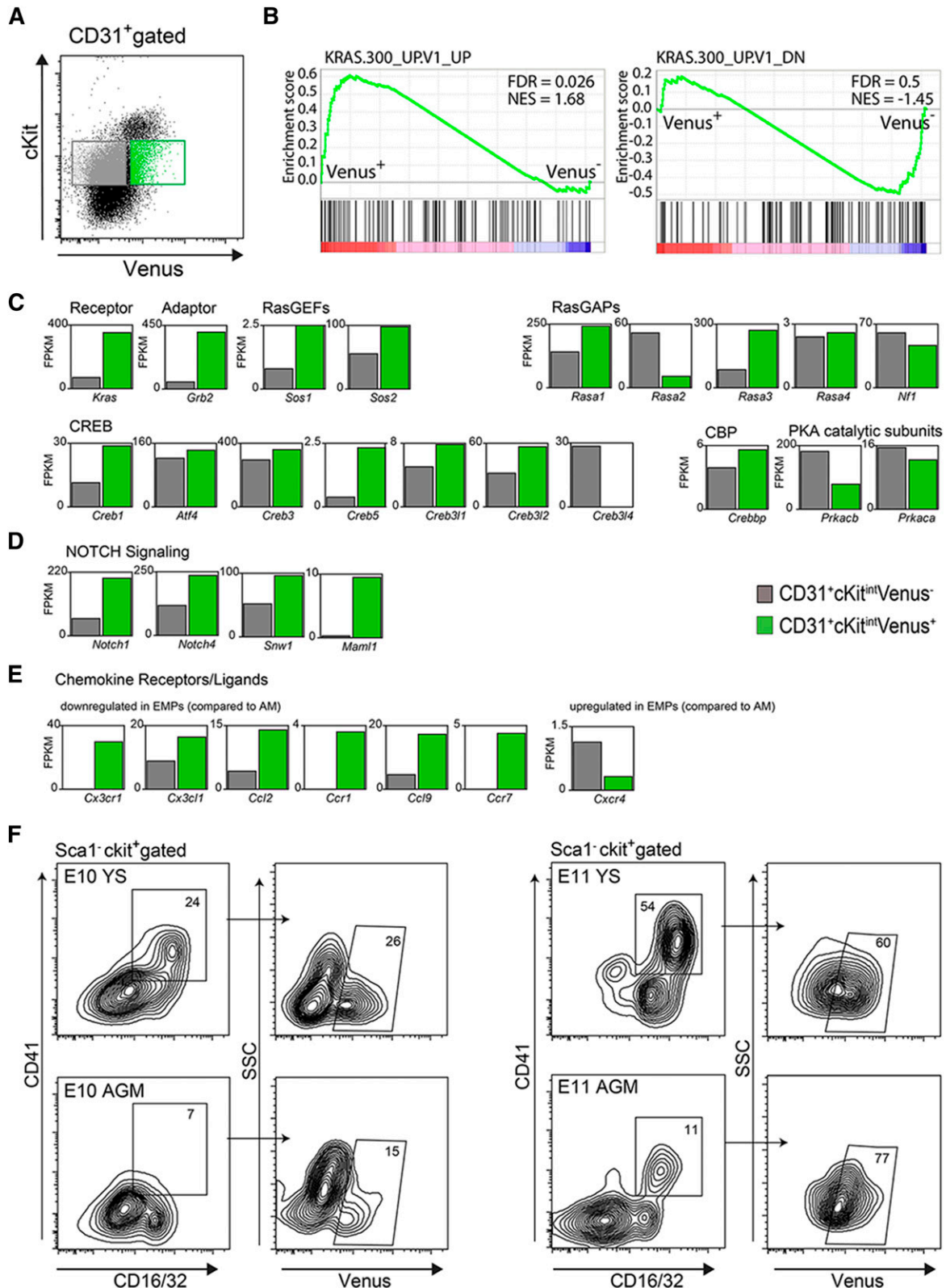
*P < .05.

**P < .01.

Figure 5. Differential expression of signaling pathway modulators in Gata2-dependent and -independent HPCs. (A) Flow cytometric sorting gates for isolation of E10.5 AGM *G2V* CD31+cKit^intVenus− (gray) and CD31+cKit^intVenus− (green) HPCs used for RNA sequence analysis. Gene Expression Omnibus data accession number is GSE76254. (B) Gene enrichment analysis for Ras signaling pathway genes. Bar graphs of fragments per kilobase million (FPKM) values obtained from RNA sequence analysis of CD31+cKit^intVenus− (gray bar) and CD31+cKit^intVenus+ (green bar) AGM cells for (C) Ras pathway and cyclic AMP response element-binding protein (CREB) and CREB-binding protein (CBP) transcription factor genes and (D) Notch pathway genes. (E) Bar graphs of FPKM values obtained from RNA sequence analysis for a selection of chemokine receptor/ligand genes (see Kierdorf et al[37]; these genes were down-/upregulated in YS EMPs compared with adult microglia [AM]). (F) Representative FACS plots demonstrating frequency of EMPs in the Venus+ fraction, as defined as Sca1−cKit+CD41+CD16/32+, in YS and AGM of E10 (left) and E11 (right) *G2V* embryos. Numbers indicate the percentages of gated cells within the parental cell population.
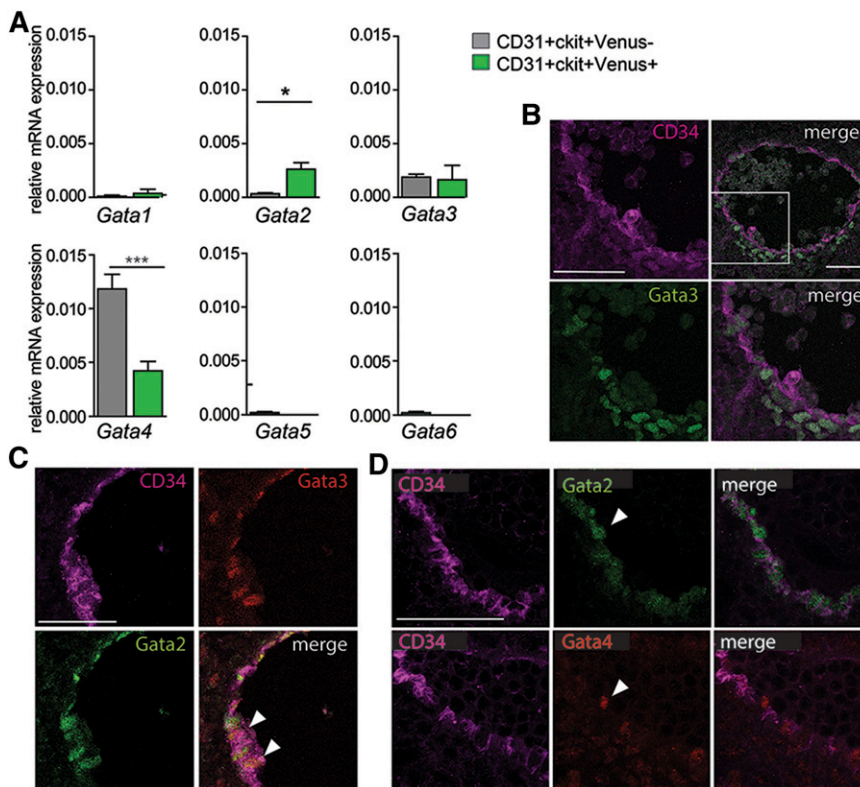
115

Figure 6. Gata family gene expression in AGM Gata2-dependent and -independent HPCs. (A) qRT-PCR for expression of *Gata1, 2, 3, 4, 5,* and *6* transcription factors (normalization with *Gapdh*) in E11 AGM CD31+cKit+Venus+ and CD31+cKit+Venus− cells. n = 3. SEM shown with *P = .05 and ***P = .001. (B) Transverse section of WT E10.5 AGM immunostained for CD34 (magenta) and Gata3 (green) showing expression of Gata3 in the aortic endothelial cells and some emerging hematopoietic cells and ventral mesenchymal cells directly under the aorta. (C) Transverse section of *G2V* E10.5 AGM immunostained for CD34 (magenta), Gata2 (green), and Gata3 (red) showing some overlapping expression of Gata2 and Gata3 in aortic endothelial cells (arrowheads). (D) Transverse consecutive sections of E11 *G2V* AGM immunostained for CD34 (magenta) and Venus (green) in the top panels and for CD34 (magenta) and Gata4 (red) in the bottom panels. Gata4 expression is observed in some ventral aortic endothelial cells and emerging hematopoietic cells (arrow).

previously appreciated. In support of this are recent data from ES cell hematopoietic differentiation cultures suggesting that there are 2 different hemogenic endothelial cell subsets[45] and the fact that, in vivo, the AGM, VA/UA, YS, PL, and head are all hemogenic tissues.[36,46-49]

The highest number of Venus− HPCs was found in E9 and E10 YS (270.0 ± 69.8 and 130.0 ± 25.5 CFU-C, respectively) compared with other tissues (PL, AGM, VA+UA). It is clear that Gata2 has an important role in EHT in the hemogenic endothelial cell compartment before or during the generation/emergence of hematopoietic cells, as evidenced by the decrease (but not absence) in the hematopoietic cluster cells in *Gata2*^{−/−} aorta, VA, and UA. However, it is as yet unclear at what frequency EHT occurs in the YS, thus raising the possibility that Gata2-independent HPCs arise differently than Gata2-dependent HPCs (perhaps directly from hemangioblasts[50]).

We found differences in the number of CFUs from E9 YS Venus− cells (270.0 ± 69) and Gata2^{−/−} cells (64.4 ± 12.2; Figures 3D and 4C; Tables 2 and 3). The fourfold lower CFU number is likely related to observations (ours and others) that colonies from *Gata2*^{−/−} embryos, YS explants, and ES cell differentiations were smaller/less proliferative than WT colonies, due to the complete absence of Gata2.[6,7] Venus− cells are not defective for Gata2, and the resulting colonies are normal in size. Whereas at the time of sorting they did not express Gata2, Gata2 expression could initiate after seeding Venus− HPCs in methylcellulose, and cells thus undergo normal proliferation/differentiation. To test whether Venus− HPCs can convert to Venus+ cells, we analyzed Venus expression in colonies derived from sorted YS fractions after 10 days of differentiation (Figure 7). Venus expression was found in colonies derived from both fractions, indicating that a portion of Venus− cells start to express Gata2 during formation of a hematopoietic colony. Interestingly, colonies derived from Venus+ cells showed a Gr1+ and Mac1+ phenotype, whereas Venus−-derived colony cells were only Mac1+. This demonstrates that Gata2 is not necessary for a

subset of HPCs and that Gata2 promotes more complex hematopoietic function in other progenitor subsets.

Gata3/Gata4 redundancy in Gata2-independent progenitors

The expression of Gata3 and Gata4 in Venus− AGM HPCs and aortic endothelial cells is intriguing and highlights the potential redundancy of Gata transcription factors in hematopoietic cell generation. *Gata2* and *Gata3* can partially rescue the erythroid phenotype in *Gata1*-deficient mice,[51,52] and although recently it was suggested that *Gata3* is redundant in HSCs,[53] others clearly show that it regulates HSC cell cycle entry[54] and self-renewal.[55] The fact that *Gata3* and *Gata4* are expressed in *Gata2*-nonexpressing enriched HPCs suggests that they may function in this early progenitor subset. *Gata3*-deficient embryos show decreased numbers of FL HP/SCs.[56] Gata3 affects HSC development non-cell autonomously by activating the expression of *Th* (tyrosine hydroxylase) and hence, catecholamine production in the ventro-lateral cells of the sympathetic nervous system underlying the embryonic aorta.[38] HSC production was rescued when catecholamines were administered to the pregnant dams. These investigators also found that some aortic endothelial cells express a *Gata3LacZ* reporter, leaving open the possibility of a direct and overlapping role for Gata3 in some HPCs.

Much less is known concerning Gata4 in hematopoietic development. In zebrafish, there is a close relationship between anterior hemangioblasts and cardiac precursors.[57] Together with *Gata5* and *Gata6, Gata4* specifies these 2 anterior mesoderm derivatives. In mice, *Gata4* is a key component of the cardiac developmental program, with close associations between cardiac, vascular, and hematopoietic lineages.[58-60] Moreover, a subset of mouse endocardial and YS endothelial cells express cardiac markers, possess hemogenic potential, and give rise to transient definitive erythroid/myeloid progenitors.[61] Our results suggest the Gata4 aortic endothelial cells and Venus−

Figure 7. Gata2 is expressed by Venus⁻ cells after culture. Schematic diagram showing method and FACS analysis by which Gata2 expression was found in the progeny of sorted Venus⁻ HPCs. *G2V* YS tissue was FACS sorted into Venus⁻ and Venus⁺ fractions. Cells were subsequently seeded in methylcellulose, and colonies were analyzed after 10 days of culture. Colonies were harvested from the dish, cells were washed and stained (with anti-Gr1 and anti-Mac1 antibodies), and Venus, Gr1, and Mac1 expression was analyzed by FACS. FACS plots (top) indicate Venus expression in cells harvested from Venus⁻ (left) and Venus⁺ (right) CFU-C experiments. Note that both FACS analyses indicate Venus expression in both cultures. FACS plots (bottom) show Gr1 and Mac1 expression in Venus⁻ and Venus⁺ populations in both cultures and that cells harvested from the Venus⁺ culture show a more immature phenotype.
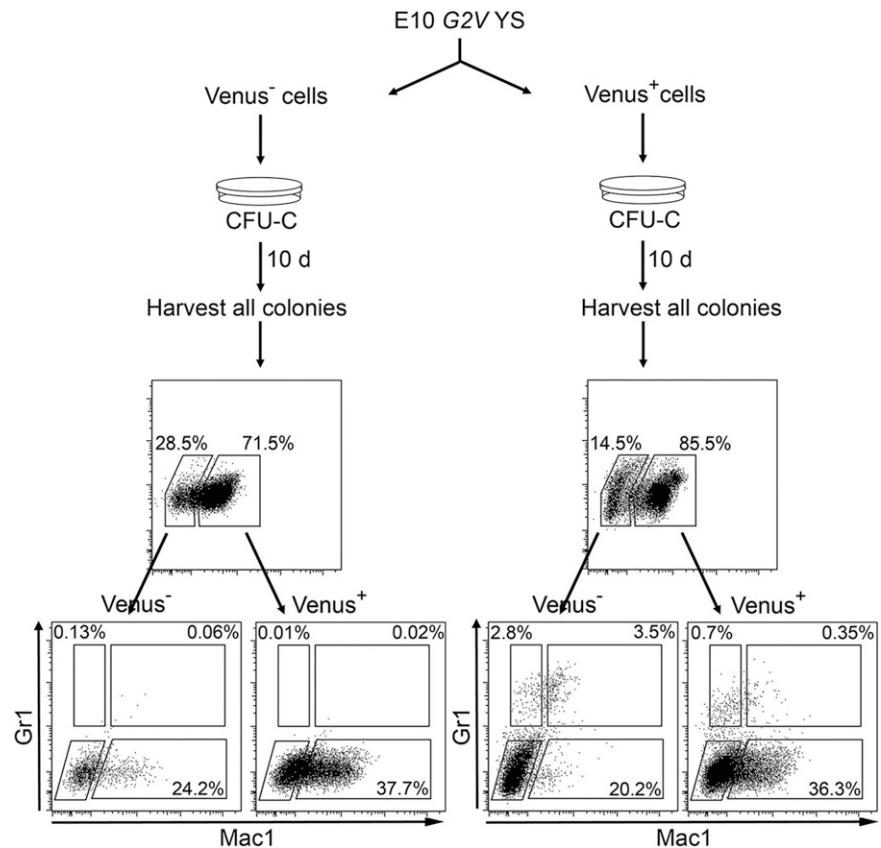
Gata4-expressing HPCs may be derivatives of mesodermal cells with a genetic program that retains cardiac-vascular-hematopoietic potential and can produce HPCs. Further examination of double reporter and deficient mice should reveal the overlapping and/or redundant roles of these Gata factors.

Gata2 as a pivotal regulator of complex hematopoietic function

RNA sequence comparisons of the functionally distinct Venus⁺ and Venus⁻ HPC subsets revealed a strong upregulation of *Kras* and *Ras* pathway genes in Venus⁺ HPCs. This pathway is particularly important in cell differentiation, acting as a molecular switch to relay extracellular growth signals.[62] *Kras* mutations confer a competitive-repopulating advantage to BM HSCs in transplantations and initiate leukemia in mice.[63] In humans, *Kras* mutations (together with other cooperating gene mutations) are prevalent in patients with various forms of myelomonocytic and myeloid leukemia.[64] Interactions between oncogenic Ras and Gata2 have been proposed.[65] The normal function of Kras has not yet been explored fully. However, conditional deletion of *Kras* by *Vav-Cre* or *Mx1-Cre* does not affect HSCs or the adult hematopoietic system.[66] However, chimeric mice, produced by *Kras*⁻/⁻ ES cell blastocyst injection, show no contribution of *Kras*⁻/⁻ cells to the hematopoietic system, suggesting that Kras may be important during the embryonic development of the hematopoietic system but not after its generation.

The low expression of *Notch1*, *Notch4*, and coactivators in the Venus⁻ compared with the Venus⁺ HPC fraction supports the fact that early hematopoietic cells are generated independent of this signaling pathway or implies that these are differentiated cells that have turned off Notch signaling.[67,68] Others have shown that *Notch1* deletion impairs the development of HSCs and angiogenesis,[69] but not YS primitive or definitive hematopoiesis. Moreover, *Gata2* expression

in the aortic endothelium is lost when *Jagged1* (ligand) is deleted.[70] Our data demonstrate a direct relationship for Notch and Gata2 expression, strongly supporting a pivotal role for this pathway in the generation of functionally complex hematopoietic cells. In the absence of Notch signaling, less complex HPCs emerge in the AGM or are immigrants from the YS.[18,69,70] In addition, our observed upregulated expression of some CREB genes in Venus⁺ HPCs supports the involvement of these regulators in definitive hematopoietic cell generation.[71] Our *Gata2Venus* model, in combination with recently reported *Gata2* distal enhancer-*Evi1* mouse model, will allow for a direct examination of the cells relevant to leukemogenesis.[12]

In conclusion, we enriched, localized, and characterized Gata2-dependent and -independent subsets of hematopoietic progenitors in *Gata2Venus* embryos. The combination of this reporter with other reporter and knockout models will lead to a better understanding of the role of Gata2 (and other factors) in the development and function of multipotential HP/SCs in health, leukemogenesis, and reprogramming.

Authorship

Contribution: P.K., E.d.P., C.E., M.-L.K., M.J., C.S.V., and T.Y. performed research; P.S.K. analyzed RNAseq data; R.v.d.L.

performed/analyzed flow cytometric data; D.M. provided reagents; P.K., E.d.P., C.E., D.M., and E.D. designed experiments and analyzed and interpreted the data; and P.K., E.D., E.d.P., and C.E. wrote the manuscript.

Correspondence: Elaine Dzierzak, University of Edinburgh, Centre for Inflammation Research, Queens Medical Research Institute, 47 Little France Crescent, Edinburgh EH16 4TJ, United Kingdom; e-mail: e.dzierzak@erasmusmc.nl or elaine.dzierzak@ed.ac.uk.

References

1. Wilson NK, Foster SD, Wang X, et al. Combinatorial transcriptional control in blood stem/progenitor cells: genome-wide analysis of ten major transcriptional regulators. *Cell Stem Cell.* 2010;7(4):532-544.

2. Solaimani Kartalaei P, Yamada-Inagawa T, Vink CS, et al. Whole-transcriptome analysis of endothelial to hematopoietic stem cell transition reveals a requirement for Gpr56 in HSC generation. *J Exp Med.* 2015;212(1):93-106.

3. Swiers G, Baumann C, O'Rourke J, et al. Early dynamic fate changes in haemogenic endothelium characterized at the single-cell level. *Nat Commun.* 2013;4:2924.

4. Fujiwara Y, Chang AN, Williams AM, Orkin SH. Functional overlap of GATA-1 and GATA-2 in primitive hematopoietic development. *Blood.* 2004;103(2):583-585.

5. Tsai FY, Keller G, Kuo FC, et al. An early haematopoietic defect in mice lacking the transcription factor GATA-2. *Nature.* 1994; 371(6494):221-226.

6. Tsai FY, Orkin SH. Transcription factor GATA-2 is required for proliferation/survival of early hematopoietic cells and mast cell formation, but not for erythroid and myeloid terminal differentiation. *Blood.* 1997;89(10):3636-3643.

7. de Pater E, Kaimakis P, Vink CS, et al. Gata2 is required for HSC generation and survival. *J Exp Med.* 2013;210(13):2843-2850.

8. Ling KW, Ottersbach K, van Hamburg JP, et al. GATA-2 plays two functionally distinct roles during the ontogeny of hematopoietic stem cells. *J Exp Med.* 2004;200(7):871-882.

9. Rodrigues NP, Janzen V, Forkert R, et al. Haploinsufficiency of GATA-2 perturbs adult hematopoietic stem-cell homeostasis. *Blood.* 2005;106(2):477-484.

10. Hsu AP, Johnson KD, Falcone EL, et al. GATA2 haploinsufficiency caused by mutations in a conserved intronic element leads to MonoMAC syndrome. *Blood.* 2013;121(19):S3830-S3837.

11. Gröschel S, Sanders MA, Hoogenboezem R, et al. A single oncogenic enhancer rearrangement causes concomitant EVI1 and GATA2 deregulation in leukemia. *Cell.* 2014;157(2): 369-381.

12. Yamazaki H, Suzuki M, Otsuki A, et al. A remote GATA2 hematopoietic enhancer drives leukemogenesis in inv(3)(q21;q26) by activating EVI1 expression. *Cancer Cell.* 2014;25(4): 415-427.

13. Heyworth C, Gale K, Dexter M, May G, Enver T. A GATA-2/estrogen receptor chimera functions as a ligand-dependent negative regulator of self-renewal. *Genes Dev.* 1999;13(14):1847-1860.

14. Persons DA, Allay JA, Allay ER, et al. Enforced expression of the GATA-2 transcription factor blocks normal hematopoiesis. *Blood.* 1999;93(2): 488-499.

15. Nandakumar SK, Johnson K, Throm SL, Pestina TI, Neale G, Persons DA. Low-level GATA2 overexpression promotes myeloid progenitor self-renewal and blocks lymphoid differentiation in mice. *Exp Hematol.* 2015;43(7):565-577.

16. Minegishi N, Suzuki N, Yokomizo T, et al. Expression and domain-specific function of GATA-2 during differentiation of the hematopoietic precursor cells in midgestation mouse embryos. *Blood.* 2003;102(3):896-905.

17. Ottersbach K, Dzierzak E. Analysis of the mouse placenta as a hematopoietic stem cell niche. *Methods Mol Biol.* 2009;538:335-346.

18. Robert-Moreno A, Espinosa L, de la Pompa JL, Bigas A. RBPjkappa-dependent Notch function regulates Gata2 and is essential for the formation of intra-embryonic hematopoietic cells. *Development.* 2005;132(5):1117-1126.

19. Gao X, Johnson KD, Chang YI, et al. Gata2 cis-element is required for hematopoietic stem cell generation in the mammalian embryo. *J Exp Med.* 2013;210(13):2833-2842.

20. Lim KC, Hosoya T, Brandt W, et al. Conditional Gata2 inactivation results in HSC loss and lymphatic mispatterning. *J Clin Invest.* 2012; 122(10):3705-3717.

21. Orlic D, Anderson S, Biesecker LG, Sorrentino BP, Bodine DM. Pluripotent hematopoietic stem cells contain high levels of mRNA for c-kit, GATA-2, p45 NF-E2, and c-myb and low levels or no mRNA for c-fms and the receptors for granulocyte colony-stimulating factor and interleukins 5 and 7. *Proc Natl Acad Sci USA.* 1995;92(10):4601-4605.

22. Sakai K, Miyazaki J. A transgenic mouse line that retains Cre recombinase activity in mature oocytes irrespective of the cre transgene transmission. *Biochem Biophys Res Commun.* 1997;237(2):318-324.

23. Yokomizo T, Yamada-Inagawa T, Yzaguirre AD, Chen MJ, Speck NA, Dzierzak E. Whole-mount three-dimensional imaging of internally localized immunostained cells within mouse embryos. *Nat Protoc.* 2012;7(3):421-431.

24. Medvinsky A, Taoudi S, Mendes S, Dzierzak E. Analysis and manipulation of hematopoietic progenitor and stem cells from murine embryonic tissues. *Curr Protoc Stem Cell Biol.* 2008;Chapter 2:Unit 2A.6.

25. Trapnell C, Hendrickson DG, Sauvageau M, Goff L, Rinn JL, Pachter L. Differential analysis of gene regulation at transcript resolution with RNA-seq. *Nat Biotechnol.* 2013;31(1):46-53.

26. Mootha VK, Bunkenborg J, Olsen JV, et al. Integrated analysis of protein composition, tissue diversity, and gene regulation in mouse mitochondria. *Cell.* 2003;115(5):629-640.

27. Subramanian A, Tamayo P, Mootha VK, et al. Gene set enrichment analysis: a knowledge-based approach for interpreting genome-wide

expression profiles. *Proc Natl Acad Sci USA.* 2005;102(43):15545-15550.

28. Johnson KD, Hsu AP, Ryu MJ, et al. Cis-element mutated in GATA2-dependent immunodeficiency governs hematopoiesis and vascular integrity. *J Clin Invest.* 2012;122(10):3692-3704.

29. Dzierzak E, de Bruijn M. Isolation and analysis of hematopoietic stem cells from mouse embryos. *Methods Mol Med.* 2002;63:1-14.

30. Gekas C, Dieterlen-Lievre F, Orkin SH, Mikkola HK. The placenta is a niche for hematopoietic stem cells. *Dev Cell.* 2005;8(3):365-375.

31. Nardelli J, Thiesson D, Fujiwara Y, Tsai FY, Orkin SH. Expression and genetic interaction of transcription factors GATA-2 and GATA-3 during development of the mouse central nervous system. *Dev Biol.* 1999;210(2):305-321.

32. Pimanda JE, Ottersbach K, Knezevic K, et al. Gata2, Fli1, and Scl form a recursively wired gene-regulatory circuit during early hematopoietic development. *Proc Natl Acad Sci USA.* 2007; 104(45):17692-17697.

33. Yokomizo T, Dzierzak E. Three-dimensional cartography of hematopoietic clusters in the vasculature of whole mouse embryos. *Development.* 2010;137(21):3651-3661.

34. Impey S, McCorkle SR, Cha-Molstad H, et al. Defining the CREB regulon: a genome-wide analysis of transcription factor regulatory regions. *Cell.* 2004;119(7):1041-1054.

35. Zhang X, Odom DT, Koo SH, et al. Genome-wide analysis of cAMP-response element binding protein occupancy, phosphorylation, and target gene activation in human tissues. *Proc Natl Acad Sci USA.* 2005;102(12):4459-4464.

36. McGrath KE, Frame JM, Fegan KH, et al. Distinct sources of hematopoietic progenitors emerge before HSCs and provide functional blood cells in the mammalian embryo. *Cell Reports.* 2015; 11(12):1892-1904.

37. Kierdorf K, Erny D, Goldmann T, et al. Microglia emerge from erythromyeloid precursors via Pu.1- and Irf8-dependent pathways. *Nat Neurosci.* 2013;16(3):273-280.

38. Fitch SR, Kimber GM, Wilson NK, et al. Signaling from the sympathetic nervous system regulates hematopoietic stem cell emergence during embryogenesis. *Cell Stem Cell.* 2012;11(4): 554-566.

39. Nutt SL, Metcalf D, D'Amico A, Polli M, Wu L. Dynamic regulation of PU.1 expression in multipotent hematopoietic progenitors. *J Exp Med.* 2005;201(2):221-231.

40. Khandekar M, Brandt W, Zhou Y, et al. A Gata2 intronic enhancer confers its pan-endothelia-specific regulation. *Development.* 2007;134(9): 1703-1712.

41. Butko E, Distel M, Pouget C, et al. Gata2b is a restricted early regulator of hemogenic endothelium in the zebrafish embryo. *Development.* 2015;142(6):1050-1061.

42. Ginhoux F, Greter M, Leboeuf M, et al. Fate mapping analysis reveals that adult microglia derive from primitive macrophages. *Science.* 2010;330(6005):841-845.

43. Gomez Perdiguero E, Klapproth K, Schulz C, et al. Tissue-resident macrophages originate from yolk-sac-derived erythro-myeloid progenitors. *Nature.* 2015;518(7540):547-551.

44. Herbomel P, Thisse B, Thisse C. Zebrafish early macrophages colonize cephalic mesenchyme and developing brain, retina, and epidermis through a M-CSF receptor-dependent invasive process. *Dev Biol.* 2001;238(2):274-288.

45. Ditadi A, Sturgeon CM, Tober J, et al. Human definitive haemogenic endothelium and arterial vascular endothelium represent distinct lineages. *Nat Cell Biol.* 2015;17(5):580-591.

46. Palis J, Yoder MC. Yolk-sac hematopoiesis: the first blood cells of mouse and man. *Exp Hematol.* 2001;29(8):927-936.

47. Frame JM, McGrath KE, Palis J. Erythro-myeloid progenitors: "definitive" hematopoiesis in the conceptus prior to the emergence of hematopoietic stem cells. *Blood Cells Mol Dis.* 2013;51(4):220-225.

48. Lux CT, Yoshimoto M, McGrath K, Conway SJ, Palis J, Yoder MC. All primitive and definitive hematopoietic progenitor cells emerging before E10 in the mouse embryo are products of the yolk sac. *Blood.* 2008;111(7):3435-3438.

49. Rhodes KE, Gekas C, Wang Y, et al. The emergence of hematopoietic stem cells is initiated in the placental vasculature in the absence of circulation. *Cell Stem Cell.* 2008;2(3):252-263.

50. Jaffredo T, Nottingham W, Liddiard K, Bollerot K, Pouget C, de Bruijn M. From hemangioblast to hematopoietic stem cell: an endothelial connection? *Exp Hematol.* 2005;33(9):1029-1040.

51. Takahashi S, Shimizu R, Suwabe N, et al. GATA factor transgenes under GATA-1 locus control rescue germline GATA-1 mutant deficiencies. *Blood.* 2000;96(3):910-916.

52. Tsai FY, Browne CP, Orkin SH. Knock-in mutation of transcription factor GATA-3 into the GATA-1 locus: partial rescue of GATA-1 loss of function in erythroid cells. *Dev Biol.* 1998;196(2):218-227.

53. Buza-Vidas N, Duarte S, Luc S, Bouriez-Jones T, Woll PS, Jacobsen SE. GATA3 is redundant for maintenance and self-renewal of hematopoietic stem cells. *Blood.* 2011;118(5):1291-1293.

54. Ku CJ, Hosoya T, Maillard I, Engel JD. GATA-3 regulates hematopoietic stem cell maintenance and cell-cycle entry. *Blood.* 2012;119(10):2242-2251.

55. Frelin C, Herrington R, Janmohamed S, et al. GATA-3 regulates the self-renewal of long-term hematopoietic stem cells. *Nat Immunol.* 2013;14(10):1037-1044.

56. Pandolfi PP, Roth ME, Karis A, et al. Targeted disruption of the GATA3 gene causes severe abnormalities in the nervous system and in fetal liver haematopoiesis. *Nat Genet.* 1995;11(1):40-44.

57. Peterkin T, Gibson A, Patient R. Common genetic control of haemangioblast and cardiac development in zebrafish. *Development.* 2009;136(9):1465-1474.

58. Fehling HJ, Lacaud G, Kubo A, et al. Tracking mesoderm induction and its specification to the hemangioblast during embryonic stem cell differentiation. *Development.* 2003;130(17):4217-4227.

59. Huber TL, Kouskoff V, Fehling HJ, Palis J, Keller G. Haemangioblast commitment is initiated in the primitive streak of the mouse embryo. *Nature.* 2004;432(7017):625-630.

60. Van Handel B, Montel-Hagen A, Sasidharan R, et al. Scl represses cardiomyogenesis in prospective hemogenic endothelium and endocardium. *Cell.* 2012;150(3):590-605.

61. Nakano H, Liu X, Arshi A, et al. Haemogenic endocardium contributes to transient definitive haematopoiesis. *Nat Commun.* 2013;4:1564.

62. Pierre S, Bats AS, Chevallier A, et al. Induction of the Ras activator Son of Sevenless 1 by environmental pollutants mediates their effects on cellular proliferation. *Biochem Pharmacol.* 2011;81(2):304-313.

63. Sabnis AJ, Cheung LS, Dail M, et al. Oncogenic Kras initiates leukemia in hematopoietic stem cells. *PLoS Biol.* 2009;7(3):e59.

64. Chang YI, You X, Kong G, et al. Loss of Dnmt3a and endogenous Kras(G12D/+) cooperate to regulate hematopoietic stem and progenitor cell functions in leukemogenesis. *Leukemia.* 2015;29(9):1847-1856.

65. Katsumura KR, Yang C, Boyer ME, Li L, Bresnick EH. Molecular basis of crosstalk between oncogenic Ras and the master regulator of hematopoiesis GATA-2. *EMBO Rep.* 2014;15(9):938-947.

66. Damnernsawad A, Kong G, Liu Y, Chang Y-I, et al. Kras plays an important role in generating differentiated blood cells [abstract]. *Blood.* 2013;122(21). Abstract 2451.

67. Richard C, Drevon C, Canto PY, et al. Endothelio-mesenchymal interaction controls runx1 expression and modulates the notch pathway to initiate aortic hematopoiesis. *Dev Cell.* 2013;24(6):600-611.

68. Bertrand JY, Cisson JL, Stachura DL, Traver D. Notch signaling distinguishes 2 waves of definitive hematopoiesis in the zebrafish embryo. *Blood.* 2010;115(14):2777-2783.

69. Kumano K, Chiba S, Kunisato A, et al. Notch1 but not Notch2 is essential for generating hematopoietic stem cells from endothelial cells. *Immunity.* 2003;18(5):699-711.

70. Robert-Moreno A, Guiu J, Ruiz-Herguido C, et al. Impaired embryonic haematopoiesis yet normal arterial development in the absence of the Notch ligand Jagged1. *EMBO J.* 2008;27(13):1886-1895.

71. Kim PG, Nakano H, Das PP, et al. Flow-induced protein kinase A-CREB pathway acts via BMP signaling to promote HSC emergence. *J Exp Med.* 2015;212(5):633-648.

CHAPTER 6

Discussion

Discussion

The adult hematopoietic system is established in a stepwise manner as a progressive generation of hematopoietic cells with increasing complexity, ultimately culminating in the generation of long-lived self-renewing HSCs. HSCs are on top of the hematopoietic hierarchy giving rise to all terminally differentiated blood cell lineages. They are capable of repopulating the adult organism providing life-long blood supply, thus HSC transplantation is a pivotal treatment strategy for curing blood disorders. As there are limited resources of patient compatible HSCs for transplantations, generating blood from other sources, such as by iPSC/ESC differentiation, has been a long term goal in blood research.

Kinetic analysis has suggested that blood cells are generated from iPSC/ESC in a sequential order with growing complexity (Keller et al., 1993; Wiles and Keller, 1991) implying that with the progression of the culture, HSCs could be ultimately generated and isolated with the use of right markers. Although several markers, and marker combination has been used to characterise and isolate cells from different stages of this process, these approaches have not resulted in the establishment of a robust method to generate HSCs. This is largely due to the lack of relevant markers to enrich for cells with HSC identity and a defined molecular program.

Transcriptional control is the most important regulator affecting cell fate during EHT and the development of HSC/HPC (reviwed in Kaimakis et al., 2013). Although the precise spatial and temporal onset of the HSC identity is as yet debatable, it is certain that it is controlled by a set of transcription factors that work in a combinatorial manner to activate the transcription of downstream target genes relevant to hematopiesis (Wilson et al., 2010). In concert, these factors drive the determination of hematopoietic (progenitor/stem) cell fate by regulating their temporal expression pattern and the expression levels of their target genes.

Gata2 has proven to be one of the key players in this set of factors, as the deletion of Gata2 causes severe hematopoietic defects and is lethal at the time of the first HSC emergence (Tsai et al., 1994). *Gata2*$^{+/-}$ embryos generate profoundly fewer HPCs and HSCs, and the HSCs are qualitatively challenged. However, the definitive erythroid cell compartment is unchanged (Rodrigues et al., 2005). On the other hand, differentiation of ESCs over-expressing *Gata2* show that lymphoid cell potential is severely affected when there is more Gata2 (Nandakumar et al., 2015). Together, these data suggest that the levels of Gata2 are involved in the fate determination of HPCs/HSCs, as well as of several mature blood lineages. This evidence also implies that levels of Gata2 may play a role in the stepwise progression of ESC hematopoietic differentiation, and may potentially discriminate different (progenitor) blood cells with growing complexity that emerge in ESC differentiation cultures. However, as Gata2 is a transcription factor, previously it was not possible to isolate live Gata2 expressing cells for functional assays to characterise their potential in ESC cultures. Although a *Gata2-GFP* knockout/knockin reporter was generated, these results only indicated hematopoietic cells produced in a state of *Gata2* haploinsufficiency (Minegishi et al., 2003), and thus, did not reflect the physiological function of Gata2.

We have generated a *Gata2Venus* reporter ESC line that facilitates the isolation and characterization of live cells expressing endogenous levels of Gata2 that emerge

throughout the ESC differentiation, and used these ESCs to establish a reporter mouse to understand the role of Gata2 in the embryonic development of HPCs/HPCs *in vivo.* **This thesis research has shown the following:**

The *Gata2Venus* reporter discriminates stages of hematopoietic potential emergence that are analogous to *in vivo* waves of hematopoietic generation, and it marks all functional HPCs in ESC differentiation cultures and HSCs in the mouse embryo

In the mouse embryo, the first hematopoietic cells arise from the YS blood islands harbouring bipotential Flk1 expressing hemangioblastic cells. They give rise to endothelial and primitive hematopoietic cells. *Gata2* expression in the YS is detected as early as E7, and is involved in erythroid cell generation (Silver and Palis, 1997). Our *Gata2Venus* ESC differentiation data show that Gata2 is co-expressed with Flk1, and that this cell population has endothelial as well as primitive erythroid potential giving rise to the first hematopoietic cells in ESC cultures at day 4 of differentiation (Chapter 2). Thus, Gata2 function in the early stage of the *Gata2Venus* ESC differentiation is similar to that at the onset of hematopoietic cell generation *in vivo*.

With the progression of the ESC differentiation culture, an increase in the phenotypic EMP (CD16/32$^+$cKit$^+$) population was observed at day 10 of differentiation within the Venus$^+$ population. This may reflect another wave of hematopoietic cell generation (but of a more complex potential) marked by Venus expression in the ESC differentiation. In contrast to the earliest ESC-derived (unipotent) blood cells, Venus$^+$ cells generated at this stage, shared functional similarities with the YS derived EMPs that *in vivo* are generated from E8.25 onwards (Frame et al., 2016; Frame et al., 2013) (Chapter 2). Our FACS and imaging data of *Gata2Venus* embryos demonstrated Venus expression in the E9 YS. Analysis of Venus$^+$ and Venus$^-$ cells of the E9-E10 YS and AGM, revealed the presence of Gata2 dependent and independent EMPs. The highest numbers of Gata2 independent EMPs were found at E9, which declined by E10 (Chapter 5). Likewise, EMP activity in the ESC differentiation cultures was found in the Venus$^+$ population, with some phenotypic EMPs detected in the Venus$^-$ fraction. The frequency of the Venus$^-$ EMPs declined over time during the ESC differentiation towards more definitive hematopoietic cell generation (Chapter 2), thus indicating similarities between the *in vivo* and *in vitro* developing Venus$^+$ cells.

After 14 days of *Gata2Venus* ESC differentiation, we observed an increase in the frequency of cKit$^+$CD31$^+$ cells within the Venus$^+$ compartment. *In vivo* phenotypic hematopoietic cluster cells are defined by co-expression of cKit and CD31, thus, implicating the emergence of another (perhaps more potent/aorta-like) hemogenic endothelium in the ESC cultures. It was not accompanied with an increased frequency of Venus$^+$ cells. However, it is possible that immature hemogenic cells express Gata2 at a very low levels, and therefore, an increased readout is not detected by our reporter expression. In the embryo, hemogenic endothelium is distinguished from the rest of the endothelial cells by the expression of the *Ly6AGFP* reporter. It also marks all HSCs, but does not label the YS stage hematopoiesis, making it a specific marker for immature definitive hematopoietic cells (de Bruijn et al., 2002; Ma et al., 2002). We used *Ly6AGFP* ESCs as a reporter to distinguish the later hematopoietic potential arising in the ESC

cultures. RNA Sequencing of E10.5 AGM cells shows *Gata2* expression in Ly6AGFP^{+} cells undergoing EHT (Solaimani Kartalaei et al., 2015), thus indicating that the hemogenic endothelial cells generated in the *Gata2Venus* ESC cultures, that express low levels of Gata2, might be labelled by *Ly6AGFP*. Moreover, our transplantation assays with E11 AGM derived Venus[+] and Venus^{-} sorted cells revealed that all HSCs express Venus (Chapter 5), thus implying that the most immature (HSC-like) potential arising in the ESC cultures, would be labelled by both markers. Indeed, FACS analysis revealed a profound increase in the CD31^{+}cKit^{+} cell frequency also in the Ly6aGFP^{+} fraction that overlapped temporally with the CD31^{+}cKit^{+} increased frequency in Venus^{+} cells. Using two individual reporter lines has allowed us to sub-fractionate hematopoietic cells (Figure 1) but has not yet led to a complete understanding of the late hematopoietic potential arising in ESC cultures.

Therefore, the next step towards more accurate delineation of the definitive hematopoietic cells generated in the ESC differentiation, would be the combination of these reporters in one ESC double reporter line. This would allow us to isolate the hematopoietic cells emerging in the third (and possibly even later) wave of hematopoietic cell generation. One probable readout for the emergence of a more complex hematopoietic program, is the detection of lymphoid activity (Kennedy et al., 2012). In the mouse embryo, after the appearance of EMPs at E8.25, cells with lymphoid potential are detected from E8.5 onwards (Godin et al., 1995). Therefore, B and/or T cell potential would indicate for the further progression of the differentiation culture, and indicate that the stepwise culture maturation is highly analogous to the *in vivo* waves of hematopoietic cell generation, and thus imply that ultimately cells with HSC potential may emerge (Fig 1). Given that the *Ly6aGFP* and Gata2Venus reporters are well described in mouse embryogenesis, they facilitate a comparison between *in vivo* waves of hematopoiesis and *in vitro* hematopoietic cell generation. However, the use of these reporters, is only beginning to dissect the hematopoietic cell potential of the *in vitro* cultures. It is likely that complex reporter combinations, marking the expression of several *in vivo* well described intrinsic factors is required for the isolation of cell populations with HSC-like characteristics. The *Gata2Venus:Ly6aGFP* double reporter would facilitate this when combined with additional gene reporters that mark *in vivo* definitive hematopoiesis/EHT/HSCs, such as *Runx1*. Runx1 transcription factor has a pivotal function for the progression of EHT (Kissa and Herbomel, 2010) and thus, in combination with *Ly6aGFP* (marks hemogenic endothelium and HSCs) and *Gata2Venus* (marks all HSCs) would sub-fractionate the hemogenic endothelial cells that are acquiring HSC potential.

The Gata2 target gene *Gpr56* is required for *in vitro* HPC generation, and has a redundant expression and function with *Gpr97*

The emergence of HSCs via EHT is associated with the upregulation of heptad transcription factors, including Gata2, and the transcriptional activation of their downstream targets. One such target, Gpr56, has been previously reported to positively regulate EHT and HSC development in the zebrafish embryos (Solaimani Kartalaei et al., 2015). However, there have been contradictory suggestions about the function of Gpr56 in the mouse hematopoiesis (Rao et al., 2015; Saito et al., 2013) and its role is still under debate.

The *Gata2Venus* reporter ESCs serve as an excellent tool to unravel the involvement of Gpr56 in mouse HPC/HSC development as it allows for the specific enrichment of functional hematopoietic cells expressing Gpr56. Our differentiation data with ESCs expressing *Gata2Venus* and WT *Gpr56* suggest that Gpr56 may have a role in the ESC hematopoietic commitment (Chapter 3). Surprisingly, when we subjected *Gata2Venus Gpr56 KO* ESCs to hematopoietic differentiation, we detected much higher hematopoietic activity in the *Gpr56* null Venus$^+$ cells as compared with WT Venus$^+$ cells. These data corroborate with the results of a study using *Gpr56$^{-/-}$* adult mice (Rao et al., 2015) and suggest that high level of Gpr56 is dispensable for HSC development (Rao et al., 2015). Strikingly, we found that the expression of *Gpr97* (another GPCR encoded on the same locus as *Gpr56*) and *Gpr56* are redundant. Thus, the compensatory mechanisms by Gpr97 may account for the increased hematopoietic activity in the *Gpr56* KO cells. It is tempting to think that possible upregulation of *Gpr97* expression in the *Gpr56$^{-/-}$* embryos explains the lack of hematopoietic defects in these embryos. Our differentiation data with *Gpr56* null cells where *Gpr97* was knocked down, support this view. The fact that Gpr56 was shown to be involved in the maintenance of stem/progenitor cells in *a* 32D cell model of neutrophil differentiation (Solaimani Kartalaei et al., 2015), suggests that Gpr56 is required during the development of HPCs/HSCs by playing a role in their maintenance. To further explore the mechanism how Gpr56 regulates hematopoietic cell development, we will assess the dynamics of *Gpr56* expression in *Gpr97* KO cells. Furthermore, our study revealed Collagen III as a potential hematopoietic inducible factor that could possibly be used to stimulate the *in vitro* generation of HPCs/HSCs. Our ongoing experiments will address the specificity of Collagen signaling axis and the effect of concentration dependent Collagen III supply on promoting HPC/HSC development.

Taken together, Gpr56 is a novel exciting player in hematopoietic development, however, recent studies exploring its function have been complicated by the function of redundant GPCR(s). Our further studies will take into account the redundant receptors and aim to address how Gpr56, and these overlapping receptors, are involved in the EHT.

Gata2Venus reports all mast cell progenitors and mast cells generated from differentiated pluripotent stem cells

Gata2 expression is downregulated during HSC/HPC differentiation into mature blood cell lineages, with the exception of mast cells. Both, immature and mature mast cells, retain high Gata2 expression. Thus, Gata2 is an important mast cell marker, and *Gata2Venus* an excellent and advantageous reporter for the isolation of these cells. Mast cells are the major effectors of allergic responses and mast cell dysfunction causes severe disorders such as anaphylaxis and mastocytosis. Despite this knowledge, and the fact that mast cells can be grown in culture, new mast cell disease treatment strategies are hampered due to the lack of a robust, rapid and high yield mast cell generation method. We have described a novel approach to rapidly and robustly generate large numbers of mast cells (Chapter 4) utilizing our novel *Gata2Venus* reporter ESCs, where Venus specifically marks highly proliferative mast cell progenitors and mast cells, that appear in the culture after only 14 days of mouse *Gata2Venus* ESC differentiation. We show that the method is applicable to human ESCs and iPSCs - phenotypic human mast cells/mast cell progenitors emerge only after 12 days of human *GATA2Venus* ESC/iPSC differentiation culture, which is at least 6 times faster than current protocols (Kovarova et al., 2010). We are currently further optimizing this method, so as to provide a rapid,

efficient and accessible source of mouse and human mast cells for drug screening and patient specific research applications.

Our approach exploits co-culture of Venus[+] hematopoietic progenitor cells on a layer of OP9 stroma resulting in a rapid induction of Gata2 expression that is marked by significantly increased Venus intensity. These data suggest that hematopoietic progenitor cells have low levels of Gata2, however, induction of *Gata2* expression is a prerequisite for the commitment to mast cells (Chapter 4). This is in line with the previously held view that Gata2 functions in a dose dependent manner and Gata2^{+} cell identity is defined by its expression levels (Ling et al., 2004; Nandakumar et al., 2015; Rodrigues et al., 2005). Delineating direct inducers of *Gata2*, that are expressed by OP9 stromal cells, would reveal potential mast cell-specific stimulators that could be used in order to generate these cells from PSCs. This approach would facilitate the derivation of stroma and serum free protocol with defined medium components making this approach more relevant for clinical applications. We are currently testing some of the known *Gata2* inducers, such as BMP4 and Notch1 for the induction of mast cell commitment (Maeno et al., 1996; Robert-Moreno et al., 2005). Moreover, we have shown in this thesis that OP9 cells express high levels of *Col3a1* (Chapter 3), thus it would be interesting to explore whether Collagen III signaling has a role in regulating the levels of Gata2 in mast cell commitment.

Conclusion and Future Perspectives

In conclusion, we have established *Gata2Venus* reporter embryonic stem cell and transgenic mouse line, and characterized the involvement of Gata2 in the stepwise differentiation and development of hematopoietic cells (Fig 1). Our study demonstrates the fundamental role of Gata2 in embryonic hematopoiesis, and indicates that in combination with other reporters (such as the *Ly6aGFP*), all hematopoietic activity arising in the ESC differentiation cultures, can be detected. *Gata2Venus* and *Ly6aGFP* reporters are just beginning to dissect and provide understanding of all the different cell types and hematopoietic potential emerging during embryonic development. The combination of these reporters with others, such as the reporters for heptad transcription factors (Wilson et al., 2010), will allow to determination of the specific molecular signatures arising in the hematopoietic development and differentiation. This will greatly advance the field and will enable the development of future strategies in directly translating the perspectives into therapeutic applications.
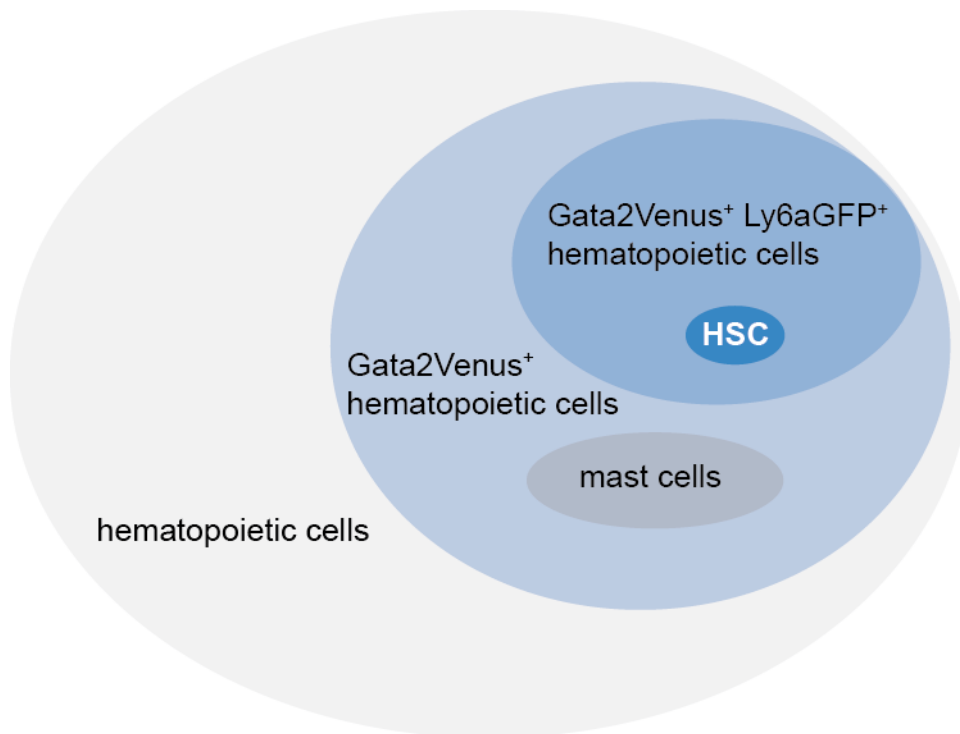
Figure 1. *Gata2Venus* and *Ly6aGFP* reporter expression in hematopoietic cells. The *Gata2Venus* reporter labels the majority of hematopoietic cells, including mast cells. The *Ly6aGFP* reporter distinguishes a subset of Gata2Venus$^+$ cells, including the hematopoietic stem cells (HSC).

References

de Bruijn, M.F., Ma, X., Robin, C., Ottersbach, K., Sanchez, M.J., and Dzierzak, E. (2002). Hematopoietic stem cells localize to the endothelial cell layer in the midgestation mouse aorta. Immunity *16*, 673-683.

Frame, J.M., Fegan, K.H., Conway, S.J., McGrath, K.E., and Palis, J. (2016). Definitive Hematopoiesis in the Yolk Sac Emerges from Wnt-Responsive Hemogenic Endothelium Independently of Circulation and Arterial Identity. Stem Cells *34*, 431-444.

Frame, J.M., McGrath, K.E., and Palis, J. (2013). Erythro-myeloid progenitors: "definitive" hematopoiesis in the conceptus prior to the emergence of hematopoietic stem cells. Blood Cells Mol Dis *51*, 220-225.

Godin, I., Dieterlen-Lievre, F., and Cumano, A. (1995). Emergence of multipotent hemopoietic cells in the yolk sac and paraaortic splanchnopleura in mouse embryos, beginning at 8.5 days postcoitus. Proc Natl Acad Sci U S A *92*, 773-777.

Kaimakis, P., Crisan, M., and Dzierzak, E. (2013). The biochemistry of hematopoietic stem cell development. Biochim Biophys Acta *1830*, 2395-2403.

Keller, G., Kennedy, M., Papayannopoulou, T., and Wiles, M.V. (1993). Hematopoietic commitment during embryonic stem cell differentiation in culture. Mol Cell Biol *13*, 473-486.

Kennedy, M., Awong, G., Sturgeon, C.M., Ditadi, A., LaMotte-Mohs, R., Zuniga-Pflucker, J.C., and Keller, G. (2012). T lymphocyte potential marks the emergence of definitive hematopoietic progenitors in human pluripotent stem cell differentiation cultures. Cell Rep *2*, 1722-1735.

Kissa, K., and Herbomel, P. (2010). Blood stem cells emerge from aortic endothelium by a novel type of cell transition. Nature *464*, 112-115.

Kovarova, M., Latour, A.M., Chason, K.D., Tilley, S.L., and Koller, B.H. (2010). Human embryonic stem cells: a source of mast cells for the study of allergic and inflammatory diseases. Blood *115*, 3695-3703.

Ling, K.W., Ottersbach, K., van Hamburg, J.P., Oziemlak, A., Tsai, F.Y., Orkin, S.H., Ploemacher, R., Hendriks, R.W., and Dzierzak, E. (2004). GATA-2 plays two functionally distinct roles during the ontogeny of hematopoietic stem cells. J Exp Med *200*, 871-882.

Ma, X., de Bruijn, M., Robin, C., Peeters, M., Kong, A.S.J., de Wit, T., Snoijs, C., and Dzierzak, E. (2002). Expression of the Ly-6A (Sca-1) lacZ transgene in mouse haematopoietic stem cells and embryos. Br J Haematol *116*, 401-408.

Maeno, M., Mead, P.E., Kelley, C., Xu, R.H., Kung, H.F., Suzuki, A., Ueno, N., and Zon, L.I. (1996). The role of BMP-4 and GATA-2 in the induction and differentiation of hematopoietic mesoderm in Xenopus laevis. Blood *88*, 1965-1972.

Minegishi, N., Suzuki, N., Yokomizo, T., Pan, X., Fujimoto, T., Takahashi, S., Hara, T., Miyajima, A., Nishikawa, S., and Yamamoto, M. (2003). Expression and domain-specific function of GATA-2 during differentiation of the hematopoietic precursor cells in midgestation mouse embryos. Blood *102*, 896-905.

Nandakumar, S.K., Johnson, K., Throm, S.L., Pestina, T.I., Neale, G., and Persons, D.A. (2015). Low-level GATA2 overexpression promotes myeloid progenitor self-renewal and blocks lymphoid differentiation in mice. Exp Hematol *43*, 565-577 e561-510.

Rao, T.N., Marks-Bluth, J., Sullivan, J., Gupta, M.K., Chandrakanthan, V., Fitch, S.R., Ottersbach, K., Jang, Y.C., Piao, X., Kulkarni, R.N.*, et al.* (2015). High-level Gpr56 expression is dispensable for the maintenance and function of hematopoietic stem and progenitor cells in mice. Stem Cell Res *14*, 307-322.

Robert-Moreno, A., Espinosa, L., de la Pompa, J.L., and Bigas, A. (2005). RBPjkappa-dependent Notch function regulates Gata2 and is essential for the formation of intra-embryonic hematopoietic cells. Development *132*, 1117-1126.

Rodrigues, N.P., Janzen, V., Forkert, R., Dombkowski, D.M., Boyd, A.S., Orkin, S.H., Enver, T., Vyas, P., and Scadden, D.T. (2005). Haploinsufficiency of GATA-2 perturbs adult hematopoietic stem-cell homeostasis. Blood *106*, 477-484.

Saito, Y., Kaneda, K., Suekane, A., Ichihara, E., Nakahata, S., Yamakawa, N., Nagai, K., Mizuno, N., Kogawa, K., Miura, I.*, et al.* (2013). Maintenance of the hematopoietic stem cell pool in bone marrow niches by EVI1-regulated GPR56. Leukemia *27*, 1637-1649.

Silver, L., and Palis, J. (1997). Initiation of murine embryonic erythropoiesis: a spatial analysis. Blood *89*, 1154-1164.

Solaimani Kartalaei, P., Yamada-Inagawa, T., Vink, C.S., de Pater, E., van der Linden, R., Marks-Bluth, J., van der Sloot, A., van den Hout, M., Yokomizo, T., van Schaick-Solerno, M.L.*, et al.* (2015). Whole-transcriptome analysis of endothelial to hematopoietic stem cell transition reveals a requirement for Gpr56 in HSC generation. J Exp Med *212*, 93-106.

Tsai, F.Y., Keller, G., Kuo, F.C., Weiss, M., Chen, J., Rosenblatt, M., Alt, F.W., and Orkin, S.H. (1994). An early haematopoietic defect in mice lacking the transcription factor GATA-2. Nature *371*, 221-226.

Wiles, M.V., and Keller, G. (1991). Multiple hematopoietic lineages develop from embryonic stem (ES) cells in culture. Development *111*, 259-267.

Wilson, N.K., Foster, S.D., Wang, X., Knezevic, K., Schutte, J., Kaimakis, P., Chilarska, P.M., Kinston, S., Ouwehand, W.H., Dzierzak, E.*, et al.* (2010). Combinatorial transcriptional control in blood stem/progenitor cells: genome-wide analysis of ten major transcriptional regulators. Cell Stem Cell *7*, 532-544.

Summary

The mammalian hematopoietic system is maintained by the self-renewing, long-lived HSCs that provide the organism with a life-long supply of all blood lineage cells. HSCs are used in cell therapy applications for treating blood disorders. To overcome the shortage of compatible donor derived HSCs, approaches to generate HSCs *de novo* by reprogramming, or deriving them from other sources, such as pluripotent stem cells, have been taken. It is essential for the derivation of *de novo* HSCs to dissect the extrinsic and intrinsic signals that drive the HSC program *in vivo*, as well as exploring the compounds of the surrounding niche and microenvironment. Recent progress has pushed the field forward, however, we still do not know all the characteristics of HSC identity.

Transcriptional control is the most important regulator in the process of defining cell identity. Gata2 is one of the key transcription factors whose precisely controlled expression levels have an essential role in the development of HSCs, HPCs as well as in several mature blood lineage cells, such as mast cells. This thesis focuses on the involvement of Gata2 in embryonic hematopoiesis. We characterize the involvement of Gata2 in *in vivo* HSC/HPC development and in the generation of blood (progenitor) cells *in vitro*. We exploit a novel *Gata2Venus* reporter, that, for the first time, allows to trace, characterize and isolate live cells expressing unperturbed levels of Gata2.

The introduction in **Chapter 1,** provides a background to the current knowledge about the embryonic development of the adult hematopoietic system, focusing on endothelial-to hematopoietic cell transition, and on some of the pivotal transcriptional regulators, including Gata2, and their targets involved in this process, and in the generation of HSCs. It introduces the scope of this study as well as specific goals of this thesis research.

In **Chapter 2**, we demonstrate that *Gata2Venus* reporter expression in ESC differentiation cultures distinguishes all *in vitro* generated blood cells that are generated in a stepwise manner with growing complexity. The most immature cells arising in late cultures, are also marked by another hematopoietic reporter, *Ly6AGFP*, that *in vivo* distinguishes all HSCs, but does not mark primitive hematopoietic stages. These novel reporters show that ESC differentiation is highly similar to the progressive development of hematopoietic cells *in vivo* and enables the isolation of the *in vitro* grown hematopoietic cells.

In **Chapter 3,** we use the *Gata2Venus* ESC hematopoietic differentiation to dissect the hematopoietic requirement of Gata2 downstream target *Gpr56*. We show that the expression and function of Gpr56 and another GPCR, Gpr97 are redundant. The deletion of *Gpr56* and *Gpr97* together blocks the definitive hematopoietic program, thus revealing a requirement for Gpr56 in the generation of HPCs. Moreover, our data reveal that the putative ligand of Gpr56, Collagen III, has a positive effect on HPC generation, and could possibly be used as a novel stimulator of *de novo* generation of HPCs/HSCs.

In **Chapter 4,** we introduce a novel approach to robustly generate mast cells, the immune cells that play a key role in allergic reactions and inflammatory disease. Mast cell related research is challenged due to the long and expensive protocols in the generation of mature functional mast cells. Our protocol utilizes the advantageous *Gata2Venus* reporter and we show that Venus marks and enables the isolation of all functional mast

cells and mast cell precursors as they are produced from mouse and human PSCs with significantly shorter culture time than previously reported.

In **Chapter 5**, we utilize the *Gata2Venu*s ESCs to establish a *Gata2Venus* reporter mouse model. We show that all HSCs, and the majority of HPCs are Gata2 expressing, and reveal a Gata2 independent progenitor population with a distinct functional output and molecular signature. These data contribute to the knowledge needed to dissect the full program of HSC identity and the factors, that are essential in the reprogramming, and PSC differentiation approaches.

The final chapter, **Chapter 6** provides an overview of the major findings and their impact in the field of developmental hematopoiesis, as well as introduces the future perspectives of this thesis study.

Samenvatting

Het hematopoietische systeem van zoogdieren wordt in stand gehouden door zelfvernieuwende, lang levende hematopoietische stamcellen (HSC's) die het organisme voorzien van een levenslange voorraad aan alle verschillende bloedcellen. HSC's worden gebruikt in celtherapie toepassingen voor de behandeling van bloedziekten. Om het tekort aan compatibele donor-afgeleide HSC's te boven te komen, zijn benaderingen gezocht voor de *de novo* generatie van HSC's door reprogrammering of afleiding vanuit andere bronnen, zoals pluripotente stamcellen (PSC's). Het ontleden van de ex- en intrinsieke signalen die het HSC programma *in vivo* aansturen, en het verkennen van de onderdelen van de omringende nis, zijn essentieel voor de derivatie van *de novo* HSC's. Recente vooruitgang heeft het veld verder gebracht, echter we weten nog steeds niet alle details van HSC indentiteit.

Transcriptionele controle is de belangrijkste regulator van het proces van het definiëren van cel identiteit. Gata2 is één van de sleutel transcriptiefactoren wiens precies gecontroleerde expressieniveaus een essentiële rol spelen in de ontwikkeling van HSC's, hematopoietische progenitor cellen (HPC's) en meerdere soorten rijpe bloedcellen, zoals mastcellen. Dit proefschrift focust op de betrokkenheid van Gata2 gedurende de embryonale hematopoiese. We karakteriseren de rol van Gata2 in HSC/HPC ontwikkeling *in vivo* en gedurende de generatie van bloed (voorloper) cellen *in vitro*. We exploiteren een nieuwe *Gata2Venus* reporter, die ons voor de allereerste keer in staat stelt om levende cellen welke onverstoorde niveaus van Gata2 tot expressie brengen te volgen, karakteriseren en isoleren.

De introductie in **Hoofdstuk 1**, geeft een achtergrond over de huidige kennis van de embryonale ontwikkeling van het volwassen hematopoietische systeem, gefocust op de endotheliale-naar-hematopoietische celovergang, en op enkele van de hoofd transcriptionele regulatoren, inclusief Gata2, en hun doelwitten betrokken bij dit proces, en in de generatie van HSC's. Het introduceert de strekking van deze studie en de specifieke doelen van dit promotieonderzoek. In **Hoofdstuk 2** demonstreren we dat de *Gata2Venus* reporter expressie in embryonale stamcel (ESC) differentiatie kweken alle *in vitro* gegenereerde bloedcellen onderscheidt die gegenereerd worden op een stapsgewijze manier met een toenemende complexiteit. De meest onrijpe cellen die onstaan gedurende de late kweken, worden ook gemarkeerd door een andere hematopoietische reporter, *Ly6AGFP*, welke *in vivo* alle HSC's maar niet de primitieve hematopoiese markeert. Deze nieuwe combinatie van reporters laat zien dat ESC differentiatie in grote mate overeenkomt met de progressieve ontwikkeling van hematopoietische cellen *in vivo* en maakt het mogelijk om de *in vitro* gegenereerde hematopoietische cellen te isoleren.

In **Hoofdstuk 3** gebruiken we de *Gata2Venus* ESC hematopoietische differentiatie om de hematopoietische behoefte van het Gata2 'downstream' doelwit *Gpr56* te ontleden. We laten zien dat de expressie en functie van Gpr56 en een andere GPCR, Gpr97, overlappend zijn. De deletie van *Gpr56* en *Gpr97* samen blokkeert het definitieve hematopoietische programma, en laat zien dat Gpr56 belangrijk is voor de generatie van HPC's. Bovendien laten onze data zien dat het vermeende ligand van Gpr56, collageen III, een positief effect heeft op HPC generatie, en mogelijk gebruikt kan worden als nieuwe stimulator voor *de novo* generatie van HPC's/HSC's.

In **Hoofdstuk 4** introduceren we een nieuwe benadering om op een robuuste manier mastcellen, de immuuncellen welke een hoofdrol spelen in allergische reacties en ontstekingsziekten, te genereren. Mastcel gerelateerd onderzoek is moeilijk door de lange en dure protocollen die nodig zijn voor de generatie van rijpe functionele mastcellen. Ons protocol gebruikt de zeer nuttige *Gata2Venus* reporter en we laten zien dat Venus alle functionele mastcellen en mastcel voorlopers markeert en hun isolatie mogelijk maakt wanneer ze worden geproduceerd vanuit muis en humane pluripotente stamcellen met een significant kortere kweektijd dan voorheen gerapporteerd.

In **Hoofdstuk 5** maken we gebruik van de *Gata2Venus* ESC's om een *Gata2Venus* muis reporter model te maken. We laten zien dat alle HSC's, en de meerderheid aan HPC's Gata2 tot expressie brengen. Dat model onthult ook een Gata2 onafhankelijke voorloper cel poplulatie met een aparte functie en eigen moleculair patroon. Onze studie, die laat zien dat Gata2 een essentiële rol heeft in het bepalen van het HSC lot, maar niet in de generatie van functionele HPC's, draagt bij aan de kennis die vereist is voor het volledig ontleden van het programma voor het genereren van HSC identiteit en van de factoren die essentieel zijn in de benadering van de reprogrammering en differentiatie van PSC

Het laatste hoofdstuk, **Hoofdstuk 6**, geeft een overzicht van alle resultaten en conclusies van dit proefschrift onderzoek. De belangrijkste bevindingen en hun impact binnen het veld van de ontwikkelingshematopoiese worden besproken en geeft een introductie van de toekomstperspectieven van deze proefschrift studie.

Kokkuvõte

Imetajate vereloome süsteemi aluseks on vereloome tüvirakud, mis tagavad organismile kogu tema elu jooksul kõigi erinevate vererakkude tagavara. Vereloometürivakkude siirdamise tulemusena on võimalik ravida leukeemiaid ning mitmeid teisi verahaigusi. Edukaks siirdamiseks on vaja sobivat doonorit, kuna erinevate inimeste vererakud on väga erinevad. Võõra vere siirdamisel tekib patsiendis äge vastureaktsioon, sest organism võitleb teistsuguste rakkudega kui sissetungijatega. Et aga sobivaid doonoreid esineb harvadel juhtudel, tuleb leida meetod *de novo* vereloometüvirakkude tootmiseks alternatiivsetest allikatest. Viimasteks on näiteks pluripotentsed tüvirakud (embrüonaalsed ning indutseeritud pluripotentsed tüvirakud). Edukaks *de novo* vereloometüvirakkude tegemiseks on vaja õppida tundma signaaliradu ning transkriptsioonifaktoreid, mis reguleerivad vereloometüvirakkude arengut organismis.

Gata2 on üks olulisemaid vereloomega seotud transkriptsioonifaktoreid. Gata2 väga hoolikalt kontrollitud ekspressioonitase määrab vere(tüvi)rakkude saatuse. Lisaks vereloometüvirakkudele on Gata2 oluline faktor ka mõnedes täiskasvanud funktsionaalsetes vererakutüüpides, näiteks nagu nuumrakkudes. Minu doktoritöö uurib Gata2 rolli vereloome arengus. Täpsemalt, iseloomustan Gata2 rolli vereloometüvirakkude arengul organismis ning progenitorrakkude tekkes pluripotentsetest rakkudest laboritingimustes (*in vitro*). Oma katsetes kasutan uudset *Gata2Venus* reporter raku- ja hiireliini, mis esmakordselt võimaldab jälgida ning eraldada elusaid rakke, mis ekspresseerivad Gata2 faktorit endogeensel tasemel.

Sissejuhatus (esimene peatükk) annanb ülevaate vereloomearengu uurimissuuna hetkeseisust, keskendudes endoteelirakust vererakuks ülemineku protsessile (*endothelial-to-hematopoietic transition*) ning olulistele transkriptisioonifaktoritele selles protsessis, nagu näiteks Gata2 ning tema sithmärkvalgud. Sissejuhatuse lõpus püstitan oma lõputöö probleemi ning toon välja selle eesmärgid.

Teises peatükis tutvustan Gata2 rolli embrüonaalsete tüvirakkude hematopoieetilises diferentseerumises, kasutades selleks *Gata2Venus* reporterrakuliini. Minu tulemused näitavad, et Gata2Venus märgib kõik verepotentsiaaliga rakud, mis on loodud embrüonaalsetest tüvirakkudest. Nende tekkimine rakukultuuris toimub järk-järgult tõusva potentsiaaliga, luues esialgselt primitiivsed vererakud ning hiljem komplsekssed suure potentsiaaliga progenitorrakud. Progenitorrakud, mis on loodud hilisemas kultuuris, on ka märgitud teise hematopoieetilise markeri, Ly6aGFP poolt, mis organismis märgistab kõik vereloometüvirakud. Selline järk-järguline vererakkude teke on väga sarnane organismis toimuvale vere(tüvi)rakkude arengule ning, koostöös edasiste uuringutega, loob suured eeldused *in vitro* vereloometüvirakkude genereerimiseks.

Kolmandas peatükis kasutan *Gata2Venus* reporterrakuliini uurimaks Gata2 sihtmärkvalgu, Gpr56 rolli vereloome arengus. Minu tulemused näitavad, et Gpr56 rolli kompenseerib selle puudumisel sama geenilookuse poolt kodeeritud Gpr97, mille ekspressioon tõuseb, kui Gpr56 rakkudest deleteeritakse. Gpr56 ja Gpr97 ko-deleteerimisel kaotavad embrüonaalsed tüvirakud aga võime genereerida vereprogenitorrakke, seega viidates nende geenide olulisele funktsioonile vereloomes. Embrüonaalsete tüvirakkude poolt vereprogenitoride tootmine aga suureneb, kui neid töödeldakse Kollageen III-ga, mis on Gpr56 potentsiaalne ligand. Seega, minu töö näitab, et Gpr56-l ning Gpr97-l on kompensatoorne, kuid vajalik

positiivne roll vereloomes ning Gpr56 potentisaalne ligand Kollageen III võimaldab indutseerida *in vitro* vereloomet.

Neljands peatükis tutvustan innovatiivset mudelit nuumrakkude kiireks ning robustseks tootmiseks. Nuumrakud on allergiate, astma ning muude põletikuprotsesside initsiaatorid. Nende põhjustatud haiguste uurimine on senini olnud pärsitud, kuna funktsionaalsete nuumrakkude genereerimisprotokollid on äärmiselt pikaajalised ning kallid. Minu väljatöötatud meetod põhineb teadmisel, et nuumrakud ekspresseerivad kõrgel tasemel Gata2 transkriptsioonifaktorit ning kasutab ära *Gata2Venus* reportertüvirakuliini. Minu tulemused näitavad, et Venus märgib kõik funktsionaalsed nuumrakud ning nende eellased, mis saadakse hiire ja inimese pluripotentsete tüvirakkude diferentseerimisel. Seega, minu meetod võimaldab toota suuri koguseid funktsionaalseid nuumrakke teadustööks märkimisväärselt kiiremini ning odavamalt kui see oli võimalik seni, luues võimalusi nuumrakkude põhjustatud haiguste uurimiseks ning ravi väljatöötamiseks.

Viiendas peatükis genereerime *Gata2Venus* embrüonaalsetest rakkudest reporterhiiremudeli, millega katsed näitavad, et kõik vereloometüvirakud, ning enamus progenitorrrakke organismis ekspresseerivad Gata2 faktorit. Lisaks esineb Gata2-st iseseisev progenitorrakkude populatsioon, millel on spetsiifiline geeniekspressiooniprofiil ning funktksioon. Need andmed näitavad, et Gata2 on vereloometüvirakkude arenguks äärmiselt vajalik ning loob suured eeldused dedasiseks teadustööks vereloometüvirakkude *de novo* genereerimise meetodi väljatöötamiseks.

Viimases, kuuendas peatükis annan ülevaate kogu oma lõputöö tulemustest, nende olulisusest ning aplikatsioonidest.

List of acronyms

AGM   aorta-gonad-mesonephros
AML   acute myeloid leukemia
BAC   bacterial artificial chromosome
BFU-E   burst forming unit-(definitive) erythroid
BL-CFC   blast-colony forming cell
BM   bone marrow
BMP-4   bone morphogenetic protein 4
bp   base pairs
CB   cord blood
Cbf   core binding factor
CFU-C   colony forming unit-cell
CFU-EryP   colony forming unit-(primitive) erythroid
CFU-GEMM   colony forming unit granulocyte-erythrocyte-monocyte-
              macrophage
CFU-GM   colony forming unit granulocyte-macrophage
cKit   proto-oncogene receptor tyrosine kinase
CLP   common lymphoid progenitor
CMP   common myeloid progenitor
Col III   collagen III
CPA-3   carboxypeptidase A3
D   day of differentiation
DKK   dickkopf WNT signaling pathway inhibitor
E   embryonic day
EB   embryoid body
Ed   definitive erythroid
EGM   endothelial cell growth medium
EHT   endothelial to hematopoietic transition
EMP   erythroid-myeloid progenitor
EPO   erythropoietin
Erg   avian erythroblastosis virus E-26 (v-ets) oncogene related
ESC   embryonic stem cell
EVI-1   ectopic viral integration site-1
FcεR1α   Fc receptor, IgE, high affinity I, alpha polypeptide
FcεR1γ   Fc receptor, IgE, high affinity I, gamma polypeptide
FGF   fibroblast growth factor
FL   fetal liver
Fli1   friend leukemia integration 1
Flk1   kinase insert domain protein receptor
Flt3L   Fms-related tyrosine kinase 3 ligand
FPKM   fragments per kilobase of transcript per million mapped reads
Gata   GATA binding protein
GFP   green fluorescent protein
GM-CSF   Granulocyte-macrophage colony-stimulating factor
GMP   granulocyte/monocyte progenitor
GP(C)R   G-protein coupled receptor
G2V   Gata2Venus

HEC	hemogenic endothelial cell
HPC	hematopoietic progenitor cell
HPRT	hypoxanthine phosphoribosyltransferase
HSC	hematopoietic stem cell
IAHC	intra aortic hematopoietic cluster cell
IGF-1	insulin like growth factor
IRES	internal ribosome entry site
iPSC	induced pluripotent stem cell
KO	knockout
LG	Ly6a(Sca1)GFP=Ly6Agfp
Lmo2	LIM domain only 2
LN	lymph node
Lyl1	lymphoblastomic leukemia
MC	mast cell
MCP	mast cell progenitor
MEP	megakaryocyte/erythroid progenitor
mMCP-1	mast cell protease (chymase)
mMCP-5	mast cell chymase 1
mMCP-6	mouse tryptase beta
MPP	multipotent progenitor
NK	natural killer cell
NT	neural tube
OB	olfractory bulb
PB	human peripheral blood
PL	placenta
PSC	pluripotent stem cell
RT	reverse transcription
Runx1	Runt-related transcription factor 1
Sca-1	Stem cell antigen-1
SCF	stem cell factor
Sp	somite pairs
Tal1	T cell acute lymphocytic leukemia 1
TPO	thyroid peroxidase
UA	umbilical artery
UTR	untranslated region
VA	vitelline artery
V^+	Gata2Venus expressing
V^-	Gata2Venus non-expressing
VEGF	vascular endothelial growth factor
WT	wild type
YS	yolk sac

Curriculum Vitae

Personal details

Name   Mari-Liis Kauts
Date of birth   16.04.1988
Nationality   Estonian

Education

2013-present   ***PhD***
                    Department of Cell Biology, Erasmus University
                    Medical Center, Rotterdam, The Netherlands
                    Prof. Dr. Elaine Dzierzak (promoter)

                    Centre for Inflammation Research, University of
                    Edinburgh, Edinburgh, United Kingdom
                    Prof. Dr. Lesley Forrester (promoter)

2010-2012   ***MSc, cum laude***
                    Institute of Gene Technology, Tallinn University of
                    Technology, Tallinn, Estonia
                    Dr. Alla Piirsoo (supervisor)
                    Prof. Dr. Toomas Neuman (co-supervisor)

2007-2010   ***BSc, cum laude***
                    Institute of Gene Technology, Tallinn University of
                    Technology, Tallinn, Estonia
                    Piret Michelson (supervisor)
                    Prof. Dr. Priit Kogerman (co-supervisor)

Employment

2011-2013   Cellin Technologies LLC; Tallinn, Estonia;
                    Researcher
2009-2011   East-Tallinn Central Hospital, Diagnostic Clinic,
                    Tallinn, Estonia, Clinical; Laboratory Technologist
2008-2010   Tallinn University of Technology, Department of
                    Gene Technology, Tallinn, Estonia; Undergraduate
                    intern

Publications

An innovative approach to rapidly generate functionally mature mast cells from Gata2 reporter pluripotent stem cells **Kauts ML**, De Leo B, Kaimakis P, Rodriguez Seoane C, Glykofrydis F, Wilkinson AC, Göttgens B, Saunders P and Dzierzak E (submitted)

Differentiation of Gata2Venus and Ly6aGFP reporter embryonic stem cells corresponds to in vivo waves of hematopoietic cell generation in the mouse embryo **Kauts ML**, Kaimakis P, Hill U, Cortes X, Mendez S, Dzierzak E (submitted)

Hematopoietic (stem) cell development-how divergent are the roads taken? **Kauts ML**, Vink CS, Dzierzak E // FEBS Lett. 2016 Aug 20.

Functional and molecular characterization of mouse Gata2-independent hematopoietic progenitors Kaimakis P, de Pater E, Eich C, Solaimani Kartalaei P, **Kauts ML**, Vink CS, van der Linden R, Jaegle M, Yokomizo T, Meijer D, Dzierzak // Blood. 2016 Mar 17;127(11):1426-37

Protein kinase inhibitor SU6668 attenuates positive regulation of Gli proteins in cancer and multipotent progenitor Piirsoo A, Kasak L, **Kauts ML**, Loog M, Tints K, Uusen P, Neuman T, Piirsoo M // Biochim Biophys Acta. 2014 Apr;1843(4):703-14

CCL5/CCR1 axis regulates multipotency of human adipose tissue derived stromal cells **Kauts ML**, Pihelgas S, Orro K, Neuman T, Piirsoo A // Stem Cell Res. 2013 Mar;10(2):166-78

PhD Portfolio

Personal data

Name	Mari-Liis Kauts
Erasmus MC department	Cell Biology
PhD period	January 2013-April 2017
Promoters	Prof. Dr. Elaine Dzierzak
	Prof. Dr. Lesley Forrester

PhD training Courses

2013 Cell and Developmental Biology course
2013 Biochemistry and Biophysics course
2013 Personal Licence laboratory animal training course
2013 Adobe Illustrator and Photoshop workshop
2014 Genetics course
2014 Health and safety training
2014 Late and lone work training
2014 Liquid nitrogen training
2014 Radiation protection training
2015 Confocal microscopy training
2015 Flow cytometry training
2015 FlowJo training
2015 Statistics course

Conferences and meetings

2016 iForum Meeting, Paris (poster presentation)
2015 ISEH 44th Annual Meeting, Kyoto (poster presentation, travel grant award)
2015 BSDB and BSCD Joint Spring Meeting, Warwick (poster presentation, travel grant award)
2015 ISEH 43th Annual Meeting, Montreal (poster presentation, travel grant award)
2013 ISEH 42th Annual Meeting, Vienna (poster presentation)
2013 DSDB meeting, Utrecht
2013 MGC Symposium, Rotterdam
2012 ISSCR 10th Annual Meeting, Yokohama (poster presentation)
13-17 Lab and Departmental Research in Progress meetings (oral presentations)
14-17 Monthly Edinburgh Hematopoiesis Meetings (oral presentations)
13-16 Journal Clubs

Teaching

2016 Bachelor of Science Honors program student thesis research supervision

Acknowledgements